Università degli Studi di Palermo

AREA RICERCA E TRASFERIMENTO TECNOLOGICO
SETTORE DOTTORATI E CONTRATTI PER LA RICERCA
U. O. DOTTORATI DI RICERCA

Dottorato in Energy
Dipartimento di Ingegneria
IIND-07/A

INTEGRATION OF THERMAL ENERGY SYSTEMS IN RENEWABLE ENERGY COMMUNITIES

IL DOTTORE
GIUSEPPE EDOARDO DINO

IL COORDINATORE
PROF.SSA ELEONORA RIVA SANSEVERINO

IL TUTOR
PROF. ANTONIO PIACENTINO

CO TUTOR
PROF. PIETRO CATRINI

CICLO XXXVII
ANNO CONSEGUIMENTO TITOLO 2025

Riconoscimenti

Arbusta iuvant humilesque myricae

Giovanni Pascoli pone questo verso sul frontespizio della sua raccolta poetica dal titolo *Myricae* per sottolineare l'importanza delle piccole cose semplici della vita quotidiana, meritevoli di essere incluse nell'empireo della poesia. Il verso è volutamente contrapposto all'originale *"Non omnis arbusta iuvant humilesque myricae"*, tratto dalla IV Egloga di Virgilio, in cui, al contrario, si esaltava la superiorità della poesia dotta in contrapposizione al linguaggio quotidiano, impiegando la metafora botanica delle tamerici (*myricae*). Le tamerici sono cespugli bassi, piante certamente non ornamentali né dal fusto alto. Pascoli, nella sua raccolta, le eleva a simbolo della poesia semplice, quotidiana e campestre, che costituisce uno dei capisaldi della sua poetica.

Sono stato ispirato dal concetto delle *Myricae* per estendere il mio riconoscimento personale a tante persone che hanno avuto un ruolo essenziale nel mio percorso formativo e professionale. Ho avuto la fortuna, infatti, di incontrare tante *Myricae* che hanno saputo trasmettermi valori e contenuti elevatissimi senza mai sfociare nella superbia o nell'alterigia, ma rimanendo sempre nella sobrietà, nella semplicità e nel genuino sorriso quotidiano.

I primi anni di formazione sono cruciali per lo sviluppo delle capacità cognitive, dello spirito critico e del ragionamento. Sarò sempre grato ai miei maestri elementari (preferisco chiamarli così, piuttosto che con termini burocraticamente più corretti, ma meno efficaci), tante piccole *myricae* che spargono semi di conoscenza, competenza e metodologia, che vedono sbocciare solo dopo tanti anni e quindi lavorano sempre con uno sguardo di prospettiva. Un ricordo e un ringraziamento particolare al caro maestro di matematica, il compianto Serafino (Fifì) Licata, che ha fatto sviluppare in noi bambini la capacità di ragionamento logico e calcolo elementare mediante metodologie apparentemente semplici e rudimentali, ma efficacissime e strategiche per il prosieguo formativo. Come dimenticare lo studio delle frazioni mediante la suddivisione delle barrette di cioccolato? Grazie anche ai professori delle scuole medie che hanno avuto l'arduo compito di traghettarci dall'infanzia alla giovinezza, trasmettendoci valori ancora oggi indelebili e insegnamenti scolpiti nella nostra memoria. Come non menzionare la cara prof.ssa Irene Purpi, che con il suo rigore metodologico e disciplinare ci ha spianato la strada verso la crescita personale e culturale e mi ha trasmesso l'amore per il teatro, coinvolgendomi per la prima volta a salire su un palco con un copione vero e proprio? Un pensiero speciale al compianto prof. Nino Scelfo, il primo che ci fece costruire un piccolo circuito elettrico elementare, facendoci accendere la "lampadina" della conoscenza tecnica; indimenticabile la sua ironia, la sua voglia di vivere, di scherzare e di stare insieme nei momenti di convivialità. Sono trascorsi poco più di vent'anni, ma sembra quasi un'altra epoca, in cui la didattica e la vita quotidiana non erano basati sull'utilizzo di dispositivi elettronici, come quello che sto impiegando per scrivere questa tesi.

Grazie ai professori del Liceo, per averci preso per mano quasi bambini e lasciati quasi adulti. Sono particolarmente grato a tutti loro per aver impresso in noi lo sviluppo del pensiero complesso, invitandoci a guardare il mondo mediante una sfumatura di colori diversi e non necessariamente in bianco e nero. Un ringraziamento particolare alla prof.ssa Vazzano per averci accompagnato nell'intero percorso scolastico; con i suoi insegnamenti di latino ci ha permesso di sbloccare delle strutture logiche che si sono rivelate fondamentali in tanti campi della conoscenza. Un caro e sentito ringraziamento al prof. Massimo Genchi, che purtroppo ho incontrato solo nell'ultimo anno di liceo e che è stato un propulsore di conoscenza della matematica e della fisica. Grazie a lui, l'impatto con le lezioni universitarie di Analisi 1 è stato (quasi) indolore.

Esprimo profonda gratitudine ai docenti del corso di laurea in Ingegneria Energetica. Pur essendo arrivato in un momento di "rodaggio didattico", il corso è stato in grado di fornire non solo le conoscenze scientifiche, ma anche la metodologia di approccio ai problemi ingegneristici correlati al

vastissimo settore raggruppato sotto il comune denominatore dell'energia. Impossibile dimenticare anche i colleghi di corso, compagni di avventura, il cui imperativo era l'ironia e la risata.

Dopo poco meno di dieci anni dall'esperienza universitaria, ho deciso di ritornare a frequentare le aule e i dipartimenti di UNIPA grazie a due *Myricae* speciali, senza le quali non avrei mai deciso di intraprendere il percorso di dottorato: il prof. Antonio Piacentino e il prof. Pietro Catrini. Il primo mi aveva impressionato nel corso delle sue lezioni di "Gestione dell'energia" per il modo con cui riusciva a trasmettere concetti complessi ed estremamente innovativi. Il prof. Piacentino aveva trovato quella chiave interpretativa e didattica che ci ha consentito di traguardare nuove prospettive scientifiche. Con Pietro ho condiviso una buona parte del cammino studentesco. A conclusione delle lezioni del prof. Piacentino, quando tutto sembrava scontato e facilmente comprensibile, tutti noi ci accorgevamo che quei contenuti non erano affatto facili e ci scontravamo con i nostri limiti di studio e comprensione. Pietro, invece, mi ha sempre stupito per la semplicità, la dedizione e la genialità con cui affrontava queste e altre tematiche, concludendo poi con ottimi risultati il suo percorso. Quando ho deciso di iniziare il percorso di dottorato di ricerca, l'ho fatto perché sapevo di contare su queste due guide di riferimento, a cui sarò per sempre grato.

Non finirò mai di ringraziare il prof. Michele Bottarelli e l'amico e collega Marco Bortoloni dell'Università di Ferrara. Grazie a loro sono stato introdotto nel mondo della ricerca e mi sono appassionato ad esso. Grazie a loro ho iniziato a fare attività di ricerca, cominciando proprio dalla ricerca sperimentale pura, sporcandomi le mani quotidianamente, sbattendo la testa su mille difficoltà che mai, prima di allora, avevo incontrato. Loro mi hanno trasmesso rigore scientifico e metodologico, unito a un profondissimo spirito di abnegazione e dedizione a questo lavoro. Non è stata un'esperienza facile, ma condividere le difficoltà, la fatica e i momenti critici ha rinsaldato anche i nostri rapporti umani, che rimarranno indissolubili. Indimenticabili le missioni nel deserto del Negev con le valigie piene di attrezzi da lavoro necessari per le operazioni sul sito sperimentale di Yeruham.

Grazie ai colleghi della Frigoveneta per la brevissima esperienza aziendale che mi ha permesso di aprire gli occhi su una realtà diversa da quella accademica. La mia presenza tra Emilia e Veneto mi ha permesso di smentire tanti luoghi comuni legati a quella meravigliosa parte d'Italia. Un'altra tappa cruciale nel mio percorso professionale la devo al CNR ITAE di Messina, in particolare al dott. Andrea Frazzica e alla dott.ssa Valeria Palomba. In quei laboratori ho continuato con la ricerca sperimentale, seppur su un settore profondamente diverso rispetto a Ferrara. Ad Andrea e Valeria devo moltissimo; al centro testing del CNR ITAE ho potuto affinare molti aspetti di questa professione grazie al loro validissimo supporto e al coinvolgimento in progetti di ricerca internazionale. Un percorso di crescita umana e professionale molto importante che mi ha consentito di prendere la scelta definitiva di andare avanti e puntare su questo settore in maniera definitiva.

L'ultima tappa, in ordine cronologico, è l'approdo in ENEA, con un contratto di lavoro a tempo indeterminato che mi ha permesso di innalzare l'orizzonte temporale delle mie prospettive. Anche qui ho avuto il piacere di incontrare persone che coniugano una solida base professionale e scientifica alla semplicità e sincerità dei rapporti umani. Un grazie sincero al mio responsabile di unità, dott. Francesco Gracceva, con il quale ho già condiviso momenti importanti, sebbene il mio impegno sia stato più dedicato al dottorato di ricerca che all'attività in ENEA. Il primo impatto è stato inusuale, in quanto io parlavo una "lingua" diversa rispetto a Francesco e ai colleghi di unità, avendo percorsi formativi totalmente diversi. Questa apparente debolezza sta diventando sempre più un punto di forza, consentendoci di rafforzare il nostro operato mediante la complementarità.

Ciò che siamo è frutto di tanti contributi; la crescita professionale è certamente influenzata dalla relazione con le persone incontrate nell'ambito formativo e lavorativo, ma il contesto sociale, familiare e affettivo scolpisce un'impronta profonda e determinante in ognuno di noi. Non possono mancare i ringraziamenti ai tanti amici con cui ho condiviso molte tappe della mia vita, che mi hanno coinvolto in contesti profondamente diversi da quello lavorativo e accademico, consentendomi di aprire lo sguardo a mondi che altrimenti non avrei mai conosciuto. Grazie a loro ho potuto vivere

emozioni grandissime, partecipando ad esperienze culturali, di volontariato, teatrali, cinematografiche, naturalistiche. Tutto mosso dall'unico scopo di voler fare comunità, di aggregarsi con un mordente ogni volta diverso, ma con un obiettivo sempre comune. Un ricordo speciale, pieno di tutti i sorrisi che abbiamo condiviso, agli amici che ci hanno dovuto lasciare prima del tempo, cristallizzandosi nella nostra memoria per sempre: Calogero, Giorgio e Daniele.

Il luogo in cui siamo nati e cresciuti, dove abbiamo vissuto le nostre prime esperienze e abbiamo avuto il primo approccio con il mondo, spesso ha un'influenza determinante sulla nostra vita. Per questo motivo sono grato alla mia piccola grande casa, Petralia Sottana, che costituisce più di un luogo fisico. Ho raggiunto questa tappa di vita anche grazie al contesto in cui sono cresciuto, da cui ho ricevuto innumerevoli stimoli culturali e dove la mia personalità si è forgiata, tra aspetti positivi e inevitabilmente negativi. Il riconoscimento verso questa comunità ha preso vita in un progetto di crescita collettiva che mi ha portato ad impegnarmi in un percorso di impegno civile e politico di prima linea, arduo ma edificante.

Per ultimo, le mie *Myricae* più care, i miei familiari, a loro va la dedica di questo lavoro e di questa esperienza.

Ad Erica, ormai parte indissolubile della mia vita, organo vitale di me stesso e preziosissimo sostegno, con la quale riesco a guardare al futuro senza essere distratto dai tanti problemi della quotidianità. Alla sua famiglia, che con immensa generosità e amore mi ha accolto sin dal primo momento, offrendomi tutto il meglio di sé, a loro va la mia più profonda gratitudine.

A mia madre, per il suo amore puro profuso verso di me sin dal primo istante in cui sono venuto al mondo. Gli eventi della vita non le hanno riservato un cammino facile, ma, nonostante tutto, la sua fragile condizione ci permette ogni giorno di fare tesoro degli elementi puri della nostra "tavola periodica" esistenziale. Le sono grato per la lezione di vita che quotidianamente mi offre.

Infine, a mio padre, che sin da piccolo ha stimolato la mia curiosità e la mia cultura scientifica. Oggi sono arrivato a questo punto grazie alla sua spinta, ai suoi incoraggiamenti ed alla sua infinta generosità. Per un piccolo imprevisto con la vita non potrà assistere fisicamente a questo traguardo, ma sono certo che ne sarà fiero con il suo sorriso ironico sotto il baffo.

Grazie di cuore a tutte le *Myricae* della mia vita.

Con infinita gratitudine

Giuseppe Edoardo Dino

Sommario

1. Introduction

The EU27 final energy consumption share in the household sector for 2022 accounted for 26.9% (1411 TWh) [1], transports have the highest share at 31%, and commercial and public services range up to 13.4% share (Figure 1).

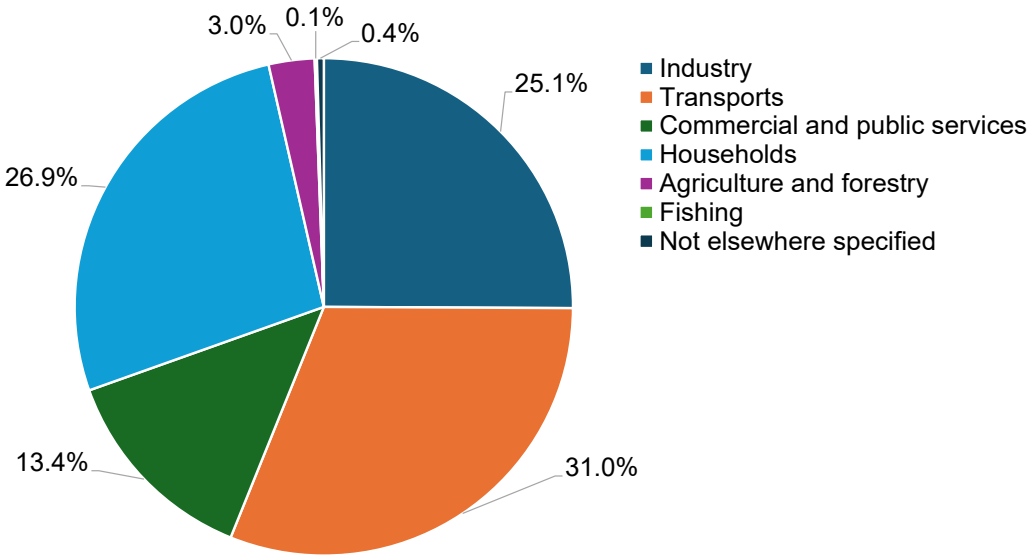

Figure 1: Final energy consumption by sector - Year 2022 [1]

The main use of energy by households in the EU in 2022 was for space heating (63.5% of final energy consumption in the residential sector - Figure 2), with renewables accounting for more than a quarter (31.4%) of EU households space heating consumption [2]. Water heating has the second highest rate, while space cooling has a minor role with increasing perspectives.

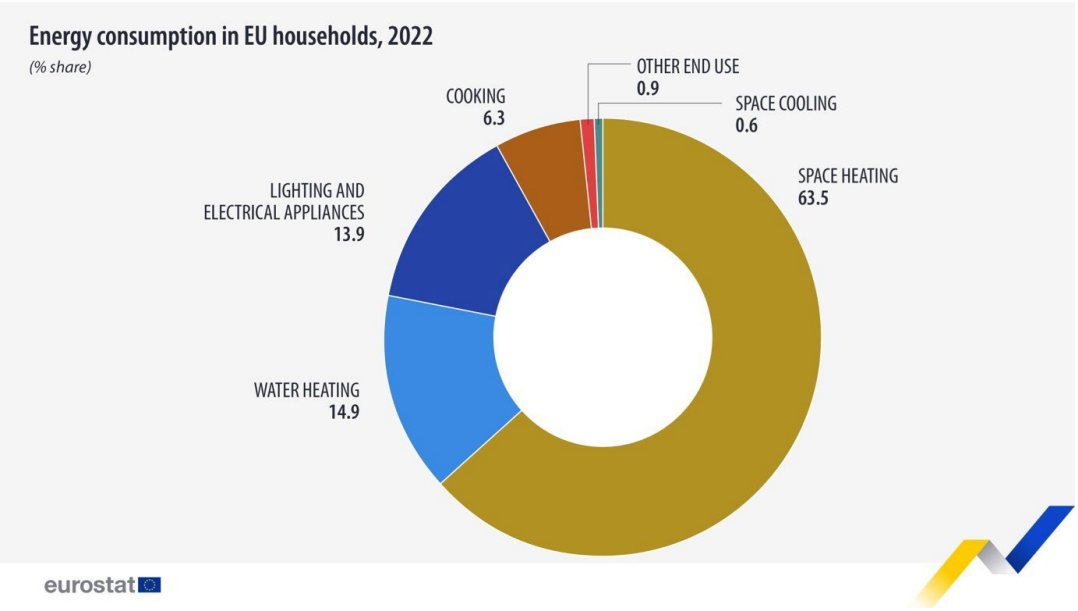

Figure 2: Energy consumption in households - Year 2022 [2]

The disaggregated final energy consumption analysis in households (Figure 3) reveals that space heating is supplied for its majority share by fossil fuels: 36.3% natural gas, 13.1% Oil

and petroleum products, 3.4% solid fossil fuels, and peat [1]. Heat pumps cover a minority share, while “Heat” (District Heating) covers 9.7%. An analog distribution is observed for water heating, also in this case fossil fuels have a higher share, while solar thermal emerges with 5.7%, and district heating rises to 13.7%.

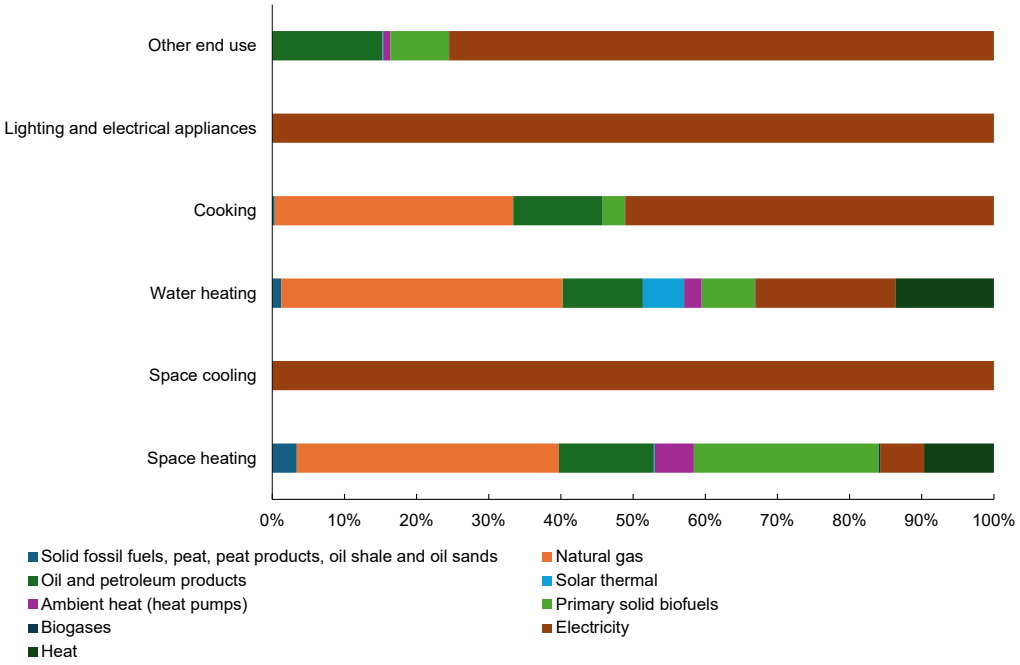

Figure 3: Disaggregated final energy consumption in households – Year 2022 [1]

Due to the increasingly dangerous effects of climate change and its correlation with carbon emissions, the decarbonization of energy systems has emerged as a critical priority for governments, industries, and communities alike. As underlined by the most recent available European data shown before, the household and civil sectors, which account for a significant portion of global energy consumption and greenhouse gas emissions, are at the forefront of this transition. Among the various strategies to achieve decarbonization, district heating systems (DHS) have gained prominence as an effective solution for providing sustainable and efficient thermal energy to urban populations.

District heating refers, in general, to a centralized system that converts heat from a variety of sources (from fossil fuels to renewable energy) and supplies it through a pipeline network to multiple consumers, including residential buildings, commercial establishments, and public facilities. The interface between DHS and the final user is the thermal substation which is one of the core components of these systems and will be an object of focus and detailed analysis of the present work.

One of the key advantages of district heating systems is their capacity to implement a diverse variety of heat sources. This flexibility allows for the incorporation of renewable energy technologies, such as solar thermal, biomass, geothermal, and waste heat recovery, into the heating mix. Through the exploitation of these sustainable resources, district heating can significantly lower carbon emissions associated with space heating or water heating, which is particularly important in regions where individual heating solutions are heavily reliant on natural gas or oil. Furthermore, district heating systems can operate at lower

temperatures, which further enhances their association with renewable energy sources and improves overall system efficiency.

In addition to their environmental benefits, district heating systems offer economic advantages. By centralizing heat production, these systems can achieve economies of scale, leading to lower operational costs, reduced energy prices for consumers, and increased supply reliability. Moreover, the integration of smart technologies and digital solutions in district heating networks can optimize energy distribution, enhance demand-side management, and improve the overall reliability of heating services. This represents a viable path to guarantee the stability of the energy grid, particularly concerning the behavior of intermittent renewable energy sources increases.

Furthermore, the role of district heating in the decarbonization of the household and civil sector is further highlighted by its potential to promote energy resilience and security. As urban populations continue to grow, the demand for reliable and affordable heating solutions will increase. District heating systems can provide a robust framework for meeting this demand while simultaneously addressing the challenges presented by climate change. By promoting energy efficiency, reducing emissions, and enhancing the integration of renewable energy, district heating can play a pivotal role in creating sustainable urban environments.

Figure 4 illustrates a trend in heating networks over the past 150 years, shifting from centralized fossil fuel sources, which presented significant heat losses, to decentralized renewable energy sources operating at low temperatures with minimal heat losses in smart thermal grids. Fourth-generation district heating networks (4GDH), through lowering the operating temperature, have introduced smart thermal grids that enhance efficiency using renewable energy sources [3]. These smart thermal grids allow for the sharing of renewable energy across entire districts, and the network itself can serve as a form of heat storage [4]. As a result, the transition to 4GDH and the implementation of smart thermal grids globally is becoming essential.

However, a significant challenge with smart thermal grids and the utilization of waste heat is that energy at low-temperature levels cannot be directly employed within 4GDH systems. To address this, the Fifth Generation District Heating and Cooling (5GDHC) system was introduced, characterized by operating at temperatures close to ground levels [5]. These systems are characterized to be decentralized, and bidirectional, and enable direct exchange between warm and cold return flows [6]. This makes them particularly suitable for integrating renewable energies, which are often decentralized and operate at very low temperatures, close to the ambient one, thus minimizing heat losses. Furthermore, utilizing geothermal systems as a heat source can enhance heat gains through the distribution network [7].

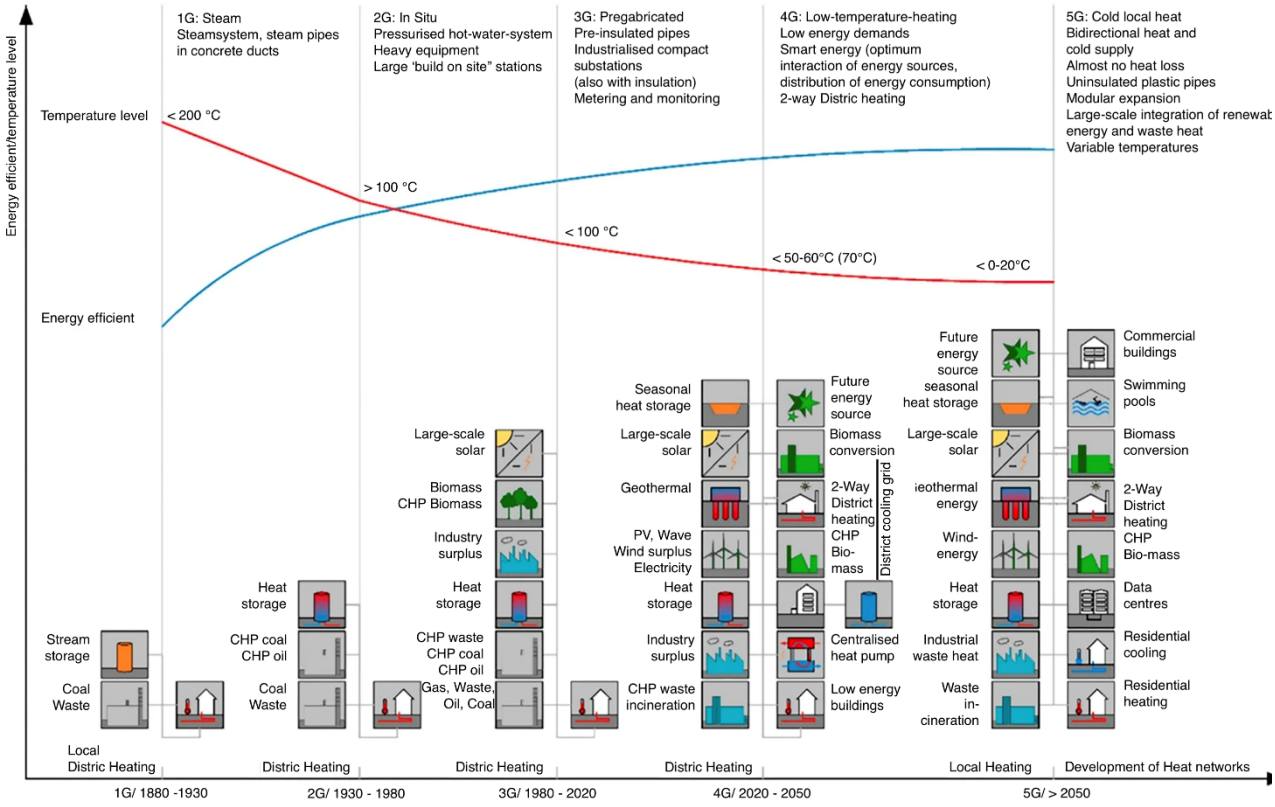

Figure 4: Evolution of district heating networks from the first to the 5th generation over the last 150 years

1.1. The District Heating and Cooling in Italy

As of December 31, 2022, the building stock connected to district heating networks in Italy reached a volume of nearly 393 million cubic meters [8]. The extension of new networks in 2022 is approximately 53 km, while, compared to the last survey reported in 2021, the existing networks have increased by about 68 km. Therefore, as of December 31, 2022, the total length of urban heating networks in Italy reached nearly 5.000 km, excluding connections. From 2000 to the present, this development shows a significant growth factor of almost 4.6 (meaning that in just over 20 years, the network length has nearly quintupled). However, while between 2000 and 2010 the growth factor was 2.54, between 2010 and 2022 it decreased to 1.8, confirming the downward trend already observed. As for user plants, by the end of 2022, a total of 90.223 substations had been installed. This represents an increase of 1.864 compared to the previous year, confirming the trend of recent years. The importance of the equipment that supplies heat for both heating and domestic hot water remains significant, accounting for almost 71% of installed plants (in 2012, this type made up 66% of installed substations, and in 1997, it was only 50%). At the end of 2022, the potential by type of production units that feed district heating networks is reported in Table 1. Table 1 does not account for the electrical power from waste-to-energy from residual municipal waste plants and that of thermoelectric power plants from which heat is drawn for district heating networks. The principle adopted is to consider only the electricity produced in cogeneration, excluding any shares of energy that, although produced by the same

combined production plant, are generated in a dissipative or partially dissipative regime. Essentially, the principle relies on separating the combined production unit into two parts: the full CHP portion and the Non-Full CHP portion. Only the energy flows from the Full CHP portion are considered in the preparation of the energy and environmental balance of the district heating system. The method adopted for separating the Full CHP portion is indicated by the Italian Ministerial Decree of August 4, 2011 [9]. The share of bioenergy plants represents almost 19% of the installed capacity (3908 MWt excluding supplementary and reserve boilers), which, when added to the remaining share from waste-to-energy recovery, geothermal energy, heat pumps, industrial recovery, and solar thermal, brings the percentage to 45%. Bioenergy plays a significant role, with a total of 736 MWt installed, of which 482 MWt comes from simple combustion and 255 MWt from cogeneration plants.

Table 1: Energy conversion plant typology. (1) Plants powered by fossil fuels, (2) Boilers powered by bioenergy, landfill gas, and sludge

Plant Typology	**Installed capacity on 31st December 2022**		**Installed Capacity on 31st December 2021**	
	Electric MWe	**Thermal MWt**	**Electric MWe**	**Thermal MWt**
Thermoelectric power plants		1.204		1.155
Cogeneration plants(1)	808	933	808	919
Waste-to-energy from residual municipal waste plants		681		685
Simple production from bioenergy(2)		482		459
Bioenergy cogeneration plants	91	255	88	248
Geothermal plants		156		156
Industrial waste heat		118		78
Heat pumps		78		52
Solar Thermal		1,65		1,55
Backup boilers		5.586		5.533
Total	**899**	**9.494**	**896**	**9.287**

The primary energy sources mix employed in the Italian district heating systems is reported in Table 2. The comparison between 2012 and 2022 data underlines several significant considerations. Overall, there is a shift from fossil sources to renewable sources. It is also confirmed that renewables are typically used as a base source. Natural gas has decreased

significantly by almost 10 percentage points, from 78.5% to 69.8% (of the total output), but it remains by far the primary source and the waste-to-heat source showed an increase from 9.7% to 16.1%. Among renewable sources, bioenergy (primarily biomass) plays a prominent role, constituting today the third most used fuel in district heating systems in Italy (10.7% of the input). Solar energy, absent in 2012, nowadays is active but with encouraging perspectives, geothermal energy has shown a significant increase over the past ten years, but despite its development potential and the environmental benefits associated with its use, it remains in a very marginal position: 1.5%. Finally, it is worth noting the dismantling of coal in the analyzed decade

Table 2: Primary energy sources mix employed in the Italian District Heating Systems. (1) Since 2013 the terminology "Bioenergy" includes biomass, biogas, and liquid biofuels. (2) Consumption of the National Electric System for electricity drawn from the grid.

Energy sources	**2022**		**2012**	
	tep	**%**	**tep**	**%**
Natural Gas	1.353.550	69.8	1.288.738	78.5
Waste-to-energy from residual municipal waste	312.764	16.1	159.278	9.7
Bioenergies(1)	206.672	10.7	105.918	6.4
Coal	-	0	43.131	2.6
Oil derivates	1.797	0.1	12.317	0.7
Geothermal	29.596	1.5	14.684	0.9
Industrial waste heat	7.943	0.4	858	0.1
Solar	77	0	-	0
Fossil primary energy by National Electric System(2)	26.537	1.4	17.409	1.1
Total Fossil sources	**1.381.884**	**71**	**1.361.595**	**83**
Total Renewables	**557.053**	**29**	**280.738**	**17**
Total	**1.938.937**	**100**	**1.642.333**	**100**

The plants supplying district heating networks operating in Italy produced 6535 GWh_e, 11515 GWh_t, and 167 GWh_f. The net useful energy (without network losses and plant self-consumption) amounts to 6111 GWh_e (approximately 94% of production), 9173 GWh_t (approximately 80% of the energy delivered to the networks), and 155 GWh_f (93% of production). The thermal energy converted by cogeneration from fossil sources accounts for

approximately 49.7% of the total energy fed into the grid, while the integration of energy produced by simple boilers constitutes 22.6%. The remaining 27.7% comes from renewable sources (among these, heat pumps account for about 1%). Overall, the contribution of fossil cogeneration and renewable sources covers about 77.4% of the thermal energy fed into the networks.

As regards district cooling, the prevalent technology, in terms of cooling energy supplied, is the centralized vapor compression chiller with 59.5% of the total. The remaining part is supplied by centralized absorption chiller (11.3%) and by decentralized ones supplied by heat delivered by the district heating network (29.2%). The comparison with historical data series underlines several critical issues that hinder the penetration of this technology:

- High transportation network costs (for centralized plants)
- High cost of cooling energy production, particularly in plants with decentralized chillers, where single-stage absorption chillers with COP ranging between 0.60 and 0.65 are installed.
- Low number of hours of utilization of the installed systems.
- Cost of cooling energy is strictly dependent on the performances of the installed chiller and climate conditions.

Table 3: Cooling energy produced and installed capacity of cooling DH plants for 2022

Plant typology	**Cooling Energy produced in 2022**			**Installed capacity in 2022**		
	Compression	**Absorption**	**Total**	**Compression**	**Absorption**	**Total**
	MWh_f	**MWh_f**	**MWh_f**	**MW_f**	**MW_f**	**MW_f**
Centralized	99369	18891	118261	108.1	32.6	140.8
Decentralized		48632	48632		108.6	108.6
Total	**99369**	**67523**	**166892**	**108.1**	**141.2**	**249.4**

A synthetic overview of the characterization of district heating and cooling systems in Italy is presented in Table 4.

Table 4: Global overview of district heating and cooling networks in Italy. (1) Cogeneration plants fully dedicated to the DHN, supplied by fossil fuels and biofuels. (2) Cogeneration plants fully dedicated to the DHN, part of full CHP mode of non-fully dedicated plants, supplied by fossil fuels and biofuels. (3) Including Industrial process waste heat, waste-to energy from residual municipal waste, bioenergy, geothermal, heat pumps. (4) Only primary network until substation, excluded the distribution pipelines from user substation to the user final dwellings. (5) Emission factor for conventional thermos-electric plants: 564 g CO_2/kWh

		Year	
		2012	**2022**
Number of cities supplied by DHCN	n.	109	232
DHN management entities	n.	68	166
Number of networks	n.	148	279
Hot water	n.	105	234
Super-heated water	n.	37	39
Steam	n.	6	6
Overall building volume heated	Mm^3	279.4	392.7
Cogenerative installed electric power (1)	MWe	849	898
Cogenerative installed thermal capacity (2)	MWt	2682	3113
Thermal energy supplied to the users	GWht	8005	9173
Renewable energy sources and waste heat (3)		22.7%	27.7%
Cogeneration from fossil fuels		50.2%	49.7%
Fossil fuel combustion		27.1%	22.6%
Cooling energy supplied to the users	GWhf	101.4	155.1
Electrical energy supplied to the grid	GWhe	5592	6111
Ratio between electrical energy supplied to the grid and thermal energy delivered to the users		0.70	0.67
District Network length (4)	km	3161	4989
User substations	n.	57492	90223
Avoided CO_2 emissions (5)	Mt	1.4	1.8

1.2. Thermal Prosumers

Energy-sharing models could contribute to achieving environmental, economic, and social sustainability. In this regard, the “Integrated Energy Communities” will offer new opportunities to create smarter, more flexible, and integrated local systems [10]. Although the “Electrical Energy Communities” have already achieved a recognized and organized structure, “Thermal Energy Communities” still need research efforts to overcome some barriers that make their feasibility more difficult [11]. Among those barriers, challenges are related to the capability of dealing with the increasing number of renewable energy producers that could supply heat to thermal grids [12]. Indeed, a typical heat consumer who is connected to the network could become a producer for some hours in a day due to the energy produced by renewable energy plants installed onsite [13] or waste heat.

Thanks to the innovations introduced in terms of the enlargement of supply sources for DHN and smart digital systems, positive interactions can take place among heat sources within the supply structure. As in the case of the electricity grid, such an actor is not more classified as “only-consumer”, but it is a “prosumer” (i.e., “producer-consumer”). A user who consumes energy from the grid and returns it at different times is known as a “prosumer” [14]. A typical example of a prosumer is a residential building that extracts heat during the winter and cooling during the summer months. This interaction can also occur among various consumers, such as when a housing development is linked with a data center. When prosumers are interconnected, the system is termed a bidirectional network, as the energy flow is not exclusively directed from the energy source to the users.

Thermal prosumers can include a heterogeneous range of participants, such as residential households equipped with solar thermal panels or heat pumps, commercial buildings utilizing waste heat recovery systems, and industrial facilities that generate excess heat during production processes. Thanks to the diversification of energy sources, prosumers can reduce their reliance on conventional individual heating methods, which are often dependent on fossil fuels. This shift not only lowers greenhouse gas emissions but also enhances energy security and resilience, particularly in urban areas where heating demand is concentrated, and the air quality index is scarce due to the emission of individual heating systems.

The integration of thermal prosumers into existing energy systems shows several advantages. Firstly, it leads to an intermediate solution between fully centralized heat production and individual heating systems, thus allowing for a more localized approach to heat generation. This decentralization can lead to reduced transmission losses, as heat is produced closer to where it is consumed. Additionally, the presence of thermal prosumers can enhance the flexibility of energy systems, enabling better demand-side management and the optimization of energy flows. By actively participating in the thermal energy market, prosumers can contribute to balancing supply and demand, particularly during peak heating periods. Moreover, thermal prosumers play a crucial role in the integration of renewable energy sources into heating systems. As the share of renewable energy in the overall energy mix continues to grow, the ability to utilize locally generated heat becomes increasingly important. Thermal prosumers can effectively exploit surplus heat from renewable sources, such as solar thermal systems or biomass, thereby reducing the carbon footprint of heating

systems. This not only supports the decarbonization of the heating sector but also aligns with broader climate goals and policies aimed at promoting sustainable energy practices.

The rise of thermal prosumers is also facilitated by advancements in technology and digitalization. Smart meters, energy management systems, digital twins, and digital platforms enable prosumers to monitor their energy production and consumption in real time, allowing for more conscious decision-making and efficient energy use. Additionally, the development of peer-to-peer energy trading platforms through innovative digital instruments (as experimented with the application of blockchain into the electrical energy communities [15]) empowers prosumers to sell excess heat to their neighbors or participate in community energy initiatives, fostering a sense of collaboration and shared responsibility in the energy transition.

The research studies that include the concept of “Prosumers” related to the DHC technologies were grouped by the main purpose of the study, in order to carry on a critical review of the main aspects belonging to the aforementioned concepts and to investigate the perspectives that the actual state of art assesses for the prosumers in the DHCN.

Name of the group	General purpose	References
Design, Assessment, and Experimental Analysis of District Heating Systems	To evaluate, design, and experimentally assess district heating systems incorporating prosumers, including their configurations and operational profiles.	[16], [17], [18], [19], [20], [21], [22], [23], [24]
Dynamic Modeling, Simulation, and Economic Optimization of Prosumer-Based District Heating Systems	To model, simulate, and optimize the performance and economic viability of district heating systems with prosumers, focusing on dynamic behavior and economic analysis.	[25], [26], [27], [28], [29], [30], [31], [32]
Integration of Renewable Energy, Waste Heat, and Theoretical Framework in District Heating Systems and reliability analysis	To explore the integration of renewable energy sources and waste heat recovery in district heating systems and their reliability while providing a theoretical background and reviewing existing literature on the subject.	[33], [34], [30], [35], [36], [37], [38], [39]

The papers in the group named “*Design, Assessment, and Experimental Analysis of District Heating Systems*” collect papers that address the multifaceted aspects of designing, assessing, and experimentally analyzing district heating systems with prosumers. They

explore several configurations and operational profiles, highlighting the potential benefits of integrating solar thermal energy and other renewable sources. The design and assessment of district heating systems with prosumers require a comprehensive understanding of various thermohydraulic parameters and operational dynamics. In fact, the integration of prosumers introduces complexities in the management of heat flows, temperature control, and energy storage. For these reasons, it is essential to develop robust models that can simulate the behavior of these systems under different scenarios. Such models enable researchers and practitioners to evaluate the performance of district heating networks, identify potential improvements, and optimize the configuration of system components. The findings from these studies contribute to the growing body of knowledge on the prosumer role within district heating systems, providing valuable insights for policymakers, engineers, and researchers aiming to enhance the sustainability and efficiency of urban energy systems.

The study presented in [16] presents a comprehensive analysis of prosumer-based district heating systems (DHS) that includes solar thermal energy and thermal storage. The study implemented a modeling framework that integrates a thermal network design and simulation model, a building energy demand model, and supply and storage technology models. This framework is designed to assess the solar fraction, equivalent annual cost, and greenhouse gas emissions of DHS. The simulations were based on GIS urban data, allowing for a detailed analysis of different district characteristics, including varying sizes, retrofitting stages, and load densities. The model specifically focused on integrating rooftop-mounted solar thermal collectors, gas boilers, and thermal storage tanks, providing a comprehensive view of the system's performance. A quantitative analysis of a prosumer-based solar DHS with thermal storage was performed, based on its energy, economic and environmental impacts. It is assumed that for DHS scenarios, each building with solar thermal collectors primarily covers self-consumption, and only when there is surplus heat available is it fed into the thermal network. This is regarded as the “prosumer state”. When available solar energy is lower than the heating load, the buildings withdraw heat from the thermal network, referred to as a “consumer state”. The results indicated that DHS generally outperforms individual heating systems (IHS) in terms of energy efficiency, cost-effectiveness, and greenhouse gas emissions, particularly when the storage volume to solar collector area ratio is optimized or in the solution with diffused solar plants and centralized storage. The study reported maximum solar fractions of 50% for non-retrofitted buildings and 63% for retrofitted cases. Smaller districts and those with retrofitted buildings show significant benefits from DHS solutions, highlighting the importance of proper sizing and configuration. The adoption of prosumer-based DHS is then proposed as a viable alternative to traditional heating systems, particularly in urban environments.

Several efforts were dedicated to creating new modeling framework, a novel Modelica library for prosumer-based heat networks is presented in [17]. The authors introduced the “ProsNet library”, designed to facilitate the dynamic and steady-state analysis of these networks. A comparative validation approach, utilizing the ProHeatNet_Sim framework, was carried on as a benchmark for assessing the accuracy of the ProsNet library. A radial heat network model comprising three prosumers was built, each configured to operate in different modes (production and consumption). Key parameters, such as pipeline dimensions, pressure loss

factors, and heat exchanger specifications, were meticulously defined to ensure realistic simulations. The models were initialized in steady-state conditions, allowing for a direct comparison of results between the two frameworks. The validation results indicated that the ProsNet library provides a more accurate representation of pressure losses and flow rates due to its incorporation of the actual Darcy-Weisbach friction factor, contrasting with the simplified flow model of ProHeatNet_Sim. The maximum relative error for pressure differences was found to be 11.7% for certain prosumers, while volumetric flow rates exhibited lower relative errors, highlighting the quadratic relationship between flow rate and pressure drop. Additionally, the heat flow rates calculated by ProsNet were lower than those predicted by ProHeatNet_Sim, attributed to the dynamic adjustment of the overall heat transfer coefficient in response to changing flow conditions. The authors concluded that the ProsNet library effectively depicts the complex thermohydraulic behavior of prosumer-based heat networks, facilitating the exploration of various operating modes and control strategies. However, challenges remain, particularly in refining the models to account for non-linearities in valve characteristics and the dynamic nature of prosumer interactions.

The paper [18] presented an exam of the role of prosumers in district heating networks, illustrating how their configurations can significantly impact system dynamics and efficiency. The study employed a simulation-based approach using SimulationX® software (based on Modelica language), specifically the Green City library, which allows for detailed modeling of energy supply systems. The authors defined several configurations for prosumer systems, implementing different heat generators (heat pumps, solar thermal collectors, and combustion-based generators) and thermal storage components. The configurations are evaluated through scenario analysis, simulating conditions such as heat extraction (consumer mode), grid absence (decentralized production), and heat feed-in (producer/prosumer). The simulation results revealed significant differences in efficiency and operational suitability among the configurations. For instance, configurations optimized for heat extraction demonstrated lower return temperatures and higher efficiency when the prosumer primarily extracts heat. Conversely, configurations designed for heat feed-in showed enhanced efficiency and feed-in potential, particularly when excess heat is available. The findings indicated that the main operational purpose of the prosumer, whether extracting or feeding in heat, must be established to select the most effective configuration. The authors concluded that the integration of prosumers into district heating networks can enhance overall system efficiency and flexibility. However, they also highlight challenges, such as the need for advanced control strategies and the potential for increased complexity in system management.

The paper [19] investigated the integration of prosumer structures within low-temperature and ultra-low-temperature district heating networks. The study aimed to analyze the impact of prosumers on energy efficiency and overall system performance, particularly in the context of a new housing district. The authors developed a dedicated model based on c#.NET language and Math.NET.Numerics library to model and analyze various heating network scenarios. This framework allows for calculating hydraulic and thermal losses based on the heat demand of connected buildings. The graph theory was adopted to solve the hydraulic model, and the multipole method to solve the thermal one. Finally, the hydraulic and thermal models coupling was performed, and the prosumer operation was included. The

study employed a real-world case study in Bergkamen, Germany, to validate the model and assess the performance of different network configurations. The study revealed that ultra-low-temperature networks can achieve up to an 80% reduction in heat losses compared to traditional low-temperature systems. The study case application showed that including prosumers in the analyzed ultra-low temperature district heating network achieved an electricity consumption reduction of about 23% for circulating pumps. Besides, heat losses have also declined by 10% in the scenario with prosumers. Overall, the results underscored the potential for prosumers to not only meet local heating demands but also contribute to a more sustainable energy system by decreasing reliance on fossil fuels. The perspectives of research opened by authors include the need for further research into seasonal thermal energy storage, the economic implications of transitioning from low to ultra-low temperature networks, and the optimization of prosumer locations within the network.

The paper [20] analyzed the integration of prosumers within district heating networks (DHNs) through the development and testing of a bidirectional substation prototype. The employed methodology involves a hardware-in-the-loop (HIL) technique, which allows for real-time simulation of the substation's performance under varying operational conditions. This approach enabled the coupling of the substation with data-driven thermal loads from a multi-family residential building and production profiles from renewable sources, in this case, the solar collector and a waste heat recovery system were considered. The physical experimental equipment was composed of the prosumer substation, while the DHN, the distributed generation, and the user load were emulated through HIL. A set of different conditions was considered. The results obtained from the experimental tests revealed significant insights into the operational efficiency of the bidirectional substation. The study indicated that the district heating contribution to the user’s load can vary according to the selected condition, ranging from 99.8% on winter days to as low as 21.8% during summer days. Furthermore, the local production contribution to the user’s load fluctuates between 24% and 100%, depending on the system configuration. This variability underscored the importance of optimizing the integration of local energy production to meet thermal demands effectively. These outcomes confirm the technical feasibility of the analyzed system, in terms of temperature control and demand-supply, and prosumers’ role in better exploiting locally available sources, solar energy, and waste heat in this experimental campaign. Transforming the DHN into a storage can be a solution for end users, and the daily net-metering model proved to be an effective method for enhancing the contribution of distributed generation to the user load, achieving up to 100% in the case of waste heat. The findings from this study could offer valuable insights for stakeholders to advocate for thermal net-metering as a strategy to facilitate a green transition in district heating and cooling systems, ensuring their long-term sustainability and competitive provision of heat and cold to end users.

The study [21] is focused on bi-directional heat trading within DHNs that includes the participation of prosumers. An experimental analysis involved three thermal energy prosumer buildings integrated into an existing thermal network. The methodology included modifying the pipe network to facilitate bi-directional flow and establishing a control system to manage heat trading between buildings. The experimental test period covered over five weeks during the cooling season, allowing for real-time data collection on temperature,

energy flow, and operational costs. The study also involved a detailed analysis of the control methods employed to optimize energy sharing among the connected buildings. The results showed that the temperature of the thermal network maintained a range of 11°C to 13°C, demonstrating the feasibility of decentralized heat supply. Furthermore, it was proved that, like the centralized heat supply case, decentralized heat prosumer buildings can be used in a thermal network by supplying an appropriate level of cooling energy to the network. Conversely, the outcomes of the experimental campaign highlighted that while the current operational model did not yield immediate economic benefits, future scenarios with increased peak power costs could enhance the cost-effectiveness of the bi-directional heat trading system. The study concluded that integrating heat prosumers into thermal networks can significantly improve energy efficiency and sustainability. However, challenges remain, particularly regarding the economic viability of such systems under current energy pricing structures. The authors emphasized the need for supportive policies and incentives to encourage the adoption of prosumer models.

An experimental study on the integration of heat prosumers within a small-scale centralized district heating and cooling system is presented in [22]. An existing high-efficiency urban district was adopted as an experimental field, three thermal energy prosumers were considered: a high school, a childcare center, and a management center. The study utilized a control logic system to manage the flow of heating and cooling energy among the buildings, allowing for real-time adjustments based on demand and supply conditions. Experimental operations were conducted to assess the effectiveness of the bi-directional energy trading method, with a specific focus on the thermal load profiles and energy flow dynamics. The results revealed that the integration of prosumers significantly improved the overall efficiency of the thermal network. On a typical operational day, the total recorder thermal load was 4,702.2 kWh, with the management center supplying 798.7 kWh (17% of the total load) from seasonal thermal energy storage (STES) and 2,270.5 kWh (48%) from the heat pump. The childcare center contributed 295.2 kWh (6%) through its geothermal heat pump. The results demonstrated that the prosumers could effectively share excess thermal energy, thereby optimizing resource utilization and reducing operational costs. The proposed method of constructing a bidirectional thermal network can be used to implement heat transactions between buildings on a heat network with multiple heat energy prosumers, and the results of the demonstration operation allow each thermal prosumer to appropriately share the amount of heat energy supply in consideration of economy and eco-friendliness The authors highlighted the importance of further research to refine the operational strategies and to explore the scalability of such systems in broader contexts.

The study [23] employed a synthesis between simulative case studies and scientific deduction to explore the intrinsic characteristics of these networks, which differ significantly from conventional district heating systems. A reference concept for prosumer-dominated thermal networks was given, which is the basement for the further analysis developed in the study. The simulation models offered an overview to investigate the behavior of these networks under various operational scenarios, focusing on the switching of prosumers between production and consumption modes. This approach allows for a detailed examination of the thermal dynamics and the impact of prosumer interactions on network performance. The results revealed that the switching behavior of prosumers significantly

influences local temperature variations within the network. For instance, when a prosumer switches from production operation to consumption one, the local temperature in the cold subnetwork rises sharply, while the warm subnetwork experiences a slight increase. This behavior is due to the rapid inversion of mass flow directions and the gradual cooling of inlet temperatures. The complexity of managing thermal energy flows in a network characterized by high variability and interdependence among prosumers emerged from all the presented simulations. The authors concluded that traditional design methodologies for district heating systems are inadequate for prosumer-dominated networks due to their inherent variability. For this reason, the paper identifies several challenges, including the lack of representative design cases, the need for effective cost allocation in thermal markets, and the integration of variable temperatures into market mechanisms.

The experimental study presented in [24] aimed at investigating the challenges faced by experimental facilities to test a DHC system. The methodology integrated commercial hardware with Power Hardware in the Loop (PHIL) simulations, allowing for realistic experimentation without impacting user comfort. The laboratory consists of five thermal and electric prosumer houses connected through an adjustable DHC grid, enabling the emulation of various operational scenarios. The results obtained from the experimental campaign show significant insights into the dynamics of DHC systems. The case studies conducted revealed that prosumer integration into flexible DHC grids can lead to reduced overall heating costs. However, the findings also indicated that simplistic control strategies may not suffice when multiple prosumers are simultaneously feeding into the system. The research highlighted the necessity for intelligent control concepts to manage transfer stations and heat generators effectively, as neglecting temperature and pressure constraints can lead to inaccuracies in system performance. The laboratory's capability to replicate complex phenomena is emphasized, and future scenarios foreseeing tests on the same topics are conceptualized. The paper also outlines the challenge of the use of a PHIL emulator to replicate the thermal dynamics of prosumer houses located at short distances. This system may not fully capture pressure behavior in the thermal network. Additionally, the laboratory's design limits research to 3rd and 4th generation DHC systems, as older systems requiring temperatures above 100 °C cannot be tested.

Dynamic modeling and simulation play a crucial role in understanding the behavior of prosumer-based district heating systems. The studies collected in the group “*Dynamic Modeling, Simulation, and Economic Optimization of Prosumer-Based District Heating Systems*” let to understand the evolution of the dynamic simulation approaches regarding the heat prosumers involved in bi-directional DHNs. These methodologies allow for the analysis of time-dependent interactions between various components of the system, including heat generation, distribution, and consumption. By describing the dynamic nature of energy flows and the influence of external factors such as weather conditions and user demand patterns, dynamic models provide a privileged framework for system performance. Furthermore, they enable the exploration of different operational scenarios, facilitating the identification of optimal strategies for managing energy resources.

Economic optimization is another critical aspect of prosumer-based district heating systems, the discussion is open still now. With the evolution of energy markets and the increasing

penetration of renewable energy sources, the economic viability of district heating systems must be carefully assessed. Optimization techniques can help determine the most cost-effective configurations and operational strategies, considering factors such as capital investment, operational costs, and potential revenue streams from energy sales. A clear economic framework will help the stakeholders contribute to the broader goals of energy transition.

As previously explained, the integration of prosumers into district heating systems presents both opportunities and challenges. On one hand, prosumers can contribute to the decentralization of energy production, reducing reliance on centralized fossil fuel sources and enhancing the overall sustainability of the system. They can also provide flexibility and reliability, as their energy production can be adjusted in response to demand fluctuations. On the other hand, the presence of multiple prosumers introduces complexities in terms of coordination, control, and economic interactions. The operation management of these systems requires innovative concepts that rely on advanced modeling and optimization techniques. In this context, the research presented in this group focuses on dynamic modeling, simulation, and economic optimization of prosumer-based district heating systems. Starting from state-of-the-art methodologies and tools, the studies aim to enhance the understanding of system dynamics, improve operational efficiency, and optimize economic performance. The outcomes of these researches have the potential to give new perspectives and technical instruments to policymakers, energy planners, and industry stakeholders, guiding the development of more sustainable and flexible district heating systems that can effectively integrate prosumers and renewable energy sources.

The paper [25] underlines the transformative potential of prosumers in enhancing the sustainability of district heating systems. The authors developed a model that simulates a ring-shaped DHN serving a cluster of ten residential users in Palermo, Italy. The model incorporated various scenarios, including the presence of prosumers equipped with heat pumps, operated during peak solar hours, to evaluate their effects on energy generation and consumption. The model, implemented in TRNSYS, required inputs such as climate data, pipe specifications, and load descriptions, allowing for flexibility in simulating different operational conditions. The results indicated significant energy savings and reductions in CO_2 emissions when prosumers are integrated into the DHN. Specifically, the study reports a 31.3% reduction in energy produced by the centralized plant and a 17.6% decrease in energy consumed for pumping when prosumers are active. The results also highlighted that the energy required for pumping is reduced by 73% during winter months compared to the base case. The presence of prosumers leads to a more balanced flow rate within the network, resulting in lower pressure drops and enhanced overall efficiency. Finally, the paper acknowledged challenges such as the need for accurate data on user behavior and the variability of renewable energy generation. Additionally, the model's structure may be influenced by the geographical and infrastructural context of the DHN, necessitating further research to optimize the integration of prosumers in different configurations.

The research [26] employed a dynamic simulation approach using the Dymola software, which utilizes the Modelica language for detailed physical modeling. an existing model of a local low-temperature DH grid was updated to include prosumers, specifically data centers

and food retail stores, which have distinct surplus heat characteristics and profiles. A data set of DH demand profiles from modern buildings in Trondheim (Norway) was retrieved, and then, various scenarios were simulated by considering the presence or absence of prosumers and different temperature levels within the DHN. The simulation aimed to assess the energetic and environmental benefits of surplus heat delivery from prosumers. The results showed that the inclusion of prosumers can significantly change the heat supply dynamics within the DH grid. Prosumers were shown to provide sufficient heat to meet local demand during peak production times, particularly in summer, leading to potential flow reversals in the pipeline. The study confirmed that dynamic modeling is effective for simulating small-scale DH grids with decentralized heat supply, highlighting the ability of prosumers to cover substantial portions of the heating demand. The authors underlined that the introduction of seasonal thermal storage could be strategic in shifting the availability of heat surplus to the colder seasons. Finally, the study identifies the need for effective control strategies to manage differential pressure issues that may arise from decentralized heat supply.

In [27] the authors introduced a holistic mathematical model that captured the thermohydraulic steady state of the bi-directional thermal networks, which is crucial for understanding the interactions between control variables and system performance. The developed system of equations integrated balance equations with physical models of network components, including hydraulic actuators and heat transfer mechanisms. The model embedded the nonlinear behavior of pumps and valves, as well as the flexible modes of prosumers. The hydraulic and thermodynamic equation systems, together with the component models, form a set of governing equations for bidirectional prosumer heat networks. This comprehensive approach allowed for the simulation of system states under various control inputs and their assessment to optimize heat exchanges. The model's implementation in Python, available as open-source software, facilitated flexibility in testing different scenarios. The simulation results demonstrated the sensitivity of the thermohydraulic steady state to small changes in control variables. For instance, a minor adjustment in the pump speed at one prosumer significantly alters the power supply dynamics within the network, thus showing the propagation of variation through the other prosumers. The results indicated that the model effectively captures the complex interactions and dependencies among prosumers, highlighting their critical role in the overall system performance. The presented model successfully links high-level energy management with the thermohydraulic conditions at the prosumer level, enabling a more integrated approach to energy distribution. From these outcomes derive the necessity to set a novel model framework that accounts for dynamic behaviors of prosumer thermal grids, especially in the presence of fluctuations due to renewable energy sources.

The paper [28] presented a comprehensive study on optimizing the distribution temperature in heat-prosumer-based district heating systems, emphasizing the integration of renewable energy sources and thermal energy storage (TES). A generalized heating price model based on existing literature from the Scandinavian heating market was formulated, it is represented by four price components: Energy Demand Component (EDC), Load Demand Component (LDC), Flow Demand Component (FDC), and Fixed Component (FXC). Then a dynamic optimization framework was designed to minimize heating costs while considering the

coupling between supply and demand sides of the DH systems. It is applied to a typical heat-prosumer-based DH system, which includes a distributed heat source (DHS) and a short-term TES. The study applied the model to a case study of a campus DH system in Norway, retrieving real operational data to validate the proposed model. The results indicated that the optimal economic distribution temperature significantly influences both energy efficiency and peak load management. While lower distribution temperatures can enhance energy efficiency, careful consideration of peak load impacts is necessary, since it can increase investment and operational costs. The study highlighted that peak load-related components constitute a substantial portion of heating pricing models, with a notable share of 28% on average. The role of heat prosumers is strategic in this model, and their participation allows for a more decentralized approach to DH systems, facilitating the integration of renewable energy sources such as waste heat and solar thermal energy. Furthermore, the results demonstrated that varying storage capacities and renewable fractions (RF) among prosumers can lead to different optimal distribution temperatures, thereby affecting overall system performance and economic viability. Even this study underlines the necessity of deeper knowledge about heat prosumer modeling through more extensive studies to explore the complexities of integrating prosumers into DH systems.

A systematic investigation into optimizing the economic performance of heat prosumers within district heating (DH) systems is presented in [29], concerning the current heating price models. The heat pricing model and the application to a real case study are the same presented in [28]. The study integrated water tank thermal energy storage (WTTES) with varying storage capacities into the DH system. Then, the optimization problem formulated aims to minimize heating costs while maximizing the self-utilization rate of heat generated by prosumers. This is crucial as the current unidirectional heating price models do not incentivize prosumers to supply heat back to the central DH system, thereby limiting their economic benefits. The evaluation of the results is based on the economic indicators arising from the dynamic simulation performed in Dymola environment. Initially, the results indicated that the economic performance of prosumers significantly improves when employing an hourly method to define peak load, as opposed to a daily method. This finding underlined the importance of the precise definition of peak load in contractual agreements, as they directly influence the economic viability of integrating WTTES. The study also highlights that optimal thermocline conditions within the WTTES can enhance performance, suggesting that careful management of thermal storage can yield substantial economic benefits. The introduction of the WTTES into the heat prosumer networks led to the peak load being shaved by up to 39%, and the waste heat self-utilization rate being increased from 79% to 96%. The conclusions emphasized the necessity for further research into the economic feasibility of integrating thermal energy storage systems for prosumers, particularly given the high initial investment costs and long payback periods associated with these technologies. Then, a precise economic configuration and identification for heat prosumer should be done.

In [30] the authors employed a bi-level programming approach to model the interactions between the regional tariff service (upper level) and the district heating system (lower level). The upper level focuses on regulating tariffs for household consumers, aiming to minimize the heat tariff while ensuring the economic balance of the DHS. The lower level optimizes

heat production and distribution based on consumer demand, maximizing profits for heat sources while staying in line with physical and technical constraints. The mathematical formalization included equations that represent the hydraulic network and optimal flow distribution, allowing for a detailed analysis of the system's performance. The model showed how the prosumer’s participation can enhance the efficiency and cost-effectiveness of heat supply. By simulating various scenarios, emerged that involving prosumers leads to a more responsive and adaptive heating system, capable of meeting fluctuating demand while optimizing resource allocation. The integration of prosumers introduces complexities in managing demand and supply, necessitating further research to refine the model and enhance its applicability in real-world scenarios.

A perspective on future DHNs is given in [31]. The methodology employed involves a modular simulation framework (Matlab+Simulink) that allows for the dynamic analysis of energy flows within a 5GDHC network. The model designed a set of different users joined by a closed low-temperature loop that supplies decentralized WSHP. The results obtained from the simulations indicate a promising thermal efficiency of 1.69, highlighting the potential for rational energy use within the network. The model assesses global performance indicators, such as thermal efficiency and electric index, which provide insights into the energy dynamics of the system. The findings suggested that the coupling of diverse users within the network can lead to significant energy savings and improved operational efficiency. In this way, the introduction of prosumer can become interesting for low-temperature thermal grids as the simulated one.

The effects of the bidirectional trade of surplus heat between thermal grids on overall operational efficiency were studied in [32]. The methodology employed an event-based empirical correlation formulation, which allows for the assessment of new operating conditions without the need for extensive additional simulations. This approach enhances the reliability of the results by leveraging actual operational data to derive correlation formulas that reflect the interconnected thermal grid's performance. The simulation results indicated that the activation of bidirectional heat trade can significantly improve operational efficiency and economic performance. Specifically, the analysis revealed that gas engines demonstrate higher performance in terms of energy-saving rate and economic performance if compared to other prime movers, such as gas turbines and combined cycle gas turbines (GTCC). The sensitivity analysis highlighted that fuel prices have a dominant effect on operating profits, with a notable increase in profitability observed when fuel prices decrease, as expected. Additionally, the results showed that operating profits are more sensitive to electricity sales prices than to heat sales prices, underscoring the importance of market conditions in determining economic feasibility. The conclusions drawn from the study emphasize the potential benefits of implementing bidirectional heat trade in thermal grids through prosumers, particularly in enhancing energy efficiency and reducing operational costs.

A theoretical framework for the integration of renewable energy and waste heat in district heating systems is necessary to include various aspects, including energy generation, distribution, storage, and consumption. It provides a structured approach to analyze the performance of district heating systems under different operational scenarios and to

evaluate the impacts of integrating renewable energy and waste heat on system efficiency, reliability, and economic performance. By employing advanced modeling and simulation techniques, the dynamics of these integrated systems can be explored, and optimal configurations are identified to assess the potential benefits of various integration strategies.

Moreover, the theoretical framework supports the identification of potential synergies between renewable energy sources and waste heat recovery. For instance, solar thermal energy can be effectively combined with waste heat from industrial processes to create a more stable and reliable heat supply for district heating systems. This integration not only enhances the overall efficiency of the system but also contributes to the reduction of energy costs and greenhouse gas emissions.

The studies presented in the group named "*Integration of Renewable Energy, Waste Heat, and Theoretical Framework in District Heating Systems*" rely on the integration of renewable energy, waste heat, and the development of a theoretical framework for district heating systems. The group aims to advance the understanding of how these elements can be effectively combined to optimize the performance of district heating networks. The findings of this research have significant implications for policymakers, energy planners, and industry stakeholders, as they seek to design and implement more sustainable and efficient district heating systems.

The paper [33] provided a systematic analysis of the dual role of data centers as both energy consumers and producers (prosumers) within district energy systems. The methodology involved a thorough examination of various studies related to data centers' energy consumption patterns, cooling technologies, and waste heat recovery techniques. The literature works were categorized into a set of operating fields:

- techniques in the data centers' demand response control for increasing renewable energy utilization;
- application of data centers' waste heat for district heating, including the locations for waste heat recovery, the connection architecture, and the connection on both sides;
- projects that consider either upstream renewable energy integration or downstream waste heat reuse in district heating or consider both of them;
- Analysis of the data centers' performance as prosumers in the district energy system from aspects of energy, economy, and environment;
- Identify future research directions, which can help to improve the data center's overall performance as energy prosumers in district energy systems.

The review highlighted successful projects that have implemented renewable energy solutions and waste heat recovery systems, demonstrating the feasibility and benefits of these approaches. Furthermore, the study aimed to emphasize that the role of data centers should shift from net consumer to prosumer, concluding that this concept allows for a more holistic understanding of their role in energy systems, emphasizing the potential for energy trading and enhanced efficiency. The paper also identified several challenges, including the need for advanced control systems to optimize energy use and the variability of renewable energy sources. The integration of prosumers into the model is crucial, as it allows for a dynamic interaction between energy supply and demand, ultimately leading to improved

energy efficiency and reduced emissions. Future research should focus on developing innovative technologies and strategies to enhance the performance of data centers as prosumers.

A detailed investigation into the integration of waste heat into the district heating system at the Forschungszentrum Jülich (FZJ) campus in Germany is presented in [34]. The methodology proposed to extend an existing simulation model in Modelica to consider multiple heat sources, specifically focusing on the integration of waste heat from a newly constructed high-performance computing (HPC) facility. The simulation model implemented an open-loop approach, allowing for the hydraulic decoupling of mass flow inputs and outputs, which simplifies the analytical complexity of the system. The study analyzed a set of waste heat integration scenarios, specifically analyzing shares of 20%, 30%, and 40% of the total heat supply. Additionally, the researchers explored the implications of reducing supply temperatures from the current high temperatures (95-132 °C) to medium temperatures (80-100 °C). This reduction is significant as it can lead to lower heat losses and improved efficiency in heat pump operations. The results indicated that integrating up to 40% waste heat is feasible without compromising the operational integrity of the district heating network. Keeping the design return temperature at 65 °C is crucial for the operational constraints of the combined heat and power (CHP) units. The inclusion of prosumers into the model is addressed, emphasizing their role in providing additional flexibility and resilience to the heating network. Prosumers can contribute to the heat supply, thus influencing the overall heat ratio and operational dynamics of the system.

A systematic review of Photovoltaic Thermal District Heating (PVT DH) was performed in [35], The methodology followed the PRISMA (Preferred Reporting Items for Systematic Reviews and Meta-Analyses) principles, systematically reviewing records through a three-phase process. PVT DH systems can ensure higher performances than conventional solar technologies by leveraging the cooling effect of thermal output on PV cells, which enhances their electrical efficiency. Furthermore, the overall system performances are enhanced by the synergistic relationship between PVT systems and heat pumps, where the thermal output from PVT can significantly reduce the electricity consumption of heat pumps. Due to lower operating temperatures if compared to traditional solar collectors and vacuum ones, PVT technology could play a crucial role in the transition towards fourth-generation district heating (4GDH), particularly in urban settings where space is limited. In addition to PVT-assisted heat pump district heating systems, there are many other configurations of the various PVT types with a range of electrical and thermal storage, which are open for research and demonstrations in different applications. The conclusions identified several drivers for the development of PTH DH: progression towards 4th generation district heating, solar technology and storage technological advancement and cost reduction, mutual system performance improvement with heat pumps, and green legislation/policies. The critical analysis identified a gap in knowledge regarding the optimization of PVT array performance and the integration of thermal storage solutions. It underscored the importance of maintaining low temperatures in PVT systems to prevent electrical efficiency degradation, which poses a challenge for effective system design and operation.

A theoretical mathematical model for 4th generation bidirectional thermal grids is presented in [36]. A bottom-up approach was adopted to develop a dynamical model of an Ectogrid-type heat network. This model is constructed by applying physical laws to individual components, which are then interconnected to form a network capable of energy sharing among users. The model incorporated heat pumps to facilitate the transfer of excess energy from one user to another, thereby enhancing the overall efficiency of the system. The authors also established existing conditions for stable steady states within the network, utilizing convex optimization techniques to derive energy-optimal configurations. The results showed that the proposed model allows for the balancing of heat production and consumption, which can temporarily eliminate the need for a centralized heating plant. This flexibility is particularly beneficial in scenarios where energy demand fluctuates. The results demonstrated that the integration of prosumers into the heat network not only stabilizes the system but also optimizes energy distribution, leading to reduced waste and improved efficiency. The variability in energy production from prosumers can lead to local fluctuations that may complicate the overall stability of the network. Additionally, the need for advanced control strategies to manage these fluctuations is highlighted as a critical area for future research.

An analysis of the effects of supplying failure and reliability of prosumers in DH systems is given in [37]. The research relied on mathematical modeling that describes both system state analysis (Markov model) and flow distribution. The methodology included the use of nodal reliability indices, which allow for a detailed assessment of the reliability of heat supply to individual consumers. The Markov processes are implemented to analyze the dynamics of system failures and repairs. The approach distinguished between passive time redundancy, resulting from heat accumulation and thermal energy storage, and active time redundancy, provided by additional heating sources owned by the prosumer. This dual consideration enabled a comprehensive evaluation of how prosumers can mitigate heat supply vacancies during system failures. Results showed that optimizing the time redundancy of prosumers can lead to a significant reduction in heat undersupply during failure states. The study demonstrated that prosumers, by utilizing their own heating sources and storage capabilities, can mitigate the load on centralized heating systems, thereby improving the overall reliability of the DHS. In this way, joint optimization of prosumer time redundancy and system component restoration rates can yield cost-effective solutions that enhance the reliability of both the prosumer and the overall heating system. The proposed methods are applicable to real-world scenarios, considering the unique characteristics of actual DHS.

A methodology for ensuring the reliability of heat supply in a thermal prosumer network is presented in [38]. A Markov model was developed to describe the random functioning of the system over time, allowing for the analysis of potential failures in both the district heating system and its components. Then, a flow distribution model from hydraulic circuit theory, and nodal reliability indices, was structured to analyze the system's performance. The methodology focuses on optimizing the reliability parameters of system components, such as failure and restoration rates, while considering the heat capacity and redundancy provided by the prosumer's heat source: The results indicated that adjusting the prosumer's heat capacity to 67% of its heat load, the system can achieve a higher level of reliability,

reflected in a failure-free operation probability (FOP) of 0.92. The sensitivity analysis showed that this configuration leads to a total cost of 1.95 M$ for ensuring reliability; conversely, a slightly lower reliability level (FOP of 0.90) reduces costs to 1.51 million, demonstrating a clear trade-off between reliability and economic expenditure. The study demonstrated that the integration of prosumers significantly enhances the reliability of heat supply in DHS. By utilizing their own heat sources, prosumers can provide additional capacity and redundancy, thereby reducing the overall load on centralized heating sources and improving service quality for all consumers. The need for accurate modeling of failure rates and the complexities involved in integrating prosumers into existing DHS frameworks emerges in conclusions.

The topic of reliability is analyzed thereby in the study [39]. The research employed a mathematical modeling framework that incorporates reliability analysis and optimization techniques. Markov random processes are implemented to model the reliability parameters of system components, including failure and restoration rates. The integrated reliability parameter is a key concept, representing the overall reliability of the system based on individual component performance. The methodology also included the analysis of nodal reliability indices, which assess the reliability of heat supply at various points in the network. The mathematical model is validated through a case study. The results indicate that the optimal operation of prosumers' heat sources (HS) can significantly enhance the reliability of heat supply. The study revealed that prosumers should ideally cover 60-80% of their thermal energy load with their own HS, which not only reduces the load on district sources but also provides a buffer during emergencies. The results demonstrated that integrating prosumers leads to a decrease in the overall failure rates of the system, thereby improving reliability for all consumers, including those without their own HS. Future research directions should include exploring structural redundancy in heat networks and the integration of energy storage solutions to further enhance reliability.

1.3. Motivation of the research

From the literature analysis emerges the common need to deepen the knowledge about prosumer integration in DHC networks. Some key aspects were identified:

- several studies investigate DHNs from a systemic point of view, by considering the general aspects and its global operation and performances. All the papers underline the necessity to focus on single components to create a more complex theoretical and modeling framework;
- although the concept of the thermal prosumer is introduced in the academic field, it should be characterized by investigating its technical configuration;
- the prosumers should be characterized under the dynamic behavior within a DHCN, by exploring opportunities and challenges from the technical and economic points of view;
- a clear statement of factors that can affect the inclusion of prosumers within a DHCN (availability of excess heat, temperature alignment with DHCN requirements, economic viability to produce heat locally for self-consumption and/or for selling to the grid).

From the previous analysis, the motivation for this research arises from the urgent need to address critical gaps in the understanding and implementation of prosumer integration within District Heating and Cooling Networks. As energy systems evolve towards decentralized and participatory models, the role of prosumers will be more and more relevant. Despite the growing academic focus on DHCNs, several unresolved challenges persist, particularly regarding the inclusion and effective operation of thermal prosumers in these networks.

From a technical perspective, the literature highlights a systemic approach to DHCNs, often focusing on general operations and overall network performance. The studies rely on a global and systemic point of view and often don’t deepen the knowledge of the heart of the bidirectional exchange of prosumers. Precisely, the integration of prosumers demands a granular understanding of their specific technical configurations, dynamic behavior, and interaction with the network. Factors such as the availability of excess heat, temperature alignment with network requirements, and the technical feasibility of locally producing and distributing heat remain inadequately characterized and need a focus. To build robust and efficient networks, it is essential to shift focus towards the characterization of individual prosumers and their dynamic contributions to the energy balance and hydraulic performance of DHCNs.

The present research work will try to answer these open issues by proposing a novel modeling framework, based on experimental data, that was tested to be extremely flexible to several approach studies: from approaches that focus more on technical issues (energy balances, temperature levels, hydraulic characterization) to ones that shift on economic considerations.

Economic viability is another critical dimension driving this research. Prosumers must navigate challenges such as balancing self-consumption with opportunities to sell surplus energy to the grid. Economic considerations include the cost-effectiveness of technologies required for prosumer participation, financial incentives for decentralized energy production,

and the long-term sustainability of participatory energy models. By developing a flexible modeling framework, this research seeks to evaluate the economic implications of various integration strategies, enabling the identification of cost-effective pathways for prosumer inclusion. The economic and administrative relationships with DHN dealers are decisive in understanding how a third party can be included in existing markets. This understanding is crucial for promoting financial accessibility and ensuring that the economic benefits of thermal energy communities are equitably distributed.

The emergence of thermal energy communities introduces a novel participatory model that redefines the traditional producer-consumer relationship in energy systems. As happened with electrical energy communities, beyond technical and economic aspects, these communities offer profound social implications by fostering local collaboration, enhancing energy democracy, and promoting sustainable practices. However, their success depends on overcoming significant barriers, such as the lack of standardized frameworks, public awareness, and user engagement. By addressing the factors influencing prosumer integration, this research contributes to creating inclusive energy models that empower individuals and communities, bridging the gap between technological innovation and societal adoption.

This research aims to provide a comprehensive overview of these multidimensional challenges by developing a novel, data-driven modeling framework. Grounded in experimental data, the proposed framework is designed to be versatile, enabling both technical analyses (e.g., energy balances, temperature optimization, and hydraulic characterization) and economic evaluations. Additionally, it offers insights into the social potential of thermal energy communities by exploring how technical and economic optimizations can align with broader societal goals.

Ultimately, this work seeks to advance the integration of prosumers in DHCNs by addressing the intertwined technical, economic, and social aspects of these participatory models. In doing so, it not only contributes to the academic understanding of decentralized energy systems but also provides practical tools and strategies to facilitate the transition toward sustainable, inclusive, and resilient energy communities.

2. District Heating and Cooling Capacity Expansion Analysis

District heating and cooling (DHC) systems are vital parts of today's urban energy infrastructure, providing centralized heating and cooling solutions for homes, businesses, and industries. These systems distribute heat, typically in the form of hot water or steam, through a network of insulated pipes, and they also offer cooling through chilled water systems. As urban areas expand and energy demands grow, the idea of "capacity expansion" becomes increasingly important. This ensures that DHC systems can meet future energy needs while addressing environmental and economic concerns.

Capacity expansion involves increasing a DHC system's ability to produce and distribute more thermal energy to meet rising demand. This can be achieved through various strategies, such as building new heat generation facilities, extending existing networks, integrating renewable energy sources, and improving energy efficiency. The main objectives of capacity expansion are not only to meet both current and future energy demands but also to strengthen the resilience and sustainability of the energy supply. Various factors, such as population growth, urbanization, technological advancements, and policies aimed at reducing carbon emissions, influence how capacity expansion is approached in DHC systems. Research shows that expanding district heating networks can bring significant benefits, such as lower energy costs, improved air quality, and better energy security. However, it's essential to evaluate the economic feasibility of these expansions to ensure they are affordable for consumers and don't lead to higher costs.

The planning methodologies for capacity expansion can vary relevantly. Some studies use a top-down approach, relying on aggregated data to create large-scale heat maps that guide regional or national expansion strategies. This approach helps planners understand heat demand patterns and potential supply sources, enabling more strategic planning. On the other hand, a bottom-up approach involves detailed analyses of specific areas, offering a closer look at local heat demands and supply options. This method often uses advanced modeling techniques to simulate how DHC systems would perform under different scenarios, helping planners identify the best strategies that balance economic, environmental, and technical factors.

Economic feasibility is a key consideration in capacity expansion for DHC systems. Economic analysis can be divided into socio-economic and consumer-economic perspectives. Socio-economic analyses consider the broader societal benefits of district heating expansion, such as reducing greenhouse gas emissions and improving public health. In contrast, consumer-economic analyses focus on the direct costs and benefits to end-users, including the impact of taxes and subsidies on heating costs.

Despite the advantages of expanding DHC systems, several challenges must be addressed. Technical challenges, such as the need for infrastructure upgrades and integrating new technologies, can complicate expansion efforts. Financial constraints and the need for significant upfront investments can also discourage stakeholders from moving forward with expansion projects.

Furthermore, social acceptance and regulatory frameworks are crucial for the success of capacity expansion initiatives. Building support among communities and stakeholders is

essential for overcoming resistance and ensuring successful project implementation. Policymakers must also create favorable regulatory environments that encourage investment in DHC systems and support the integration of renewable energy sources.

A recent review [40] provided a comprehensive analysis of the methodologies and strategies necessary for the effective planning and design of district heating (DH) systems, particularly in countries where DH has not yet gained significant diffusion. The review is organized into several sections, addressing critical aspects such as the identification of DH potentials, heat demand prediction methodologies, integration of sustainable heat sources, and optimal planning techniques. The authors highlighted the necessity of developing a high-quality heat atlas, which serves as a geospatial representation of heating and cooling demands alongside potential supply sources. This atlas is considered essential for effective DH planning, particularly in areas where existing data is scarcely available. The review showed various methodologies for predicting thermal energy demand and integrating sustainable resources into DH systems. The authors discuss the technical barriers that hinder the implementation of these sustainable heat sources, such as economic feasibility and infrastructural limitations. They also explore innovative configurations and upgrading measures for existing DH systems, which can enhance efficiency and reduce carbon emissions.

The research studies that include the concept of “capacity expansion” related to the DHC technologies were grouped by the adopted methodology and main purpose of the study, to carry on a critical review of the main aspects belonging to the aforementioned concept and to investigate the future perspectives of DHC.

Table 5: Group of papers based on DHC expansion potential analysis

Name of the group	General purpose	References
Techno-Economic Analysis and Optimization of District Heating Systems	To analyze and optimize the economic and technical aspects of district heating systems.	[41], [42], [43], [44], [45], [46], [47]
Topological optimization Feasibility Studies	To assess the potential for expansion of district heating networks within a defined area and conduct feasibility studies.	[48], [49], [50], [51], [52], [53], [54], [55]
Modeling and Simulation Approaches	To develop models for simulating and analyzing district heating capacity expansion	[56], [57], [58], [59], [60], [61], [62] [63],

The group named “*Techno-Economic Analysis and Optimization of District Heating Systems*” encompasses a collection of research papers that delve into the intricate relationship between technological advancements and economic viability in the context of district heating (DH) systems. This group of studies collectively emphasizes the importance of optimizing

district heating networks to enhance their efficiency, reduce carbon emissions, and ensure economic feasibility, particularly in the face of evolving energy markets and sustainability goals. The common thread among these papers is the application of multi-objective optimization techniques to evaluate and improve the performance of district heating systems. Each study addresses the emerging need for a transition towards low-carbon energy solutions, highlighting the role of district heating as a crucial component in achieving decarbonization targets. The authors explore various methodologies for techno-economic analysis, focusing on the integration of renewable energy sources, cogeneration units, and innovative technologies that can enhance the operational efficiency of DH systems.

One of the key themes is the assessment of district heating potentials and the identification of optimal expansion strategies. Then, the studies investigate the feasibility of expanding existing networks or implementing new systems, considering factors such as heat demand predictions, energy market prices, and the integration of sustainable heat sources. Another element that is underlined among all studies is the necessity of developing comprehensive heat atlases and employing advanced modeling techniques to accurately predict thermal energy demands and optimize resource allocation. Moreover, the papers highlight the significance of cost and carbon allocation methods in cogeneration units, which are pivotal for understanding the economic implications of district heating systems. By employing multi-objective optimization approaches, the authors aim to minimize total costs while maximizing exergy efficiency and reducing environmental impacts. This dual focus on economic and environmental performance is essential for ensuring the long-term sustainability of district heating networks.

The researches finally address the challenges associated with the implementation of low-temperature district heating systems, which are increasingly recognized for their potential to utilize a wider range of heat sources, including waste heat, geothermal energy, and solar thermal energy. The optimization of these systems is crucial for enhancing their competitiveness against individual heating solutions, particularly in regions where natural gas prices are low.

In [41] the authors developed a model that focuses on minimizing total costs and carbon emissions while maximizing exergy efficiency. It is capable of optimizing supply capacities, including thermal storage, and managing the system's hourly operations throughout the entire year. The allocation method translated the power loss resulting from heat production into the operational costs and carbon emissions of the combined heat and power (CHP) system, which are then assigned to heat production. The model was applied to a DHN case study located in Northern Croatia, with a continental climate. The DHN solution is considered more convenient than a single-user one when it shows a lower carbon factor and levelized cost of heat (LCOH). Without heat allocation methods, no district heating solutions outperformed individual heating when natural gas prices for households are low. However, when cost allocation is applied, some Pareto solutions show better performances than individual natural gas heating, although those with the highest exergy efficiency do not. Finally, regarding the district cooling, a small increase in specific costs allows for the inclusion of cooling energy production within the district heating system. This integration can enhance the overall efficiency and utility of the system, providing additional benefits such as

improved resource exploitation and potentially lower operational costs in long-term perspectives. The presented work represents a viable methodology to assess the feasibility of DHC technologies, but a systematic comparison with individual heating solutions is still needed. Furthermore, the barriers related to retrieving monitoring data and the computational intensity of the multi-objective optimization process may limit practical applicability in real-world scenarios.

In [42] a systematic approach that integrates clustering techniques for heat and cooling (H&C) load analysis with techno-economic modeling is proposed. Utilizing the free database released within Hotmaps project [64], H&C load data were aggregated into hectare-sized cells, which were then clustered based on the capacity of available Neutral-Temperature District Heating and Cooling (NT-DHC) heat sources, typically less than 1 MW. The clustering process was executed by testing various algorithms (K-Means, Spectral Clustering, and Gaussian mixture methods). Finally, the Spectral Clustering method was selected since it provided satisfactory results in terms of producing more evenly sized clusters compared to other algorithms. The Persson method [65] was adopted as a geometrical optimization algorithm for DHC pipeline length and distribution, the techno-economic analysis relies on Net Present Value (NPV) maximization. The results indicated that NT-DHC systems are particularly advantageous in densely populated urban areas, where they can outperform individual heating and cooling solutions. The model's validation through the demo case (Ospitaletto case study, Italy) showed its applicability across different scenarios, yielding accurate estimates of energy metrics and network costs. The authors underlined that even with simplified inputs, the model can be executed rapidly, making it a practical tool for feasibility-stage planning. Despite its strengths, the paper acknowledges certain challenges, such as the need for further research in areas with varying heat densities and climatic conditions. Additionally, the integration of energy storage solutions and the comparison with other district heating models, like 4GDH, are suggested as paths for future exploration.

In [43] a comprehensive analysis of the optimization strategies for expanding district heating networks (DHNs), focusing on the design and operation of energy centers, is presented. A mixed-integer linear programming (MILP) approach was adopted to develop a methodology that identifies the optimal investment schedule for marginal DHN extensions. This methodology integrates the spatial network extension, selection of technologies, their phasing, and operational optimization, thereby addressing both cost savings and greenhouse gas (GHG) emissions reduction. Model inputs included aggregated heat demand, hydraulic connection, pipe extension, and the techno-economic features of various heat sources, including thermal storage. The model can be applied to existing network capacities and realistic connection scenarios, which are crucial for effective planning. The authors underlined the importance of stakeholder engagement in determining connection strategies, which significantly influence the overall performance of the energy center. A real DHN was adopted as a case study, the results show that cost optimization models indicate the installation of combined heat and power (CHP) units, with biomass boilers being added later. The findings implied that anticipating capacity expansion and oversizing heat production can lead to higher revenue and operational flexibility. Conversely, when the objective function is the minimization of GHG emissions, the results indicate the installation

of technologies that are less reliant on fossil fuels, such as biomass boilers and heat pumps, particularly as the carbon intensity of the electricity grid decreases over time. The approach selected to connect the heat clusters significantly affects both the selection of plants and the operational strategy of the energy center. While subsidies can influence technology selection, careful analysis of electricity export rates will be essential for informed decision-making.

The study presented in [44] shows an interesting application of the MANGO (Multi-stage Energy Optimization) and MANGOret models, which are designed to optimize energy systems and retrofitting strategies. The model performs a multi-stage and multi-objective optimization (cost vs. CO_2) to determine a long-term retrofitting and energy system investment strategy at the district level considering a building-level resolution. The authors proposed an extension of the MANGO model with additional constraints specifically related to network development and operation to depict the expansion and utilization of district heating. The representation of the DHN expansion and building connection is based on the transshipment problem. This approach reproduced the energy flow as a good that can reach its destination through multiple itineraries. Specifically, the transshipment problem is applied for the modeling of energy distribution across different sites, ensuring that the connections between buildings and the DHN are efficiently managed. In the presented research, two binary variables were utilized: one to indicate if a site is connected to another one and another to determine if a site is connected to the DHN. The proposed framework was applied to two case studies in Chur, Switzerland: a dense inner-city neighborhood and a typical residential one. The results showed that in the inner-city district, DH reduces both total system costs and emissions thanks to the integration with a low-emission DH supply ensured by the installation of Carbon Capture Storage technology. On the other hand, in the residential neighborhood, decentralized heating systems offer the best cost versus emission trade-offs. Since in the actual economic models the costs are unequally distributed between the DHN operator, the building owners, and the tenants, future studies should reflect on a novel perspective regarding the cost distribution. Further studies are needed to understand the distributional effects that various scenarios and Pareto points have on the three stakeholders, as well as how to achieve a fair distribution of costs. Incorporating this perspective on cost distribution will enhance the model's value by aiding in the identification of politically viable solutions that balance costs and emissions trade-offs at the district level. The study provides valuable insights into the complexity of urban energy planning and the critical role of integrated approaches in achieving sustainability goals.

The paper [45] presented the development of a MILP model that supports endogenous decision-making about investments in the connecting between different DH systems. This model was a significant advancement over previous frameworks, as it enhanced the automation of connecting piping design and incorporates a differentiated range of technologies, including gas combined heat and power (CHP) plants, electric boilers, heat pumps, and thermal energy storage systems. CHP lets model the sector coupling between power and heat sectors from the technical and economic point of view, thus providing a reliable tool for assessing the feasibility and benefits of DH expansion. The authors assessed the parameters and variables used in the model, including operational and maintenance costs, fuel costs, CO_2 emissions, and revenues from electricity sales (CHP).

The objective function was set to minimize the overall socio-economic costs of the system. This included the annualized investment costs, both fixed and variable operating and maintenance (O&M) costs, unit start-up expenses, carbon and fuel costs, along with the annualized sunk costs related to the investment decision for constructing the piping connection. By employing a binary decision-making process, the model evaluated the economic viability of investments in interconnectors, enabling a nuanced analysis of the trade-offs involved in expanding DH networks. The model was applied to the case of the City of Zagreb and the two adjacent smaller cities. The results revealed that the interconnection of DH systems can lead to substantial economic benefits, quantified in a remarkable 29.2% reduction. The findings indicated that, in scenarios where interconnectors are allowed, the dependence on electric boilers decreased significantly, while the utilization of cogeneration units increases. This change not only enhances the profitability of the DH systems but also contributes to a reduction in CO_2 emissions, thus aligning the urban strategies with the broader European sustainable frameworks. On the other hand, when allowed by the model constraints, the optimal solution was to install both heat pumps and electric boilers across all three geographic areas in the absence of interconnectors. In this scenario, electric boilers addressed peak demand, while heat pumps satisfied a substantial portion of the overall heat demand. Moreover, the study underlined the transition from tree-like structures of DH systems to more efficient ring-shaped or meshed configurations, which improved heat transfer capacity and reduced the risk of supply failures due to pipeline technical issues. This structural evolution is crucial for enhancing the resilience and reliability of DH networks, particularly in urban agglomerations.

The paper titled [46] tried to give a pathway for exploring the possible solutions to the debates on whether DHN must be expanded or partially decommissioned to sustain profitability in the future. An enhanced mixed-integer linear programming (MILP) open-source model was adopted to assess the techno-economic results of various transformation scenarios. This model was specifically designed to optimize the network topology by balancing infrastructure costs, thermal and hydraulic losses, and revenue from heat sales (by the DHN manager, not by prosumers). A myopic optimization approach was employed, dividing the planning horizon into smaller time segments. This lets the model adapt dynamically to variable conditions, as it didn’t consider the future parameters during optimization. The model incorporated several transformation-related target states, including reductions in supply and return temperatures and potential post-densification strategies. The depicted model was applied to a real case DHN, installed in a larger city in the center of the German state of Baden Württemberg. The results showed that without setting clear transformation targets, the reduction in heat demand densities leads to an unavoidable network expansion to stay profitable. The study identified six distinct transformation scenarios, each varying in post-densification potentials and temperature reduction targets. The results underscored the necessity of strategic planning to avoid unnecessary expansion and to optimize existing infrastructure. Furthermore, network expansions can be significantly reduced or completely avoided by both utilizing post-densification potentials within the existing DHN and by moderate reductions of supply and return temperatures. The paper highlights also several challenges, including the limited existing literature on comprehensive transformations of DHNs and the complexities associated with predicting future heat

demand. The authors underlined that static optimization methods prevalent in current research do not adequately address the dynamic nature of DHN transformations. They push for more robust methodologies that can incorporate uncertainties and provide reliable insights for network operators facing the transition to low-temperature systems.

The liberalization of energy markets requires the Generation Expansion Potential (GEP) problem to be studied as a price-based and decentralized decision-making process. In the paper [47] a market-based approach that enhances the interaction between generation companies (GENCOs) and district heating system operators (DHSCOs) is employed, facilitating a more efficient allocation of resources. The methodology relies on a two-loop iterative algorithm that combines a price loop and Bender's decomposition loop. The price loop facilitates the calculation of locational marginal prices (LMPs) based on the operational status of generating units, which are then used to inform the expansion plans of GENCOs and DHSCOs. The Benders decomposition technique is implemented to manage the complexity of the optimization problem, allowing for a more tractable solution process. A fuzzy load duration curve (FLDC) model is introduced to represent the temporal variations in load more accurately, utilizing clustering techniques to condense 8760 hourly load values into a manageable number of states. The results showed the effectiveness of the proposed method in achieving a balanced and economically viable expansion plan over a 10-year horizon. The integration of fuzzy logic in load modeling significantly enhances the accuracy of demand representation, leading to more reliable LMP calculations. The case study based on the modified IEEE 30-bus system illustrates the framework's capability to optimize investments while considering the operational constraints of both power and heating systems. Coupling power and heat systems is a key to understanding the complexity of the supply market. Finally, the authors suggested that future research should focus on enhancing the prediction methods for load and renewable energy variations and developing more detailed load-shedding cost models to improve the accuracy of LMPs.

The group named “*Topological Optimization Feasibility Studies*” collects a selection of research papers that explore the viability and potential for expanding DHC systems in various urban contexts. One of the leading arguments of these studies is the focus on assessing the capacity for growth within existing DHC networks while evaluating the economic, technical, and environmental implications of such expansions. Each paper contributes to a better understanding of how DHC systems can be adapted to increasing energy demands, the increasing need to integrate renewable energy sources, and enhance sustainability in urban environments.

The papers in this group look at the DHC expansion potential from a different point of view than group 1. They examine factors such as population growth, urbanization, and technological advancements that drive the need for enhanced thermal energy supply. By employing both top-down and bottom-up approaches, the studies provide comprehensive insights into heat demand patterns and the feasibility of integrating new heat generation facilities, as well as the expansion of existing networks. This dual perspective allows for a novel analysis of local and regional energy needs, enabling planners and policymakers to make supported decisions regarding DHC system expansions.

A significant focus of the research is on the economic feasibility of expanding DHC networks by implementing GIS-based models and tools. The studies differentiate between socio-economic and consumer-economic analyses, highlighting the broader societal benefits of district heating expansion, such as reduced greenhouse gas emissions and improved public health outcomes, alongside the direct costs and benefits experienced by end-users. This articulate evaluation ensures that the proposed expansions are not only technically feasible but also economically sustainable for consumers, thus fostering greater acceptance and support for DHC initiatives.

Finally, the papers address the challenges and barriers associated with capacity expansion in DHC systems. Technical obstacles, such as the need for infrastructure upgrades and the integration of innovative technologies, are discussed alongside financial constraints that may hinder investment in expansion projects. The importance of social acceptance and regulatory frameworks is also stressed, as engaging with communities and stakeholders is crucial for defeating resistance and ensuring the successful implementation of DHC projects.

The study proposed in [48] proposed a spatial analysis using GIS tools, specifically ArcMap 10.2, to locate existing district heating zones and identify areas currently lacking such infrastructure. Publicly available spatial data, including the Danish Heat Atlas, are implemented to calculate heating demand and the number of buildings in these zones. The analysis categorized urban areas based on their heating supply status, allowing for a clear understanding of where district heating could be feasibly expanded. Following this, an economic analysis is conducted, comparing the socio-economic costs of district heating with consumer-economic considerations, which include the financial implications for households. The cost of heat attributed to customers belonging to the expanded DHN line is considered the same as for the existing customers in the nearest district heating network, although the marginal cost may be higher than the present average cost. The spatial analysis assessed the distance to the nearest district heating network for each of the urban zones outside the district heating zones actually served. In the economic analysis, it is assumed that the nearest district heating zone is the one that the urban zone can potentially connect to. The results indicated a socio-economic potential for expanding district heating to cover 13% of Denmark's total heat demand, while the consumer-economic potential is slightly lower at 9%. It is worth noticing that only 6% of the expansion potential overlaps between the two approaches. This discrepancy is attributed to the favorable taxation conditions on biomass, which make it a more attractive option for consumers despite its lower socio-economic viability. While the socio-economic approach guided long-term investment decisions, consumer-economic ones are crucial for evaluating the feasibility of these investments under current market conditions. It’s evident how political decisions regarding taxation and subsidies significantly influence these dynamics and, secondarily, indirect effects such as impacts on GDP and employment that were not included in the analysis.

The paper reported in [49] employed a GIS-based model to assess the technical feasibility of expanding the existing DH infrastructure, which is crucial for enhancing energy efficiency in urban contexts. A fluid-dynamic network model was implemented to simulate the mass flow rates within the DH system, considering various technical limitations such as geographical barriers (e.g., the Po River) and the integration with existing building heating

systems. The analysis of the case reported a detailed assessment of the current DH network, which supplies approximately 55% of the heat demand in Turin. The study categorized buildings into residential, public, commercial, and industrial types, calculating the volumes connected to the DH network and identifying those that are potentially connectable. The model is validated using energy consumption data from the DH company, ensuring accuracy in the projections. The results indicated a significant technical potential for expanding the DH network: up to 20% of connectable users can be integrated without necessitating changes to the existing pipeline infrastructure. The short-term expansion can cover the consumers that are more easily connectable, while long-term scenarios may require investments for new pipelines to accommodate a broader range of users. The study highlighted the importance of optimizing energy demand across different user types to enhance the sustainability of the DH system. One of the most relevant challenges is the need for gradual retrofitting of buildings which can lead to potential resistance from users with individual heating systems. The authors suggested that future research should explore innovative solutions, such as distributed thermal storage units, to further enhance the network's efficiency and resilience.

The work proposed in [50] presents a systematic analysis of district heating systems, focusing on their potential to transition towards renewable energy sources. The authors adopted a methodology that includes both the development of a heat atlas and a district heating expansion model, which are essential for assessing the feasibility and efficiency of future scenarios. The creation of a heat atlas, utilizing data from Denmark's national building register, foresees to acquire detailed information about building properties, energy supply types, and energy demand. This data is complemented by the FIE database (Danish Supply Companies Reporting Model for Energy Consumption), which collects energy demand data from various suppliers. The periodic update of this database is considered strategic by the authors since it is projected to cover approximately 80% of heated buildings in Denmark once fully implemented. This comprehensive data collection composed the main structure of the analysis, allowing for a deep understanding of heat demand across different building types. Also in this work, a GIS analysis was implemented to build a DH expansion model, and the methodology was applied to a study case of the Northern Denmark Region. The model included three scenarios: the first is a reference case with standard temperatures and heat demand, the second considers heat savings, and the third considers heat savings in combination with low-temperature district heating. The key findings indicated that the potential for district heating is greatest in the standard scenario that does not incorporate any heat savings. When heat savings are implemented, the feasibility of expanding district heating systems generally diminishes due to increased costs. Although the adoption of low-temperature district heating slightly enhances the expansion potential by lowering overall costs compared to scenarios with standard temperatures and heat savings, these savings are insufficient to render the expansion potential as viable as in the standard scenario without heat savings. Furthermore, the sensitivity analysis revealed that while the standard scenario maintains the highest number of buildings with prices below 200 €/MWh, the low-temperature scenario shows potential for buildings priced below 150 €/MWh. This suggests that integrating low-temperature operations can enhance the economic viability of district heating systems. The conclusions drawn from the study highlight the critical balance

between heat supply and demand, promoting strategies that prioritize heat savings alongside supply improvements.

The paper [51] presented a comprehensive methodology aimed at optimizing the connection of additional buildings to existing large district heating (DH) networks, with a focus on minimizing pumping costs and reducing CO_2 emissions. The methodology integrated three steps: firstly, the data collection on building positions and heating demands performed by a Geographic Information System (GIS) tool, then the technical assessment of flow constraints performed by a fluid-dynamic model, and, finally, setting the pump strategies through the optimization algorithm. The approach began with the GIS tool, which identifies potential buildings that can be connected to the DH system based on their thermal demand and location close to existing infrastructure. This step is crucial as it lets to make a precise analysis of urban areas where additional connections can be made without relevant investment in new pipelines. The fluid-dynamic model simulated hydraulic behavior within the network, accounting for existing pumping stations and their operational constraints. This step is essential for recognizing how increased connections will affect pressure and flow rates throughout the system. Results from applying this methodology to the Turin district heating network (one of the largest in Italy) indicated that approximately 26% more buildings can be connected with minimal investment costs. This strategy achieved a significant reduction in CO_2 emissions, exceeding 13%, thereby enhancing the environmental benefits of the DH system. The study highlighted the importance of optimizing existing resources rather than incurring additional costs for infrastructure development. A relevant issue underlined by the results refers to the management of the thermal grid and is regarded as the optimal management of pressure and flow rates to prevent system overloads. The authors suggested that further research could explore the relaxation of constraints on pumping stations to improve results even more.

A comprehensive assessment of the potential for district heating in Italy is presented in [52]. The primary objective was to identify areas where DH can be economically feasible compared to individual heating systems, facilitating the transition to renewable-based DH solutions. The methodology employed a five-step framework designed to estimate the potential diffusion of DH at a large scale. The analysis started by mapping heat demand (step 1) from residential and tertiary buildings at a granular level, utilizing census data to ensure high spatial resolution. Based on the resulting map, The available heat sources were clustered (step 2), and the heat sources were mapped (step 3), then, a virtual energy graph was built, connecting demand and supply points through triangulation and routing algorithms (step 4). At the end, (step 5) the optimization algorithm indicated what are the optimal heat demand clusters and heat sources to be connected and how. The core of the methodology relied on a linear programming optimization model developed using the open-source framework “oemof”, which optimizes heat flows to minimize overall delivery costs. This approach allows for a detailed simulation of network topology, addressing a significant gap in existing literature that often relies on threshold values and empirical equations. The elaborated methodology is applied to the case of the Italian territory to estimate the potential of RES and WH (Waste Heat) based district heating at the national level. The results indicated an interesting potential for DH in Italy, with an estimated capacity of 38 TWh, which could meet approximately 12% of the civil sector's heat demand. This potential is positioned

within a broader context, comparing it with other studies that suggest varying estimates of DH market share and heat demand. The results demonstrated robustness, aligning with recent European assessments while highlighting a higher expansion margin than previously reported national forecast. The aim proposed by the authors is to extend the range of considered heat sources, by considering heat recovery from water basins through heat pumps, to improve the estimation of solar thermal potential starting from space availability and solar irradiation, and to improve the backup technology modeling. Overall, the paper contributes significantly to the discourse on sustainable energy solutions, providing a framework for future studies in district heating optimization and a reliable instrument for energy planners, local authorities, DH operators, and policymakers.

The necessity of developing effective urban planning tools to achieve sustainable energy targets is underlined in [53]. The study adopted a GIS-based model to assess energy consumption in residential buildings and optimize district heating networks and is focused on the retrofit of buildings and the refurbishment of the district heating network in the “Centro Residenziale Europa” area of Turin (CRE). The methodology process started with the collection of Base Year (2010) data, including GDP, population, floor area, and energy use. The geographic information systems were used to geo-reference buildings and district heating networks, thus creating a detailed GIS database that characterizes the building stock and existing energy infrastructure. Then, a thermal model was applied to calculate the heating and DHW energy demands for each building. This bottom-up approach allowed for the simulation of several energy scenarios, considering supplying different energy sources (natural gas, electricity, and district heating vectors). A synthetic indicator, based on socio-economic factors, was elaborated to evaluate the feasibility of renovation works in residential buildings. The results indicated a significant potential for energy savings within the building sector. The GIS-based model effectively identified optimal routes for new distribution networks and assessed the energy demands of the building stock. The analysis reveals that targeted interventions can lead to substantial reductions in energy consumption, aligning with the European Union's sustainability goals. The most important conclusion is that integrating GIS tools into energy planning processes is crucial for developing effective strategies to reduce energy consumption in urban areas and can drive rational solutions. The study highlighted the importance of a systematic approach to energy modeling, which can inform policymakers and stakeholders about the potential impacts of various interventions.

The research presented in [54] proposed a systematic approach that integrates graph preprocessing to enhance the efficiency of the optimization process. The methodology accounted for two main steps. Initially, a linear thermal power flow optimization is carried out to analyze the district heating topology. In this way, the district heating network was represented as a graph. This step aimed at calculating the flow distribution through the network, excluding the unnecessary piping connections, and limiting the selection of discrete pipe diameters. Thereafter, detailed nonlinear optimization is performed on the preprocessed system. In this second phase the nonlinear pressure and temperature drops were calculated, providing a more realistic representation of the network's behavior. The authors assumed water as the heat carrier medium at a constant temperature of 60 °C, simplifying the analysis by neglecting temperature dependencies of fluid properties within a

specified range (ΔT=40°C). Finally, the optimization function was set to minimize investment and operational costs. The optimization method was applied to a small district heating system including 42 consumers. The results showed a significant improvement in the efficiency of the network: the desired heat demand is met with 95 % of the desired heat, thus minimizing the operational costs. Overall, the total efficiency for the heat distribution of 98.01 % is reached. The optimization successfully minimized both investment and operational costs, showcasing the method's potential for practical applications in real-world scenarios. The authors underlined that their two-step methodology effectively addresses the challenges of optimizing district heating systems. The integration of graph preprocessing not only streamlines the optimization process but also enhances the accuracy of the results. In further work, the method should be applied to larger districts to prove the scalability of the method. Moreover, the discrete pipe sizing method should be improved to eliminate all non-discrete diameters in the final results of the optimization. The optimization should also be developed to account for the profitability of the district heating network considered. From a future perspective, the discrete pipe sizing method requires refinement to eliminate non-discrete diameters in the final optimization results. Future work should focus on incorporating profitability assessments into the optimization framework, ensuring that economic viability is considered alongside technical performance. In this context, the role of prosumers will be crucial.

Another example of the employment of GIS tools for analyzing DHN expansion is presented in [55]. The GIS-based model allowed for spatial analysis of the existing DH network, identifying areas with potential for energy savings and retrofitting operations. A comprehensive dataset that includes building characteristics, energy consumption patterns, and demographic information was used in the study. The model was applied to the case study of the city of Turin (Italy). Energy savings hypotheses were examined by assessing various energy-saving trends based on the existing policies. The results indicated that by focusing on critical areas, only an additional 5% of potential buildings could be connected to the existing district heating (DH) network with standard retrofitting, while this quantity could increase to 25% with advanced retrofitting. Conversely, when interventions are applied across the entire city, there is a significant reduction in energy consumption, and the percentage of buildings that can be connected to the DH network rises to 42% with standard retrofitting and 82% with advanced retrofitting, along with improved energy distribution optimization.

The group named “*Modeling and Simulation Approaches*” presents a cohesive examination of the role of advanced modeling techniques in the analysis and optimization of district heating and cooling systems. The common thread among these studies is the utilization of simulation methodologies to understand the dynamics of energy systems, evaluate performance under various scenarios, and inform decision-making processes for sustainable energy management. By implementing sophisticated modeling tools, these papers contribute to a deeper understanding of how DHC systems can be effectively designed, managed, and expanded to meet the evolving energy demands of urban environments.

The studies in this group employ a variety of modeling approaches, including mathematical optimization, nonlinear programming, and system dynamics, to capture the complexities of DHC systems. These methodologies allow researchers to simulate several operating strategies, assess the impact of various design and operating parameters, and evaluate the feasibility of integrating renewable energy sources and energy efficiency measures. By creating detailed models that reflect real-world conditions, the studies provide reliable insights into the performance of DHC systems and their potential for reducing greenhouse gas emissions and enhancing energy efficiency.

A significant focus of the research is on the optimization of district heating networks. The papers explore how modeling can be used to identify cost-effective expansion strategies, optimize network layouts, and minimize operational costs while ensuring reliable heat supply. This optimization process often involves the consideration of multiple objectives, such as economic viability, environmental impact, and social acceptance, highlighting the need for a holistic approach to energy system planning.

Moreover, the studies address the importance of scenario analysis in understanding the long-term implications of different energy policies and technological advancements. By simulating various future scenarios, based on European and international policy trends, researchers can assess the role of DHC systems to affect the markets in energy demand, fuel prices, and regulatory frameworks. This future perspective is crucial for policymakers and stakeholders as it leads to a deep understanding of the complexities of energy transition and challenges to achieve sustainability goals.

The integration of real consumption data into modeling efforts is another key aspect of this group. By utilizing empirical data, the studies enhance the accuracy and reliability of their simulations, allowing for more informed decision-making. This data-driven approach not only improves the credibility of the models but also facilitates the identification of specific areas for improvement within existing DHC systems.

The paper [56] combined GIS mapping with energy systems modeling to assess local heat demands and supplies across the EU27. This approach led to identifying the high heat density areas suitable for district heating and the mapping of local renewable energy resources, such as geothermal and large-scale solar thermal, which can be integrated into district heating networks. Then, three different scenarios were proposed and modeled into the EnergyPLAN tool. EnergyPLAN is an energy system analysis tool specifically designed to assist the design of national or regional energy planning strategies under the “Choice Awareness” theory [66] The results indicated that incorporating district heating into an energy system with low heat demands lets to maintain fossil fuel and biomass usage at levels comparable to the EU Energy Efficiency (EU-EE) reference scenario while achieving approximately 15% lower total costs for heating and cooling buildings by 2050. The study highlighted that energy efficiency measures foreseen in the Heat Roadmap Scenario (HRE-EE) are essential for reducing heat demand, but there are limits to their implementation due to the high costs, suggesting that ambitious targets should be pursued without over-reliance on heat savings alone. The HRE-EE scenario is presented as a safer and more realistic alternative to the EU-EE scenario, offering a diverse range of technologies and renewable resources, thus reducing the need for drastic heat demand reductions. By adding district

heating for buildings, it is possible to utilize surplus heat from power plants, industry, and waste incineration, while also using more renewable energy such as wind power, large-scale solar thermal, and geothermal. The most relevant barriers identified are related to the integration of various renewable energy sources into existing systems and to the technical and regulatory challenges that must be addressed to fully realize the benefits of district heating.

The paper [57] aimed to strengthen the internal validation of EnergyPLAN by synthesizing its applications across various studies, thereby forming a reference for future research. The district heating technology is evoked several times by presenting multiple case studies, as it represents a critical component in the modeling of energy systems and the validation of the tool's effectiveness in promoting sustainable energy solutions. A multi-step approach was adopted to identify relevant journal articles that utilized EnergyPLAN. The rigorous selection process allowed for a thorough analysis of the geographical coverage and the types of energy systems modeled using EnergyPLAN. The comprehensive review showed the value of district heating in facilitating the integration of fluctuating renewable energy sources. By providing a centralized heating solution, district heating systems can support the balance between supply and demand, making them essential for the transition to RES-based energy systems. The research showed also the ability of EnergyPLAN to simulate the impacts of district heating on overall energy system performance, including efficiency, emissions, and cost-effectiveness. This capability is particularly relevant for cities and regions aiming to reduce carbon footprints and enhance energy sustainability. Furthermore, several case studies where EnergyPLAN has been applied to assess the potential of district heating in different contexts were reported. These studies demonstrated how district heating can optimize energy use and improve system reliability, especially when combined with other technologies like heat pumps and RES. The review acknowledged EnergyPLAN as a valuable tool for modeling complex energy systems, particularly in the context of integrating renewable energy sources and district heating. The authors emphasized the necessity of model validation through calibration, replication, and comparisons with other models to ensure the reliability of results. A more extensive application of EnergyPLAN in diverse geographical contexts is necessary to enhance its validation and applicability and to evaluate the strength of district heating applications.

The MARKAL modeling approach is considered one of the leading methods for the elaboration of energy planning models by the scientific community. The TIMES MARKAL model generator, developed within the IEA-ETSAP (Energy Technology Systems Analysis Program), is a framework that utilizes long-term energy scenarios to conduct energy and environmental analyses [67]. These models are widely used for analyzing and simulating energy systems and informing policy decisions related to energy planning, climate change mitigation, and energy transition strategies.

By integrating technical engineering and economic approaches, the TIMES MARKAL model generator combines two distinct and complementary systematic methods for energy modeling. TIMES, functioning as a technology-rich, bottom-up model generator, is based on linear programming to optimize and generate a cost-effective energy system (MARket – ALlocation), considering various user-defined constraints, across medium to long-term

timeframes. It provides a comprehensive representation of an energy system by considering various energy sectors, technologies, and their interconnections. It allows for the optimization of energy system pathways by considering factors such as energy demand, energy supply options, infrastructure development, and environmental constraints. Once fixed energy balances, technology characterizations, and user-defined constraints, the model generator puts technologies in competition to minimize the global economic costs of the energy system for a defined timeframe.

This integrated modeling framework is particularly valuable for assessing the costs, benefits, and impacts of different energy policies, including evaluating the deployment of renewable energy technologies, energy efficiency measures, and carbon mitigation strategies. It enables detailed techno-economic analysis of energy systems while considering environmental constraints and policy objectives.

TIMES models include the entire energy supply chain: from primary resources to the demand for energy services from consumers through the processes of transformation, transportation, distribution, and conversion. On the supply side, this includes activities such as fuel mining, primary and secondary production, as well as import and export. Energy is delivered to the demand side through various carriers, and the demand side is structured into sectors like residential, commercial, agricultural, transport, and industrial. Consumers and producers act as the agents on, respectively, the energy demand and supply sides. The mathematical, economic, and engineering relationships between these producers and consumers form the fundamental framework of TIMES models. These models are based on the following basic entities:

- Commodities: fuels, energy carriers, energy services, materials, monetary flows, and emissions; a commodity is either produced or consumed by some technology.

- Processes (or technologies): representations of physical devices that transform commodities into other commodities. Processes can involve primary sources of commodities, such as mining or import activities, as well as transformation processes like electricity generation in conversion plants, energy processing in refineries, or the utilization of end-use demand devices such as cars and heating systems

- Commodity flows: links between processes and commodities (i.e. heat generation from solar radiation). In the architecture of the model, a flow has the same nature as a commodity but is linked to a particular process and represents one input or one output of that process.

The building modeling process is structured in a step-by-step process. The preliminary steps involve the definition of modeling scope geographical application and time horizon. This family of models can be applied to underline the potential development of a specific process or commodity among others or to have a general overview of the energy system. Under the geographical application, theoretically, TIMES Markal allows a huge range of analyses: from micro-scale (small groups of final demand users) to large regions or countries (continental applications such as JRC European model). The time horizon is another fundamental setting and it’s representative of the time range necessary to reach a specific goal that policymakers attempt to reach.

The second step foresees energy balance and technology database fulfillment. The energy sectors and sub-sectors (such as electricity generation, transportation, industry, and residential) have to be identified; then the energy resources, technologies, energy demand, and other relevant databases should be compiled with reliable and consistent data. This step is fundamental to formulating the energy system representation: defining the conversion processes and linkages between different energy sectors, determining the available technologies, their costs, efficiencies, and capacity limits, and introducing constraints and policies related to emissions, resource availability, and energy demand

Before running the simulation model, policy constraints and optimization objectives should be set. The future energy demand is estimated by making assumptions on macroeconomic projections, population growth, and other relevant factors. The time steps (i.e., yearly or multi-year) and the representation of energy technologies (e.g., power plants, vehicles, heating systems) are set, finally, the optimization objectives are defined, such as minimizing system costs, maximizing energy security, or achieving specific emissions reduction targets.

The simulation software attempts to solve the problem and identify the energy system that meets the demands for energy services across the entire time horizon at the lowest possible cost. It achieves this by simultaneously making decisions regarding equipment investments, primary energy supply, energy trade, and operations, considering different regions. The TIMES model assumes perfect foresight, meaning that all investment decisions are made in each period with complete knowledge of future events. It optimizes both horizontally (across all sectors) and vertically (across all imposed time periods).

The results yield the optimal combination of technologies and fuels for each period, along with the corresponding emissions required to meet the demand. The model configures the production and consumption of commodities (such as fuels, materials, and energy services) and their prices. When the model aligns supply with demand, matching energy producers with energy consumers, it achieves equilibrium. From a mathematical standpoint, this implies that the model maximizes the surplus for both producers and consumers. The model is designed in a way that the price of producing a commodity influences the demand for that commodity, while simultaneously the demand affects the commodity's price. An equilibrium is reached in a market where no consumer desires to purchase less than the quantity available, and no producer wishes to produce more than the quantity demanded, at a specific price. When all markets reach equilibrium (Figure 5), the total economic surplus is maximized, represented by the summation of producers' and consumers' surpluses.

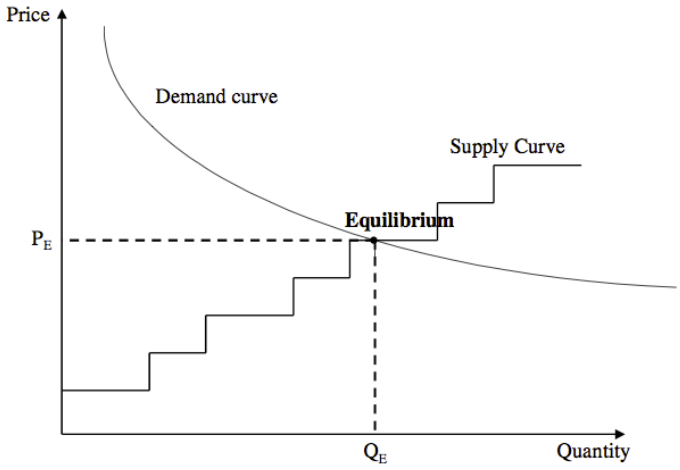

Figure 5: Market equilibrium in TIMES model

The model outputs are energy flows, energy commodity prices, GHG emissions, capacities of technologies, energy costs, and marginal emissions abatement costs. A new configuration of the energy system is obtained for each step, it is configured as able to supply the entire demand by respecting the imposed constraints (Figure 6).

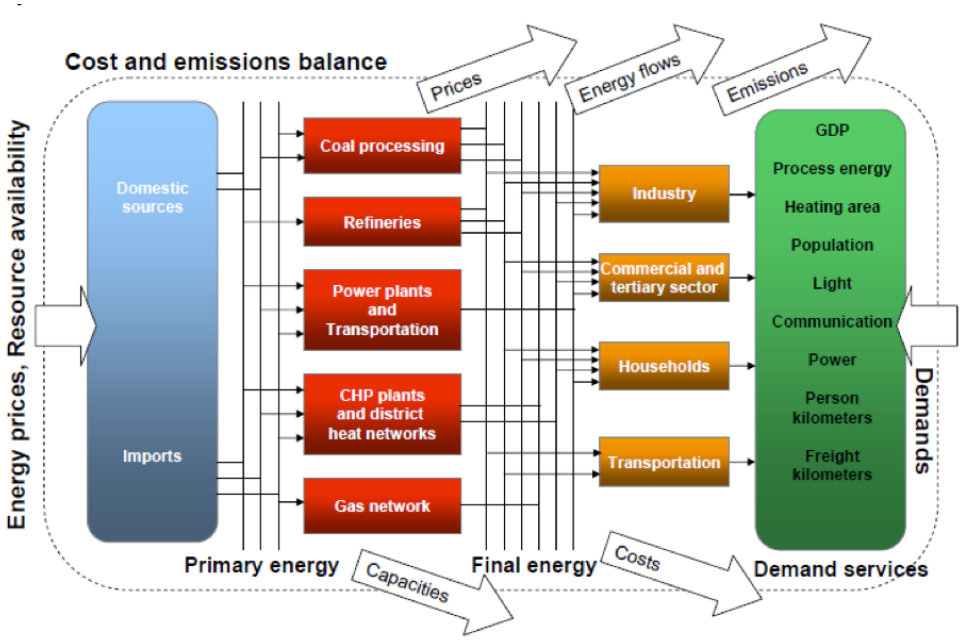

Figure 6: Layout of a TIMES model reporting inputs and outputs

Once the results are obtained, model validation and calibration are highly recommended by comparing the outputs with historical data or other independent sources. Adjusting the model parameters and assumptions is needed to improve its accuracy and reliability.

The validated model could be used to analyze different scenarios by modifying input parameters or constraints. Evaluate the impacts of policy options and inform decision-makers about the potential costs, benefits, and trade-offs associated with different energy strategies. Furthermore, technological advancements or changes in energy demand on the energy system's performance and outcomes can be analyzed in depth. The TIMES-MARKAL model generator was applied mainly to country energy planning or continental level (The JRC European TIMES Energy System Model [68]). Despite this, it found

interesting applications on a local level, with a particular focus on the development of district heating systems.

The research presented in [58] adopted a MARKet ALlocation model framework. MARKAL builds a model of economic “partial equilibrium” and it’s characterized by balancing the production and consumption of energy carriers and other goods and fixing their prices. The study implements a bottom-up modeling approach, integrating several energy generation technologies, including renewable sources, nuclear power, and carbon capture and storage (CCS) systems. The model embedded a detailed analysis of the Polish energy system, merging the energy demand framework, existing infrastructures, and future energy projections up to 2060. The utilized tool let to consider the implications of the EU Emissions Trading System (EU ETS) and the potential for energy storage solutions to face the intermittency of renewable energy sources. The results indicated a sustainable pathway for the development of district heating in the context of a transition towards a low-emission scenario. Geothermal energy and solar thermal systems were identified as relevant technologies for long-term district heating solutions. Furthermore, CHP systems, particularly biomass and waste-fired ones, can play a crucial role. The model showed that the transition from coal and natural gas to biomass and waste for CHP led to lower greenhouse gas emissions while providing efficient heat and power generation. The global overview offered by the MARKAL model allows for evaluation related to the country-level infrastructure expansion. Investment in infrastructure is necessary to support the integration of renewable energy sources into district heating systems. Finally, the analysis suggested that while the transition to low-emission district heating systems is feasible, it requires careful planning and consideration of economic factors to ensure economic sustainability.

The paper [59] presented a comprehensive analysis of the potential for utilizing urban excess heat (UEH) in district heating (DH) systems across four cities: Madrid (Spain), Nice (France), Berlin, and Brunswick (Germany). The study employed a dynamic energy system modeling approach using the TIMES MARKAL model generator, specifically developed for this research as the "TIMES_CityHeat" model. It represents the heating sector in urban areas, which includes both district heating (DH) production and individual heating in buildings. The electricity system and international fuel markets are considered exogenous factors. The objective function of the model was the minimization of the costs associated with fulfilling the heating demand of both residential and service sectors in cities, considering constraints such as emissions limits and restricted energy resources. The overall system cost reflects the net expenses of heat supply, which includes income from electricity sales (based on externally determined prices) generated by combined heat and power (CHP) plants. The model optimization calculated the share of DH compared to individual heating systems. Furthermore, the analysis focused on how UEH can affect fuel and electricity use, primary energy consumption, and overall system costs in urban heating supply. The results indicated that the integration of UEH into DH systems can significantly enhance their competitiveness compared to individual heating solutions, such as boilers. The use of UEH for DH in the case cities could be feasible and cost-efficient regardless of climate policy scenario; however, the available potential of UEH was larger than what was cost-efficient to use The study found that cities with a high share of individual heating solutions, like Madrid and Nice, could benefit substantially from the earlier introduction of large heat pumps (HPs)

that utilize UEH. This shift could lead to reduced CO_2 emissions and lower system costs, particularly under stringent carbon pricing scenarios. The use of UEH in large heat pumps (HPs) can enhance the competitiveness of district heating systems relative to individual heating options, such as boilers and ambient-temperature source HPs in buildings. The results indicate also that utilizing UEH in large HPs could serve as a significant catalyst for the development of DH in cities like Madrid and Nice, which currently have limited DH infrastructure. In the presence of local CO_2 emissions reduction requirements, the implementation of large HPs in DH systems in cities with a high reliance on individual heating solutions (like Madrid and Nice) could be implemented earlier than in cities with a greater proportion of combined heat and power (CHP) systems, such as Berlin. The analysis highlights that leveraging low-temperature UEH sources can play a crucial role in advancing both the heating and electricity sectors toward more sustainable practices. Additionally, utilizing UEH can lead to a decrease in primary energy consumption by substituting fuel or electricity used for heat production. Future work should focus on enhancing geographical resolution in modeling UEH sources and analyzing the cost-efficiency of thermal storage investments.

An analog point of view is offered in [60] that evaluated the energy system and the effects on system costs of the most cost-effective heat supply options for new LEB areas in Sweden by 2050, using a dynamic energy system modeling approach from a Nordic regional perspective. The analysis was conducted through scenario assessments and the incorporation of new LEB areas and low-temperature district heating (DH) within Sweden's energy system model. A TIMES model generator was adopted, more specifically the Open Nordic TIMES (ON-TIMES) model was selected as representative of that specific geographical area. A scenario analysis was carried out to evaluate the cost-effectiveness of decentralized low-temperature district heating (LTDH) compared to traditional heating methods. This methodology enabled the identification of optimal heat supply strategies that align with national energy and climate objectives. Despite the consistently low heat demand of LEBs throughout the year, the selection of heat supply systems for these buildings influences system costs, energy flows, and the technologies employed for heat and power production in achieving Sweden's energy and climate objectives. The study demonstrated that constructing LEBs in decentralized locations together with supplying decentralized low-temperature district heating (LTDH) to these buildings, led to a decrease in electricity consumption for heating within the building sector. It was also shown that the decentralized LTDH option in LEB areas could decrease the annual average energy system cost by nearly 2 billion EUR (5%) between 2020 and 2050 in Sweden. The study reveals also several challenges. These include uncertainties related to future energy markets, the need for robust scenario analysis to validate the findings, and the potential variability in local conditions that may affect the implementation of district heating systems. Additionally, the authors underline the importance of considering technological advancements and policy frameworks that could influence the future perspectives of district heating in Sweden.

The impacts of the Nationally Determined Contribution (NDC2) targets in Moldova were examined in [61], with a special focus on the potential role of distributed heat pumps in transforming Moldova's district heating. The TIMES model generator was employed, and three scenarios were defined: a Reference scenario that maintains current trends, a

Sustainable scenario with a limit of 36% CO_2 by 2030 and 65% CO_2 by 2050 (compared to 2019), and a Decarbonization scenario with a limit of 52% CO2 by 2030 and 85% CO_2 by 2050 (compared to 2019). In both Decarbonization and Sustainable scenarios higher levels of subsidies for buildings and the rapid implementation of new technologies were foreseen. The results indicate a shift from gas-fired combined heat and power (CHP) systems to distributed heat pumps, particularly under the Sustainable and Decarbonization scenarios. Furthermore, the implementation of advanced heat pumps could lead to a reduction in CO_2 emissions while providing efficient heating solutions. The total discounted system cost is projected to increase slightly under the Sustainable scenario, highlighting the financial implications of transitioning to cleaner technologies. This transition not only aligns with global climate commitments but also stresses the need for affordable and clean heating solutions for the population.

A combination of TIMES and EnergyPLAN modeling for the expansion potential of District Heating in Ireland is presented in [62]. The methodology is structured in two main phases: first, the TIMES model is employed to frame the initial future energy system, focusing on long-term scenario development. This model incorporated a comprehensive database of over 1300 technologies and evaluated energy service demands, fuel prices, and available resources to identify the least-cost energy system over a long horizon (e.g., to 2050). Since the TIMES model generator is not suitable for investigating operational aspects of heating scenarios due to its lack of hourly resolution, EnergyPLAN was adopted for detailed hourly simulations of both electricity and heating systems. This dual-model approach enabled a more nuanced analysis of the operational dynamics of district heating compared to individual heating systems. The specific scenario analyzed is the CO_2-80 scenario, which aims for an 80% reduction in carbon emissions. The study compares the operational efficiency and cost implications of implementing district heating versus maintaining individual heating systems. The results arising from TIMES MARKAL model were set as input for the hourly simulation in EnergyPLAN. The study takes into account the uncertainty of the performance of the district heating grid implemented, while does not discuss the implementation of heat savings, but recognizes its potential impact on the result. The results indicated that the transition of 37% of Ireland's heat demand to district heating is a viable solution to increase global efficiency if compared to individual heating solutions. Furthermore, incorporating district heating along with combined heat and power results in lower annual costs than those associated with individual heating systems. Despite being more investment-heavy, the fuel savings generated by district heating more than offset the initial costs, leading to an estimated annual cost reduction of approximately 300 million euros compared to individual heating systems. However, the paper also identifies challenges, such as the need for substantial upfront investments and the potential resistance to changing existing heating infrastructures.

2.1. Focus: Scenarios for Italian District Heating

The REWARDHeat project [63] demonstrated a new generation of Low Temperature District Heating and Cooling networks, which will be able to recover Low Temperature Heat and Renewable Energy sources available within the urban context. For this study, a specialized

heating sector model called TIMES_Heat was developed and applied to each demonstrator. The TIMES_Heat model captures the heating sectors in the countries under study, covering both heat generation in district heating systems and individual heating units in buildings. The electricity system and international fuel markets are considered as external factors in the analysis. Energy efficiency measures and heat demand forecasts are also incorporated as external inputs to the model. The TIMES_Heat model is designed to minimize the cost of meeting heating demand in each country, while taking into account constraints defined within the model, such as emissions, resource availability, and other factors. The model begins in the year 2015, where the heating sector is depicted using the existing fuel mix and heat generation technologies of that time. As the model progresses, these existing technologies are gradually phased out and replaced by new ones, based on factors like cost, efficiency, availability, and lifespan. The main modeling parameters are considered as follows:

- Start year of the model: 2015
- Time horizon: 2015-2052
- Time resolution: Eight time slices per year (four seasons, day and night)

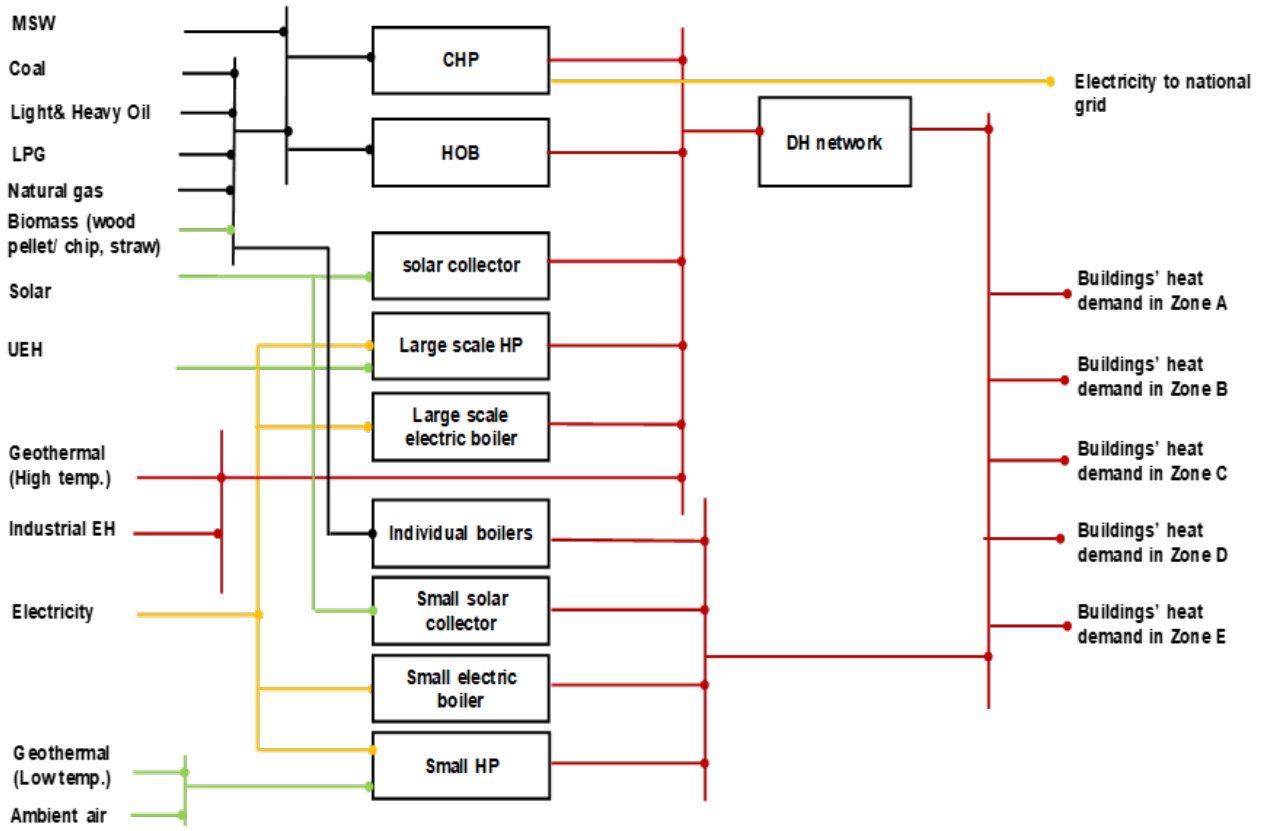

Figure 7: Simplified representation of the heating sector in the TIMES_Heat model implemented in REWARDHeat project and adopted from [59]

Within the RewardHeat project, 9 scenarios were developed and modeled in TIMES model generator. These 9 scenarios result from a combination of 3 heat supply scenarios and 3 climate policy options.

Three heat supply scenarios:

1. **Conventional DH** - Conventional district heating without low-temperature heat sources. In this scenario, the current DH systems remain without low-temperature heating sources.
2. **Transition DH** - Conventional district heating with low-temperature heat sources. In this scenario, the current DH systems remain. In addition to this low-temperature heating sources are introduced to the system.
3. **Future DH** - Low-Temperature district heating with low-temperature heat sources. Low-temperature district heating technologies are introduced with the availability of low-temperature heating sources.

Three climate policy options:

1. **Ambitious** - Net zero emission by 2030 compared to 2015 Local and international CO_2 emission reduction of 100% by 2030 compared to 2015
2. **WEO-SD** - World Energy Outlook Sustainable Development Scenario total CO2 reduction by 95% by 2050 compared to 2015 Local and international CO2 emission reduction of 95% by 2050 compared to 2015
3. **WEO-NP** - World Energy Outlook New Policies Scenario total CO2 reduction by 60% by 2050 compared to 2015 Local and international CO2 emission reduction of 60% by 2050 compared to 2015

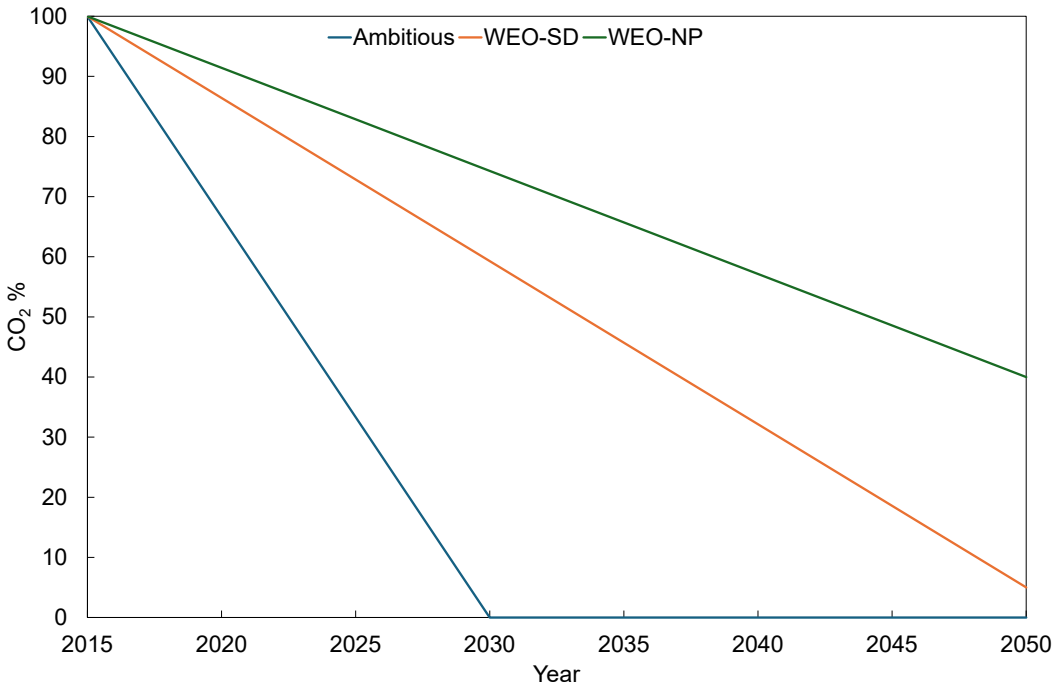

Figure 8: Climate policy options as defined in the REWARDHeat project

The combination of **"Conventional DH" + "Ambitious"** let to achieve a significant reduction in heat demand by 2050. Furthermore, there is a goal to achieve a 100% reduction in CO_2 emissions, both locally and internationally, by 2030, compared to 2015 levels, a faster growth rate in renewable electricity generation by 2050 is also expected. However, while the cost of fossil fuels is projected to decrease, the cost of biomass is likely to increase and investment costs for DH networks are expected to be lower, though this may come with

higher losses. Additionally, the efficiency of biomass and natural gas CHPs and boilers is expected to decline, and large-scale heat pumps are not anticipated to be implemented.

The combination of **"Conventional DH" + "WEO-SD"** lead to a significant reduction in heat demand by 2050. The environmental goal foresees cutting CO_2 emissions by 95%, both locally and internationally, by 2050 compared to 2015 levels. The generation of renewable electricity is projected to accelerate by 2050; however, while the cost of fossil fuels may decrease, the cost of biomass is likely to rise. DH networks are expected to have lower investment costs, although this could lead to higher losses. Additionally, the efficiency of biomass and natural gas CHPs and boilers is anticipated to decline, and large-scale heat pumps are not expected to be introduced.

The combination of **"Conventional DH" + "WEO-NP"** foresees a modest reduction of heat demand by 2050. Meanwhile, the CO_2 emissions have to be reduced by 60% both locally and internationally, compared to 2015 levels. The growth in renewable electricity generation is projected to be slower by 2050, fossil fuel costs are anticipated to rise, while biomass costs are expected to decrease. Although investment costs for DH networks might be lower, this could result in higher losses. Additionally, the efficiency of biomass and natural gas CHPs and boilers is expected to decline.

The combination of **"Transition DH" + "Ambitious"** let to achieve a significant reduction in heat demand by 2050. Additionally, there is a target of a 100% reduction in CO_2 emissions, both locally and internationally, by 2030 compared to 2015 levels. Renewable electricity generation is expected to grow at a faster pace by 2050, while fossil fuel costs are expected to decrease, the cost of biomass may increase. Investment costs for DH networks are projected to be lower, but this could lead to higher losses. The efficiencies of biomass and natural CHPs and boilers are expected to decline, a similar trend is shown by the COP of large-scale heat pumps.

The combination of **"Transition DH" + "WEO-SD"** shows a high rate of heat demand reduction by 2050 and the environmental aim is to achieve a 95% reduction in CO_2 emissions both locally and internationally by 2050, compared to 2015 levels. Renewable electricity generation is projected to increase at a faster rate by 2050, then, the cost of fossil fuels is expected to decrease, conversely, the cost of biomass may rise. Investment costs for DH networks show a decreasing trend, although this might result in higher losses. Additionally, the efficiency of biomass and natural gas CHPs and boilers is expected to decline, along with a lower COP for large-scale heat pumps.

The combination of **"Transition DH" + "WEO-NP"** foresees a low rate of heat demand reduction by 2050, furthermore, the local and international CO_2 emissions will show by 60% reduction by 2050 compared to 2015. The growth in renewable electricity generation is anticipated to be slower, fossil fuel costs are likely to increase, while biomass costs are expected to decrease. Investment costs for DH networks may be lower, but this could lead to higher losses. Additionally, the efficiency of biomass and natural gas combined CHPs and boilers is expected to decline, along with a lower COP for large-scale heat pumps.

The combination of **"Future DH" + "Ambitious**" is characterized by a high rate of heat demand reduction by 2050. There's also the ambitious goal to achieve a 100% reduction in

CO_2 emissions, both locally and internationally, by 2030 compared to 2015 levels. Renewable electricity generation is expected to grow at a fast rate by 2050, meanwhile, fossil fuel costs are likely to decrease, while biomass costs may rise. Investment costs for DH networks are expected to be higher, but this could result in lower losses. Additionally, the efficiency of biomass and natural gas CHPs and boilers is expected to improve, along with a higher COP for large-scale heat pumps.

The combination of **"Future DH" + "WEO-SD**" a high rate of heat demand reduction by 2050 is set, moreover, local and international CO2 emission reduction of 95% by 2050 compared to 2015 is foreseen. The generation of renewable electricity is expected to accelerate by 2050; meanwhile, fossil fuel costs are likely to decrease, while the cost of biomass may increase. DH networks may require higher investment costs, but this could lead to lower energy losses. Additionally, the efficiency of biomass and natural gas CHPs and boilers is expected to improve, as well as the COP of large-scale heat pumps.

The combination of **"Future DH" + "WEO-NP**" foresees a minimal reduction in heat demand by 2050. The CO_2 emissions should be cut up to 60% both locally and internationally compared to 2015 levels and a slow growth in renewable electricity generation is expected. On the cost side, fossil fuels are expected to become more expensive, while biomass costs may decrease. Investment in DH networks might require higher costs, but this could result in lower energy losses. Additionally, the efficiency of biomass and natural gas CHPs and boilers is expected to improve, along with a better COP for large-scale heat pumps.

Three air pollutants: Nitrogen Oxides (NOx), Sulfur Oxides (SOx), and particles less than 2.5 μm (PM2.5) were estimated for all heat production technologies that are supplying the heat demand for each scenario. The methodology used in the model is the multiplication of heat output from the respective technologies (PJ) and emissions factors per each substance, technology, and fuel (kt/PJ). For air pollutant calculations, the TIMES model is soft linked with the GAINS model [69]. Heat output is retrieved from the TIMES_Heat model and linked with the unique emission factor for the respective technology defined in the GAINS model:

$$Emission\ (kt) = Heat\ output\ (PJ) * Emission\ Factor\ (\frac{kt}{PJ}) \quad (1)$$

Finally, the model calculates total system cost discounted to 2015 as well as undiscounted variable costs (including energy flow cost, activity cost, taxes, and subsidies), fixed operation and maintenance, and capital costs for each demo-city and each model year. From the model results, average annual system cost savings for each demo-city are calculated based on equations (1) and (2) where: "i" is either WEO-SD or WEO-NP "j": variable cost, fixed operation, and maintenance cost or capital costs:

$$AC_{sav,j} = \frac{AC_j(i, Conventional\ DH) - AC_j(i, Transition\ DH\ or\ Future\ DH)}{Heat\ Supply_{av}} \quad (2)$$

$$AC_{sav} = \sum AC_{sav,j} \quad (3)$$

where:

- $AC_{sav,j}$: Average annual cost(j) saving for each year from 2020 to 2050

- AC (j, Conventional DH): Average annual cost(j) for each year from 2020 to 2050 for a selected climate policy and Conventional DH technology system
- AC (j, Transition DH or Future DH): Average annual cost(j) for each year from 2020 to 2050 for a selected climate policy and Transition DH or Future technology system
- Heat $Supply_{av}$: Average total heat supply

The tool was run to evaluate the future scenarios for the Italian DHN expansion perspectives and personal data elaboration was performed.

For the “Conventional DH” heat supply scenario, a comparison between the three climate policy options is shown in Figure 9, specifically, Figure 9a) depicts the trend of End-Use devices capacity, and Figure 9b) depicts the trend of District Heating capacity.

About the End-Use Capacity (Figure 9 a), all three climate options show an identical trend for the natural gas boiler capacity, even the ambitious one foresees a drastic decrease after 2030, by maintaining a minority share until 2040. A relevant role is observed for Electric ASHP. In the AMB and WEO-SD options, an analog trend arises from the simulation: an increase until 2030 and then a slight decrease up to the end of the simulated period (2050); WEO-SD shows absolute values that are, on average, 20% lower than the ambitious one. The same trend occurs for GSHP in both scenarios, together with ASHP it replaces the capacity occupied in the first ten years by gas boilers, by determining a deep electrification of the Italian heating system capacity. It is important to underline the role that the WEO-NP scenario offers to the ASHP: differently to the other scenarios, this technology is predominant from 2030 and no share of GSHP is foreseen with a peak of 172 GW in 2030 and 2035. The scenario that guarantees the major share of DH about end-use devices is the WEO-SD with a peak of 85 GW in 2045, in AMB and WEO-NP options the District Heating capacity doesn’t exceed 69 GW, maintaining a similar trend. Finally, it is worth noticing the dismantlement of oil boilers and electrical after 2025 for each scenario and the small capacity of biomass boilers that disappear in WEO-SP and WEO-SD after 2025 but, conversely, it’s maintained until 2040 in the AMB scenario. While in the last two reference years (2045 – 2050) the AMB and WEO-SD scenarios show a capacity share among DH, ASHP, and GSHP, WEO-NP shows that the capacity is mostly covered by ASHP and DH and a minority share of Natural Gas HP is foreseen.

The District Heating capacity (Figure 9b), shows the district heating capacity in gigawatts (GW) for the examined period (2015 - 2050), the conventional district heating technology, and under the three different energy policy scenarios. In the baseline year, across all scenarios (AMB, WEO-NP, WEO-SD), the district heating capacity is quite low, below 10 GW, primarily relying on Natural Gas boilers. WEO-NP and WEO-SD scenarios show an increasing introduction of the CHP technologies up to 2035: in the case of WEO-SD the natural gas CHP technology is introduced, and in the WEO-NP there is a balanced share between the natural gas and coal CHP. In the first case, the absolute capacity of DH capacity is higher than in the second. A different perspective is given by the AMB scenario: starting from 2025 a share of Solar DH is foreseen, and then, the biomass boiler is introduced with an increasing weight among the other technologies. Regarding absolute value, the AMB scenario shows comparable values with WEO-SD. In the second part of the simulated

period, even the two more conservative scenarios foresee installing solar DH technology and biomass boiler (only in WEO-NP). A preeminent role is played by Natural Gas boiler CHP (WEO-SD) and Natural Gas boiler (WEO-NP). The AMB scenario shows the progressive decrease of fossil-based sources and a smooth capacity trend after 2040. In all the scenarios a minor role is given to Industrial Excess Heat and Geothermal sources (less than 1 GW for each source).

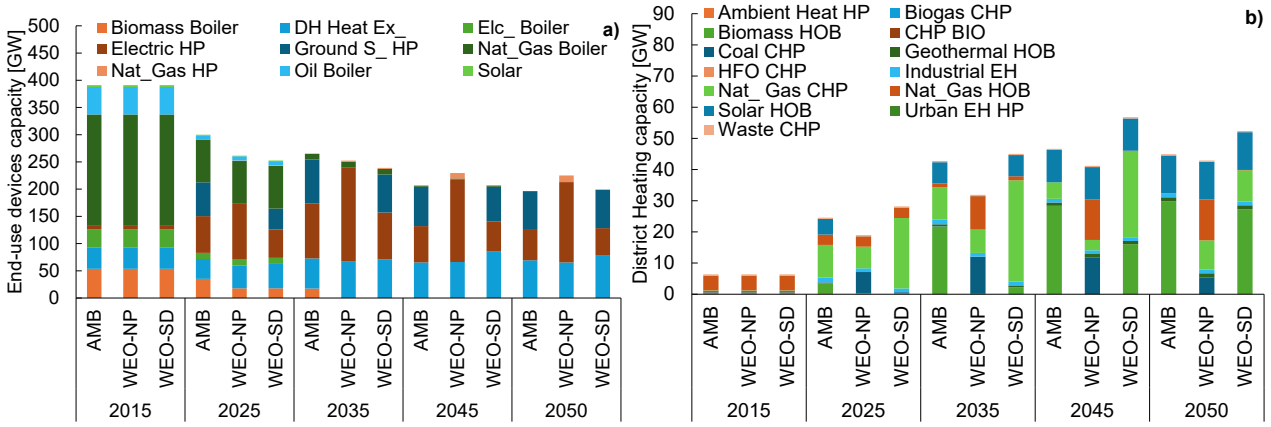

Figure 9:End-use devices capacity (a) and District Heating capacity (b) for Conventional District Heating scenario

Following the same approach, for the "Transition DH" heat supply scenario, a comparison between the three climate policy options is shown in Figure 10, specifically, Figure 10a) depicts the trend of End-Use devices capacity, and Figure 10b) depicts the trend of District Heating capacity.

About the End-Use Capacity (Figure 10 a), this case also shows analogies between the three scenarios, regarding the Gas Boiler generators. Regardless of the climate policy, a clear decrease in the implementation of this technology is visible: although the gas boiler is preeminent in the first simulated years, then its share decreases up to a minority contribution after 2030. A primary role is given to the Electric ASHP in the future perspectives of WEO-NP with a peak of 169 GW over 246 GW in 2030 and 253 GW in 2035. The other end-use technology arising from the optimization calculation in the same scenario is the external DH, with a ratio over the total capacity that ranges between 10% (initial year) and 48% (final simulation year 2050). These aspects reflect the same trend observed for WEO-NP policy applied to Conventional DH technology. AMB and WEO-SD reflect a similar trend to the Conventional DH but with different absolute values and slight differences in share for every single technology. The most relevant difference shown by these two climate policies, compared with WEO-NP, is the introduction of the GSHP. Slight differences between AMB and WEO-SD are revealed by the utilization of biomass boilers in the first climate policy until 2040. The combination of AMB + Transition DH shows a higher implementation of External DH compared to AMB + Conventional DH, since the total end-use capacity is the same, this gain is obtained by reducing the share of ASHP and maintaining the share of GSHP. The same result is arising from the comparison between the WEO-SD climate policy applied to Conventional and Transition DH. This aspect proves the environmental performance of GSHP which, despite the higher costs compared with the ASHP, is the selected technology by the TIMES optimization model.

The results regarding the district heat capacity (Figure 10b) show relevant differences among the three climate policies. Shifting from the more conservative (WEO-NP) to the more futuristic climate policy (AMB) it's possible to notice the decline of most emissive generators in favor of solar and heat pumps. In WEO-NP, in fact, the increasing capacity is covered mostly by fossil fuel generators such as natural gas boilers and CHP, coal CHP that is constantly present until 2050 with an invariant capacity. The WEO-SD policy foresees the highest absolute values of DH capacity, ranging up to 80 GW in 2050, differently from the previous one, it replaces the coal generators with natural gas ones and prefers SHCP technology instead of boilers. Furthermore, a gradual and increasing presence of solar and ASHP is foreseen starting from 2035; then, a consistent penetration of biomass boilers (21 GW over 80GW of total DH capacity) is shown in 2050. The electrification and penetration of renewables and waste heat are visible in the AMB scenario in which the ASHP plays a dominant role, followed by the natural gas CHP (that disappear in 2050) and solar technologies. The "Transition DH" scenario achieves lower temperature than the "Conventional DH" one, for this reason, the differences, within the same climate options, are marked and are underlined by the increased presence of low-temperature generators (ASHP, Solar, Excess Urban Heat). Considering the AMB policy scenario, which represents the "stricter" in terms of environmental constraints, the biomass boilers foreseen in the "Conventional DH" case are totally replaced by ASHP, and the Urban Excess Heat is introduced. Parallelly, even in the WEO-NP policy, among fossil-based technologies, the Transition DH scenario lets to introduce ASHP and Excess Heat, thus revealing the competitiveness of these technologies not only from the environmental point of view but also from the economic one. In all scenarios, a negligible presence of industrial excess heat, geothermal source, and waste CHP.

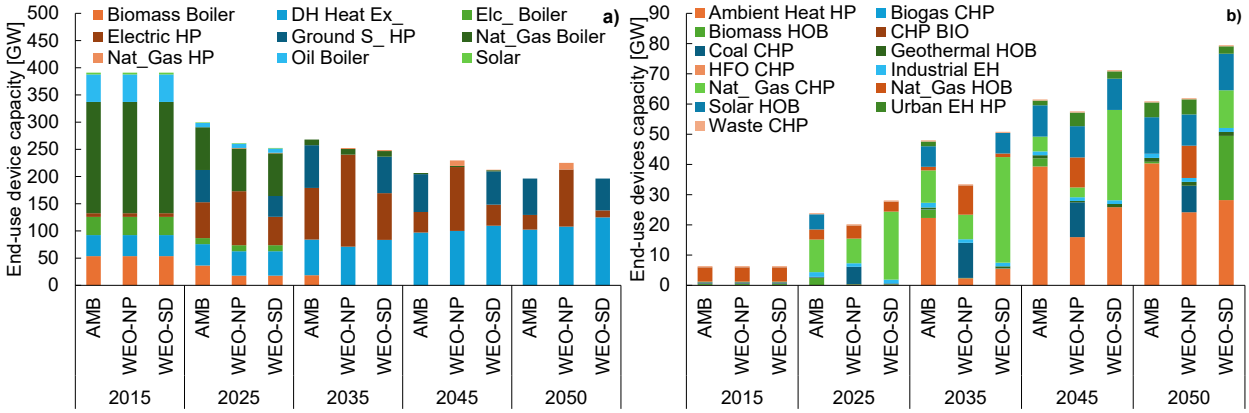

Figure 10: End-use devices capacity (a) and District Heating capacity (b) for the Transition District Heating scenario

Finally, Figure 11 depicts the same comparison carried out in the last two cases for the "Future DH" scenario.

The end-use devices capacity (Figure 11a) follows the same trend as the "Transition DH" scenario, with negligible differences in the absolute values. It is worth noticing that the diversification of sources present in the first simulation periods tends to reduce in the last years by favoring a small set of technologies.

A similar behavior is observed for the DH capacity, in this case, a higher share of low-heat sources is foreseen (mostly solar and urban excess heat).

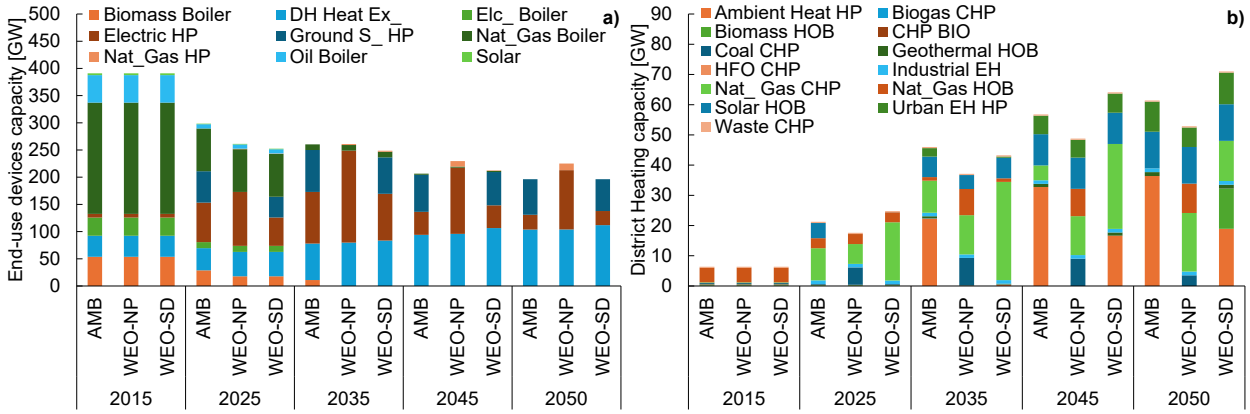

Figure 11: End-use devices capacity (a) and District Heating capacity (b) for the Future District Heating scenario

Starting from Equations (4) and (5)

$$AC_{sav,j} = \frac{AC_j(i, \text{Conventional DH}) - AC_j(i, \text{Transition DH or Future DH})}{\text{Heat Supply}_{av}} \quad (4)$$

$$AC_{sav} = \sum AC_{sav,j} \quad (5)$$

a comparison between the average annual cost of Transition DH, 4th Generation DH, and Conventional DH was carried out for WEO-SD and WEO-NP climate policy options. Figure 12 shows the average annual cost changes within the period 2020-2050 for the Italian case and the two climate policy options WEO-SD (Figure 12a) and WEO-NP (Figure 12b). In all the considered cases the cost changes show a net negative value whose meaning is a global economic saving arising from the implementation of Transition and 4th Generation DH if compared to the Conventional DH technology. More specifically, despite the higher capital costs (whose cost change is always positive) in the WEO-SD climate policy option (Figure 12 a) the 4th Generation DH technology shows better economic performances due to a minor capital cost change and higher savings achieved by the reduction of variable cost and fixed O&M ones. The variable costs change gives the major contribution ranging up to -0.343 M€/PJ for the Transition DH and -1.036 M€/PJ for the Conventional DH case. It is worth noticing that, although the 4th generation DH is a more advanced technology than the Transition DH one, the capital costs change is lower for the 4th Generation DH case: 0.280 M€/PJ vs 0.107 M€/PJ. Even the O&M costs show better performances of 4th Generation DH in comparison to Transition DH in terms of cost change (-0.098 M€/PJ vs -0.134 M€/PJ). The net average cost changes reveal the clear economic advantages of adopting a 4th Generation DH network rather than a Transition DH one, although both let to achieve an economic saving in comparison to a Conventional DH technology: -0.161 M€/PJ vs -1.064 M€/PJ (a negative value indicates a saving since the cost change is obtained by subtracting the analyzed DH technology vs the Conventional one).

The WEO-NP (Figure 12b) shows an analog trend: the 4th Generation DH achieves better economic performance than the Transition DH but with a reduced gap compared to the previous case. The Annual Average Cost change of Fixed O&M costs is negligible, and the major contribution is given by the variable cost change for which the difference between Transition DH and 4th Generation DH is clearly visible: -0.352 M€/PJ vs -0.866 M€/PJ. The capital cost change shows a slight difference between the two cases with an advantage for

4th Generation DH: 0.201 M€/PJ vs 0.175 M€/PJ. Globally, the average net annual cost change ranges up to -0.154 M€/PJ for Transition DH and -0.705 M€/PH for the 4th Generation DH.

Figure 12: Average annual cost changes 2020-2050. WEO-SD (a) - WEO-NP (b)

In Figure 13 the trend of total air emissions for Transition DH (Figure 13a) and Future DH (Figure 13b) are shown, concerning the two opposite climate policies: Ambitious and WEO-NP. The two selected heat supply scenarios show a similar trend in the comparison of climate policies. A drastic decrease of emissions in the first 10 years is resulting in all cases, the PM2.5 component is reduced to a neglecting share in WEO-NP and disappears in AMB after 2030. The SO_2 component is avoided after 2030 only in the AMB climate policy scenario, in WEO-NP there is a residual share that is present until the end of the simulated period for all cases. This is due to the presence of fossil fuel combustion technologies in the WEO-NP scenario (coal, natural gas boiler, and CHP). Slight differences between Transition DH and Future DH are due to the different technology mix employed with more shift to electrification in the second case and a consequential reduction of total emission (mainly NO_X after 2030).

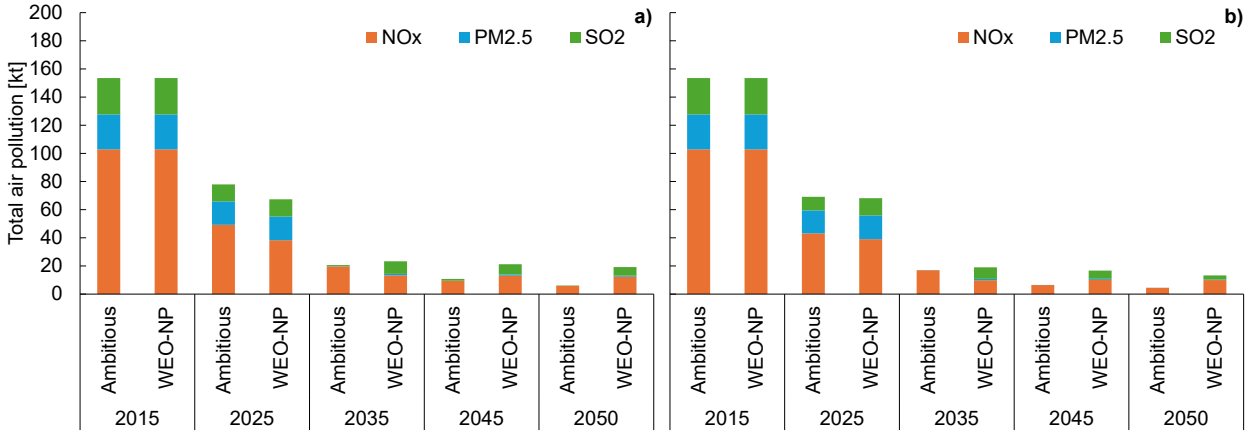

Figure 13: Total air emissions for Transition DH (a) and Future DH (b) for WEO-NP and Ambitious climate policy options

One of the main findings of the review based on District Heating Capacity Expansion is the lack of the prosumer concept. The introduction of prosumers within DHN can induce relevant changes, enabling virtuous processes of renewable energy technologies penetration and waste heat integration. Modeling frameworks should be adapted to include the prosumer role which adds a further level of complexity since it affects both technical and economic aspects. A clear hypothesis of third-party access should be defined to depict the border of the analyzed systems and explore all the possible solutions since the prosumer role needs to be ruled in a configuration in which there is a main DHN dealer and several prosumers, as occurs in the existing electrical energy communities. Reliable instruments of simulation should be assessed, starting with the analysis of the dynamic behavior of prosumers within a DHN. The economic models should rely on a defined structure of the heat markets, this remains an open issue since each DHN has its own rules and, generally, most of them are supplied mainly by natural gas and their economic conditions are strictly coupled with gas market fluctuations.

In the present Ph.D. research work, an attempt to fill a part of the research gap is made. Specifically, a focus on the thermo-hydraulic model of the prosumer substation was carried on and a virtual model, based on an experimental one, was developed in order to support the techno-economic analysis of different thermal prosumer configurations.

3. Heat Pricing and Third-Party Access

The DHN systems characterization cannot exclude an analysis of two aspects that belong to juridical and economic frameworks but relevantly affect their expansion perspective and technical operation. Heat pricing mechanisms and Third-party access are pivotal themes that should be investigated to understand how the DHN markets will evolve and how each single DHN system will operate, planning investments to shift toward more sustainable solutions. As urban centers increasingly prioritize sustainable energy solutions to meet growing heat demands, understanding these themes is essential for optimizing district heating systems, enhancing energy efficiency, and achieving climate goals.

Heat pricing is a fundamental issue in the operation and sustainability of district heating systems. It collects the methodologies and strategies used to determine the cost of heat supplied to consumers. The pricing mechanisms can significantly influence consumer behavior, the economic sustainability of district heating companies, and the overall efficiency of energy use within a community.

The complexity of heat pricing arises from various factors, including fuel costs, joint cost allocation, and the interplay between different energy sources. The studies hereafter presented show that heat pricing is not focusing only on recovering costs and making profits but also on ensuring fairness and competitiveness in a market often characterized by natural monopolies. The low-price elasticity of demand for heat further complicates pricing strategies, as consumers have limited alternatives and switching costs can be high. Therefore, developing advanced pricing mechanisms that reflect the true cost of heat production while promoting sustainability and consumer rights is crucial.

The heat pricing methodologies most adopted widespread are the following ones, discussed in-depth in [70]:

- **Cost-Plus Pricing**: a traditional method that assesses heat prices calculating the total costs incurred by the district heating company, including fixed and variable costs, plus a reasonable profit margin. While it ensures cost recovery, it may not incentivize efficiency or competition.
- **Marginal-Cost Pricing**: this approach sets prices by focusing on the cost of producing an additional unit of heat. It is often seen as more efficient, as it reflects the true economic cost of heat production and can encourage consumers to adjust their demand based on price signals.
- **Dynamic Pricing**: some systems are exploring dynamic pricing models that adjust heat prices in real-time based on demand, supply conditions, and the integration of renewable energy sources. This can enhance flexibility and promote energy efficiency.

Due to the natural monopoly in which they operate, district heating (DH) companies have significant control over heat pricing in a market with a very low elasticity. Generally, there are two primary types of heating markets: regulated and deregulated, which utilize the cost-plus method and the marginal-cost method for heat pricing, respectively.

The marginal cost of heat is influenced by various factors, including fuel costs, the allocation of joint costs, electricity prices, and time periods, all of which complicate its calculation. Consequently, in practice, this calculation has been simplified by dividing costs into two components: the fixed charge and the variable charge, which can also help mitigate financial risks associated with investment and operation.

To address the challenges linked to the cost-plus and marginal-cost pricing methods, alternative models have been proposed, such as the incremental cost model, the shadow price model, and the Equivalent Marginal Cost Pricing (EMCP) model. Additionally, there is growing concern regarding external costs, particularly non-internalized environmental costs, and it has been suggested that these should be incorporated into heat-pricing models.

The marginal-cost method is regarded as the most effective approach for optimal resource allocation, reflecting the scarcity of resources in society, and could serve as the foundation for future DH pricing models. Currently, the external costs associated with DH pricing primarily include environmental pollutants like CO_2 and SO_X. To enhance the sustainability of DH, other factors, such as utilizing waste as fuel and its related impacts, should also be considered. Furthermore, with the advancement of smart heat metering, real-time pricing mechanisms that engage consumers on the demand side can improve transparency in DH pricing and promote sustainable development, thus garnering increasing interest.

The regulatory environment plays a crucial role in shaping heat pricing. Several countries have established frameworks to ensure transparency, fairness, and non-discriminatory access to district heating networks. These regulations often assess how prices are set and reviewed, aiming to protect consumers from monopolistic practices. In Europe, the European Commission has proposed measures to enhance competition in district heating markets, including the promotion of third-party access (TPA) to encourage independent heat producers.

As expected, the integration of renewable energy sources into district heating systems is increasingly influencing heat pricing. Pricing mechanisms are being developed to reflect the lower marginal costs associated with renewable heat production, thereby incentivizing the use of sustainable energy sources. Variable heat pricing models are being explored to align heat demand with the availability of renewable energy, allowing for more efficient use of resources and reducing reliance on fossil fuels. Furthermore, the pricing mechanism connected to renewable energy sources reflects the risks arising from their volatile availability, ascribing to the final user this additional burden. Some studies advocate for the implementation of pricing structures that promote energy efficiency and demand response, allowing consumers to benefit from lower prices during off-peak periods or when renewable energy is abundant. This structure is analogous to the demand-response system that has just been adopted for the electricity infrastructure.

In conjunction with heat pricing, the concept of third-party access (TPA) applied to district heating networks is a critical area of focus. TPA allows independent heat producers to utilize existing district heating infrastructure to supply heat to consumers, thereby fostering competition and innovation within the sector. This is a key factor for the prosumer introduction within DHN markets.

Without appropriate regulations, the potential advantages of TPA may not be fully realized. For instance, utilities that operate both district heating and electricity distribution networks may impose restrictions on the installation of alternative heating technologies, such as heat pumps, thereby limiting consumer choices and stifling competition. A robust and uniform legislative framework is essential to ensure non-discriminatory access to district heating networks, protect consumer rights, and promote fair competition among heat suppliers.

TPA is often governed by national and EU regulations aimed at promoting competition and preventing monopolistic practices in district heating markets. The European Commission has proposed measures to ensure non-discriminatory access to district heating and cooling systems, particularly for heat produced from renewable sources and waste heat. Some countries have adopted varying approaches to TPA, with some implementing mandatory access models while others rely on voluntary agreements between district heating companies and third-party producers. The most common TPA models can be grouped as follows:

- **Voluntary Agreements**: in this case, third-party producers negotiate access to district heating networks with existing operators. This model can lead to inefficiencies and may not guarantee fair access for all potential suppliers.
- **Regulated Access Models**: this approach attempts to establish clear rules and conditions for access. These models aim to enhance competition and ensure that third-party producers can supply heat to the network under transparent and fair conditions.
- **Single-Buyer Model**: in cases where district heating systems are deemed inefficient, a single-buyer model may be proposed, where a central entity purchases heat from various producers and redistributes it, potentially simplifying the access process.

Advances in technology, such as smart metering and data analytics, are enhancing the feasibility of TPA by improving the management and monitoring of heat flows within district heating systems. These technologies can facilitate better coordination between producers and operators, leading to more efficient operations. Digital platforms are being developed to streamline the process of accessing district heating networks, allowing for more transparent and efficient transactions between third-party producers and district heating companies. Analog cases, for electricity sharing within renewable energy communities, are experimenting with the introduction of blockchain to regulate the energy and monetary transition between prosumers.

Most EU member states view district heating (DH) as an integrated infrastructure, which is classified as a natural monopoly that necessitates a vertically integrated supplier responsible for both the production and delivery of heat to consumers. Except for Poland, no member state has implemented full third-party access (TPA), which would enable independent heat companies to utilize the heating grid to serve their customers. In Poland, however, the option for grid access remains underutilized due to overly complex and restrictive regulations. Some EU member states do permit grid access on the production side (Producer TPA), where such access is regulated. For instance, in Estonia, when new heat production capacities are needed, the grid operator is required to issue a public call for heat producers

to identify the most cost-effective offer. In Latvia, grid operators must purchase thermal energy from all heat producers, including independent ones, as long as the price is below a specified threshold and technical conditions are satisfied. Agreements between heat producers and grid operators must comply with the stipulations of the Latvian Energy Law. A similar framework exists in Lithuania. Conversely, some countries, such as Sweden, Austria, and Germany, lack any TPA regulations, with grid access being negotiated voluntarily between the involved parties. Denmark adopts a different approach, where the DH market is primarily characterized by non-profit ownership structures and legislation that prioritizes customer interests. Consequently, policymakers do not perceive a need to enforce TPA. Nonetheless, day-ahead heat plans are created based on bids from various heat producers within the DH network of the greater Copenhagen area. However, the Danish model is not representative of most DH markets in Europe, where such socio-economic goal-driven legislation is absent.

The implications of dynamic heat pricing mechanisms were investigated in [71]. The authors analyzed two case studies in Sønderborg, Denmark, and Espoo, Finland, to explore how dynamic pricing can facilitate the integration of low-cost heat sources, such as waste heat and geothermal energy, into existing DH systems. Starting from the two real systems, a set of simulations was performed in Matlab to test the DH systems under various pricing scenarios. The authors analyzed the weighted average marginal heat prices and total turnover across different configurations, including scenarios with waste heat and geothermal heat. The methodology also included the introduction of thermal energy storage to assess its impact on pricing and turnover. This systematic approach allowed for a realistic evaluation of how dynamic pricing could alter the operational landscape of DH systems. The resulting dynamic pricing showed a reduction in total primary energy consumption and CO_2 emissions. In Sønderborg, the weighted average heat price decreased by 25.6%, while in Espoo, it dropped by 6.6%. The inclusion of low marginal cost heat sources shifted the marginal cost curves, indicating good prospects for lower prices during peak demand periods. The study highlighted that natural gas heating plants typically set marginal prices, but the integration of waste heat and geothermal sources could lead to substantial cost reductions. The dynamic pricing mechanisms are essential for fostering the integration of waste heat into DH systems, thereby enhancing sustainability and economic efficiency. The study underlined challenges related to third-party access to DH networks, which can hinder the delivery of excess heat from alternative sources. The existing monopolistic structures in DH markets often complicate the integration of third-party suppliers, necessitating regulatory reforms to facilitate equitable access.

The marginal cost-based pricing mechanism for the open district heating system in Espoo (Finland) is analyzed in [72]. The methodology employed a Matlab-based simulation to evaluate the potential for external heat sources, specifically waste heat from a metro center and solar heat plants, to contribute to the DH network. An hourly model was implemented to reflect real-time cost variations, addressing the limitations of the traditional rigid pricing systems prevalent in Finnish DH. The results of the simulations indicated substantial cost savings when integrating external heat sources. Waste heat, when combined with heat pumps, could effectively replace more expensive heating methods, particularly during peak winter demand. The analysis revealed that the total annual cost savings could be significant,

with external heat providers potentially achieving a payback period of a few years on their investments. The findings underscored the economic attractiveness of this model for all stakeholders involved, including consumers and external producers. The direction towards a market-based approach in DH pricing is paved. The authors argued that the current pricing system, characterized by its natural monopoly structure, fails to reflect actual production costs and does not incentivize energy-saving measures during peak demand periods, since rigid pricing can lead to inefficiencies and higher costs for consumers. The introduction of real-time, marginal cost-based pricing is proposed as a solution to enhance transparency and encourage more efficient energy use.

The paper [73] examined a set of pricing strategies within district heating systems, particularly in the context of monopoly markets. The importance of district heating in cold climates represents the primary source of thermal energy for both household and industrial consumers. A mathematical model, based on classical monopoly market principles, was proposed to analyze three pricing variants:

1. **Free Pricing Based on Market Equilibrium** that allows prices to be determined by the balance of supply and demand for heat energy, reflecting a liberalized market approach.
2. **Regulation Tariff Based on Average Total Costs (ATC)** in which the tariff for household consumers is set at a level that covers the average total costs of production and transportation of heat energy, allowing the Heat Supply Company (HSC) to achieve a profit margin.
3. **Regulation Tariff Based on Marginal Costs (MC)** sets the tariff for household consumers at the level of marginal costs, which are the costs associated with producing and transporting an additional unit of heat energy. While this method results in lower prices for consumers, it may not cover the fixed costs of HSC, potentially leading to financial losses for the company.

The analysis incorporated various heat production scenarios and their associated costs, providing a comprehensive framework for understanding the dynamics of heat pricing. The results revealed that the pricing strategies significantly impact on the profitability of the Heat Supply Company (HSC) and the costs borne by consumers. In the liberalized market scenario, HSC maximizes profits, while the regulated pricing based on marginal costs leads to losses due to insufficient tariff coverage of fixed costs. The discussion indicated that setting household tariffs at the level of average total costs allows HSC to achieve a modest profit, while household consumers benefit from the lowest prices under the marginal cost regulation. The transition from regulated tariffs to the free pricing model in the heating market would lead to a sharp increase in the heat energy tariffs for household consumers (by 30%) and gaining excess profit by HSC (more than 17%).

An example of the application of two different regulatory frameworks for heat pricing in South Korea is presented in [74]. A theoretical framework based on the one proposed by Joskow and Jones (1983) is proposed to analyze how price regulation influences the optimal capacity composition of combined heat and power (CHP) and heat-only boilers (HOB) in a

monopolistic market. The economic modeling approach proposed aims to assess the impact of two types of price regulation:

1. **Price-Cap Regulation (PC)**: a set maximum price can be charged to the consumers by the monopolistic district heating provider. The findings indicate that under this regulation, the heat production mix is economically optimal, encouraging the provider to minimize costs and enhance efficiency.
2. **Rate of Return Regulation (RoR)**: this mechanism allows the provider to earn a specified return on its investments. However, the study reveals that RoR regulation tends to maximize CHP investment without incentivizing cost reduction, leading to inefficiencies in the heat production mix.

A proposed way to improve the environmental value of the district heating supply without expanding CHP capacity is the replacement of fossil energy HOBs with renewable or carbon-neutral equivalents such as biomass boilers or electric boilers using renewable electricity sources such as solar and wind power, in exchange for higher investment costs. This approach may require governmental support to make district heating operators economically viable.

The paper [75] presented a comprehensive analysis of dynamic heat pricing in low-temperature district heating (LTDH) systems. This mechanism was modeled as a Stackelberg game, where the heat provider sets hourly heat prices in advance (upper-level problem), and consumers adjust their heat demand based on these dynamic prices to minimize their costs (lower-level problem). The dynamic pricing approach allowed for flexibility in heat demand response, facilitating better alignment between production and consumption while optimizing operational costs for the provider and potentially lowering costs for consumers compared to a flat pricing mode. The model is applied to a groundwater-based LTDH system involving one producer and three consumers, giving a detailed evaluation of operational costs and average heat prices compared to a flat pricing model. The results indicated that the implementation of dynamic heat pricing significantly enhances the flexibility of heat demand response. Consumers adjust their heat usage based on price signals, leading to optimized operational costs for the provider. In this way, dynamic pricing can lower consumer costs while maintaining provider profitability, thus highlighting the potential for improved economic efficiency in district heating systems.

The viability of competitive wholesale district heating systems, focusing on the implications of marginal-cost pricing (MCP) for various heat production technologies in the Netherlands is presented in [76]. A linear programming model that integrates heat supply and demand to deliver hourly dispatch and market prices is adopted. This approach is used to determine the market prices for heat production based on the short-run marginal costs of the various heat producers. The study revealed that while MCP can lead to cost-efficient dispatch of heat generators, it may not provide sufficient revenues for heat producers to recover their fixed costs, which poses challenges to the sustainability of the district heating market. The results indicated a significant under-recovery of fixed costs for most heat producers, ranging from 60% to 90%, with the notable exception of waste incineration combined heat and power (CHP) plants, which show a return on investment of 44% and 12% in different scenarios. The study highlighted that while MCP can facilitate cost-efficient dispatch, it fails to provide

sufficient revenue for heat producers to recover their investments, thus missing the economic sustainability aims of the district heating market. This underlined the critical theme of heat pricing, as the current pricing mechanisms do not adequately reflect the costs associated with maintaining and expanding heat generation capacity. Two aspects are found to be crucial in selecting appropriate methods to determine the fixed charge and payments of the heat producers: rewarding more cost-efficient generators to obtain the lowest total system cost for the end-user and allowing for the entry of new, more efficient, and environmentally friendly heat production plants.

What is the impact of the prosumers on heat pricing in the DH market? Up to now, scientific literature has not given a comprehensive overview of the state of the art. The study [77] presented a systematic review of business models (BMs) for prosumer integration in the district energy (DE) sector, focusing on the flexibility that prosumers can offer. The study showed significant diversity in how benefits are considered across the literature reviewed, with a predominant focus on marginal cost (MC) pricing as a method for evaluating the economic viability of prosumer heat. The study highlighted that while MC pricing is prevalent, it often neglects the investment costs associated with prosumer-side technologies, which can disincentivize potential investments. This finding underlined the complexity of pricing logic in the DE sector, where the price charged by DE companies and the price offered to prosumers for their heat can vary significantly. Furthermore, the computation of benefits is influenced by the control over prosumer-side technologies, which vary across different business models and specific case studies. The conclusions drawn from the analysis indicate that there is no singular pattern for prosumer integration in the DE sector, reflecting a lack of consensus on how benefits should be computed and the decision-making logic involved. The authors emphasized the need for a more unified approach to understanding the economic implications of prosumer participation, particularly concerning heat pricing.

Regarding third-party access (TPA), there are a few examples of full investigation and clear regulation. The report [78] provided a detailed examination of the potential for TPA within Finland's district heating sector. Currently, district heating in Finland is predominantly supplied through a market-based system with minimal regulation. Approximately one-third of the district heat produced is sourced from third-party producers, primarily through voluntary agreements. Most of the third-party heat sources in the Finnish Energy statistics are either industrial waste heat or heat from industrial CHP plants. In addition, an increasing amount of waste heat from data centers has been supplied for district heating. The companies actively search for available heat sources within their networks that can be utilized in district heating cost-efficiently. If the heat produced by a third-party is available at a competitive price compared to its own production, it will be utilized. The cost-efficiency of the heat source depends on the amount of available heat and potential network expansion and strengthening costs. Furthermore, the heat source must meet the technical quality requirements of the network. In the existing voluntary TPA, the district heating company buys heat from the third-party producer. The heat may be distributed to either the supply or return (lower temperature) line depending on the temperatures of the heat source and the needs of the network. The bilateral conditions include, for example, the length of the purchase agreement, division of network expansion (and strengthening) costs between the TP producer and the energy company and the temperature demands for the third-party heat.

Obviously, as the value and the temperature levels of the return water are lower than on the supply side, the prices for the heat distributed to the supply side are notably higher. In many cases, supply to return water is not possible and could have negative impacts on the network and other production capacity. The price paid by the energy company may differ during different seasons of the month as the demand for heat is higher during the heating season compared to summertime, or the TP heat is not purchased at all during summertime. The report proposed a set of simulations which aim to analyze three different TPA models:

1. **Single-buyer with open and transparent access conditions**: it is a TPA framework where the district heating company serves as the sole buyer in the wholesale heat market. It allows third-party producers to access the network through voluntary agreements, promoting transparency in pricing and connection terms. This model does not require the unbundling of heat production, distribution, and sales, simplifying regulation. A heat marketplace is established for transactions, with connection fees based on general terms to ensure fairness. The aim of this model is to enhance competition and efficiency in the district heating sector while maintaining a straightforward regulatory approach.
2. **Single-buyer with regulated wholesale competition**: in this model, the district heating company manages both the network and retail operations while purchasing heat from various producers. This model requires ownership unbundling, ensuring unbiased competition in heat production. Producers can offer their heat to a regulated marketplace, where prices are set based on marginal production costs. Although customers cannot directly choose their heat producer, the distribution company can provide different pricing options. This model aims to foster competition in the production market while maintaining regulatory oversight to ensure fair treatment of all producers and efficient operation of the district heating system.
3. **Network access (full-scale)**: this model allows all heat producers to access the district heating network on a non-discriminatory basis. In this model, customers can contract directly with heat producers or retailers, separating network operations from production. The distribution company is responsible for maintaining the network and balancing supply and demand. Customers can choose from multiple producers, fostering competition like electricity and gas markets. This model emphasizes transparency in transmission pricing and conditions, aiming to enhance competition and customer choice while potentially increasing complexity in regulation and operations.

The results showed that the first model, which reflects the current system, resulted in lower administrative costs compared to the more complex models. This model allows for voluntary agreements and does not require extensive unbundling, making it easier for district heating companies to manage. Conversely, it might not significantly enhance competition in the market, as it does not fully open the market to multiple producers. The second model showed that while it could foster competition in heat production, the administrative costs associated with unbundling production from distribution were significant. The complexity of managing multiple producers and ensuring fair pricing could lead to increased operational costs for the district heating companies. In this case, competition might be limited due to the dominance of a few large producers, which could necessitate regulatory oversight to prevent market

abuse. Finally, the simulation results for the “network access” model showed that it could significantly enhance competition by allowing customers to directly choose their heat producers. This could lead to more competitive pricing and innovation in heat production. However, the model also introduced complexities in network management and regulatory requirements, which could increase costs for the district heating companies. The need for transparent pricing and conditions for network access was emphasized. Finally, the report identifies potential challenges associated with implementing a regulated TPA model. These include the administrative burden on district heating companies, which may increase operational costs and complicate existing business models. Furthermore, the report warns that without adequate regulatory support, the integration of third-party producers could undermine the profitability of current district heating operators, potentially discouraging long-term investments.

The main challenges for an effective introduction of a comprehensive TPA regulatory framework were analyzed in [79]. The introduction of TPA adds layers of regulatory requirements that must be managed effectively. This complexity can create barriers to entry for new market participants and complicate the regulatory landscape, especially if the unbundling of services is not implemented. Then, there are several issues due to the monopoly structure: DH systems often operate as natural monopolies, which necessitates careful regulation to ensure fair and non-discriminatory access for third parties. Without adequate regulations, incumbent suppliers may exploit their market power, limiting competition and consumer choice. Without proper enforcement of competition and regulatory measures, consumers may face limited choices and higher costs. From the economic point of view, the authors highlight the challenge of determining how to allocate costs associated with maintaining and upgrading DH infrastructure. This includes balancing the financial responsibilities between existing operators and new entrants, which can affect the economic viability of TPA. Furthermore, the existing market structure and the relationships between different stakeholders can hinder the effective implementation of TPA. The paper noted that the interplay between various energy sources and technologies complicates the competitive landscape. Another topic is the relationship between TPA and the penetration of RES. TPA alone may not be sufficient to drive the integration of renewable energy sources into DH systems. Complementary policies and measures are necessary to support the transition towards more sustainable energy solutions. Finally, it is necessary to align TPA framework conditions to the national legislation. The varying institutional setups and market conditions across different EU member states present additional challenges. Tailoring TPA regulations to fit these diverse contexts is essential for successful implementation.

From the reviewed literature emerges the gap of the prosumer point of view, related to its relationship with the heat market (Heat pricing and TPA). How can the prosumer be included in a DH market? Under which conditions? How should it manage its decentralized plant to comply with the request of the DH market? An economic analysis carried out for an example of a prosumer equipped with a RES plant is given, with the aim of tracing an operational border.

4. Modeling and validation of a bidirectional thermal substation

The investigated literature on thermal prosumer highlighted the necessity of defining a modeling framework to go in-depth into the prosumer thermal systems. In the previous chapter, several studies based on thermal prosumers and DHN expansion were presented, but the majority of them is based on the analysis of DHNs on a global scale, the entire system is analyzed and there is a research gap on the study of the components that characterize these systems.

In a recently published paper, Pipicello et al. [80] introduced a design for a bidirectional substation tailored for prosumers within district heating networks (DHN), accompanied by a comprehensive experimental analysis of both full- and part-load operations. Addressing the existing gap in literature regarding the modeling of prosumer substations, this research presents a dynamic model that simulates the experimental system outlined in [80], using TRNSYS software. Experimental study is out of the scope of the present research and was taken as starting point for the modeling study. The model incorporates the control logic necessary to maintain the temperature setpoint for both the water supplied to the end user and the hot water delivered to the DHN. Initial simulations, based on experimental data from [80], are conducted to validate the model. Then, to illustrate the model's capability, an office building is assumed to be a potential prosumer thanks to the heat available from solar thermal collectors installed onsite. Note that solar thermal energy was considered here due to the large, recognized potential of this source in supplying DHNs. Finally, in general terms, the provision of validated modeling of a prosumer substation will then enable:

- assessing the potential heat output of prosumers utilizing various onsite generators (e.g., renewable cogeneration plants, solar thermal systems, heat pumps, and low-grade waste heat flows), while considering temperature and flow rate limitations;
- testing new supervisory control strategies designed to enhance energy efficiency or address technical challenges (e.g., high return line temperatures, pressure drops, etc.)

4.1. Description of the reference experimental substation

The four possible connections between the prosumer's substation and the district heating network were investigated in [81] and [82]:

- **Supply-to-return**: The fluid heated by the decentralized generation system (DG) is extracted from the supply pipe and reintroduced into the return line of the DHN. This configuration allows for the direct heating of the return flow, which can lead to an increase in the temperature of the return circuit. It is less commonly adopted due to the potential complications it introduces in network management, particularly regarding temperature control and regulation strategies.
- **Supply-to-supply**: This scheme connects only with the supply circuit for thermal energy exchange from the decentralized production system toward the distribution network. The decentralized system feeds thermal energy directly into the supply line, which can increase the supply circuit temperature. This increase may not be optimal

for utilities that require a constant temperature flow, potentially excluding other decentralized systems from receiving thermal energy.

- **Return-to-return**: Connections to feed heat produced by the DG are located at the return pipe. This scheme allows for the heating of the return flow without affecting the supply circuit directly. It is designed to maintain the existing temperature profile of the supply circuit, thus minimizing regulation issues.
- **Return-to-supply**: The fluid heated by the DG comes from the DHN return pipe and is pumped into the DHN supply pipe. This configuration modifies the current flow of the network, allowing for a more flexible integration of thermal energy. It does not necessarily increase the supply temperature, which helps in maintaining the temperature profile of the network and avoids significant regulation problems. This scheme is widely adopted in existing smart district heating networks due to its efficiency and adaptability.

Figure 14 shows the layout of the experimental substation developed in [80]. The authors proposed the "*return-to-supply*" configuration since it allows the prosumer substation to heat the fluid up to the DHN supply temperature without altering the temperature levels of both the DH supply and return pipes. This configuration is advantageous for downstream users, as it maintains a constant temperature, and it also facilitates thermal management within the DH central plant, especially when additional prosumers are involved in feeding heat into the DHN.

The feed-in flow is drawn from the return line of the district heating network and heated to the supply line temperature by the local generator. Simultaneously, the water flow returning from the served building is primarily heated using the heat generated by the DG, and subsequently, by hot water sourced from the DHN supply line. To facilitate the bi-directional heat exchange, three heat exchangers are employed. Specifically:

- HE1 connects the hydronic loop of the served building directly to the supply and return lines of the DHN, supplying thermal energy to the user from the DHN.
- HE2 links the hydronic loop of the served building to the DG circuit.
- HE3 connects the DG directly to the DHN, operating to transfer any surplus heat produced onsite by the DG to the DHN.

In the experimental setup, the heat generated by the DG is mainly delivered to the user through HE2, and any excess heat is sent to the DHN via HE3, provided that the temperature of the water produced by HE3 meets the supply line temperature setpoint. If the energy supplied by the DG is insufficient to meet the user load, the DHN compensates for the shortfall by exchanging heat through HE1. As illustrated in Figure 14, the testing rig is equipped with a monitoring system that includes temperature, pressure, and flow rate sensors, which are not shown in this schematic; further details can be found in [80].

The operating principle foresees that the thermal output from the DG is primarily utilized to meet the thermal demands of the user, with any excess heat produced by the DG being supplied to the network when it meets the temperature requirements of the supply side. Specifically, the user's thermal load is met by the DHN and/or the DG system through HE1 and HE2, respectively. If the DG system can satisfy the user's load, HE1 remains inactive;

otherwise, it works in conjunction with HE2. In the absence of DG heat production, HE2 does not operate, and the DHN fully meets the user's load. Regarding the heat supplied to the DHN, if the DG production surpasses the user's needs, HE3 transfers the surplus thermal power into the DHN. The prosumer substation contributes heat to the DHN only if the DG can elevate the temperature of the fluid drawn from the DH return pipe to the DH supply level, in which case HE1 is not active.

It is important to underline that the configuration of the substation does not include any thermal storage. This decision was made to focus on evaluating the dynamic behavior of the proposed substation under challenging conditions.

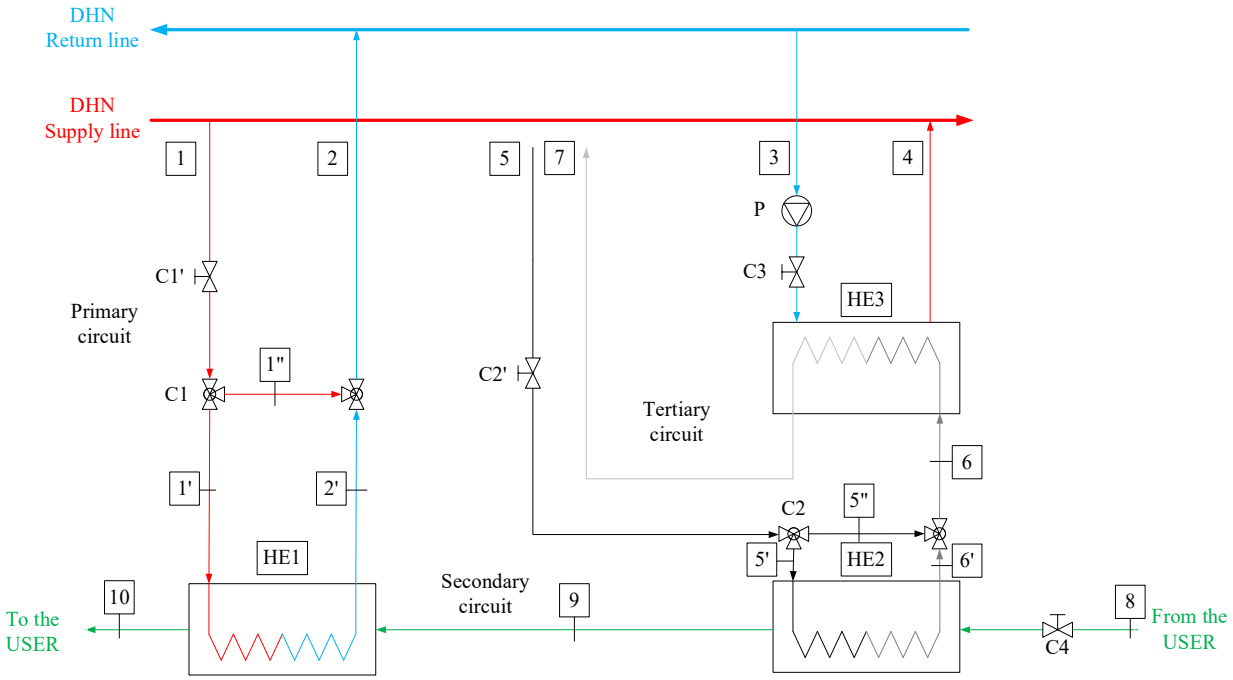

Figure 14: Scheme of the prosumer's substation proposed and tested in [80]

The nominal size of the heat exchangers was selected based on the operating temperatures of the DHN and the hydronic loop of the building. In particular, regarding the DHN, it was considered a return and supply temperatures equal to 50 °C and 80 °C, respectively. These values are typical of a 3rd generation DHN according to [83]. The other nominal temperature levels are 90 °C for the supply line coming from DG, and 60 °C and 40 °C respectively for the supply and return lines of the user circuit. Design parameters are reported in Table 6.

Table 6: Design parameters of the heat exchangers of the substation tested in [80]

Heat Exchanger	Primary side		Secondary side	
HE1	$F_{1'}$	1.20 m^3/h	F_9	1.80 m^3/h
	$T_{1'}$	80 °C	T_9	40 °C
	$T_{2'}$	50 °C	T_{10}	60 °C
	Q	42 kW		
	UA	2.90 kW/°C		
HE2	$F_{5'}$	3.60 m^3/h	F_8	1.80 $0m^3/h$
	$T_{5'}$	90 °C	T_8	40 °C
	$T_{6'}$	80 °C	T_9	60 °C
	Q	42 kW		
	UA	1.20 kW/°C		
HE3	F_3	2.14 m^3/h	F_6	2.80 m^3/h
	T_3	50 °C	T_6	90 °C
	T_4	80 °C	T_7	67 °C
	Q	75 kW		
	UA	5.59 kW/°C		

The substation is equipped with five valves that can be categorized into two types based on their operational logic, as follows (referencing Figure 14):

- Valves C1', C2', and C4 regulate the flow rate of their respective circuits;
- Valves C1 and C2 control the flow rate on the primary side of the heat exchangers, according to the setpoint temperature at the outlet of the secondary side.

To effectively manage the bidirectional heat exchange and meet the user's requirements while adhering to temperature and flow rate constraints, a comprehensive control logic for the substation has been developed. This logic governs the proper functioning of the system (including valve operations, pump speeds, etc.) based on the set points of the control variables. The nominal values for these variables are detailed in Table 7.

Table 7: Substation control variables and nominal values.

Control variables	Nominal value
DG system flowrate (F_7)	2.80 m^3/h
Flowrate from the DHN to HE1 (F_2)	1.80 m^3/h
User flowrate (F_8)	1.80 m^3/h
Minimum feed-in flowrate in the DHN ($F_{3,\,min}$)	0.80 m^3/h
User supply temperature (T_{10})	60 °C
Minimum temperature difference between DG and user ($\Delta T_{5,\,min}$)	5 K
Substation supply temperature to the DHN (T_4)	80 °C
Minimum inlet temperature in the primary side of HE3 ($T_{min,\,DHNfeed}$)	82 °C

Table 8 outlines the controlled variables (C) necessary to achieve the setpoints (SP) for each actuator (A). Additionally, the state of each actuator is contingent upon specific conditions, which may result in it being closed/OFF (for valves) or inactive (for pumps). The implemented control logic utilizes Proportional-Integral-Derivative (PID) controllers.

Table 8: Control logic scheme with reference to the substation layout indicated in Figure 14

Actuator (A)	Controlled Variable (C)	SetPoint (SP)	Condition	Actuator state
C1'	F_2	$F_{2,SP}$	$T_9 \geq T_{10,SP}$ or $F_8=0$	C1' closed
C1	T_{10}	$T_{10,SP}$	$T_9 < T_{10,SP}$	C1' action
C4	F_8	$F_{8,SP}$		C1 action
C2'	F_7	$F_{7,SP}$	($T_5 < T_8+\Delta T_{5,\,min}$) or ($T_6 < T_{min,\,DHNfeed}$ and $F_8=0$)	C4 action
			($T_5 \geq T_8+\Delta T_{5,\,min}$ and $M_8>0$) or ($T_6 \geq T_{min,\,DHNfeed}$ and $M_8=0$)	C2' closed
C2	T_9	$T_{10,SP}$		C2 action
P	T_4	$T_{4,SP}$	$T_6 \geq T_{min,\,DHNfeed}$	P action
			$M_7=0$ or $T_6 < T_{min,\,DHNfeed}$	P OFF

This control logic allows the bidirectional substation to interface with various decentralized generators (DGs), such as solar thermal collectors, micro-cogenerators, or heat recovery units. It is also adaptable for different end-users, including residential buildings, offices, or small industries. However, it is crucial to emphasize that for optimal performance, the control system of the substation must effectively interact with the controls of both the DG and the user's heating system. Nonetheless, verifying the control logic of the substation is essential for ensuring the system operates effectively.

4.2. Description of the virtual model

The described experimental system was reproduced in a virtual environment to create a model that can be scalable and suitable to be implemented into more complex models. The simulation software selected for such a scope was TRNSYS 18. The high flexibility of this software allows for modifying, adding, and connecting several components. In this case, TRNSYS allows for simulating the transient behavior of a substation integrated into a

thermal grid in the case of a variable user's demand or a variation of the heating distributed generation (i.e., solar thermal production strictly related to varying weather conditions).

The modeling phase followed two steps. First, the model was replicated in TRNSYS 18, and the resulting layout is shown in Figure 15. Here, each icon, called "type", represents the physical components of the physical system (valves, heat exchangers, and so on) and controllers. Second, its validation was carried out by replicating the dynamic tests performed in [80].

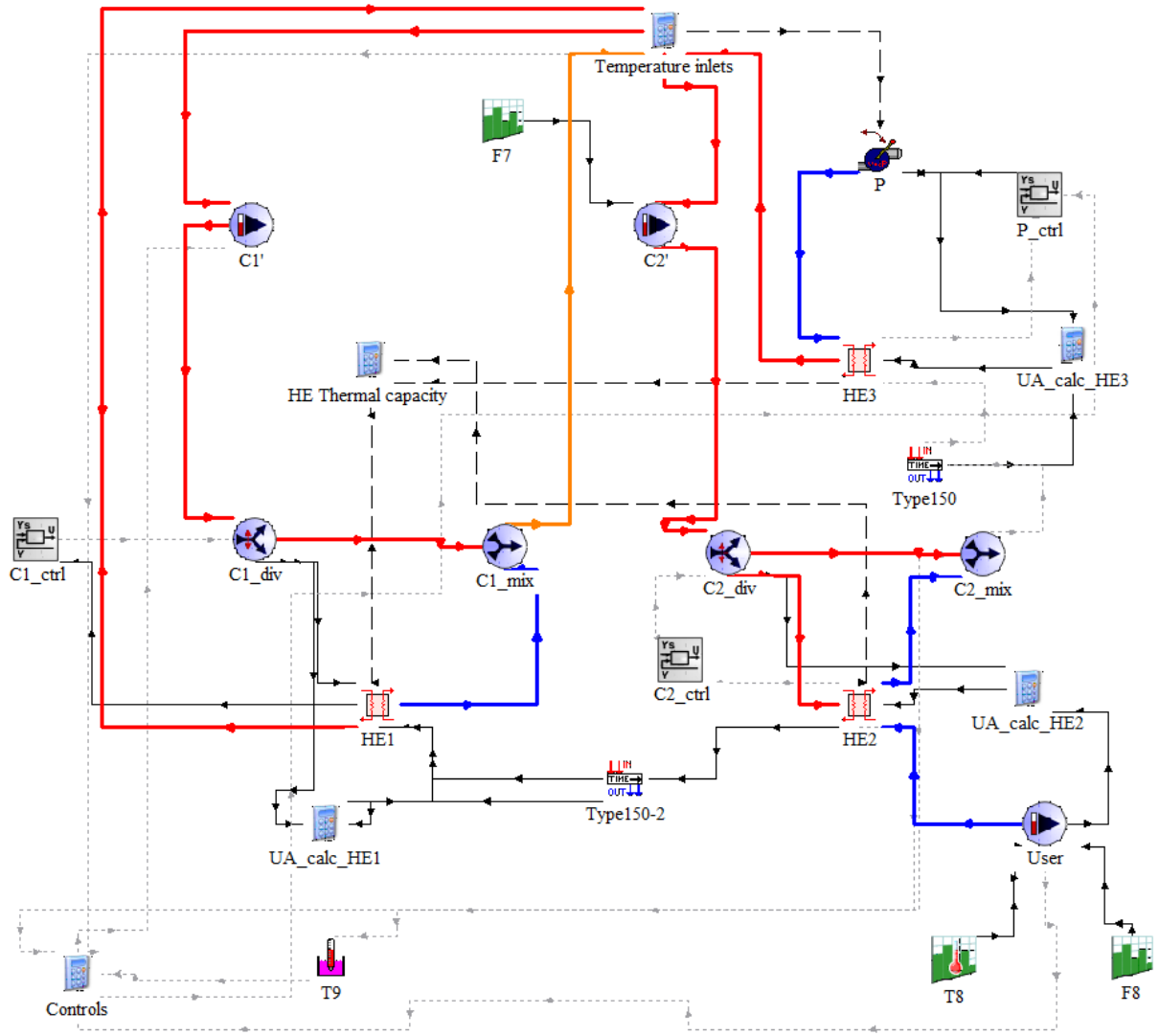

Figure 15: TRNSYS layout of the substation proposed in Figure 14

The heat exchangers were modeled using type 5b (counter-flow heat exchanger). After establishing the specific heat of the fluids flowing through the heat exchanger, type 5b requires the input of both fluids' temperature and flow rate, along with the overall heat transfer coefficient (UA). Since this coefficient is highly dependent on the flow rate, a constant value was inappropriate for this application. Therefore, it was necessary to determine a correction factor for UA to account for variations in flow rates compared to the nominal values. In this study, a simplified approach was utilized. Specifically, by knowing the heat transfer coefficient under nominal flow rate conditions (UA_n), the objective was to achieve the same coefficient under varying flow rates (UA*). The ratio of the heat transfer

coefficients is proportional to the ratio of the Nusselt numbers, which can be expressed in this context using the Dittus-Boelter equation [84]:

$$Nu = 0.023 Re^{4/5} Pr^{n} \quad (6)$$

Considering that the temperature variation from the nominal conditions is not large (a ΔT<30 $°C$ is typically observed for both hot and cold fluids), it was assumed that Pr_n=Pr*, and the ratio between the UA coefficient is proportional to the Reynolds number ratio:

$$Nu = 0.023 Re^{4/5} Pr^{n} \quad (7)$$

$$\frac{UA_n}{UA^*} = \frac{U_n}{U^*} \cong \frac{Nu_n}{Nu^*} \cong \left(\frac{Re_n}{Re^*}\right)^{4/5} \quad (8)$$

Finally, a correlation between flow rate and UA was found as follows:

$$\frac{UA^*}{UA_n} = \frac{\left(\frac{m_h^*}{m_{h,n}}\right)^{4/5} * \left(\frac{m_c^*}{m_{c,n}}\right)^{4/5} * \left[1 + \left(\frac{m_{c,n}}{m_{h,n}}\right)^{4/5}\right]}{\left(\frac{m_c^*}{m_{h,n}}\right)^{4/5} + \left(\frac{m_h^*}{m_{h,n}}\right)^{4/5}} \quad (9)$$

Equation (9) was implemented in a calculator type that, for given nominal and operation flow rates on the hot and cold sides, calculates the overall heat transfer coefficient for each heat exchanger and each simulation time step. This approach gives high flexibility to the model that can be scalable for several applications.

As previously noted, the valves C1' and C2' facilitate the flow passage according to the control logic employed; in the model, these were replaced with pumps (type 110) that operated using the same algorithm as the experimental setup for controlling the valves. The diverter and mixing valves were represented by type 11f and type 11h, respectively, with the flow rate division on the diverter managed by an iterative feedback controller (type 22). This controller was designed to simulate a real feedback controller (e.g., PID) that continuously adapts its control signal or utilizes a discrete timestep significantly shorter than the TRNSYS simulation timestep. The "*C1_ctrl*" depicted in Figure 15 monitors the controlled variable T_{10} and sends a signal to the diverter valve C1, adjusting the flow rate to HE1's primary side from the DHN supply line to maintain T_{10} at the fixed set point of 60 °C. Similarly, "*C2_ctrl*" operates on diverter C2 to keep T_9 as close to 60 °C as possible by varying the water flow from the DG entering the primary side of HE2.

Initial simulations indicated instability due to the interaction between the controllers, prompting the introduction of a delay effect (type 150) to address this problem. It is important to note that this delay effectively represents the hydraulic inertia of the system.

Lastly, the pump "P" shown in the experimental layout was modeled using type 741. An iterative feedback controller adjusts the flow rate of the pump, using the outlet temperature on the load side of HE3, T_4, as the controlled variable. Specifically, the controller aims to

maintain T_4 at 80 °C. The pump will stop when the inlet temperature T_6 on the source side of HE3 falls below a minimum threshold, set at 82 °C. This function ensures a stable feed-in temperature on the DHN supply line. The pump activation controls that replicate the ones set in the experimental rig were implemented in the calculator type “Controls”. In this calculator a set of equations was introduced to model the operating conditions that let to allow the flow rate circulation in the primary circuit by activating valve C1’, in the tertiary circuit by activating valve C2’, and in the cold side of HE3 by activating the pump P (Figure 14). The control equations are detailed below:

- C1’ is activated if $\begin{cases} T_9 < T_{9,\mathrm{SETPOINT}} \\ F_8 = 0 \end{cases}$ $T_{9,\ \mathrm{SETPOINT}}$ is monitored by a thermostat that is set at 59 °C with a centered dead band of 1 K
- C2’ is activated if $\begin{cases} T_5 < T_8 + \Delta T \\ F_8 = 0 \end{cases}$ V $\begin{cases} T_6 > T_{\mathrm{min,DHN}} \\ F_8 = 0 \end{cases}$ ΔT=5K, $T_{min,DHN}$=82 °C
- P is activated if $\begin{cases} T_6 > T_{\mathrm{min,DHN}} + \Delta T \\ F_7 > 0 \end{cases}$ $T_{min,DHN}$=82 °C

4.3. Model validation

In the experimental study, three dynamic tests were performed by varying temperature and flow rate on the three circuits, to replicate the system operation under severe conditions. The operating conditions of these tests as reported in Table 9. The variation in the user demand was simulated by varying the user return temperature (T_8) and the flow rate (F_8), and a variable DG profile was achieved through a predefined flow rate variation profile (F_7).

Table 9: Operating conditions of the experimental tests performed in [80]

	Test_prod_only	Test_cons_only	Test_pros
HE1	Not operating	Operating	Operating
HE2	Operating	Operating	Operating
HE3	Operating	Not Operating	Operating
F_2 [m^3/h]	-	1.80	1.80
F_7 [m^3/h]	2.80	2.80	0.90-2.80
F_8 [m^3/h]	0-1.80	1.80	0-1.80
T_1 [°C]	-	80	80
T_3 [°C]	50	-	50
T_4 [°C]	80	-	80
T_5 [°C]	90	90	90
T_8 [°C]	40-50	30-40	40-50
T_{10} [°C]	60	60	60

Figure 16 visually illustrates the operation of the three heat exchangers during the proposed tests. *Test_prod_only* concentrated on the functioning of HE2 and HE3 under varying levels of user thermal demands (Figure 16a) and was based on the DG production, which was partially allocated for self-consumption and partially for the DHN. Similarly, *Test_cons_only* assessed the performance of the substation when HE1 and HE2 were in operation (Figure 16b) and was based on the "consumer" mode, where both the DG and DHN meet the entire demand. Lastly, *Test_pros* combined the boundary conditions set in the previous tests and evaluated the system by operating all the heat exchangers while varying the user load and the DG energy production profile (Figure 16c), representing the complete "prosumer" condition.

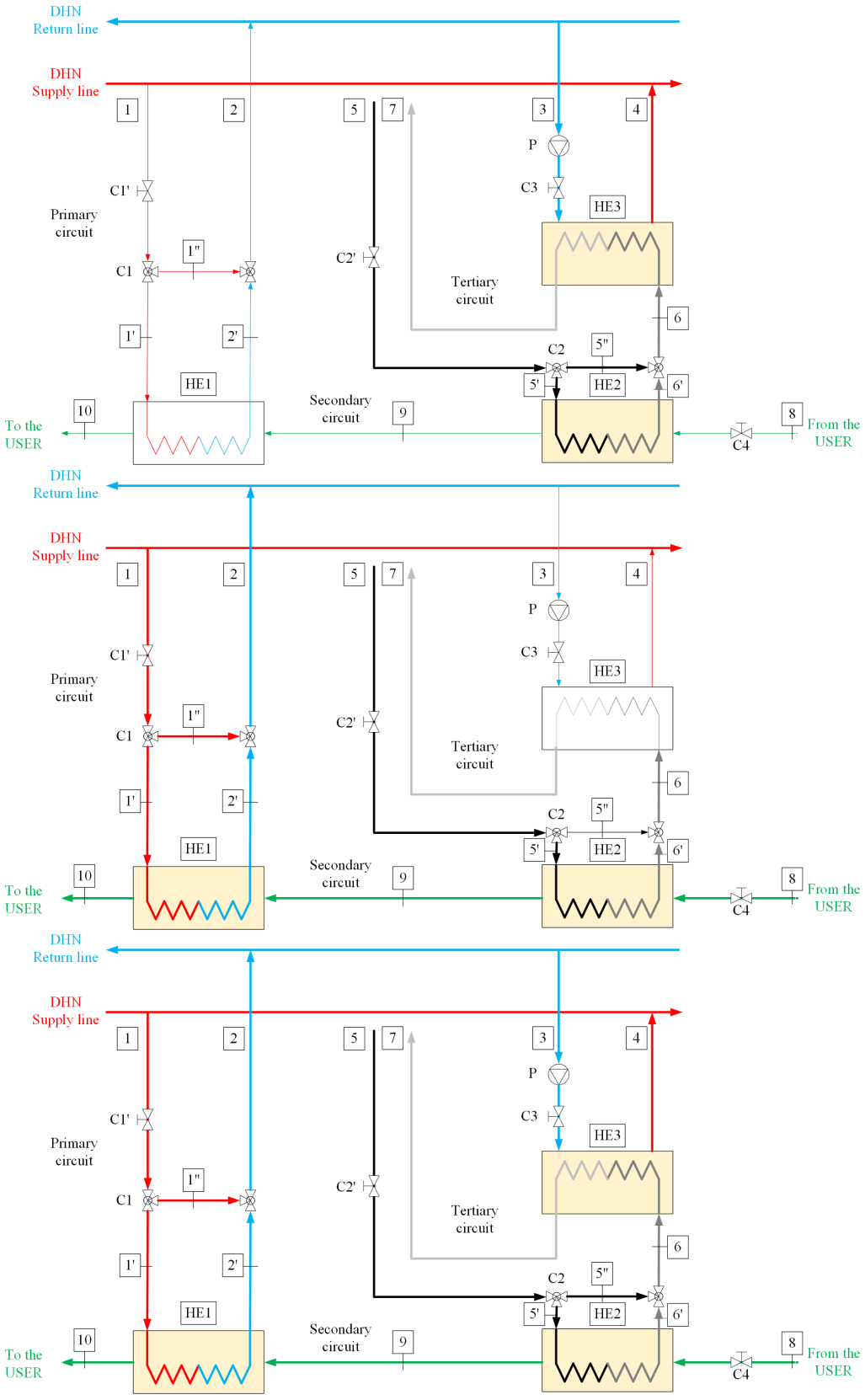

Figure 16: Focus on heat exchangers and lines activated for each test. a) Test_prod_only, b) Test_cons_only, c) Test_pros

The tests listed in Table 9 were replicated in the model using schedule TRNSYS types implemented in type 14h and type 14e, allowing for a comparison between the experimental

and simulation results. The simulation time step was set to 1 minute to accurately reflect the operation of the iterative feedback controller. The duration of the simulation matched that of the experimental campaign, which was seven hours. The test conditions for each experiment are illustrated in Figure 17. The simulation results were then compared with the experimental results presented in [80].

The dynamic timings of the experimental tests were not specified in the adopted study and were out of the scope of the present one. The virtual model aims to reproduce the general trend of the experimental test with a good approximation and, mainly, to achieve the same global results in terms of energy balance. Slight deviations from the instantaneous temperature or heat capacity values were due to: uncertainty of the measurement chain (widely presented in the adopted study), dynamic behavior of the experimental control system (not specified in the adopted study), and computational error in the TRNSYS calculations. As can be observed in the following paragraphs, the virtual model achieved a satisfactory qualitative representation of the experimental system, reproducing the dynamic trend with an acceptable quantitative approximation.

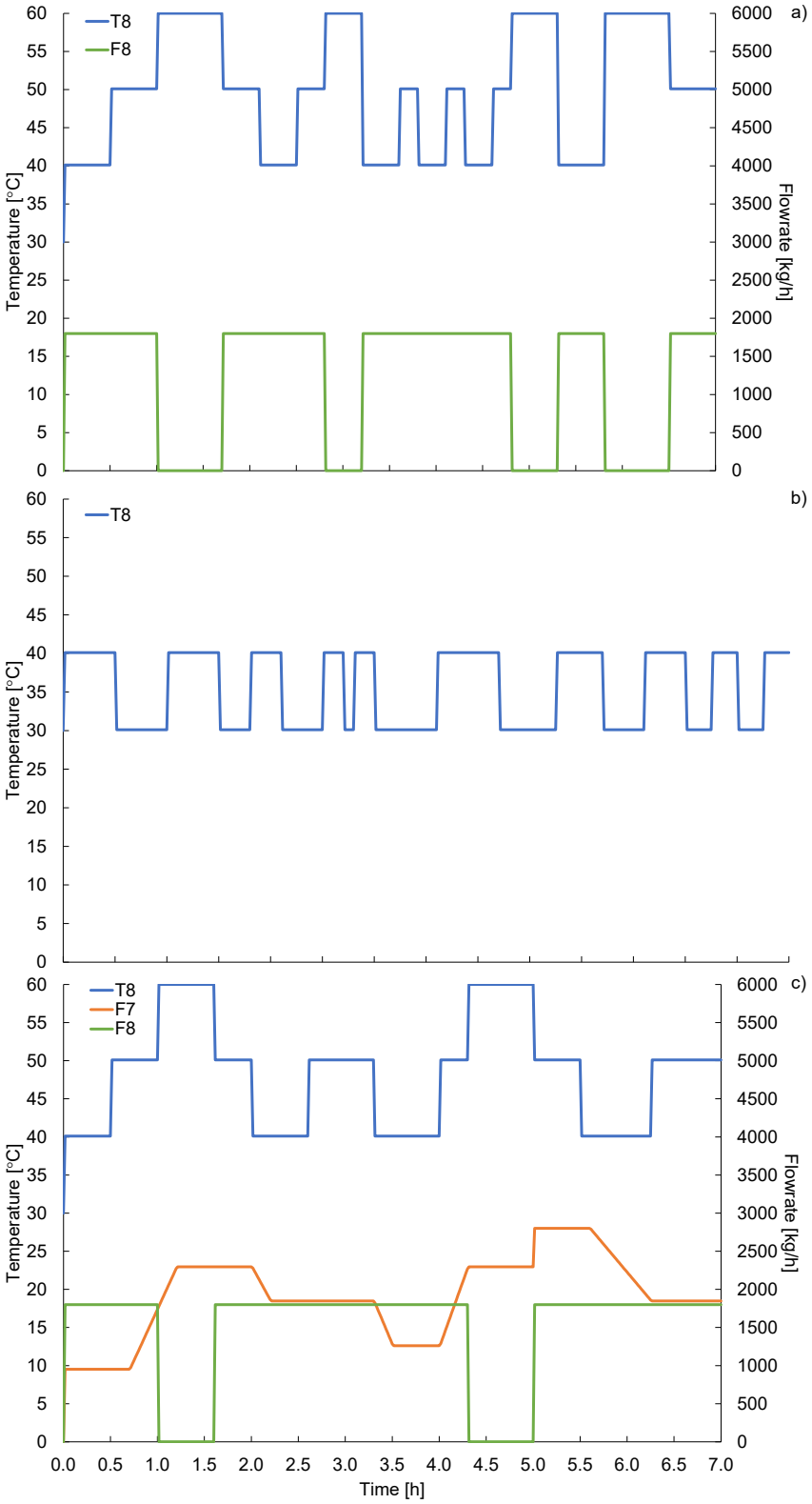

Figure 17: Dynamic conditions imposed on the experimental tests carried out in [80] and replicated in the virtual model. a) Test_prod_only - b) Test_cons_only - c) Test_pros

In *Test_prod_only*, the flow rate and temperature of the user return line were adjusted according to a specified schedule depicted in Figure 17. Specifically, T_8 was varied between 40 °C and 50 °C (representing the maximum and minimum load for *Test_prod_only*), while the flow rate alternated between 1800 kg/h (the nominal value) and 0 kg/h (indicating no user demand). The simulation results demonstrated a strong correlation with the

experimental data. In this context, the temperature profiles at the outlets of HE1 (T_{10}), HE3 (T_4), and the C2 mixer (T_6) are presented in Figure 18.

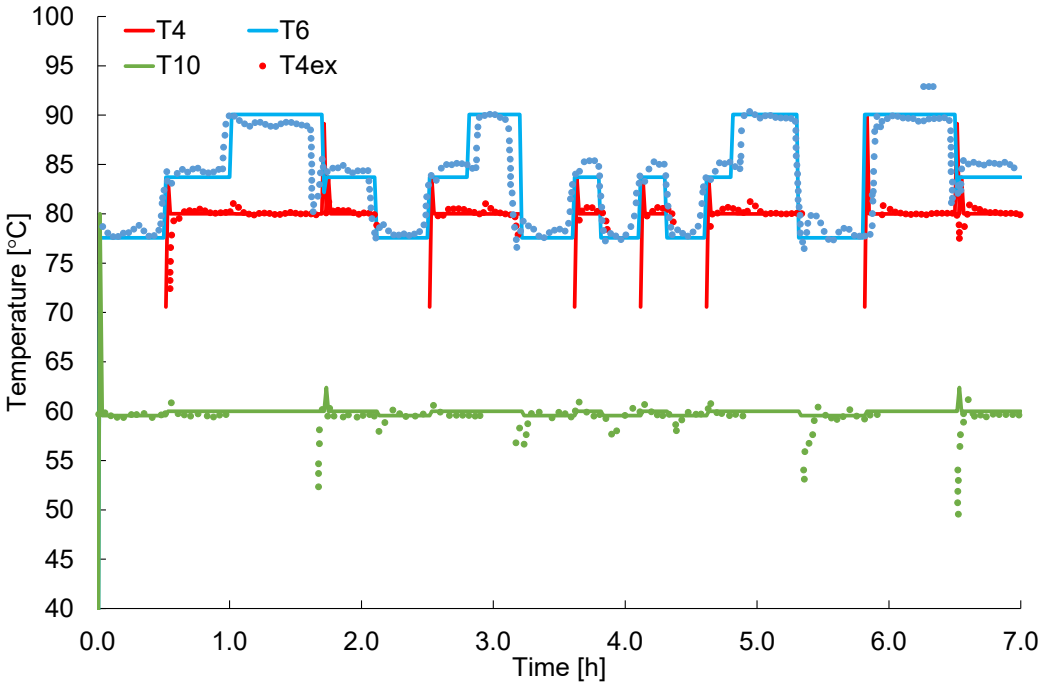

Figure 18: Comparison between simulated and experimental results for Test_prod_only: temperature profiles

The heat transfer profiles illustrated in Figure 19 showed a good agreement for HE2, although a slight discrepancy was observed for HE3. Nevertheless, since the difference between the simulated and experimental values remained, on average, below 10% for Test_prod_only, the model validation was deemed satisfactory.

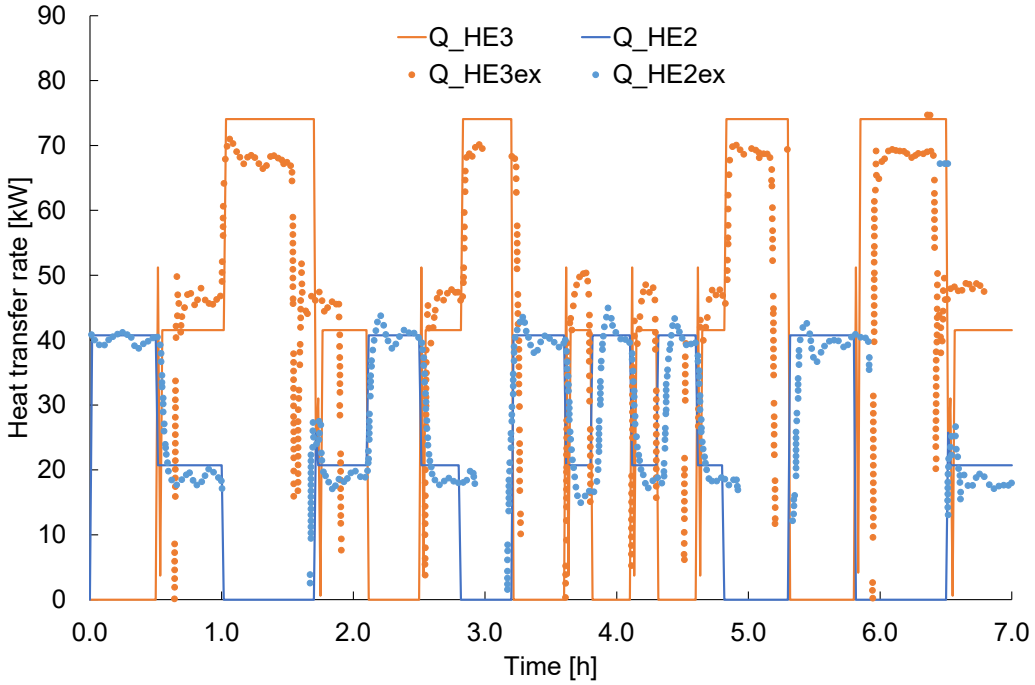

Figure 19: Comparison between simulated and experimental results for Test_prod_only: heat exchanged on HE2 and HE3

In Test_cons_only, only T8 was varied with a defined schedule between 30 °C and 40 °C (maximum and minimum load for the test), and the maximum demand from the users

required the operation of both HE1 and HE2. As in the previous test, good matching was achieved for temperature (Figure 20) and heat transfer rate profiles (Figure 21), with a better correspondence for HE1 rather than HE2. However, a difference of lower than 5% between experimental and simulated values was found.

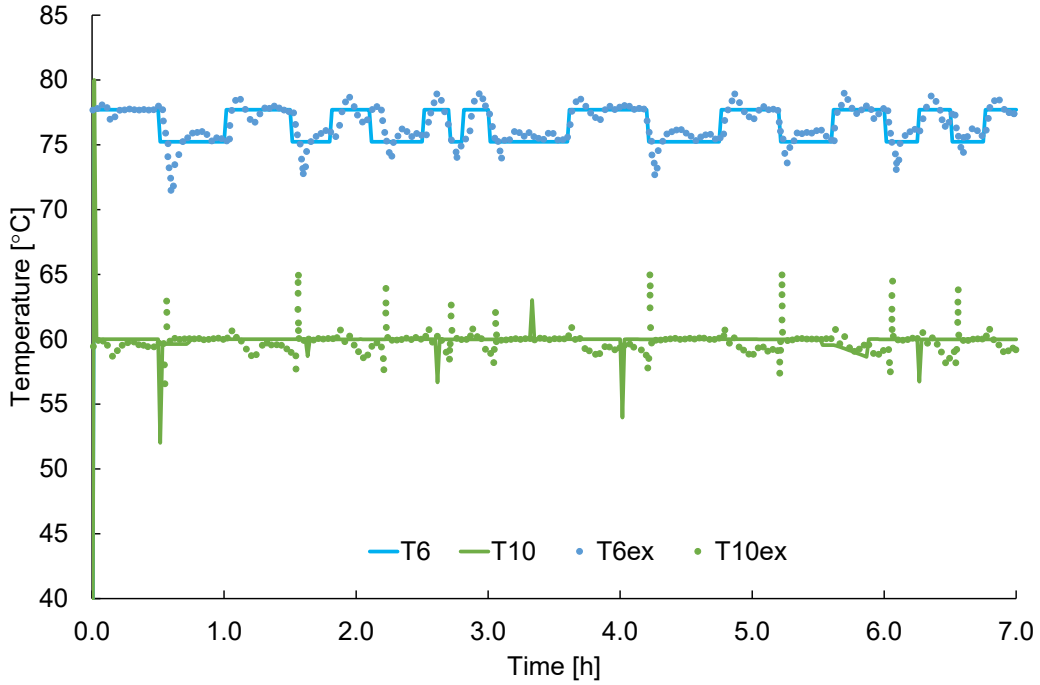

Figure 20: Comparison between simulated and experimental results for Test_cons_only: temperature profiles

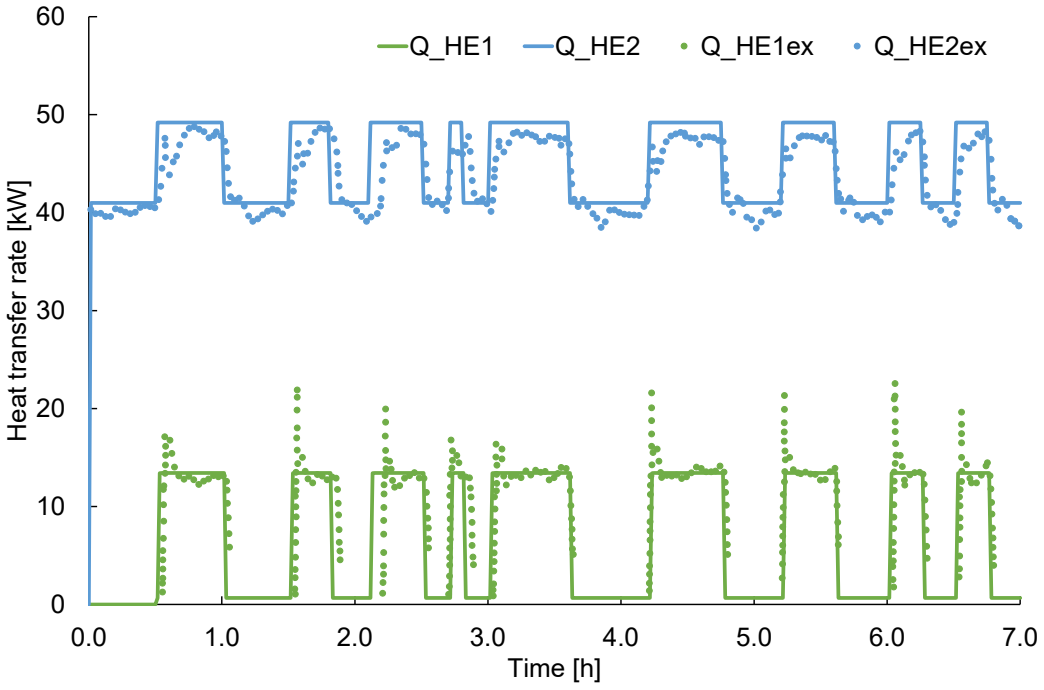

Figure 21: Comparison between simulated and experimental results for Test_cons_only: heat exchange on HE1 and HE2

Test_pros combines variable profiles of the user's demand and DG production, thus involving the operation of all heat exchangers. As shown in Figure 22 and Figure 23 the simulated temperature and heat transfer profiles are like experimental ones. In both figures,

the experimental profiles for T_4 and the heat transfer rate of HE3 show an oscillating behavior between 4-6 hours and 6-7 hours that is not replicated by the simulation results. This is due to the typical thermostat on/off behavior that was not replicated by the simulation model. Conversely, the model reflects both stationary and dynamic trends when no frequent on/off operations occur.

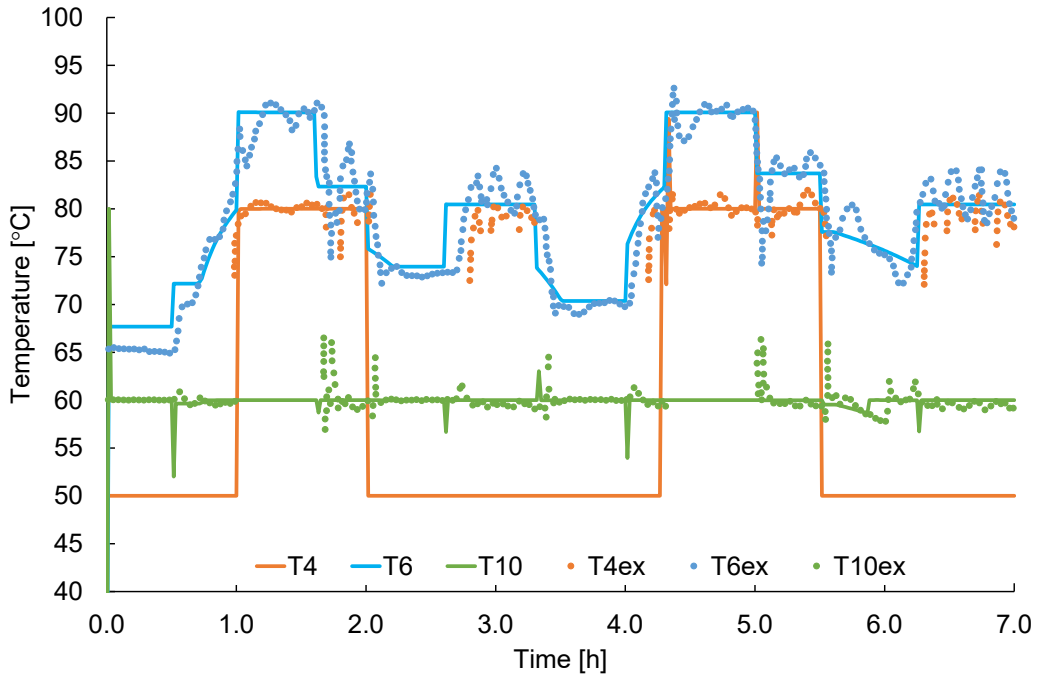

Figure 22: Comparison between simulated and experimental results for Test_pros: temperature profiles

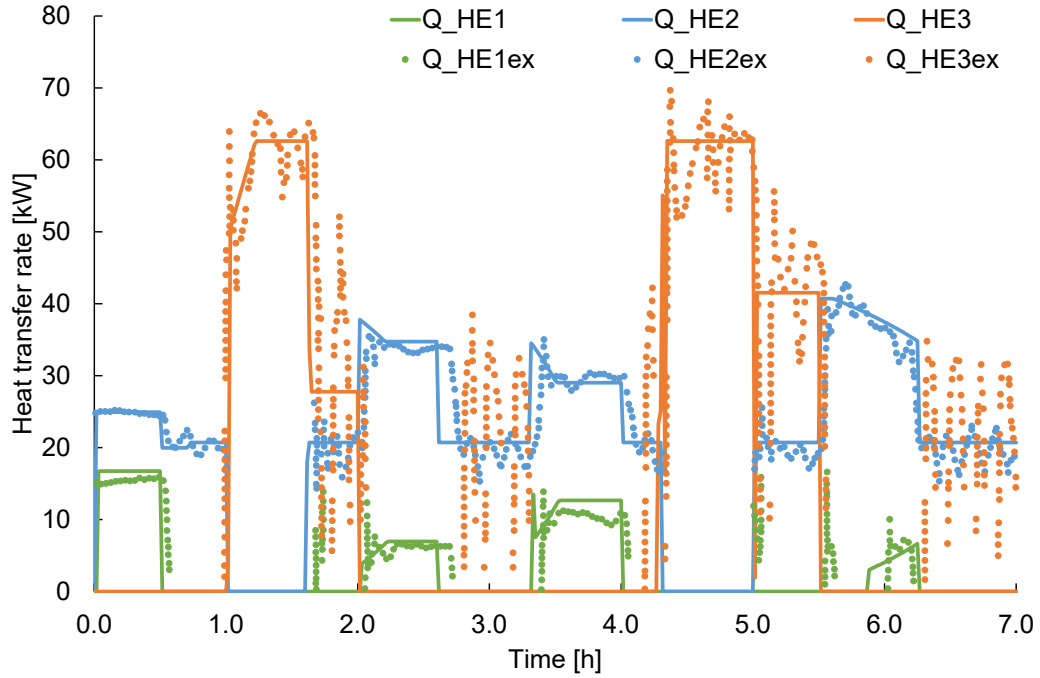

Figure 23: Comparison between simulated and experimental results for Test_pros: heat exchanged in HE1, HE2, and HE3.

The results obtained by the experimental test in terms of the energy balance of the substation and shares of the DG heat production were compared with the simulation results.

The comparison for energy balance, reported in Figure 24, shows a satisfactory correspondence between experimental and simulation outcomes. The thermal losses were neglected in the simulation model since their contribution is not relevant in the overall energy balance.

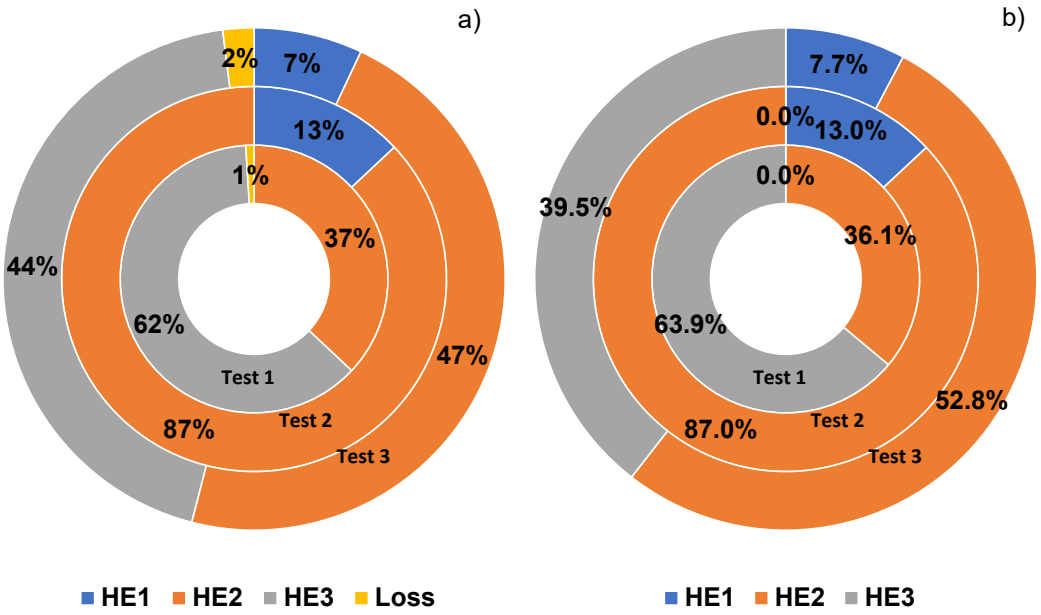

Figure 24: Comparison of energy balance on the heat exchangers. a) experimental results - b) simulation results

Figure 25 reports the comparison of experimental and simulation results in terms of DG energy share between the user (HE2) and the DHN (HE3). Even in this case, the overall balance comparison is considered acceptable, since the differences between experimental and simulation results are neglectable.

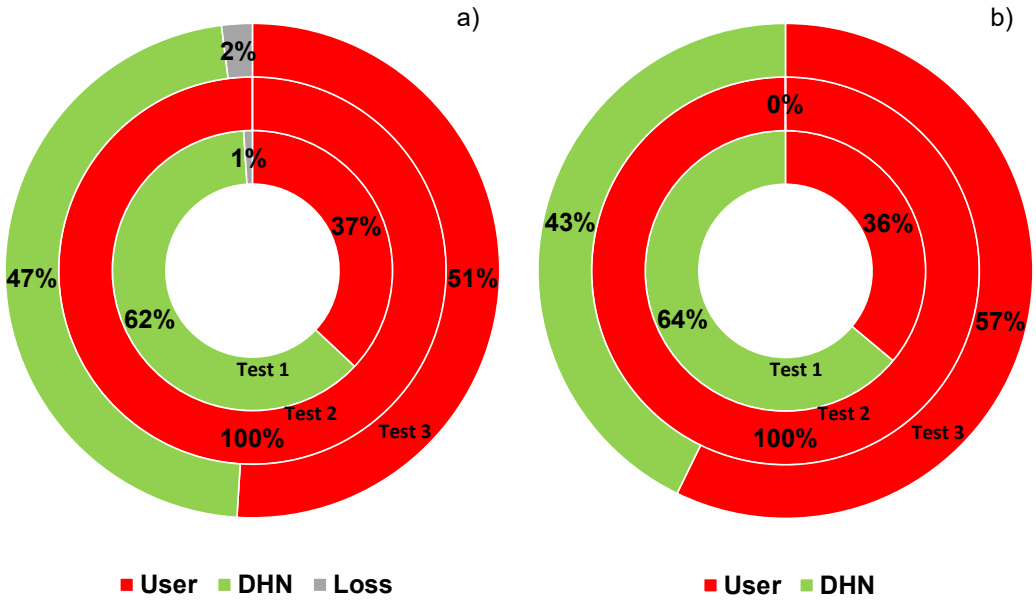

Figure 25: Comparison of DG energy shared between the user and DHN. a) experimental results - b) simulation results

The simulation model reproduced in TRNSYS environment is considered reliable and adequately validated on the experimental values. It is able to reproduce the dynamic trend of the prosumer substation and its overall energy balance.

4.4. Application of the validated model to an example case study

Among renewable energy sources for heat supply in DHNs, solar thermal energy is recognized to play a key role in the decarbonization process [85], [86]. In this regard, in Europe, several DHNs supplied by solar thermal technologies are successfully operating with some promising results [87], [88], [89]. For this reason, the effect of coupling a bi-directional thermal substation with a solar heating system was here investigated. More specifically, the solar thermal system was composed of high vacuum solar collectors whose data, retrieved from the Solar Keymark certificate [90], are reported in Table 10. The performances of the chosen high vacuum solar thermal collectors are aligned to those presented in (reference), coherently with solar Keymark data.

Table 10: Solar Keymark Parameter of the chosen high vacuum solar thermal collector.

Parameter	Value	Unit
Zero loss efficiency (η_0)	0.732	-
First-order coefficient (a_1)	0.50	W/m^2K
Second-order coefficient (a_2)	0.006	W/m^2K^2
Incidence angle modifier IAM (50°)	0.95	-

An office building characterized by a peak of 100 kW_{th} in thermal demand was assumed as the reference user. Two different climates were chosen to evaluate the behavior of this prosumer: Palermo (Southern Italy, Csa climate according to Köppen classification) and Berlin (Germany, Cfb climate according to Köppen classification). Both weather files were retrieved from METEONORM [91] database ("Palermo Punta Raisi" and "Potsdam"). The yearly profiles of heating load were developed by using a "synthetic load" approach.

The Building Energy Signature (BES) [92], [93] can be used to quickly characterize the hourly distribution of the thermal loads of a building whenever the influence of both internal and solar heat gains is neglected. As first introduced by [94] and described in the EN 15603 standard [95], BES is defined as the thermal power P_b required by a building as a function of the dry bulb temperature of the outdoor air T_{ext}.

$$P_b(i) = P_{des} \cdot \left[\frac{T_{HLET} - T_{ext}(i)}{T_{HLET} - T_{des}} \right] \qquad (10)$$

In Eq. (10), P_{des} is the design heat load of the building calculated at the outdoor design temperature T_{des}. T_{HLET} is the outdoor air temperature at which the net heat load of the building is equal to zero. For assessing the influence of heat loads on the seasonal performance of heat pumps, the adoption of T_{HLET} = 16 °C is recommended [96]. Following other studies, based on dynamic modeling of a building's thermal loads [97] or through analysis of experimental data [98], [99], this value has been estimated to be approximately T_{HLET} = 20 °C. Thus, if the series of outdoor air temperature values at each i^{th} hour during the periods when the heating system is on is known, it is possible to calculate the building's annual heat energy demand through the following summation:

$$E_b = \sum_{i=1}^{N} P_b(i) \qquad (11)$$

where N is the total number of plant operating hours in the year.

The simulation was performed for one year of operation. The yearly load profiles of the heating demand for the selected sites are shown in Figure 26.

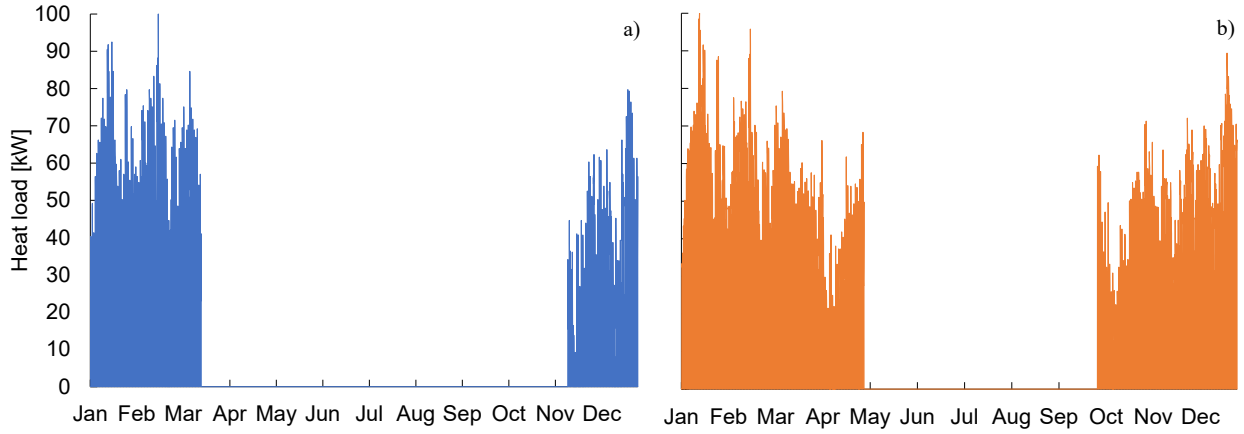

Figure 26: Heat load profile for the selected sites: Palermo (a) and Berlin (b)

The monthly energy request is shown in Figure 27. Yearly, the total amount of heat requested is 78.92 MWh/y in the case of Palermo and 151 MWh/y for Berlin.

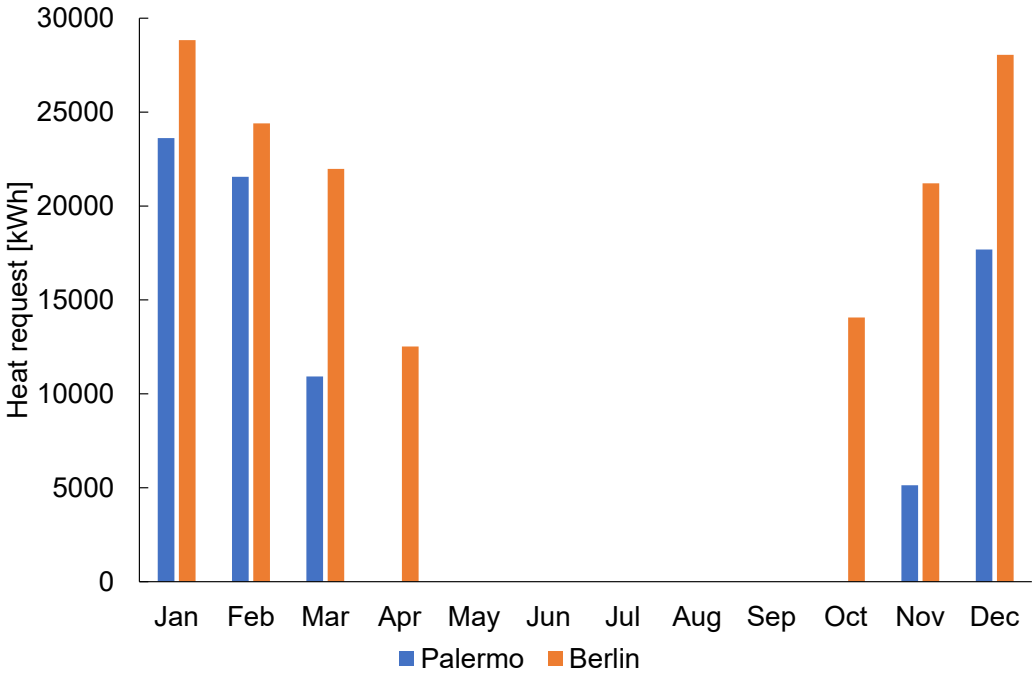

Figure 27: Monthly heating energy demand in the selected sites

The design of the solar DG system was performed according to the peak value of the thermal demand of the user and the nominal operating temperature of the DHN lines. These temperatures were assumed to be equal to 50 °C for the return line and 80 °C for the supply line. A net solar collector surface of 205 m^2 was considered with a temperature outlet set point of 95 °C, a slope of 30°, and a south-facing azimuth angle. The TRNSYS type 539 was selected to model the solar field. This type tries to keep the collector outlet to the outlet set-point temperature by varying the water flow rate. In addition, it shuts off the collector (flow rate = 0) if the collector is losing energy. This condition occurs when the control system detects a negative temperature difference at the outlet and inlet of the collector. Finally, it accounts for the effect of the collector's heat capacity. A safety controller was implemented to dissipate the solar heat surplus through a dry cooler (type 511), thus avoiding overheating and stagnation of solar panels. Finally, the solar field was connected to a stratified buffer tank (type 340) with a nominal volume of 20 m^3 that allows for equalizing the daily peak energy production of the solar system and the distributed energy request by the user. The layout of the solar loop is shown in Figure 28.

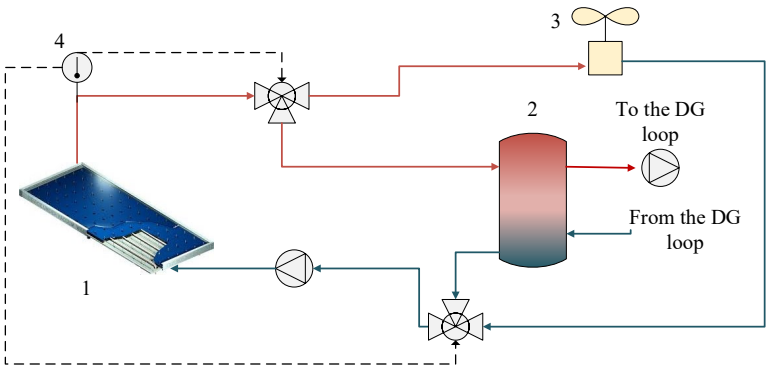

Figure 28: Layout of the solar loop. 1) High vacuum solar collectors, 2) Storage tank, 3) safety dry-cooler, 4) safety thermostat controller

The overall control logic of the substation was not changed compared to the one proposed in the previous paragraph. In particular, the control logic tries to maximize the exploitation of the heat produced by the solar collectors through HE2 and HE3, and it operates HE1 as a backup to cover the fraction of the thermal demand not met by heat available from solar collectors.

The simulation time step was fixed at 1 hour according to the variation of climatic variables and user demand. Finally, the efficiency of solar collector $\eta_{\mathrm{sol}}^{\mathrm{gross}}$ was calculated as indicated in Eq. (*12*):

$$\eta_{\mathrm{sol}}^{\mathrm{gross}} = \int \frac{\dot{Q}_{\mathrm{sol}} dt}{G_{\mathrm{col}} * A_{\mathrm{sol}}^{\mathrm{gross}}} dt \qquad (12)$$

where: $\dot{Q}_{\mathrm{sol}}$is the instantaneous thermal power output expressed in kW, G_{col} is the specific solar irradiation on the collector plane measured in kW/m^2, and *A* is the solar collector's gross surface area (measured in m^2).

The results of the dynamic simulations performed are for a typical week in winter and summer. Some insights on substation operation are also given to allow for a keener interpretation of the interactions among components and controls. Then, yearly energy results are presented.

Figure 29a-b depicts the profiles of the heat transfer rate for each heat exchanger together with the user heating demand, for six typical winter days (more specifically from January 25th to January 31st) in Palermo (Figure 29a) and Berlin (Figure 29b). Note that:

- in the case of Palermo (Figure 29a), HE2, which is supplied by the hourly thermal energy produced by the solar DG, can meet a large fraction of the user heat demand (between 25% and 100%, as indicated by the blue line), except for the last day in which the relative weight of HE1 is predominant due to the low amount of heat provided by the solar DG.
- in the case of Berlin (Figure 29b), a lower amount of heat is provided by the solar field through HE2, and the heating demand is mostly covered by HE1.

The heat transfer rate for HE2 is equal to 30 kW for Palermo and 22 kW for Berlin. In both cases, since the energy produced by the DG is entirely exchanged in HE2, the HE3 is always off. Note that HE3 does not operate for most of the heating period.

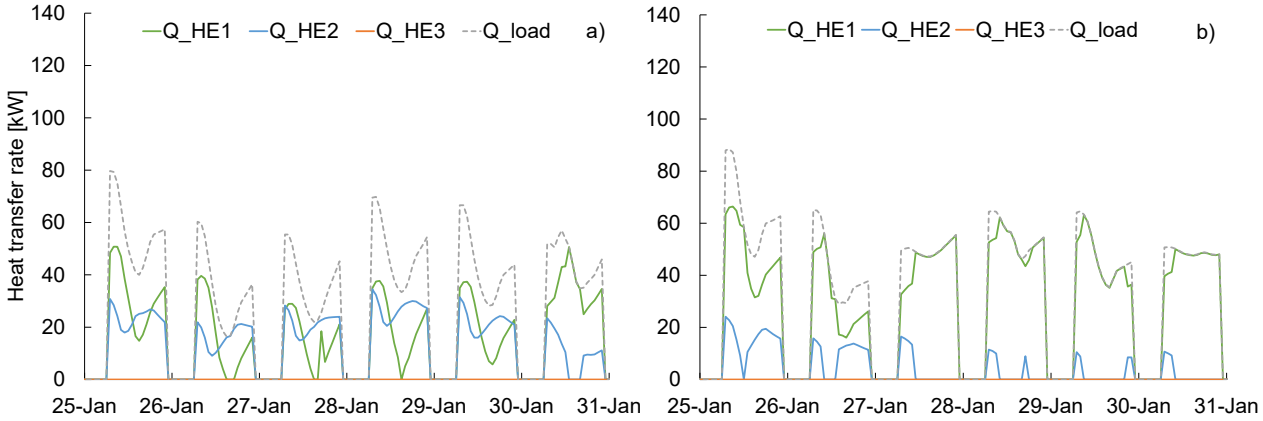

Figure 29: Heat exchangers dynamic trend for six typical winter days: a) Palermo - b) Berlin

In Figure 30 a-b the temperature profiles on the user loop (indicated in Figure 14 as T8, T9, T10,) are shown along with the inlet temperatures on the hot sides of HE1 and HE2 (T1, T5) for a winter day (more specifically, for January 25th, corresponding to the first day of the selected winter period). Following the substation layout shown in Figure 1, the water flow coming back from the hydronic circuit of the building (with a temperature equal to T8) is first heated up by the DG loop through HE2 (T5, inlet on the hot side), then by HE1 (T9 inlet on the cold side). HE1 is activated since the required set-point for T10 is not met. Worth noting that in the case of Palermo (Figure 30a), T5 values are higher than the one observed in Berlin (Figure 30b), with an average difference of 5 °C. The user flow F8 leaves HE2 by maintaining an average temperature difference with T8 of 6 °C for Palermo and 5 °C for Berlin. In both cases, T10 is equal to the desired set-point (60 °C), thus suggesting that the controller C1_ctrl1 is properly controlling the amount of water flowing through HE1. Finally, the temperature of the water exiting HE2 (T9) is higher in the case of Palermo, thus justifying the lower energy contribution of HE1 in this site.

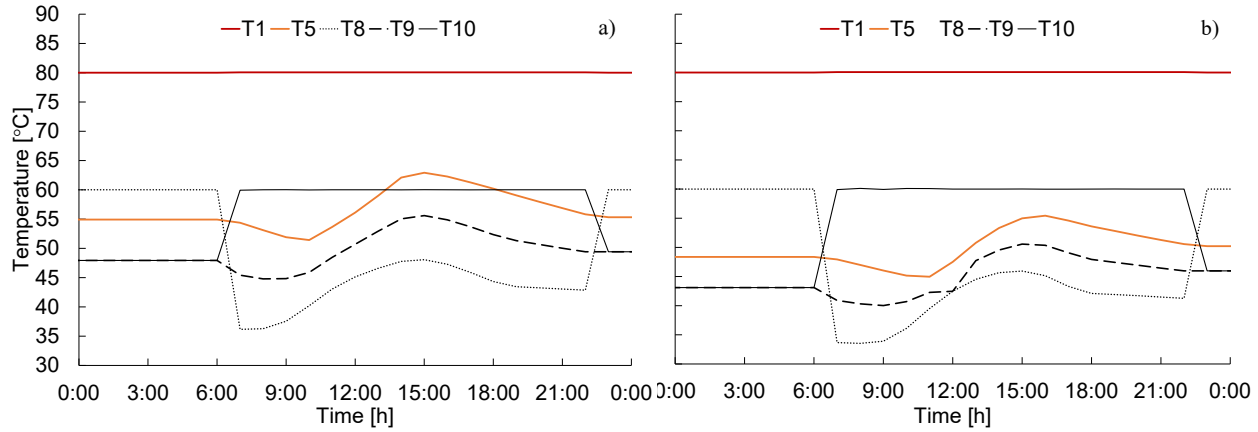

Figure 30: Temperature trends for the user temperature loop and inlet temperature on the hot side of HE1 and HE2 for a typical winter day (January 25th): a) Palermo - b) Berlin.

Figure 31 a-b shows the profiles of the heat exchanged in all heat exchangers for six typical operation days in summer in Palermo (Figure 31a) and Berlin (Figure 31b). In this case, there is no heating demand from the user, so HE1 and HE2 are always off. In the case of Palermo (Figure 31a), the thermal power exchanged with DHN through HE3 is equal to 130 kW, and the heat exchanger is operated for almost 6.5 hours per day. This is due to the continuous availability of hot water at a temperature that is higher than the desired set-point (85 °C) on the heat exchanger's hot side inlet (T6). In Berlin (Figure 31b), although the peak

heat transfer rate ranges between 100-110kW, the profile shows an oscillating behavior due to the lower amount of energy produced by DG and the unavailability of hot water at the desired set point. Once activated the HE3, the buffer tank is rapidly discharged by the energy stored and the controllers stop the operation of the pumps that provide the flow rate on the DG loop (hot side) and DHN loop (cold side).

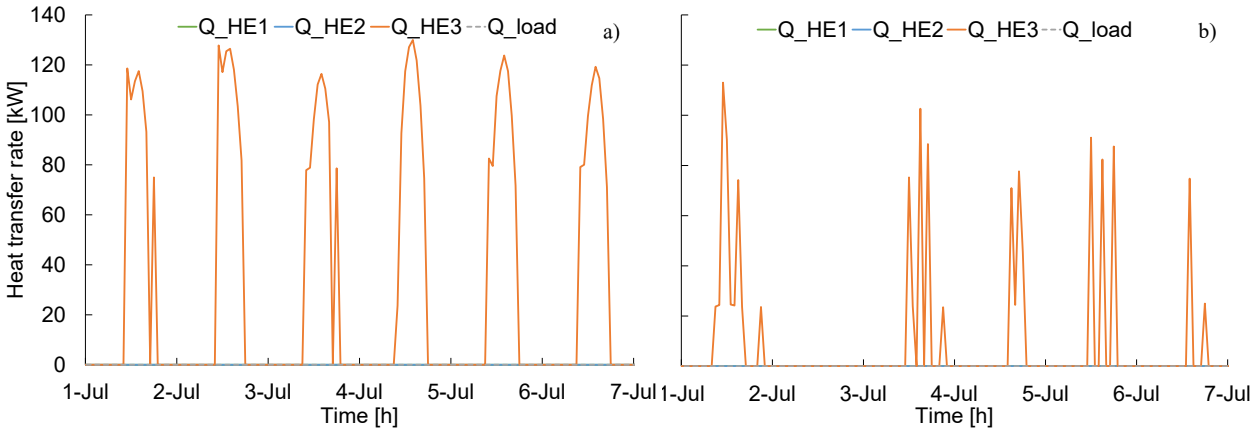

Figure 31: Heat exchangers dynamic trend for six summer operation days. a) Palermo - b) Berlin

In Figure 32 a-b the temperature profiles on HE3 are shown for a typical summer day in which there is no heat request from the user and thus HE1 and HE2 are not operating. Following the substation layout shown in Figure 14, the hot water flows from the storage tank to C2' is delivered directly to HE3, and finally, it flows back into the storage. On the cold side of the heat exchanger, the pump "P" is activated when the set-up conditions are respected (please, refer to sections 2.1, 2.3, and Appendix A) and modulates the flow rate to achieve the desired outlet temperature (DHN supply temperature). In both cases, the flow leaves the heat exchanger at the same temperature (T7=T4) when the pump is activated. It is worth noticing that in Palermo the average inlet temperature on the hot side (T6) is higher than the one observed in Berlin due to higher irradiation values. In Figure 32 is possible to notice the on-off operation due to the satisfaction of the inlet temperature requirement on the hot side of HE3 (T6). When T6<85 °C HE3 is not activated.

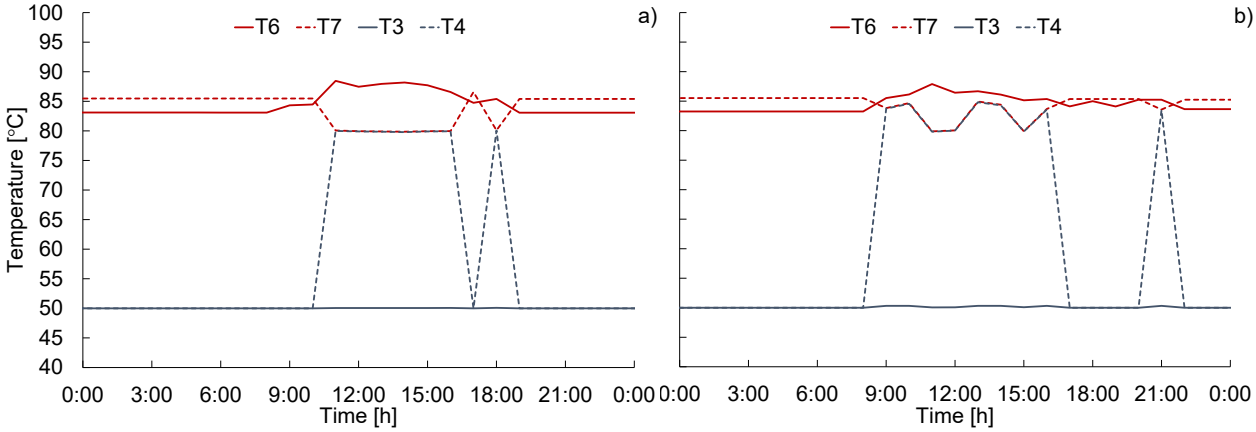

Figure 32: Temperature trends for HE3 for a typical summer day (July 1st): a) Palermo - b) Berlin

The energy production of the solar field in the selected winter week ranges between 40 kW and 90 kW for Palermo and between 38 kW and 73 kW for Berlin (respectively Figure 33a and Figure 33b). Solar radiation is related to the total net tilted surface of collectors. In

Palermo, the outlet temperature set point (95 °C) is achieved for each day of the selected period and maintained constant for almost all the diurnal hours except for the last day due to the low solar radiation.

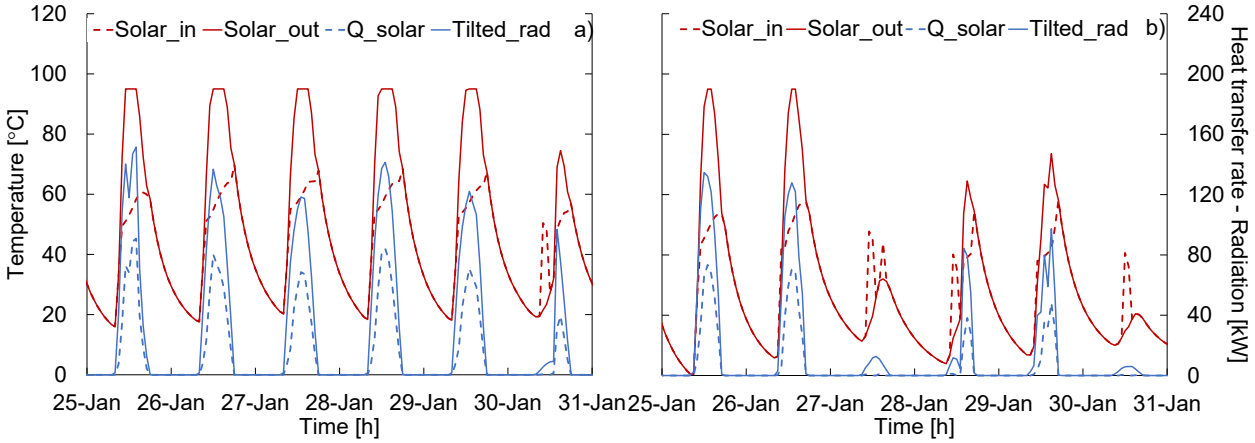

Figure 33: Profile of solar energy production and temperature profiles on a typical winter week: a) Palermo - b) Berlin.

The energy produced by the solar DG in the selected summer week ranges between 120 kW and 135 kW for Palermo and between 11 kW and 104 kW for Berlin (Figure 34 a and Figure 34 b). Since there is no heat demand from the user, all the energy produced by the collectors is delivered to HE3. Furthermore, the solar energy surplus which is not rejected through the dry cooler is delivered to the DHN when there is no heating request by the user. By using the proposed substation, energy saving is twofold: on one hand, the dry cooler is never activated, thus avoiding energy consumption for running the fans. On the other hand, the energy exchanged with DHN, produced by solar collectors, allows for a reduction of the energy produced by those centralized plants that supply the DHN, which typically use natural gas or biomass as primary fuels.

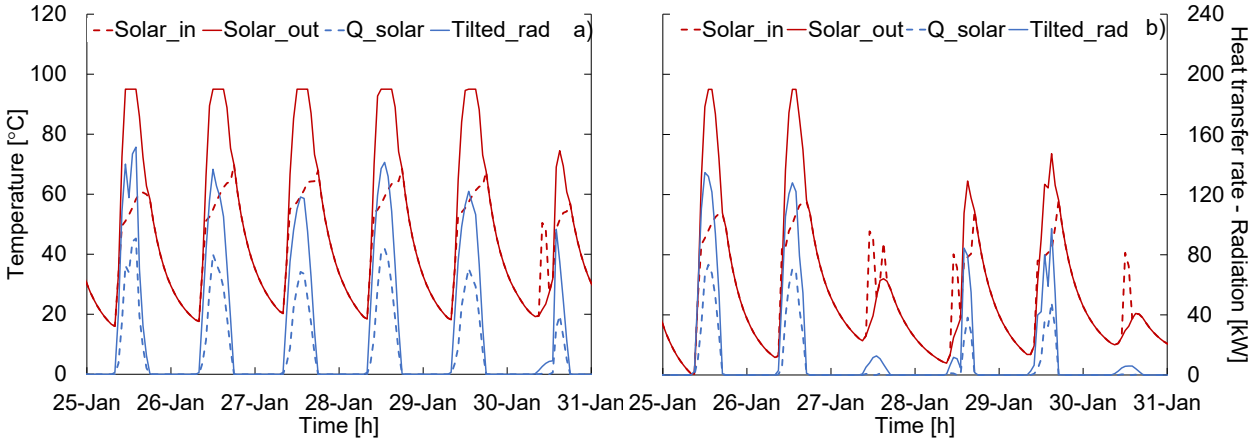

Figure 34: Profiles of solar energy production and temperature for the typical week in summer: a) Palermo - b) Berlin

Starting from the case of Palermo, Figure 35a shows the total energy balance of the substation. More specifically, it displays the ratio between the energy transferred by each HE and the total energy exchanged within the substation. As shown in Figure 35a, the heat produced by the solar system and transferred to the DHN (via HE3) represents the maximum contribution to the overall energy exchanged, accounting for almost 66%. The heat produced by the DG and supplied to the user (via HE2) accounted for 17.7%. The heat supplied by the DHN to the user (via HE1) accounted for 16.3%. Figure 35b shows the fractions of the

heat produced by the solar system, which are supplied to the user and delivered to the DHN. It is worth noting that the main contribution belongs to DHN (79% for HE3), which is due to the correspondence between the period of high radiation (summer) and the absence of heat demand from the user. This information is useful for optimizing the design of the solar system.

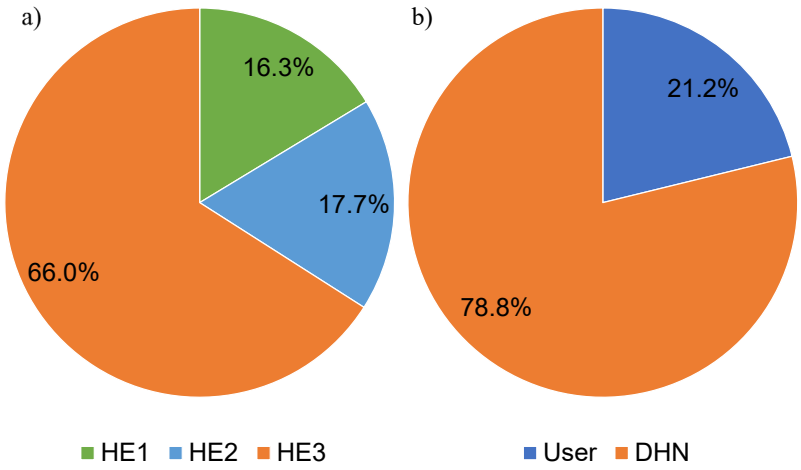

Figure 35: Energy balance on the heat exchangers (a) and DG energy distribution between the user and DHN in the case of Palermo.

Similarly, Figure 36a-b shows the total energy balance of the substation and DG in the case of Berlin. Looking at Figure 36a, it is worth noting that the heat drawn from the DHN represents the maximum contribution to the substation balance (accounting for 56.9%). In addition, a relevant role is also played by HE3 in which 29.9% of the total amount of the exchanged heat by the substation is transferred to the DHN, while only 13.2% of the thermal energy exchanged is delivered to the user due to the low radiation during the winter period. As regards the energy balance of the DG, as shown in Figure 36b, a large fraction of the heat produced is supplied to the DHN (69% for HE3).

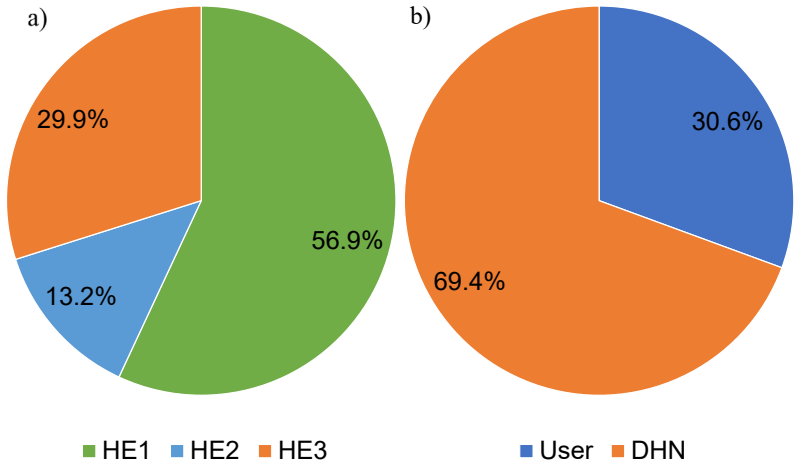

Figure 36: Energy balance on the heat exchangers (a) and DG energy distribution between user and DHN in the case of Berlin.

The above analysis highlights the importance of including detailed thermal modeling of a prosumer's substation for a more accurate estimation of the amount of energy exchanged

between the prosumer and the grid. First, as shown in Figure 30 and Figure 32, the possibility of monitoring temperature values in the substation allows for checking the meeting of the set point for the hot water supplied to the buildings and the water supplied to the DHN. In this regard, even if heat could be available from the DG, the produced heat flow is supplied to the grid only if the temperature setpoint of the produced hot water is properly met. This capability avoids the risk of overestimating the potential energy savings arising due to the presence of prosumers, which could occur when relying on a very simplified substation layout [28] or when using an energy approach [100]. In addition, the inclusion of feedback controllers allowed for (i) a more realistic description of controller actions (typically, performed by using inequality constraints), and (ii) a better description of the coordinated operation between the substation and the DG. Indeed, as shown in Figure 29b, the temperature set-point on the thermal storage leads to a discontinuous supply of heat to the DHN. Finally, the annual results show that solar collectors are a promising technology for prosumers in DHNs, although large differences in thermal energy sharing (e.g., self-consumption or heat selling) exist according to the assumed locality (see Figure 35 and Figure 36). The possibility of accurately describing such sharing is then useful for the development of a refined control strategy that aims at optimizing the economic results achieved by the prosumer.

As the main limitation of the virtual modeling proposed in this study, it can be noted that it is suitable for accurately performing only the thermal analysis of the prosumer's operation, as hydraulic modeling is not considered. In this regard, future research will aim to also include these aspects to describe pumps' operation and quantify the electrical energy consumed. In addition, the lack of constraints arising from the existence of heat demand from the DHN can be considered a further limitation of the proposed study. Indeed, if the deficit in heat production can be replaced by using the DHN, the surplus heat produced by the local DG can be critical when the architecture of the DHN is not known or not defined. A detailed heat dispatching model is then needed to better understand if a DHN can receive the huge amount of heat available from intermittent renewable energy sources. In future research, it is of utmost importance to include a supervisory control architecture that allows the exchange of information between the prosumer and the DHN dealer regarding the actual need of the DHN for the heat produced onsite by the DG. In addition, the flexibility given by the control logic will allow proposing new algorithms arising from "third party access" contracts [78], [79].

The next paragraphs will address some of the main open topics that the previous paragraphs underlined

5. Promoting the flexibility of electrical and thermal grid through the thermal prosumers

In the previous paragraphs, the urgent need for adaptation to climate change has been discussed. Furthermore, the recent geopolitical crisis raised the debate about energy security: in the REPowerEU plan, the European Union has raised the EU's binding renewable target for 2030 as a strategy for reducing energy dependency on Russian fossil fuels [101]. However, the large exploitation of RES has involved the development not only of new energy conversion systems but also of new models of energy sharing, as occurs in renewable energy communities [102], [103]. Indeed, it is widely accepted that new energy-sharing strategies can highly contribute to reducing carbon dioxide emissions and energy waste. However, to achieve these goals, technical and economic issues must still be solved [104]. For instance, the large increase of the RES capacity in the electricity sector observed during the last decades has raised the issue of unpredictable surplus and deficit of electricity production. In this respect, different solutions have been proposed to face these moments. For instance, some authors proposed solutions based on electricity storage [105], [106], the management of user demand [107], or power-to-X technologies [108], [109]. Regarding the latter, the idea of using the electricity from RES for non-electric purposes allows the coupling of the electricity sector with other sectors, such as transport, gas distribution, chemical industry, and the heating and cooling [110], [111].

Focusing on power-to-heat technologies, heat pumps are considered valid support for transmission or distribution system operators (TSO and DSO) in managing the surplus electricity in the network [112]. Indeed, through Demand Response (DR) programs implemented at the user level, HPs could provide ancillary services to TSOs [113]. HPs could be activated in the case of electricity overproduction and the produced heat which is not consumed by the user, is stored onsite in the building envelope or other storage systems [114].

Large efforts have been devoted by researchers to the investigation of HPs' capabilities to improve building flexibility. For instance, Zhang et al. [115] pointed out the need to define metrics for assessing the building-to-grid flexibility achieved through HPs, by considering the different purposes of involved actors (grid operators, final consumers, etc. Meesenburg et al. [116] found that the provision of ancillary services through HPs leads to higher exergy destruction during plant operation, which accounted in turn for 12% of the unit cost of the supplied heat. Lee et al. [117] performed a review of HPs' controls for providing ancillary services to the grid. The authors distinguished the capability of HPs when providing services for load following, reserve, or frequency regulation. The authors identified that HPs could provide flexibility while guaranteeing reduced heat costs, and higher ramp rates than other technologies, although a lack of experimental studies was pointed out. Manner et al. [118] investigated the capability of internet-connected residential HPs to provide primary frequency regulation. The authors found that only if residential HPs are aggregated, a sufficient capacity for primary frequency regulation is achieved. Bartolucci et al.[119] showed that in the case of electric microgrids, HPs coupled to thermal storage could provide ancillary service while assuring cost savings of up to 30%. Tina et al. [120] investigated the capability of commercial buildings to provide flexibility to the TSO. A Mediterranean shopping center

served by an HP was assumed as a case study, with two DR strategies compared. The authors found that a large flexibility potential exists throughout the whole year, although occupants discomfort could arise during summer. For the case of large-scale HPs, Meesenburg et al. [121] have already been shown that they to provide primary frequency capacity. Arteconi and Polonara [122] investigated the capability of air source HP coupled to an underfloor heating system to provide DR. The authors implemented an HP control based on electricity price, which decreases (or increases) the HP's temperature set-point in case of high (or low) electricity market price. A substantial decrease in the peak demand was achieved. Vivian et al. [123] found that HPs coupled to thermal energy storage in a residential district could contribute to reducing stress on the power grid. Ibrahim et al. [124] developed a dynamic model of a variable speed HP for providing frequency regulation support. The authors provided a detailed state-space model of the HPs. Rasmussen et al. [125] developed an algorithm for the activation of large-scale HP for primary frequency support. The authors found that the strategy tends to increase overall energy consumption but allows better operation of the power system reducing the peak demand. Rodríguez et al. [126] compared different strategies for implementing DR by using HPs in the case of plus-energy dwellings. The authors found that a proper combination of variable temperature setpoints and dynamic electricity pricing could lead to 15% of cost savings. Gjorgievski et al. [127] reviewed existing projects focused on DR via power-to-heat technologies. The authors pointed out that direct load control of power-to-heat technologies is more effective than real-time pricing when a quick response is required. Other studies have developed sophisticated controls for DR via HP in buildings [128] [129]. You et al. [130] evaluated the flexibility estimation of residential HP while accounting for heat demand uncertainties. Schibuola et al. [131] compared three control strategies for DR through an HP coupled with a solar thermal plant and a photovoltaic system. Two of them relied on the hourly electricity prices, and one was based on HP activation based only on electricity production from photovoltaic panels. The last one allowed for both cost and energy savings. Research has also considered the possibility of using district heating networks (DHN) as a storage of the surplus heat produced by distributed HPs [132]. Worth noting that, in this case, a user connected to the DHN which can be either heat consumers or producers is classified as "prosumer", likewise in power systems. The research focused on the integration of HPs into DHNs has covered a broad spectrum: from solving the technical issue (e.g., the different operating temperatures [133], the pressure imbalance due to the presence of multiple heat producers [134] to the lack of proper pricing mechanism [135] or well-established regulatory framework. Regarding the regulatory framework, the concepts of "third-party access" (TPA) and heat pricing were analyzed in Paragraph 3.

The previous literature review pointed out that lots of published papers have recently investigated the capability of HPs to support grid operators in moments of surplus and deficit of electricity from RES [136]. Moreover, if HPs are coupled with low-temperature DHNs, further room for increasing building flexibility exists, as the surplus heat produced on-site can be sold to the DHN. However, economic conditions (e.g., the purchasing prices of electricity and heat) and technical constraints (e.g., temperature and pressure setpoint of the DHN) will affect the operation of HPs and, then, the profits achievable by thermal prosumers.

In this framework, the present study investigates the impact of variations in the electricity purchasing prices on the operation and profits of a thermal prosumer equipped with an HP. More specifically, the study will assess whether variation in the component of the electricity price related to the “power grid management and support to the energy system” could be:

- a useful strategy for TSOs and DSOs to promote thermal prosumer flexibility. It is worth noting that no changes in the organization of the current electricity or heat market are imposed.

- an opportunity for the user equipped with a HP to become a thermal prosumer. In this respect, the unit cost of the heat produced by HPs will be highly sensitive to the purchasing prices of the electricity, and, in the case of connection to a DHN, this cost will affect the user’s decision to self-produce heat or buy it from the DHN, and finally, to the possibility of being a prosumer [137].

To show the energy and economic benefits of the proposed strategy, an office building located in Northern Italy supplied by an HP and connected to a DHN is assumed as a case study. A heuristic profit-oriented algorithm for operating HP is developed. The analysis relies on a yearly dynamic simulation performed in Transient System Simulation Studio (TRNSYS), performed by using a validated model of the prosumer’s substation in DHNs. Energy savings and economic revenues will be calculated and compared to a reference scenario characterized by using DHN only for meeting the users’ thermal demand. However, no details on the architecture of DHN are here provided, and the capability of DHN to embed the whole amount of heat injected by the prosumer is assumed. The analysis considers seven alternative scenarios based on different variations in electricity purchasing prices. The cash flows and energy exchange for the different investigated scenarios will be compared.

5.1. Description of the profit-oriented heat pump management strategy and virtual model

As previously clarified, the study case presented in this paragraph aims to analyze the effects of electricity prices on the operation of a thermal prosumer equipped with HPs in the case of the provision of ancillary services to the power grid. To perform this analysis, it is necessary to preliminary define a management strategy of the HP installed within the prosumer’s substation. In this respect, it is apparent that a thermal prosumer aims to maximize his profits by operating the HP depending on the economic boundary conditions (e.g., heat purchasing price).

Figure 37 shows a profit-oriented management strategy of HPs in a prosumer’s substation while considering economic (i.e., prices) and technical conditions. For each time step (typically, one hour), the strategy evaluates if it is profitable to activate the HP only for self-production, for selling heat to DHN, or to switch it off and use the DHN as a heat source. Looking at Figure 37, three economic conditions can affect HP’s operation (as indicated by the yellow parallelograms in the figure). The first two are the buying/selling prices of heat from/to DHN, here indicated as p_{h,DHN_buy} and p_{h,DHN_sell} respectively. The third one is the buying electricity price ($p_{e,buy}$). The buying electricity price highly contributes to the unit cost

of the heat produced on-site by HP, i.e., $c_{h,HP}$. However, it is worth noting that this unit cost depends on technological aspects as well. Indeed, the HPs' coefficient of performance (COP), controls, and interface with the substation, highly affects the amount of electrical energy required by the HP. As a first step, the measured T_{air} and the part-load ratio (briefly indicated as PLR, and given by the ratio of the user demand, D_h, and the HP heating capacity, H_c) are as input to the HP model to calculate the COP.

$$COP = f(T_{air}, PLR) \quad (13)$$

The unit cost of the heat ($c_{h,HP}$) produced by the HP is calculated by using the COP found by using Eq. (13) and the price of the electricity purchased from the grid, as shown in Eq. (14).

$$c_{h,HP} = p_{e,buy} COP \quad (14)$$

In the presence of a heat demand (i.e., $D_h \neq 0$), the algorithm suggests what is the most profitable HP operation strategy. In particular:

- When the user's thermal demand is higher than the HP heating capacity (i.e., $D_h > H_c$), if the unit cost of heat produced by the HP, $c_{h,HP}$ is greater than the heat-purchasing price, then the HP is switched off and the prosumer meets its demand by using heat from the DHN. Conversely, if the unit cost of heat produced by the HP is lower than the heat purchasing price, the HP is operated at "full capacity" and the uncovered fraction of the thermal demand (i.e., $D_h - H_c$) is met by using heat from the DHN.
- When the demand is lower than the HP heating capacity (i.e., $D_h < H_c$), if the cost of heat produced by the HP is higher than the heat-purchasing price, the HP is switched off and the prosumer meets the thermal demand by using heat from the DHN. Conversely, in this case, a further distinction should be made. Indeed, since $D_h < H_c$, it is necessary to understand if it is profitable to run the HP only to cover the user demand (i.e., modulating its capacity), or to run it at its full capacity and sell the surplus heat to the DHN. More specifically, as indicated in Figure 37, if the unit cost of the heat produced by the HP is greater than the selling heat price, the HP is modulated, conversely, it is run at full capacity

In the case of null heat demand from the user (i.e., $D_h = 0$), the strategy evaluates whether or not it is profitable to sell heat to the network by comparing the unit cost of the heat produced by the HP and the selling heat price.

Before ending, it is worth stressing that in this study a heuristic approach for the HP operation was adopted. Worth noting that, although some studies have investigated the flexibility of HP based on optimization routine [137], [138], other studies have proved that heuristics approaches could be applied to the analysis of DR with HPs [139]. In the present analysis, the adoption of a heuristic approach could be justified by considering that the study does not aim at finding an optimal management strategy for the HP in case of flexibility provision, but it investigates the sensitivity of the profits achieved by the prosumer in case variation of electricity purchasing prices.

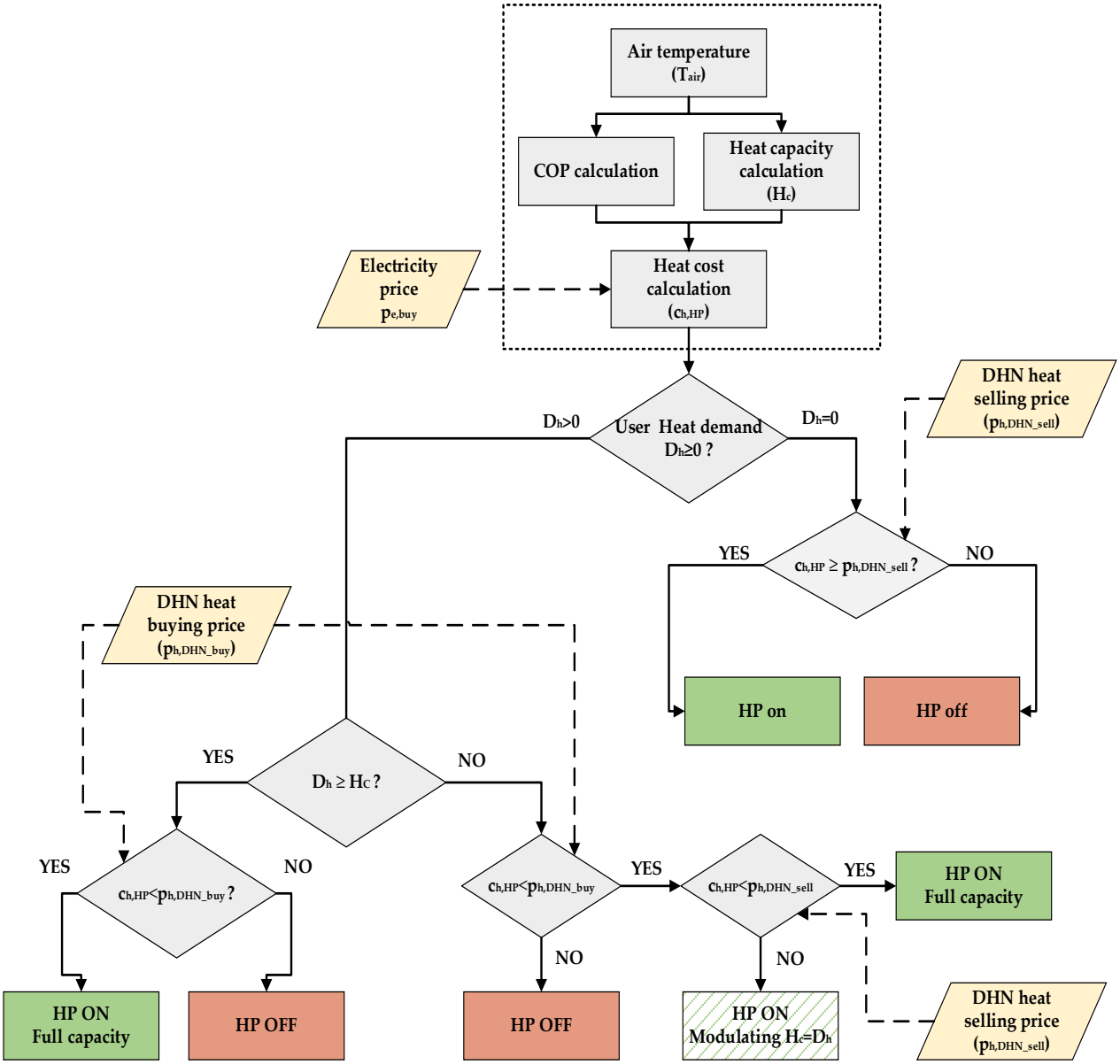

Figure 37: Flowchart of the profit-oriented management strategy of a thermal prosumer equipped with an HP in a given hour of the year

To evaluate the effects of variations in electricity prices on the profitability of HP's operation, some scenarios were here investigated. Different components are usually found in the final electricity prices, related to energy production, the management of the power grid, and taxes. In this study, in order to promote the flexibility of thermal prosumers equipped with HPs, the component of the price of the electricity related to the "network costs" and "energy system support" (briefly indicated as $p_{e,buy}^{NC\&ES}$) was varied keeping fixed the component related to the energy generation cost component $p_{e,buy}^{GEN}$.

To quantify the effects of this strategy on the profit of the thermal prosumer, different scenarios were proposed. As shown in Figure 38, the "Neutral Scenario" is characterized by the absence of incentives or penalties aimed at promoting the user's flexibility. Then, it was assumed a transition from a "Severe deficit" in electricity production from RES (during the whole year) to a constant "Severe surplus" condition, due to a large availability of electricity from RES. In the "Surplus" Scenarios (i.e., both severe and light), HPs could help TSO by

increasing its electricity consumption with the heat produced, consumed on-site, or sold to the DHN. Conversely in the "Deficit" Scenarios, the TSO could induce the users equipped with the HPs to decrease electricity consumption. In general, a severe deficit on the supply side, and a rise in the electricity price is a strategy pursued by TSOs to induce users to decrease their consumption. Conversely, in a severe surplus, a lower electricity price induces users to achieve higher energy consumption.

As shown in Figure 38, for scenarios of "deficit" in electricity production (red circles in the figure) an increase in $p_{e,buy}^{NC\&ES}$ was assumed (+100% for the "sever deficit" and +60% for the "light deficit". Conversely, for scenarios of "surplus" in electricity production (red circles in the figure) a discount in $p_{e,buy}^{NC\&ES}$ was assumed (-100% for the "sever deficit" and -60% for the "light surplus".

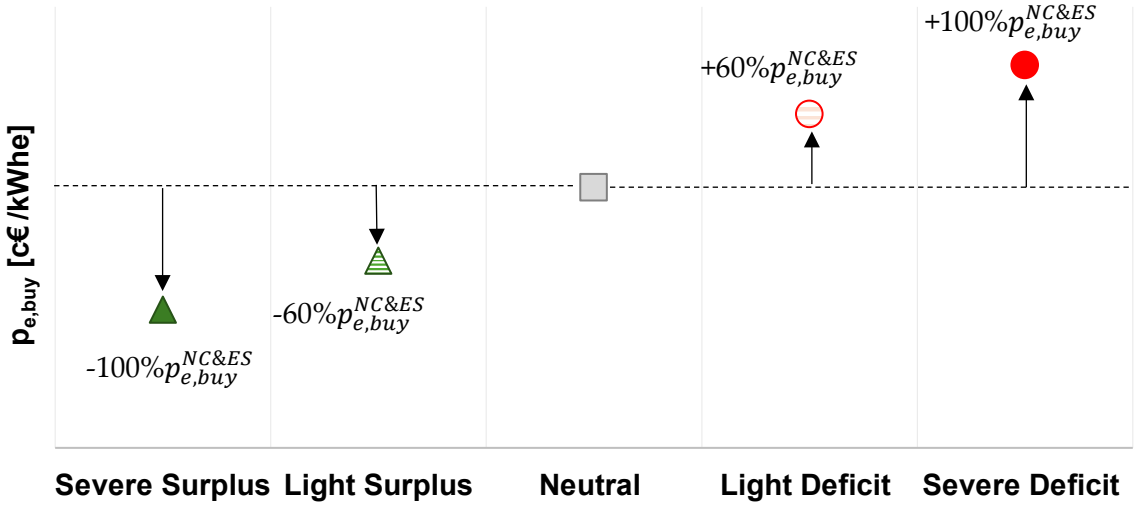

Figure 38: Variation of the electricity buying price in each scenario

Two further scenarios (not shown in Figure 38) were here investigated. More specifically, in both of them, a "random" variation (on an hourly basis) in the electricity price was assumed. More specifically, as shown in Eq. (15), in the "Random 1" scenario, the electricity buying price was randomly varied among the value of the electricity buying price in the Severe Deficit scenario (i.e., $p_{e,buy,min}^{SevSur}$ and the one of Severe Deficit (i.e., $p_{e,buy,MAX}^{SevDef}$ thus replicating unpredictable moments of electricity deficit and surplus.

In the second one, here indicated as the "Random 2" scenario, the electricity buying price values (i.e., $p_{e,buy}^{RAND2}$) varied as shown in Eq. (16). More specifically, starting from the "Random 1" scenario if the electricity price $p_{e,buy}^{RAND1}$ is lower than the maximum value of the "Neutral" scenario, then $p_{e,buy}^{RAND2}$ was assumed equal to $p_{e,buy}^{RAND1}$. Conversely, if the electricity price $p_{e,buy}^{RAND1}$ is higher than the maximum value of the "Neutral" scenario, then $p_{e,buy}^{RAND2}$ was assumed equal to $p_{e,buy,MAX}^{NEUT}$ (Eq. (16). Compared to the "Random 1" scenario, this one assumes electricity price variation to help TSO in moments of electricity deficit (i.e., "Severe deficit" or "Light deficit" situations). Conversely, electricity price is not varied in moments of electricity surplus. However, the reason for this choice will be better clarified in the result section.

$$p_{e,buy}^{RAND1} = p_{e,buy,min}^{SevSur} \leq RANDOM \leq p_{e,buy,MAX}^{SevDef} \quad (15)$$

$$p_{e,buy}^{RAND2} = \begin{cases} p_{e,buy}^{RAND1} \; IF \; p_{e,buy}^{RAND1} \leq p_{e,buy,MAX}^{NEUT} \\ p_{e,buy,MAX}^{NEUT} \; IF \; p_{e,buy}^{RAND1} > p_{e,buy,MAX}^{NEUT} \end{cases} \quad (16)$$

An office building located in Verona Villafranca (Veneto, Northern Italy) with a maximum thermal demand equal to 75 kW was assumed as the case study. The user's heat demand profile was obtained by using the Building Energy Signature method [140], [93]. This approach allows for developing the hourly distribution of the building's thermal demand D_h as shown in the following equation:

$$D_h(i) = D_{h,des} \cdot \left[\frac{T_{H,LET} - T_{air}(i)}{T_{H,LET} - T_{des}} \right] \quad (17)$$

where $D_{h,des}$ is the design heat load of the building calculated at the outdoor design temperature T_{des}, T_{air} is the dry bulb temperature of the outdoor air, $T_{H,LET}$ is the outdoor air temperature at which the net heat load of the building is equal to zero. In this analysis, $T_{H,LET}$ was fixed at 20 °C as suggested by [97] and $D_{h,des}$ was set to 75 kW (maximum thermal demand of the user). By knowing the time series for T_{air}, the hourly distribution of D_h and the total energy request for the considered period were calculated. A further load related to domestic hot water (DHW) demand was introduced in the same stream, to consider a constant energy demand during the whole simulation period, including the summer season in which there is no space heating load. The DHW demand is activated with a constant daily schedule indicated in Table 11, the daily energy required amounts to 55.2 kWh. The overall hourly thermal power and monthly energy requests, comprehensive of heating and DHW demand, are shown in Figure 39. The global yearly energy demand is 63,269 kWh.

Table 11: Daily schedule for DHW production.

Daily Hours	Temperature set-point	Hourly heat capacity
10-12 (3 hours)	55°C	11.03 kW
15-16 (2 hours)	55°C	11.03 kW

The weather file of Verona Villafranca (Cfa climate according to Köppen classification) was retrieved from the METEONORM database [91].

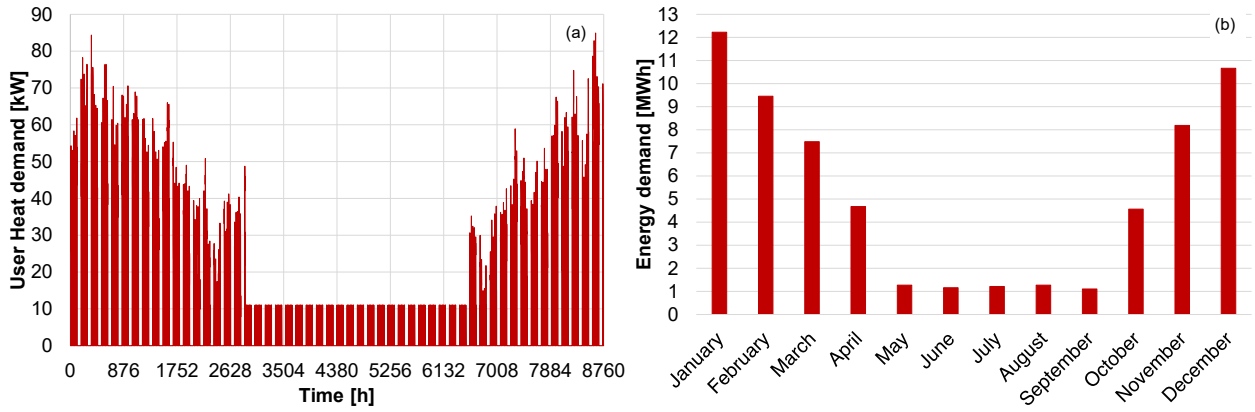

Figure 39: Data of the case study: (a) hourly heat demand of the user, and (b) monthly energy demand.

The validated model of the prosumer substation, presented in Chapter 4, was adapted to include a High Temperature Heat Pump (HTHP) as a decentralized generator (Figure 40). A "return-to-supply" configuration of the substation was assumed. It includes three heat exchangers (HE) and a High-Temperature Heat Pump (HTHP). A variable water flow rate is drawn from the return line of the DHN and heated up using the HE3 to the supply temperature (i.e., 60 °C) by the HTHP. The water flow rate returning from the hydronic loop of the building is heated using heat from the HTHP via HE2. Then, if the supply water temperature is not equal to the setpoint required by the user, the water flow rate is heated via HE1 using heat available from the DHN.

Three different circuits are then identified:

1. the primary circuit which directly connects the DHN to the substation. It includes the accessories used when the user is either a producer or consumer (e.g., HE1 and HE3). It is activated to cover the user energy demand if HE2 is not able to supply the overall energy amount requested (through HE1) or when the heat generated by HTHP is exchanged with DHN (through HE3).
2. the secondary circuit, which consists of the HE1, HE2 and other accessories used to heat the water returning from the hydronic loop of the building.
3. the tertiary circuit, where the heat produced by the HTHP is exchanged with the water returning from the building through HE2 and with the DHN via HE3.

A 4th generation DHN was assumed. For this reason, the operating temperature of the supply line of the DHN was equal to 60 °C. Details on temperature and flow rate values, and HEs' sizes, are reported in Table 12.

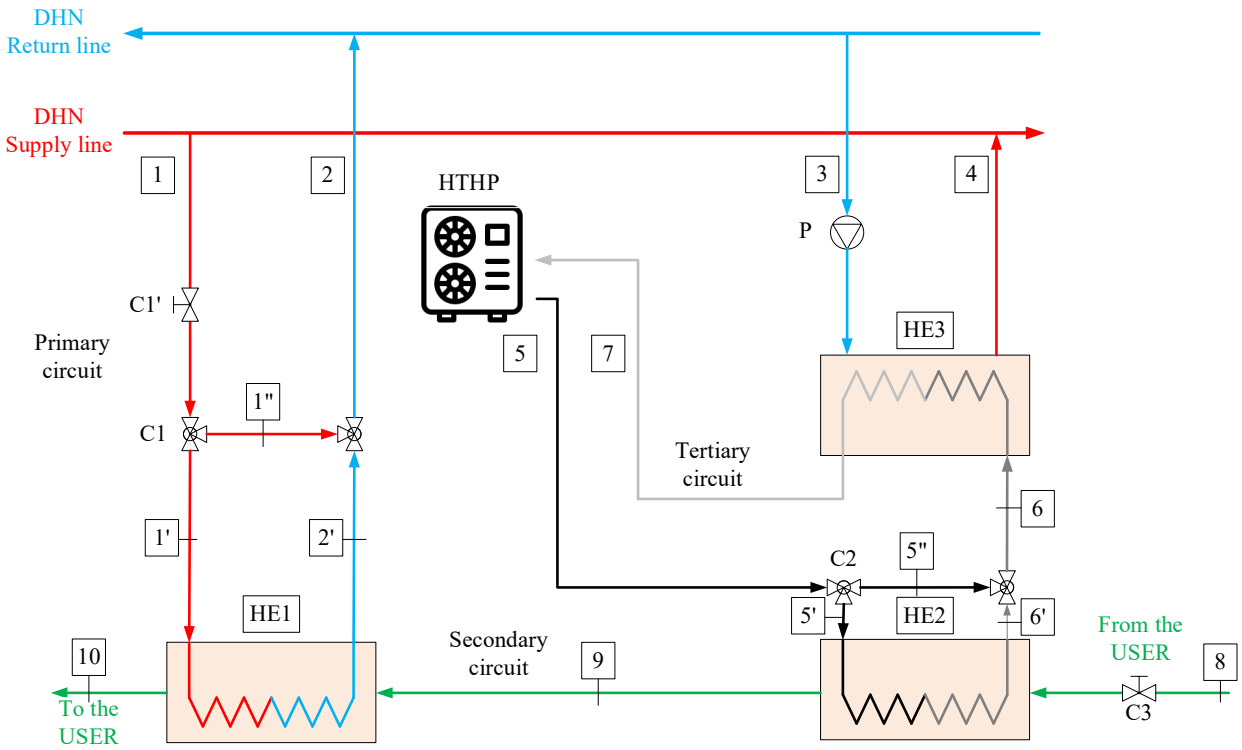

Figure 40: Scheme of the thermal prosumer's substation

Table 12: Design parameters for the heat exchanger installed with the substation.

		Primary side		Secondary side
Heat Exchanger HE1	F1'	7.30 m³/h	F9	4.87 m³/h
	T1'	60 °C	T9	40 °C
	T2'	50 °C	T10	55 °C
	Q		85 kW	
	UA		11.77 kW/°C	
Heat Exchanger HE2	F5'	3.65 m³/h	F8	4.87 m³/h
	T5'	70 °C	T8	40 °C
	T6'	50 °C	T9	55 °C
	Q		85 kW	
	UA		6.89 kW/°C	
Heat Exchanger HE3	F3	1.93 m³/h	F6	2.41 m³/h
	T3	35 °C	T6	70 °C
	T4	60 °C	T7	50 °C
	Q		56 kW	
	UA		4.54 kW/°C	

As previously mentioned, the system described was reproduced in the TRNSYS environment. More specifically, the heat exchangers were modeled through Type 5 (counter-flow heat exchanger), and the overall heat exchanger coefficient was externally calculated by considering an empirical correlation obtained by an elaboration of the Dittus-Boelter equation. HP's management strategy was implemented in TRNSYS by using a "calculator", which provides the operating signal for the HTHP. Iterative feedback controllers (type 22) were adopted to simulate the controls that regulate valves C2, C1, and the speed of pump P. They attempt to maintain the required temperature set point by varying the flow delivered

to the heat exchangers (HE1 for C1 and HE2 for C2) or the flow rate delivered by the pump P (for HE3). A detail of the iterative feedback controller settings is shown in Table 13.

Table 13: Iterative feedback controller settings

Actuator device	Controlled variable	Temperature Setpoint
C1	T_{10}	55°C
C2	T_9	55°C
P	T_4	60°C

Finally, C1' and P control the flow rate respectively on the hot side of HE1 and cold side of HE3, according to the control logic shown in Table 14.

Table 14: Settings Value for the flow rate control

Actuator device	Controlled variable	Control logic
C1'	F_2	C1' is open if: $T_9 < 55$ °C AND $F_8 > 0$
P	F_3	P is activated if: $T_6 \geq 65$°C AND $F_7 > 0$

Before ending, it is worth stressing the main assumptions of this work. First, the hydraulic modeling of the whole DHN was not included, and for this reason, constraints related to pressure setpoint values, and the maximum flow rate of hot water were accounted for. Secondly, the analysis did not consider any constraints related to the operation of DHN, *e.g.* the actual request from the DHN for the surplus heat produced *in loco* by the prosumer. All these aspects affect the operation of distributed thermal prosumer [97]. In this work, DNH was assumed to be virtual storage, whose operation is not highly influenced by the considered prosumer. However, this assumption could be justified by considering that no optimization in the management of HP is pursued.

5.2. Modelling of the High-Temperature Heat Pump included in the prosumer substation

Considering the temperature of the hot water supplied to the hydronic loop of the user (i.e., 55 °C) and the operating temperature of the DHN (i.e., 60 °C), it was necessary to select an air-to-water HP capable of producing hot water at 70 °C. The "KWP" high-temperature heat pump, provided by Kroll© was selected [141]. In Table 15 the main technical data are summarized. Figure 41 shows the heating capacity and the COP values for the case of hot water produced at T_{water}= 70 °C. Note that the profiles shown in the referenced figure consider only the variation in the COP and heating capacity with the temperature of the air entering the evaporator (i.e., T_{air}). Conversely, the effect of part-load operation was not provided.

Table 15: Technical data of the selected HTHP.

Working area	
T_{air}>-15°C	35<T_{water}≤70°C
Refrigerant	
R32 Filling quantity: 22kg GWP=675	R1234ze Filling quantity: 5kg GWP=7
Compressor	
Scroll compressor Maximum operating current: 25.7 A Maximum power consumption: 15.5 kW	Reciprocating compressor Maximum operating current: 33.2 A Maximum power consumption: 19 kW

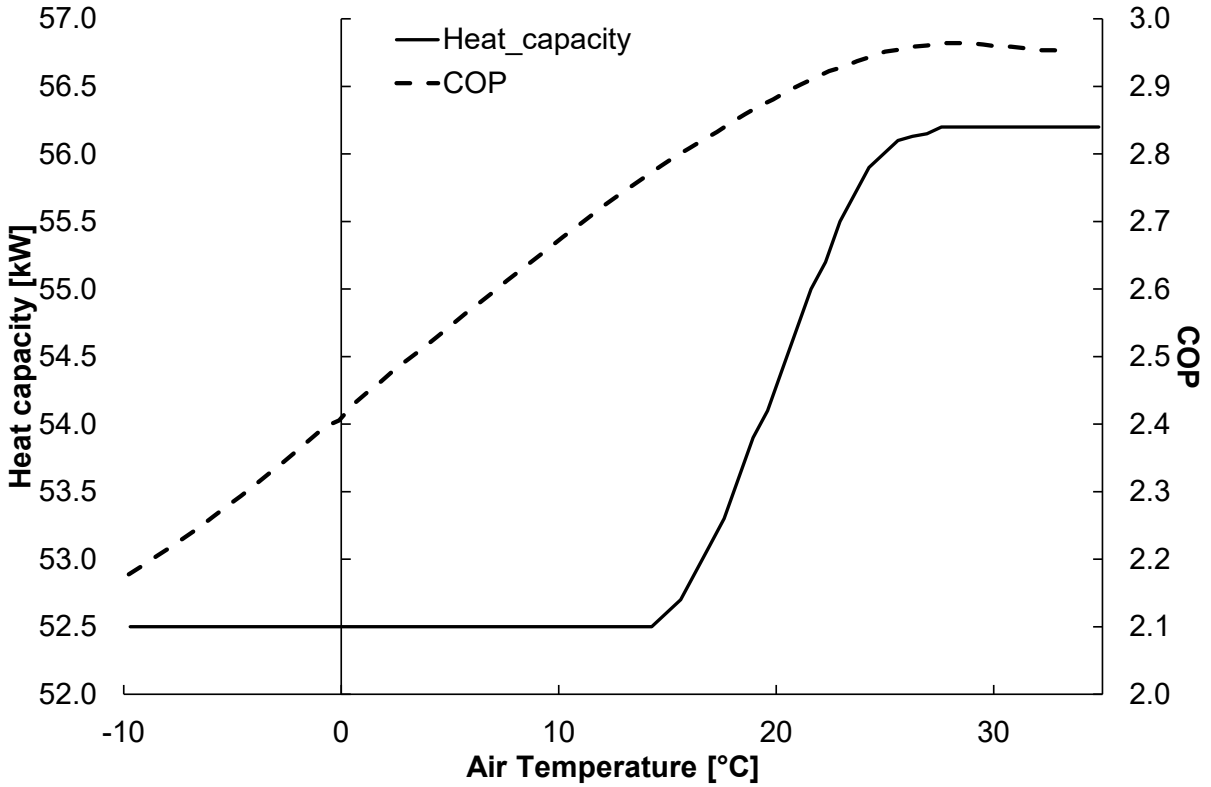

Figure 41: HTHP performance curves evaluated for T_{water}=70 °C

The data retrieved from the datasheet were processed in a statistical model to get equations that allow for a quick calculation of the performances of the HTHP by knowing only T_{air}, while keeping the temperature of the produced hot water at 70 °C. Worth noting that this "black-box" approach is very useful, for instance, for embedding experimental or empirical data in algorithms that make use of Model Predictive Controls [142]. Moreover, the approach relies on polynomial equations which usually require a low computational effort while guaranteeing good approximation [143], [144], [145].

Following this method, a non-linear regression analysis was carried out to correlate the T_{air} with the COP and heat capacity fixed in the T_{water}. A MATLAB script was used to obtain two sets of predictors for the non-linear polynomial equations that describe the HTHP performance, in the form:

$$H_C = p_1 * T_{air}^4 + p_2 * T_{air}^3 + p_3 * T_{air}^2 + p_4 * T_{air} + p_5 \quad (18)$$

$$COP = p_6 * T_{air}^4 + p_7 * T_{air}^3 + p_8 * T_{air}^2 + p_9 * T_{air} + p_{10} \quad (19)$$

the heating capacity, H_c is expressed in kW, the T_{air} in °C. The predictor coefficients and the statistical evaluation parameters are shown in Table 16. High values of R^2 (close to 1) and low values of root mean square error (RMSE) show the predictor's reliability. In Figure 42 the comparison between the datasheet and calculated performance is reported, showing the good correspondence of the black box model.

Table 16: Values of predictors and evaluation parameters of the statistical regression.

	$H_C(15°C < T_{air} < 27.5°C)$		**COP**
p_1	1.563*10^{-4}	p_6	-4.450*10^{-9}
p_2	-1.591*10^{-2}	p_7	-1.210*10^{-5}
p_3	0.574	p_8	1.068*10^{-4}
p_4	-8.466	p_9	2.628*10^{-2}
p_5	96.13	p_{10}	2.412
R^2	0.9992		0.9998
SSE	0.406		7.421*10^{-4}
RMSE	0.0395		3.353*10^{-3}
$H_C(-10°C \leq T_{air} \leq 15°C)$ 52.5 kW			
$H_C(T_{air} \geq 27.5°C)$ 56.2 kW			

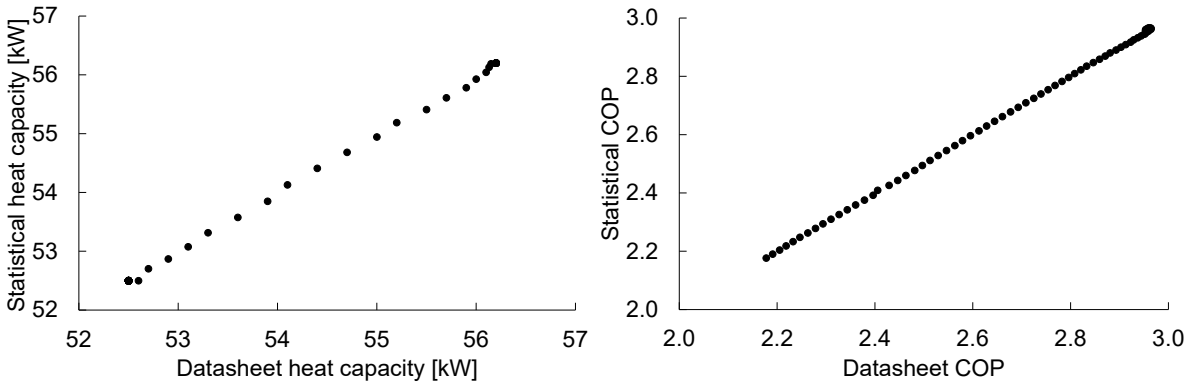

Figure 42: Graphic evaluation between data retrieved from datasheet and statistically predicted data.

The HTHP equations (Eqs. (18) and (19) were implemented in the TRNSYS model by using a "calculator". The profit-oriented strategy for the assumed HTH is an extension of the criterion shown in Figure 37. However, it is worth noting that unlike the one shown in Figure 37, here the possibility to modulate the HP's heating capacity (i.e., the possibility to operate the HTHP at PLR values between 0 and 1) is not considered, as for the considered HTHP only at full-load data were available; for this reason, the COP function is dependent only on T_{air} (Eq. (19). The outlet temperature of the water on the condenser is fixed at 70 °C, and the difference between the inlet and outlet temperature is fixed at 20 K. Since the heat capacity and COP depend only on the T_{air}, the flow rate is assumed variable and calculated through the following expression:

$$\dot{m}_{cond} = \frac{H_C}{c_p \Delta T} \ (\Delta T = 20\ K) \tag{20}$$

5.3. Definition of the economic conditions

As previously mentioned, electricity and heat prices are boundary conditions that highly affect the operation of HP. In this subsection, the heat and electricity prices for the case study are shown.

Regarding heat price, the substation was considered as a part of a DHN with one main distributor that imposes the buying price, and the TPA is allowed with a fixed buying and selling heat price for the prosumer. To account for real market heat prices, the case of Verona DHN was adopted as a reference. The detailed data of heat purchasing price, available for each trimester, were here used.

The non-household conditions were assumed, and the prices were referred to those released by DHN distribution company in 2021 for customers who require less than 29 MWh per month [146]. Since in the real case there are no prosumers, the selling price offered by the distributor to the prosumer was here assumed to be 80% of the buying price (Table 17), by considering the average ratio between the buying and selling price reported in [147].

Table 17: Reference value for heat purchasing price (from DHN to the prosumer) and heat selling price (from the prosumer to the DHN).

Heat Price	1st Jan-1st Apr	1st Apr-1st Jul	1st Jul-1st Oct	1st Oct-31st Dec
$p_{H,\ DHN,\ buy}$ [€/kWh]	0.0965	0.1009	0.1168	0.1554
$p_{H,\ DHN,\ sell}$ [€/kWh]	0.0772	0.0807	0.0934	0.1243

Regarding the electricity price, data available from the Italian Agency for Energy Market regulation were used [148]. More specifically, the Italian electricity price for both 2021 semesters and a non-household consumer with an installed power greater than 15 kW_e are assumed (Table 18). As shown in Table 18, data from ARERA showed a clear picture of the components of the electricity price related to energy production, the management of the power grid, and taxes.

Table 18: Reference value of the purchasing price of electricity

Period	Energy generation cost component $p_{e,buy}^{GEN}$ [€/kWh]	Network cost and energy system support component $p_{e,buy}^{NC\&ES}$ [€/kWh]	Final price (VAT and taxes included) [€/kWh]
2021, 1st semester	0.0736	0.0613	0.1771
2021, 2nd semester	0.1218	0.0396	0.2094

For each scenario, a cash flow (CF) was calculated as the difference between revenues arising from the heat selling and costs sustained for purchasing heat from DHN and

electricity from the grid (Eq. (21). The calculation of revenues and costs was performed for one operation year on an hourly basis (Eqs. (22 and (23). The unit heat prices are reported in Table 16 and considered constant for each scenario, while the adopted electricity prices are shown in Table 18.

$$CF = M_{revenues} - M_{costs} \tag{21}$$

$$M_{revenues} = \sum_{\tau=1}^{8760} E_{th,HE3}(\tau) \times p_{h,DHN_{sell}}(\tau) \tag{22}$$

$$M_{costs} = \sum_{\tau=1}^{8760} E_{th,HE1}(\tau) \times p_{h,DHN_{buy}}(\tau) + E_{el}(\tau) \times p_{e,buy}(\tau) \tag{23}$$

To better understand the economic benefits achievable in each scenario, a baseline condition characterized by the absence of HTHP was assumed. In this scenario, the thermal energy demand by the user is entirely met by the heat supplied by the DHN, leading to a yearly cost equal to 7,210 €. It corresponds to a negative cash flow since the revenues are equal to zero (Eq. 12).

$$CF_{base} = 0 - \sum_{\tau=1}^{8760} D_h(\tau) \times p_{h,DHN_{buy}}(\tau) \tag{24}$$

Arising from this outcome, a yearly economic saving was then calculated by the difference between the cash flows achieved in each scenario and the baseline one (Eq. (25).

$$SAV_{ref} = CF_{scenario} - CF_{base} \tag{25}$$

Finally, the economic saving was calculated by comparing the “Neutral” scenario with the other ones (Eq. (26). This information is useful to compare the same technological system under different boundary economic conditions due to the ancillary services provided to the electrical grid

$$SAV_{neut} = CF_{scenario} - CF_{neutral} \tag{26}$$

5.4. Simulation results and discussion

To assess the energy saving and the economic benefits achievable by the thermal prosumer in a scenario of DR provision, it is worth analyzing the results obtained from a one-year simulation.

Figure 43 shows the amount of energy exchanged within each heat exchanger of the prosumer substation after a one-year operation. These results are useful to gain some insights into the effect of different electricity purchasing prices on the operation of both the HTHP and the substation (e.g., interactions among the three heat exchangers, and between the substation and the DHN). Worth noting that HE2 (orange bars in Figure 43) shows a constant amount of energy exchanged for each of the proposed scenarios, except for the “Severe Deficit” scenario. Conversely, the amount of thermal energy exchanged within HE3

(grey bars) shows an increasing trend when passing from the “Severe deficit” to the “Severe surplus” scenario. This trend could be easily explained by considering that due to the decreasing electricity price, HTHP is operated for a longer period with more thermal energy available for the DHN.

In all scenarios, the thermal demand of the user is almost entirely covered by using HE2 (i.e., by using the energy supplied by the HTHP) as testified by the energy exchanged in HE1 (blue bars) which is always less than 0.05 MWh, except for the “Severe deficit” and “Light deficit” scenarios in which it ranges up to respectively 27.9 MWh and 2.2 MWh assessed on 44% and 3.5% of the entire heat demand. The “Random1” and “Random2” scenarios show equal values of heat exchanged by HE1 and HE2, respectively 14.6 MWh and 50.7 MWh, the energy exchanged by HE3 is lower in the “Random2” scenario than the “Random1” one due to the effect of less profitable prices.

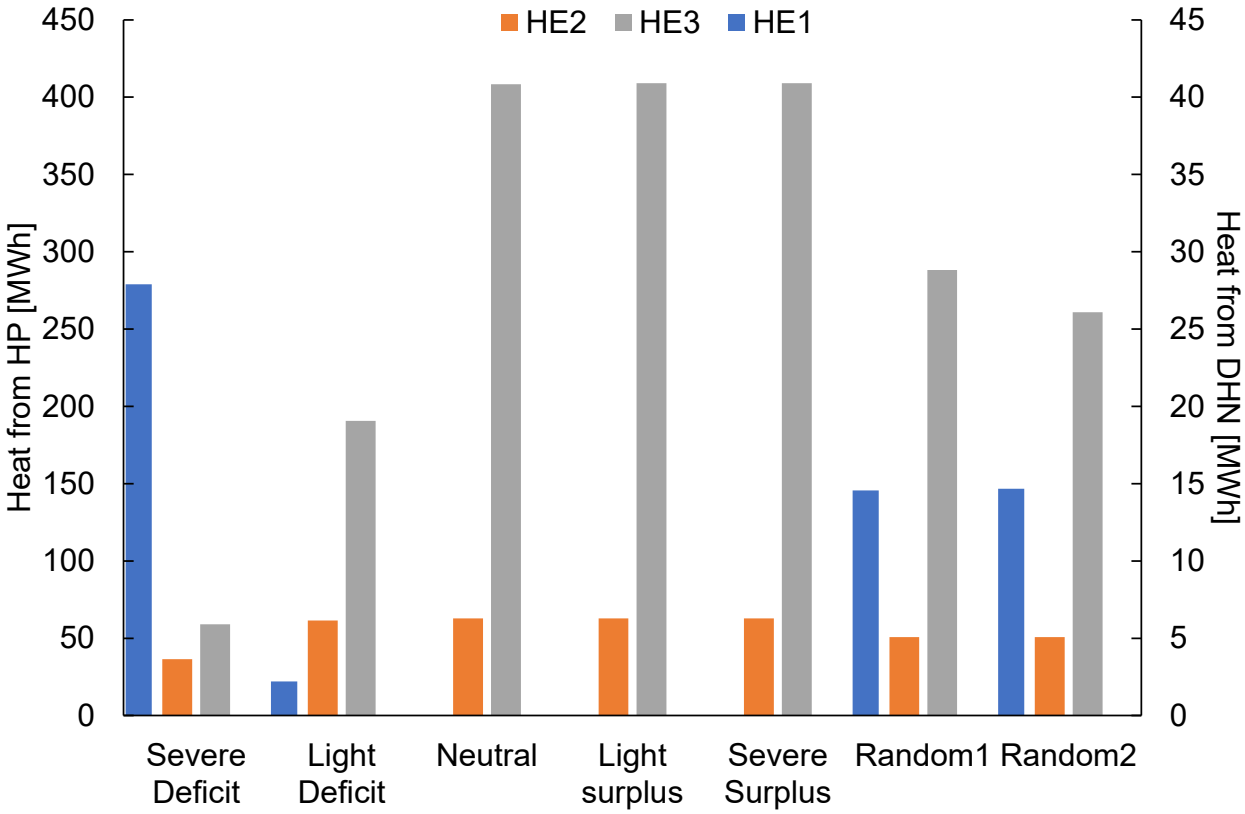

Figure 43: Thermal energy exchanged within each heat exchanger (values for HE2 and HE3 are on the left axis, HE1 to the right one)

The profiles of the heat exchanged by the three HEs are shown in Figure 44. More specifically, results found for the two opposite scenarios, i.e., “Severe Deficit” and “Severe Surplus” are presented. Comparing Figure 44a-b, the heat rate for HE1 and HE2 is identical in both scenarios, as these HEs operate to meet the energy demand on the user side. HE3 is never activated in the “Severe Deficit” scenario, while it operates for 8 hours at a constant heat transfer rate in the “Severe Surplus” one. This different behavior is due to the more profitable economic condition available in the “Severe surplus” scenario, which induces the prosumer to activate the HTHP for selling heat to the DHN. However, as shown in Figure 44b, HE3 is operated in the absence of energy demand by the user, i.e., during evening, nighttime, and early morning. In this respect, it is worth noting that this analysis did not

consider any constraints on the maximum amount of heat that could be supplied by the prosumer to the DHN during nighttime. Indeed, it was assumed that all the heat produced on-site via HP and sold to the DHN is either supplied to other users distributed along the DHN or stored in some centralized plants. This assumption, however, could be justified by considering that the main scope of this work is mainly focused on the effects of electricity prices on the operation of HTHP in the case of the provision of ancillary services.

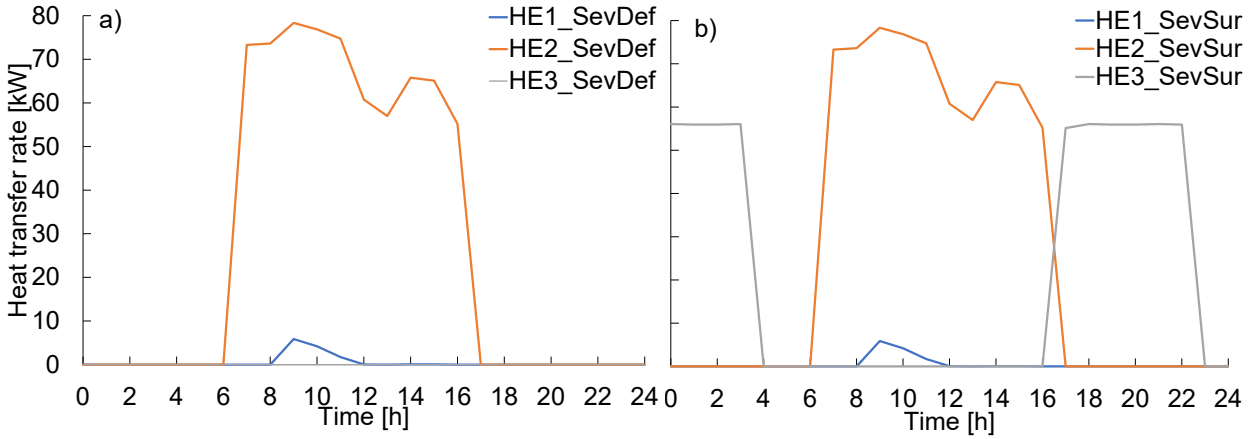

Figure 44: Substation's heat transfer rate daily trend: (a) Severe deficit scenario; (b) Severe surplus scenario

Figure 45 shows the electrical energy supplied to the HTHP for a one-year operation. Following the criterion shown in Section 5.3, it is apparent that the yearly electrical energy consumed by the HTHP increases in scenarios of lower electricity prices. This trend is confirmed: passing from the "Severe deficit" scenario to "Severe surplus", the electricity consumed passes from 35 MWh for the "Severe deficit" scenario to 172 MWh for the "Severe surplus". The "Random1" and "Random2" scenarios show an energy consumption of respectively 123 MWh and 110 MWh. Again, in this case, the Random scenarios show intermediate results between "Light deficit" and "Neutral" ones.

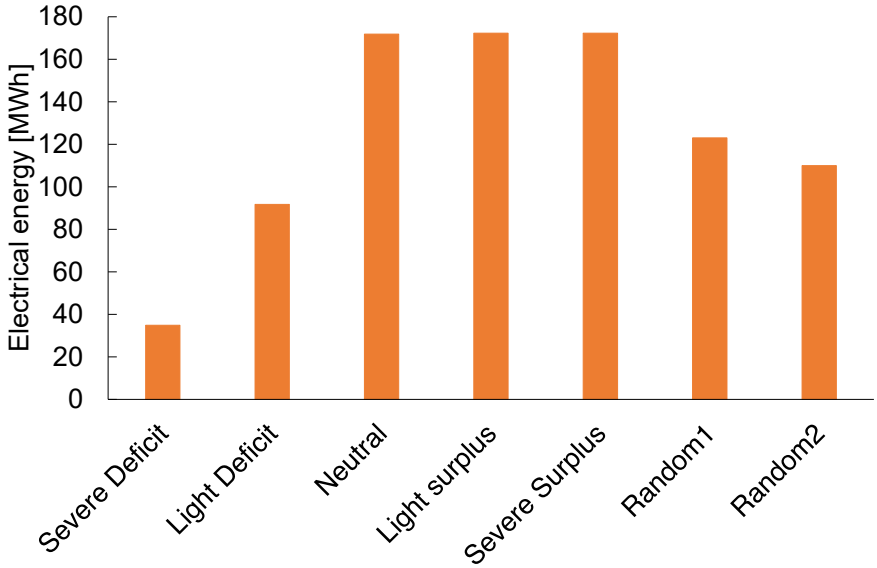

Figure 45: Yearly electrical energy supplied to the HTHP

As previously mentioned, the economic analysis considered both the savings due to the thermal energy produced by HTHP (which is not purchased from the DHN) and the revenues arising from the thermal energy sold to the DHN. The yearly economic cash flows and savings for each scenario when referring to the baseline scenario with no HTHP installed are reported in Figure 46a. In case the neutral scenario is assumed as the reference (i.e., when the HTHP is installed but with no variation in the electricity prices), cash flow and savings are shown in Figure 46b. Both the cash flow and savings follow an increasing trend when passing from the "Severe deficit" scenario to the "Severe surplus" one, due to the decreasing electricity price, ranging from -7,363 € to 21,489 € for CF and -153 € to 28,699 € for SAV_{base} in Figure 46a, and from -10,359 € to 18,493 € for SAV_{neut}. Both CF and SAV_{base} are negative for the "Severe deficit" scenario, thus suggesting that it would be more profitable to exploit the DHN as a heat source. Although in the "Light deficit" scenario the cash flow is still negative, the saving is positive since it is referred to the baseline conditions in which all the user demand is covered by DHN and there is no heat sold to it.

The "Random1" scenario achieved economic performances analogous to the "Neutral" one. The "Random2" scenario achieved a cash flow close to zero but a SAV_{base} equal to 6,763€, thus assessing the more profitable operation of HTHP if compared to the energy supplied by DHN alone. In Figure 46b the "Severe deficit" and "Light deficit" scenarios show negative results since they are referred to as the neutral scenario. This is due to the less profitable conditions imposed by the electrical grid dealer. Conversely, the "Light surplus" and "Severe surplus" scenarios achieved positive values of SAV_{neut}; the results range between - 10,359 € to 18,493 €. For the "Random1" and "Random2" scenarios, a counterintuitive result is achieved: the energetic outcomes showed that the performances of these scenarios were intermediate between the "Light deficit" and "Neutral" scenarios, while the economic outcomes show that they are closer to the "Neutral" one. This is due to the random distribution of electricity prices that affect the HTHP activation and the economic balances with different effects.

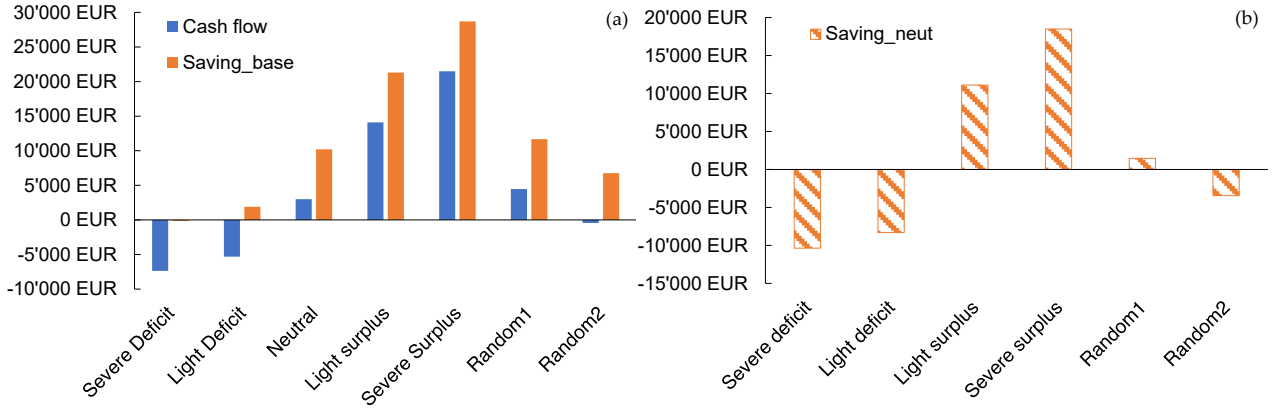

Figure 46: Cash flow and money saving for each scenario: (a) with no HTHP; and (b) assuming the "Neutral" scenario as the reference

The analysis of the described results revealed that the "Neutral" scenario led to achieving profitable results if compared to the DHN heat supply, without any other source. The introduction of tax cuts, incentives, or profitable conditions for the ancillary service leads to a relevant increase in profits. If this is operated through the introduction of public resources, the effect is the production of an extra profit generated on a system that is just able to be

profitable within a neutral condition, without taxation or incentives. If the public incentives aim at the inequality balance, these scenarios can, conversely, lead to a relevant increase in them. The “Random1” scenario comprises a distribution that considers the whole range of prices, thus balancing the less profitable conditions with the more convenient ones. From this finding, the “Random2” scenario was developed. It was structured by cutting off all the values that bring boundary conditions that aim to increase profits through public intervention. Then, electricity prices are based on a range that is not affected by any incentive but only by possible penalization in case of grid criticism (i.e., “Severe deficit” or “Light deficit” situations). Despite this penalization, the results shown in Figure 46 let to appreciate the positive results achieved by this case, due to the performances of HTHP.

To better understand the energetic and economic results here shown, it is worth comparing the yearly profile of the unit cost of heat produced by HP and the buying and selling price of heat from DHN. Looking at Figure 47a, it is possible to observe that the unit cost of heat in the “Severe Deficit” scenario is comparable with the purchasing price of the heat from the DHN (black continuous line vs pink line), thus suggesting that is not always cost saving to produce heat on-site. Regarding the selling price of heat (black dashed line), the profiles shown in Figure 47a indicate that only in the “severe” and “light” deficit scenarios there are hours characterized by no benefits achieved by selling heat to the DHN. Conversely, for the other scenarios, economic benefits are achieved by selling heat to the DHN.

In scenarios “Random1” and “Random2”, the unit cost of heat shows an oscillating behavior that, in the first scenario, allows for achieving more profitable conditions rather than the second one (Figure 47b and Figure 47c).

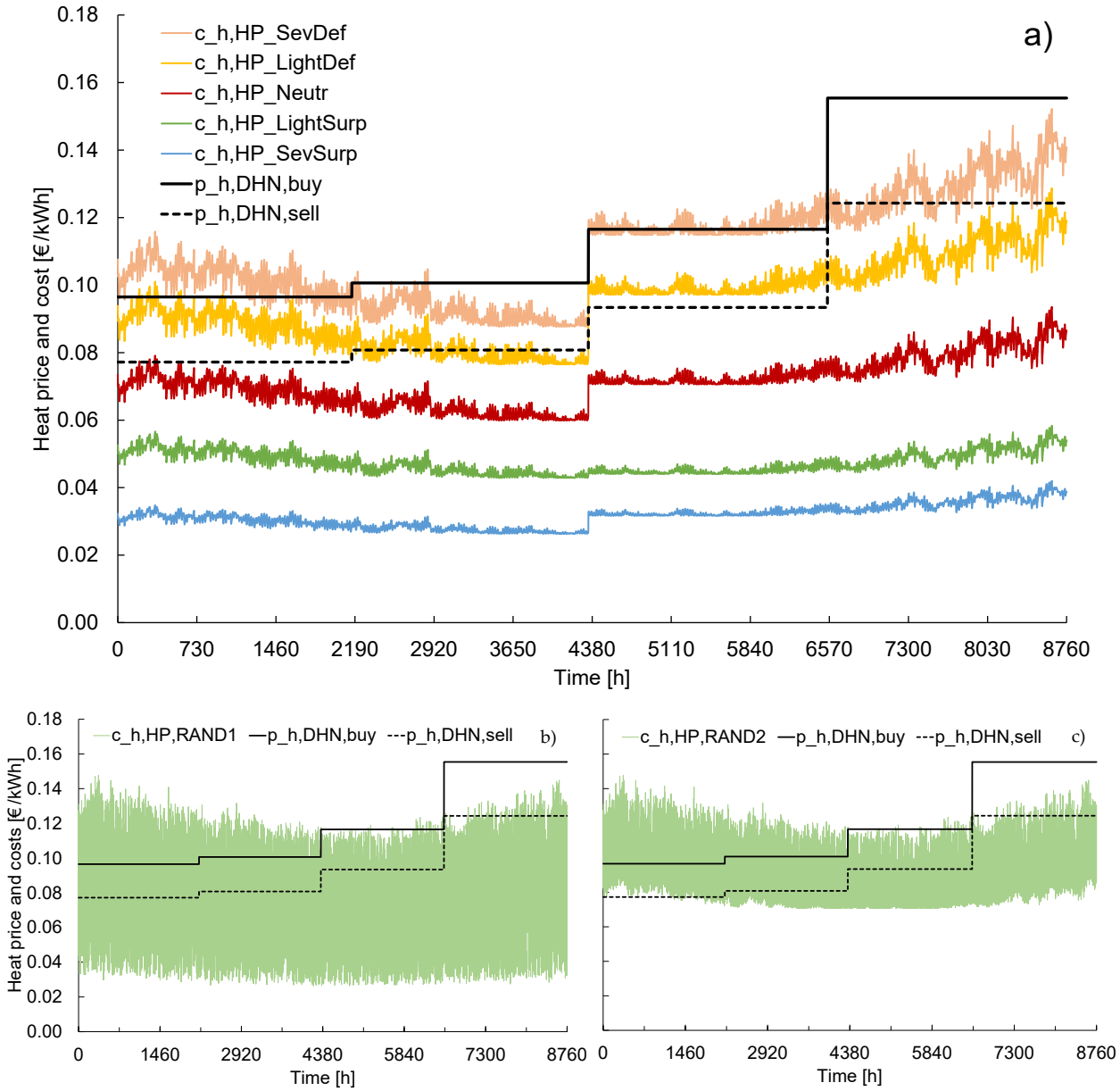

Figure 47: Comparison between DHN buying, selling heat price and the unit cost of heat produced by the HTHP for: a) Scenarios obtained by varying the NC&ES electricity price components, b) Random 1 scenario, c) Random 2 scenario

The previous analysis highlighted that the economic boundary conditions together with HP's energy performance highly affect the operation and profit of the thermal prosumer. Moreover, as previously mentioned, there is not always a match between favorable market conditions and good HP performance. It is interesting to find a correlation between the unit cost of heat and the boundary conditions previously investigated (i.e., the temperature of the outdoor environment which affects the HP's energy performance and the market price of electricity). Worth noting that other operating costs and marginal costs (e.g. maintenance costs) are here neglected but they can be easily included in the methodology

To find a correlation among c_h, T_{air}, and p_{el}, the results of the simulation were given as input to a statistical regression MATLAB model. Results from regression analysis suggested that the unit cost of heat is related to T_{air} and p_{el} according to the polynomial equation shown in Eq. (27). The values of predictors are shown in Table 19, together with the statistical evaluation parameters.

$$c_h = a_0 + a_1 \times T_{air} + a_2 \times p_{el} + a_3 \times T_{air}^2 + a_4 \times T_{air} \times p_{el} \quad (27)$$

Such a black box model allows for fast and reliable heat costing that can be directly implemented into an evaluation tree algorithm like the one here proposed in the present paper. Indeed, once known T_{air}, p_{el} from the weather forecast and market conditions imposed by the grid dealer respectively, Eq. (27) predicts the cost of heat generated onsite by the HTHP. This information is crucial for the evaluation algorithm and gives a global view of the behavior of the specific technological system.

Table 19: Values of the statistical predictors and evaluation parameters

Predictor	
a_0	1.978×10^{-3}
a_1	-4.490×10^{-4}
a_2	4.053×10^{-1}
a_3	1.557×10^{-5}
a_4	-2.701×10^{-3}
Predictor evaluation parameter	
R^2	0.0017
SSE	0.9994
RMSE	1.850×10^{-4}

The regression model of Eq. (27) was also presented in the form of a “map”, as shown in Figure 48. Such representation allows for assessing the sensitivity of the unit cost of heat with electricity prices and the outdoor condition. More specifically, when $T_{air} < 7.5$ °C, c_h is highly sensitive to the electricity prices p_{el} as testified by the rapid change of colors in in the contour plot (region at the left on the red dashed line). For higher temperature, conversely, the sensitivity of c_h with the electricity prices is greatly reduced (region at the right on the dashed line).

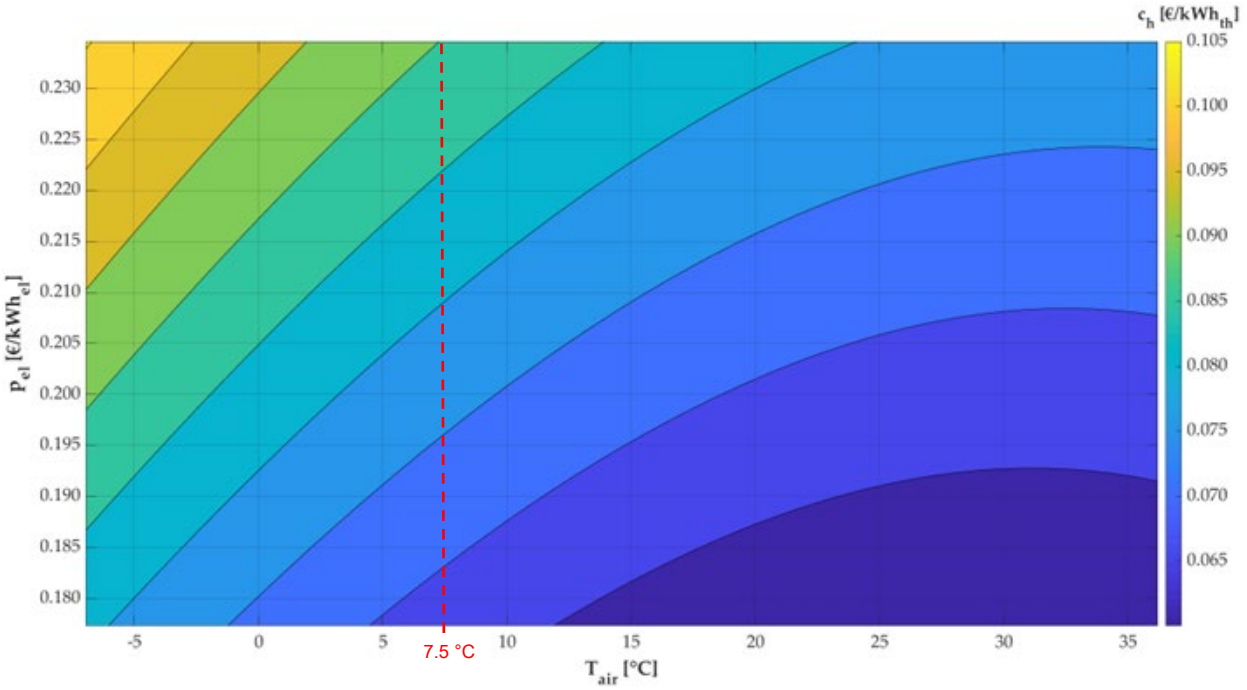

Figure 48: Map of the unit cost of heat

The analysis pointed out the key role of electricity prices in the operation of HP. Indeed, for given selling and purchasing prices of heat, the results showed an increase in the operating time of HTHP when decreasing the electricity price, as expected. Moreover, results from economic analysis highlighted that in the "Neutral" scenario, which was characterized by the absence of incentives or governmental actions that promoted flexibility, profits could be also achieved. The introduction of tax cuts and incentives for flexibility led to a relevant increase in profits in the case of a surplus in electricity production (almost +67%). In case of a deficit in electricity generation, an increase in the price component related to network cost will reduce the profits achievable by producing heat onsite through HPs. Finally, the presented study showed that in the context of smart electrical and thermal grids, HPs let to achieve flexibility for both of them and attempt to simultaneously optimize efficiency and economic profitability. The effect of incentives on the profit increase was investigated through the introduction of two simulation scenarios that include the random variation of prices in the presence or absence of incentives. The outcomes lead to reflecting on a methodology that proposes economic incentives for grid flexibility to balance the eventual inequalities, rather than to increase the profits.

The topic regarding the relationship between the prosumer and the grid will be addressed in the next paragraph, particularly as regards the amount of energy that the prosumer can deliver to the grid. The thermal curtailment concept needs to be introduced since it affects both the technical operation and economic performances of a bidirectional thermal substation

6. Techno-economic analysis of a high vacuum solar system integrated into a district heating network

The findings highlighted in the previous paragraphs reveal a lack of consensus on pricing logic and decision-making frameworks, emphasizing the need for clearer strategies to facilitate equitable third-party access and enhance the integration of prosumers into the evolving energy landscape.

Despite the great interest in novel DHC applications, it is necessary to deepen the knowledge of the potential application of thermal prosumer systems. The literature analysis underlined the necessity to propose novel analysis tools for thermal prosumer systems. Furthermore, these systems represent a technological perspective whose need for implementation is high but still requires a reference scientific framework. For this reason, scientific studies and simulation of prosumer systems are necessary to focus a general framework on the “thermal prosumer” concept and investigate technological issues that arise from these proposals, trying to study all the possible system configurations. The solar thermal prosumer is a technological concept not fully investigated that needs an in-depth analysis. Furthermore, the economic point of view of a prosumer included in the heat market needs in-depth investigations.

In this paragraph, a novel simulation tool, based on a validated model, was proposed to assess the behavior of a thermal prosumer within a bi-directional DHN. The thermal prosumer system foresees both heating and cooling operation since it is equipped with a tri-generative system supplied by high-efficiency solar collectors and absorption chillers. Two different locations and four different solar sizes were considered to investigate the effects of the heat generator scales on energy exploitation both on the user and DHN sides.

Finally, an economic analysis was conducted to design an economic framework that depends on grid operating conditions (curtailment) and market (price of heat purchased and sold), the economic performances are obtained for a wide spectrum of cases.

6.1. Building and thermo-hydraulic modeling

The analysis was performed by considering two different Italian locations, representative of two climate zones: Palermo (Csa Köppen-Geiger classification) and Verona (Cfa Köppen-Geiger classification). The climatic files were retrieved by using the Meteonorm database. In Figure 49 the monthly solar radiation and monthly average temperature for both locations are reported.

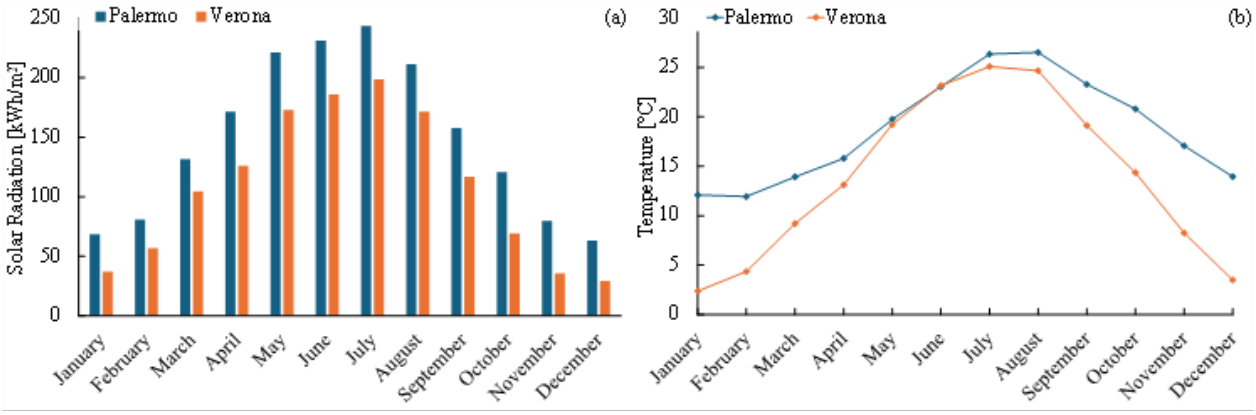

Figure 49: Monthly solar radiation (a) and monthly average temperature (b) for the selected locations

A standard building typology was adopted for the present analysis, to assess a reference benchmark for the simulation tool. The heating and cooling demand profiles were defined according to ASHRAE 90.1-2016 [149], [150] and particularized to the Italian building stock by UNI/TR 11552:2014 [151]. The adopted building consists of a standard medium office, composed of 3 floors, an aspect ratio equal to 1.5, and a window fraction of 33%. The total conditioned surface and volume are, respectively, 4980 m^2 and 19744 m^3. The heating and cooling periods were set according to Italian regulation, which also identifies 6 different climatic zones according to the standard degree days. The climatic zones are classified from zone A (hottest) to F(coldest), the selected locations belong to zones B (Palermo) and E (Verona). The crisis due to the Russian-Ukrainian war and the uncontrolled increase in energy prices led the Italian government to reduce the heating period, in Table 20 the heating and cooling periods adopted for the simulation are reported.

Table 20: Heating and cooling period adopted for the simulation

	Palermo	**Verona case**
Heating period	From 08th December to 23rd March for a maximum of 7 hours per day	From 22nd October to 7th April for a maximum of 13 hours per day
Cooling period	No restrictions – from 01st June to 30th September	No restrictions – from 01st June to 30th September

Infiltration (air infiltration allowance air changes/h), lighting, electrical equipment, and internal gains from persons, based on separate time schedules by months and day of the week, assigned by ASHRAE 90.1-2016 were defined. A different external schedule for the ideal plant, able to completely satisfy the request for heating and cooling, was realized using TRNSYS type 515, type 516, and type 519a. Thanks to the mentioned types and their interconnections, the ideal plant can operate in different configurations in the winter and summer seasons also considering the weekly schedule and annual leave. The simulation was finalized to obtain the ideal loads, the resulting values are: 27678 kWh and 73307 kWh respectively for the yearly heating and cooling load in Palermo, and 168844 kWh and 71899 respectively for the yearly heating and cooling load in Verona. Figure 50 shows the monthly heating and cooling demand for both locations.

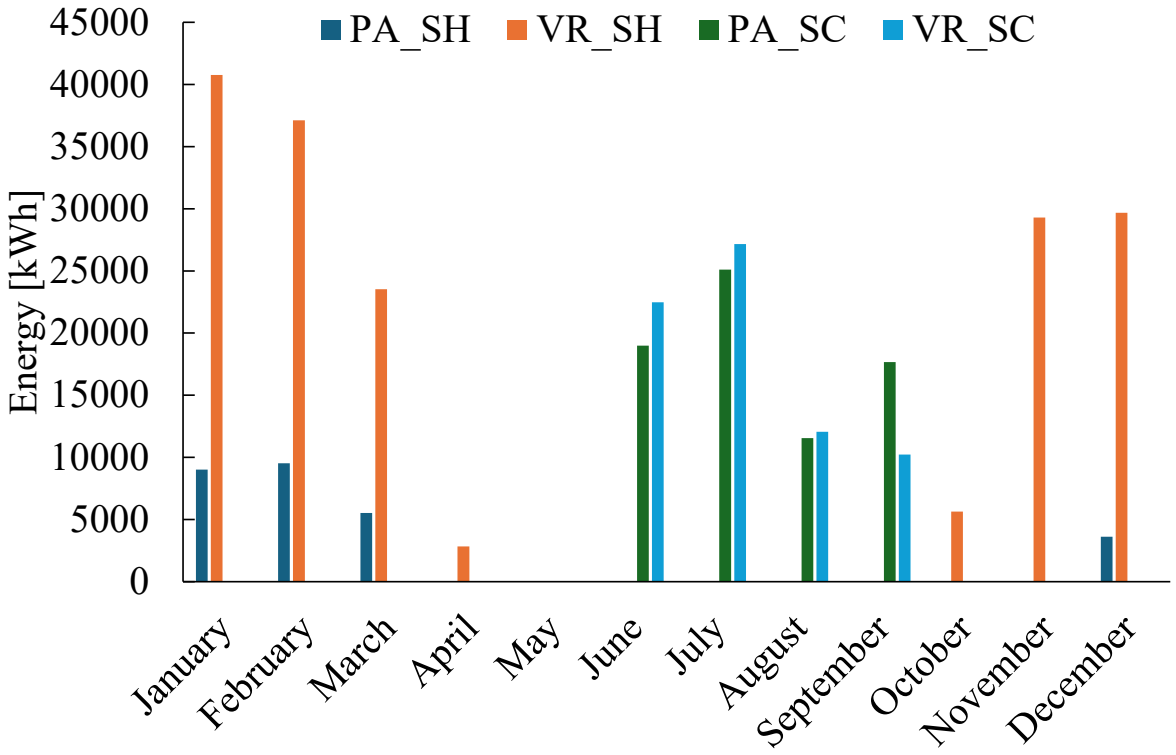

Figure 50: Heating and Cooling demands for both selected locations - Monthly values

The thermo-hydraulic system, shown in Figure 51, is composed of four main lines that connect the prosumer substation to the DHN, the heating and cooling generation systems, and the user load:

1. the primary circuit that connects the substation to DHN
2. the secondary circuit that connects the substation to the user
3. the tertiary circuit connects the substation to the local heating and cooling generation system
4. the auxiliary circuits of the solar collector system, absorption chiller, and storage tanks

The prosumer substation is configured by following the “return-to-supply” model since it ensures more reliability to the thermal system management if compared to the configuration of other thermal prosumer substations.

Three different operation modes have been set, according to the seasonal requirements.

Winter mode: the return user flow is delivered to HE2 in which it is heated up by the hot flow coming from the solar system composed of solar collectors and the storage tank. The C2 valve attempts to maintain the temperature outlet on the user line at the required set-point, if the available solar energy is not enough to reach the desired temperature set-point, the HE1 is activated. Within this heat exchanger, the user flow exchanges heat with the hot flow coming from the DHN. The seasonal S1 valve is opened on the by-pass line, to skip the vapor compression chiller that is deactivated during winter time. If the solar energy available is higher than the user demand, the excess heat is sold to the DHN through the HE3: the feed-in flow is extracted from the return line of the DHN and heated up to the temperature of the supply line by the solar plant. When there is no heat request by the user, the solar energy is entirely delivered to the HE3 and sold to the DHN.

Summer mode: through the HE2 the user flow is cooled down by the cold flow coming from the cold tank that is maintained at the desired set point by the absorption chiller. This is activated when the operating conditions occur: heat available for the absorption generator, cooling request on the cold tank, and external temperature within the operating limits admitted. If the summer set-point is not reached, the vapor-compression heat pump is operated to maintain the user cooling request. The C1' check valve is closed and the HE1 is deactivated. The seasonal valves S2 and S3 let to bypass the HE3 during the cooling operation mode. The solar energy supplies the absorption generator and the HE3 through the seasonal S4 valve that bypasses the HE2, thus avoiding heat-up of the user flow during cooling mode.

Intermediate seasons: during the intermediate seasons there is no energy requested by the user, so the entire amount of energy produced by the solar collectors is delivered to the DHN through the HE3. HE1 and HE2 are deactivated, and both chillers are turned off.

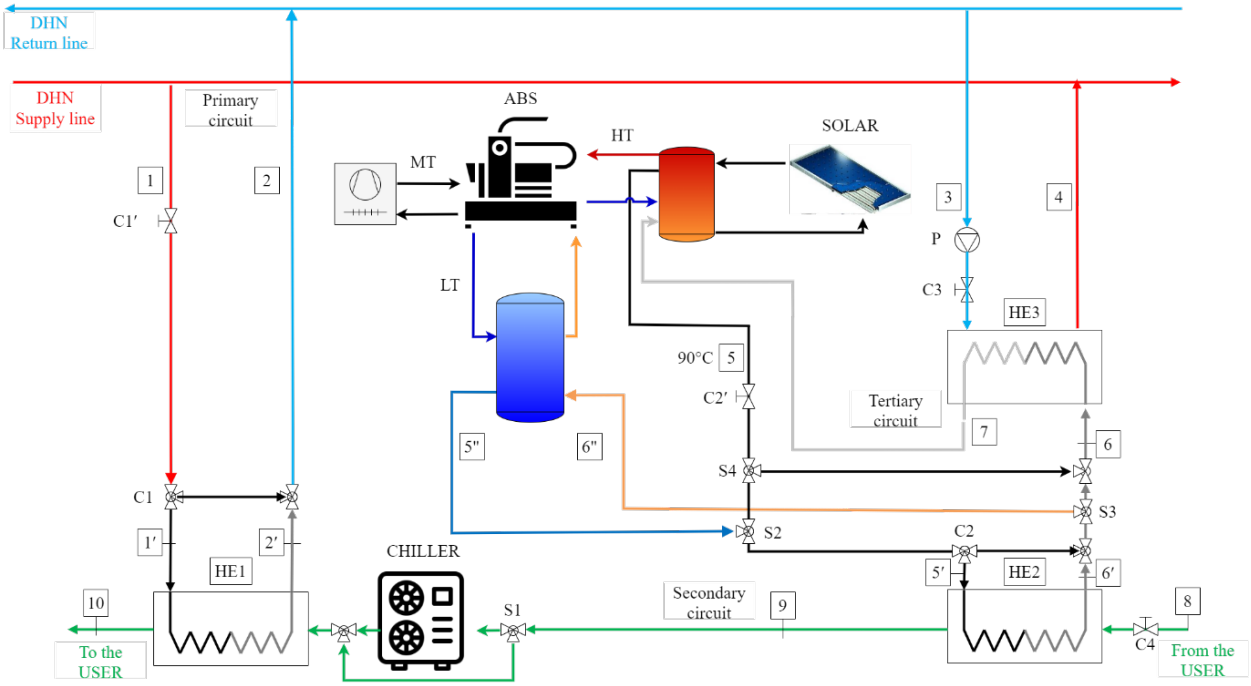

Figure 51: Layout of the thermo-hydraulic simulated model

The heat exchangers' nominal size was chosen according to the operating temperatures of both the DHN and the hydronic loop within the building. Specifically, for the DHN, return and supply temperatures of 40°C and 60°C were taken into consideration, respectively. The selected thermal levels comply with the definition of 3rd DHN generation, close to the 4th, as suggested in [83]. The user load return temperature (T8) ranges between 40°C (maximum load) and 50°C (null load) for winter, 12°C (maximum load) and 7°C (null load) for summer. The solar collector nominal set point was fixed at 95°C, but for the heat exchanger sizing the temperature inlet was set respectively at 80°C for HE2 (T5') and 95°C for HE3 (T6). The difference between T5' and T6 relies on the conservative approach implemented to ensure the correct size of HE2 even in case of lower temperatures than the nominal expected, as occurs during wintertime. The design parameters, based on winter mode, are reported in Table 21.

Table 21: Design parameters of heat exchangers belonging to the simulated prosumer substation

	Palermo case		**Verona case**	
Heat exchanger	Primary side	Secondary side	Primary side	Secondary side
HE1	F1 7558 l/h T1' 60°C T2' 45°C Q 132 kW UA 11.33 kW/°C	F9 11336 l/h T9 40°C T10 50°C	F1 18122 l/h T1' 60°C T2' 45°C Q 316 kW UA 43.82 kW/°C	F9 27182 l/h T9 40°C T10 50°C
HE2	F5 5668 l/h T5 80°C T6' 60°C Q 132 UA 5.34 kW/°C	F8 11336 l/h T8 40°C T9 50°C	F5 13591 l/h T5 80°C T6' 60°C Q 316 kW UA 12.82 kW/°C	F8 27182 l/h T8 40°C T9 50°C
HE3	F3 7085 l/h T3 40°C T4 60°C Q 165 kW UA 5.08 kW/°C	F6 5668 l/h T6 95°C T7 70°C	F3 16988 l/h T3 40°C T4 60°C Q 395 kW UA 12.18 kW/°C	F6 13591 l/h T6 95°C T7 70°C

The solar thermal system is composed of high vacuum solar collectors whose data, retrieved from the Solar Keymark certificate [90], are reported in Table 22.

Table 22: Solar Keymark Parameter of the chosen high vacuum solar thermal panel

Parameter	**Value**	**Unit**
Zero loss efficiency (η_0)	0.732	
First-order coefficient (a_1)	0.5	W/m^2K
Second-order coefficient (a_2)	0.006	W/m^2K^2
Incidence angle modifier IAM (50°)	0.95	

The design of the solar collectors (Table 23) was based on the optimization of the solar collector surface to cover the peak heating demand. Four different simulation scenarios were set by sizing the surface of collectors on different values: 100% (nominal size), 75%, 50%, and 25% of nominal size. Each string is composed of 14 collectors, and for this reason, the partial design collector surface was set to the closest theoretical value. The solar collector

system is connected to a storage tank that was sized according to the recommendation reported in [152], by considering the minimum ratio between storage volume and solar surface fixed to 0.05 m^3/m^2. For each solar system size, a simulation scenario was run to assess the influence of solar energy availability.

Table 23: Solar collector and storage tank design scenarios

Ratio of nominal size	**Palermo case**		**Verona case**	
	Solar collectors' surface	Storage tank volume	Solar collectors' surface	Storage tank volume
Nominal size (100%)	231 m^2	11.5 m^3	514 m^2	25.7 m^3
75%	180 m^2	9 m^3	385 m^2	19.3 m^3
50%	128 m^2	6.4 m^3	257 m^2	12.9 m^3
25%	51 m^2	2.6 m^3	128 m^2	6.4 m^3

The selected absorption chiller is a single-effect LiBr-H_20 manufactured by Baelz [153] the design data are indicated in Table 24. The same design size was selected for both locations since it was the closest to the peak cooling demand. The absorption chiller is connected to a storage tank whose volume was calculated as suggested by [154]. The mathematical correlation is referred to as a vapor compression chiller, that was adapted for this case. The calculated storage tank is equal to 3000 l.

Table 24: Absorption chiller nominal operating data

Hot circuit (HT)	**Cooling circuit (MT)**	**Cold circuit (LT)**
Inlet temperature 90°C	Inlet temperature 30°C	Inlet temperature 21°C
Outlet temperature 72°C	Outlet temperature 37°C	Outlet temperature 16°C
Volume flow rate 9.6 m^3/h	Volume flow rate 44.2 m^3/h	Volume flow rate 27.5 m^3/h
Heating capacity 200 kW	Heat consumption 360 kW	Cooling capacity 160 kW

The air-to-water vapor compression chiller was designed to cover the peak demand for each location, by considering the potential fault of the absorption chiller. The design data retrieved from the manufacturer [155] are shown in Table 25.

Table 25: Air-to-water chiller design operating data

Palermo case	**Verona case**
Cooling Capacity 237 kW	Cooling Capacity 188 kW
Power absorbed 74 kW	Power absorbed 58 kW
EER 3.20	EER 3.24
Dry bulb ambient air temperature 35°C	Dry bulb ambient air temperature 35°C
Water inlet temperature 12°C	Water inlet temperature 12°C
Water outlet temperature 7°C	Water outlet temperature 7°C

The methodology for modeling the absorption chiller and the vapor compression one followed the “black box approach”. Such an approach is adopted for implementing experimental data in Energy Management Systems that make use of predictive techniques to optimize energy flows [142].

The data retrieved from the Baelz datasheet (“Bumblebee model”) were processed in a statistical model to obtain equations that allow for a quick calculation of COP and Cooling Capacity by knowing the temperature inlet to the evaporator (LT_{in}), to the condenser (MT_{in}) and the generator (H_{tin}). Following this method, linear and non-linear regression analyses were carried out to find mathematical correlations between the temperature inlets and the performances, to do this a MATLAB script was used to obtain three sets of predictors:

$$COP = \frac{a_1 * HT_{in}^2 + a_2 * HT_{in} + a_3}{HT_{in} + a_4} \quad (28)$$

$$Q_{f,abs} = b_1 * HT_{in} + b_2 * MT_{in} + b_3 * LT_{in} \quad (29)$$

$$\dot{m}_{HT} = \frac{c_1 * f_{Qf} + c_2}{f_{Qf}^2 + c_3 * f_{Qf} + c_4} \quad (30)$$

$$f_{Qf} = \frac{Q_{f,abs}}{Q_{f,abs,nom}} \quad (31)$$

$$Q_{g,abs} = \frac{Q_{f,abs}}{COP} \quad (32)$$

$$Q_{c,abs} = Q_{f,abs} + Q_{g,abs} \quad (33)$$

The control logic attempts to produce chilled water at 7°C by modulating the flow rate at the generator side ($\dot{m}_{HT}$).

The statistical evaluation parameters are shown in Table 26. High values of R^2 (close to 1) and low values of root mean square error (RMSE) show the predictor’s reliability.

Table 26: Statistical evaluation parameter for the black box model of the absorption chiller

	COP	$Q_{f,abs}$	$\dot{m}_{HT}$
SSE	0.0001	8169	2.48
R^2	0.974	0.993	0.998
RMSE	0.009	3.33	0.170

The same approach was followed for modeling the vapor compression chiller. The following models were retrieved from the Aermec research engine: NRG0802X°TU°J°00 for Palermo and NRB0702°°TU°M°00 for Verona. In this case, a linear regression model was judged as suitable for the adopted technology. The EER and cooling capacity were correlated to the temperature inlet at the evaporator and the ambient air temperature. The temperature outlet was set at 7°C.

$$EER = a_1 + a_2 * T_{air} + a_3 * T_{w,in} \quad (34)$$

$$Q_{f,chiller} = b_1 + b_2 * T_{air} + b_3 * T_{w,in} \quad (35)$$

$$P_{el} = \frac{Q_{f,chiller}}{EER} \quad (36)$$

$$Q_{c,chiller} = Q_{c,chiller} + P_{el} \quad (37)$$

The statistical evaluation parameters are shown in Table 27. High values of R^2 (close to 1) and low values of root mean square error (RMSE) show the predictor's reliability.

Table 27: Statistical evaluation parameter for the black box model of the vapor compression chiller

	EER_PA	EER_VR	$Q_{f,chiller}$_PA	$Q_{f,chiller}$_VR
SSE	1.227	0.668	21.59	50.14
R^2	0.924	0.943	0.999	0.999
RMSE	0.269	0.198	1.127	1.717

The system was reproduced in TRNSYS, as described in the previous paragraphs. In addition to the prosumer substation, the absorption chiller and the vapor-compression one were modeled by introducing a black box model, implemented in the calculator TRNSYS type. The solar collector was modeled by adopting the type 539. This type tries to keep the collector outlet to the outlet set-point temperature by varying the water flow rate. In addition, it shuts off the collector (achieved by setting the water flow rate to zero) if the collector is losing energy. A quadratic correlation between the flow rate ratio and the electrical power of the circulating pump is retrieved for each scenario (Table 28).

Table 28: Correlation between the flow rate ratio of the solar system and electrical power [kW] of the circulating pump.

			Palermo case			**Verona case**		
Flow rate ratio	231 m^2	180 m^2	128 m^2	51 m^2	514 m^2	385 m^2	257 m^2	128 m^2
25%	0.163	0.135	0.135	0.026	0.105	0.093	0.17	0.135
50%	0.301	0.188	0.188	0.099	0.599	0.505	0.324	0.188
75%	0.910	0.567	0.567	0.282	1.876	1.560	0.986	0.567
100% (Nominal flow rate)	2.095	1.317	1.317	0.631	4.381	3.623	2.276	1.317

A seasonal control manages the flow delivered to the HE3 for the prosumer mode to avoid an excessive discharge of the hot storage tank: during the winter period the prosumer mode is activated when the temperature of the storage tank at the outlet node of the pipeline is higher than 65°C; during summer this reference temperature is elevated at 80°C to maintain a thermal level adequate to the absorber generator.

A set of KPIs is introduced with the purpose of better comparing the different sizing scenarios and the effect of the different locations:

$$f_{sol,w} = \frac{\int_{ti}^{tf} \dot{Q}_{load,w}\, dt}{\int_{ti}^{tf} \dot{Q}_{HE2,w}\, dt} \tag{38}$$

$$f_{DHN,w} = \frac{\int_{ti}^{tf} \dot{Q}_{load,w}\, dt}{\int_{ti}^{tf} \dot{Q}_{HE1}\, dt} \tag{39}$$

$$f_{abs,s} = \frac{\int_{ti}^{tf} \dot{Q}_{LT}\, dt}{\int_{ti}^{tf} \dot{Q}_{load,s}\, dt} \tag{40}$$

$$\varepsilon_{solar} = \frac{\int_{0}^{8760} \dot{Q}_{solar}\, dt}{A_{sol,tilt} * \int_{0}^{8760} I_{tilt}\, dt} \tag{41}$$

$$COP_{abs} = \frac{\int_{ti}^{tf} \dot{Q}_{LT}\, dt}{\int_{ti}^{tf} \dot{Q}_{HT}\, dt} \tag{42}$$

$$EER = \frac{\int_{ti}^{tf} \dot{Q}_{c}\, dt}{\int_{ti}^{tf} P_{el}\, dt} \tag{43}$$

$f_{sol,w}$ (Eq.(*38*) represents the fraction of heating demand directly covered by the solar system within the period included between t_i and t_f, in this case, the heating period. $f_{DHN,w}$ (Eq.(39) represents the complement to $f_{sol,w}$ and is the fraction of heating demand covered by the district heating in the same time period. $f_{abs,s}$ (Eq.(40) represents the fraction of cooling

demand covered by the absorption chiller during the period included between t_i and t_f, in this case, the cooling period. ε_{solar} (Eq.(41) represents the efficiency of solar collectors expressed as the ratio between the thermal energy produced by the collectors on the solar radiation incident on the tilted surface of the collectors. COP_{abs} (Eq.(42) represents the thermodynamic efficiency of the absorption chiller calculated as the ratio between the cooling energy produced at the evaporator and the heating energy demand of the generator within the whole cooling period. Finally, the EER (Eq. (43) is the energy efficiency ratio of the vapor compression chiller expressed as ratio between the cooling energy produced at the evaporator and the electrical energy absorbed by the compressor and the condenser fan within the whole cooling period.

6.2. Energy performance and thermal dynamics of the simulated system

Two reference days for each location were selected to better understand the dynamic behavior of the described system. The daily trends of the heat exchanger heat capacity are shown, and the nominal solar size and 50% size were chosen as reference for each location.

Figure 52 shows the daily trend of the substation, in terms of heat capacity exchanged by each HE. The reference days were chosen by selecting those that show activity for each HE in winter and for HE3, and the absorption generator in summer. For the Palermo case, the selected days were the 30th of January and the 10th of July. In Figure 52a it is possible to observe that during the first part of the day: the heat capacity exchanged with the solar system via HE2 and through the DHN via HE1 maintain a specular trend: in the case of nominal solar size the HE2 exchanges more heat than the 50% case, conversely, the HE1 heat capacity is reduced in the case of nominal size. In the second part of the day when the solar tank has increased the energy stored and the user load is lower than the first part, the HE2 operation is identical for both cases and the prosumer mode is operated, with relevantly higher values for the nominal solar collector size case. The excess heat is sold to the thermal grid, in the case of 230m^2 the system shows a second smaller peak in the last part of the day, while in the reduced case this event is not evident since the thermal levels of flow coming from the storage tank to the HE2 and HE3 are not enough to supply heat to the grid.

During the summer period (Figure 52b), the solar energy delivered to the absorber generator represents the maximum contribution in the first half of the morning and afternoon, with an oscillating trend of 50% solar system size case due to the thermostat activation, The prosumer operation shows a high peak of 150 kW (230 m^2 case) in the central part of the day when there is no need for cooling by the user, an analog peak is not retrieved by 50% size results. In the remaining part of the day, the prosumer mode is activated with an oscillating behavior since the thermostat is set to higher temperatures during summer, to comply with absorber generator requirements, for this reason, when the hot tank reaches the lower setpoint, the F7 flow is interrupted.

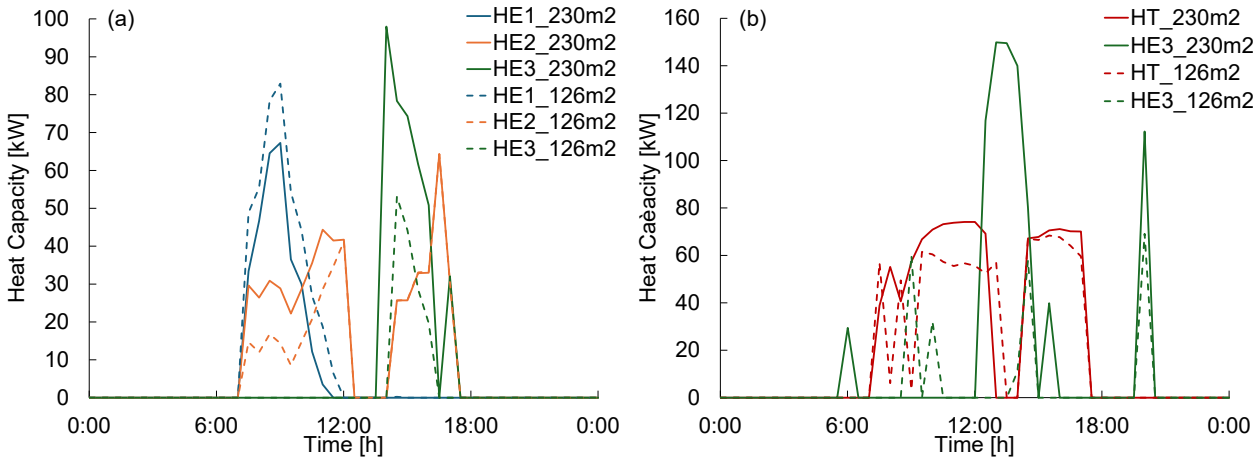

Figure 52: Dynamic trend for a reference winter day (a) and summer one (b) in Palermo

For the Verona case, the selected days were the 21st of March and the 25th of July (Figure 53). Even in this case, during winter mode (Figure 53a), the HE1 operation is relevant in the first part of the day when the solar irradiation is lower and the user load is maximum, an evident difference is noticeable between the two sizing cases, with higher values of HE2 capacity for the nominal size. In the second part of the day, both selected cases show

identical behavior for HE2, thus showing that the solar energy produced in the previous hours is enough to cover the user load request, while a high activity of prosumer mode is shown in the second part of the day with a peak of 175 kW for nominal solar sizing scenario. The oscillating behavior is evident also in this case for the reduced scenario and, finally, within the same sizing case, it is possible to observe the operation of HE1 to compensate for the lack of energy available for the user in the last part of the day.

During summer mode (Figure 53b) the absorber works for almost all day from early morning to late evening, thus allowing a constant supply of cooling energy to the cold storage with evident differences between the two selected cases: the nominal solar size case shows more availability of heat and, consequently, higher operation rate of absorption generator. The prosumer mode is active all day, including nighttime, although for the nominal size, the amount of heat sold to the grid is relevantly huger than the 50% sizing case.

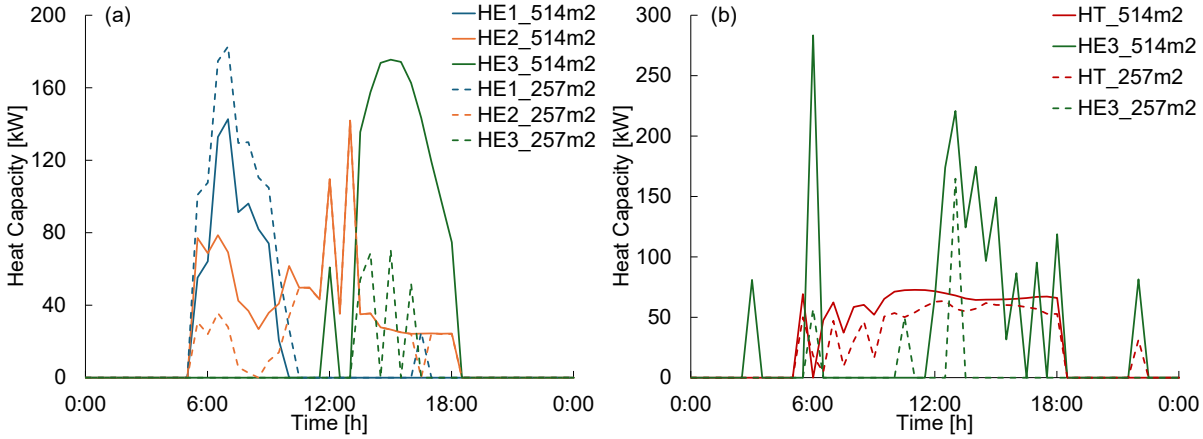

Figure 53: Dynamic trend for a reference winter day (a) and summer one (b) Verona

The active and bi-directional thermal substation model opens the view to a wide range of possible applications for future district heating systems. This approach ensures flexibility for the integration of intermittent renewable energy sources, such as solar ones. The analysis carried out until here traces the theoretical borders for thermal energy transfer from the user to the grid. A model based on a thermohydraulic system (as the one proposed in the present work) and on an energy market assessment can give a full view of the behavior of the described system. The simulation results consider that all the excess heat produced by the solar collector system is exchanged with the DHN, but in real thermal infrastructure, this operation should be approved by the network system operator, by introducing third-party agreement contracts. According to the thermal grid architecture and the mix of thermal energy sources, the network operator can forbid or require the “prosumer” operation, this aspect can strictly affect the optimal sizing of each component and the control management of the system and then, the physical operation of the system. The tri-generation system, coupled with a tertiary user, shows positive results in terms of phasing energy demand and supply, thus reducing the excess of heat. Since most energy demand is required during diurnal periods, the exploitation of energy produced by solar collectors is maximum either directly (for heating purposes) or indirectly by supplying the absorption chiller.

Starting from the case of Palermo, Figure 54 shows the total energy balance of the substation during the winter operation mode. More specifically, it displays the ratio between

the energy transferred by each HE for each solar system size and the total energy exchanged within the substation. As shown in Figure 54a, the heat produced by the solar system and supplied to the user (via HE2) represents the maximum contribution to the overall energy exchanged for the two intermediate sizes (75% and 50%), accounting respectively for 41% (19115 kWh) and 40% (15622 kWh). The 100% size case shows the prevalence of HE3 (energy produced by the solar system and injected into the grid). In comparison, the opposite case (25% size) shows a relevant prevalence of HE1 operation, thus representing the need to purchase heat from the DHN, due to the undersized solar system. The energy distribution ratio among the three heat exchangers shows a linear trend in the first three sizing scenarios, then, in the last one (25% size – 51 m^2) the HE1 energy share increase is dominant on the operation decrease of the other two heat exchangers with a share of 64.8% and 20180 kWh.

Figure 54b shows the fraction of the heat produced by the solar system which is either supplied to the user (HE2) or delivered to the DHN (HE3) during the winter operation mode. It is worth noting that the main contribution belongs to DHN (53% - 21742 kWh for HE3) only in the 100% sizing scenario (230 m^2). In the three scenarios that implement an undersized solar system, which implies the decrease of available heat produced by solar collectors, most of the heat produced by the solar system is supplied to the user through the HE2. This information is useful for optimizing the design of the solar system.

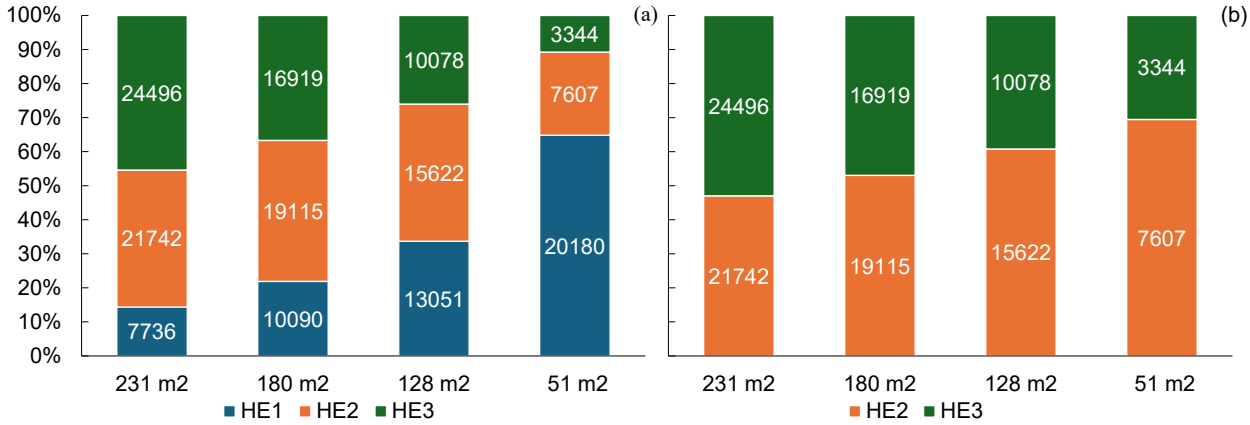

Figure 54: Energy balance (kWh) of the substation during winter in Palermo. Energy distribution among the three heat exchangers (a), and energy sharing of the amount of energy produced by the solar system (b)

The energy balance of the substation and the solar system during the summer operation mode and average season is shown in Figure 55. During the summer operation mode (Figure 55a) the heat produced by the solar system is delivered to the generator of the absorption chiller (Q_HT) and the DHN. The ratio of energy supplied to the absorber linearly increases when decreasing the solar collector surface, in the meantime, the absolute value decreases ranging from 31116 kWh and 12858 kWh. In three cases (100%, 75%, and 50% of nominal size) most of the energy produced by the solar system is injected into the DHN, only in the last scenario the simulation shows a balance between the two contributions.

In the average seasons (Figure 55b), when all the solar energy is delivered to the DHN, the decreasing trend of energy exchanged by HE3 is evident, ranging from 88896 kWh to 18117 kWh when passing from 231 m^2 to 51 m^2.

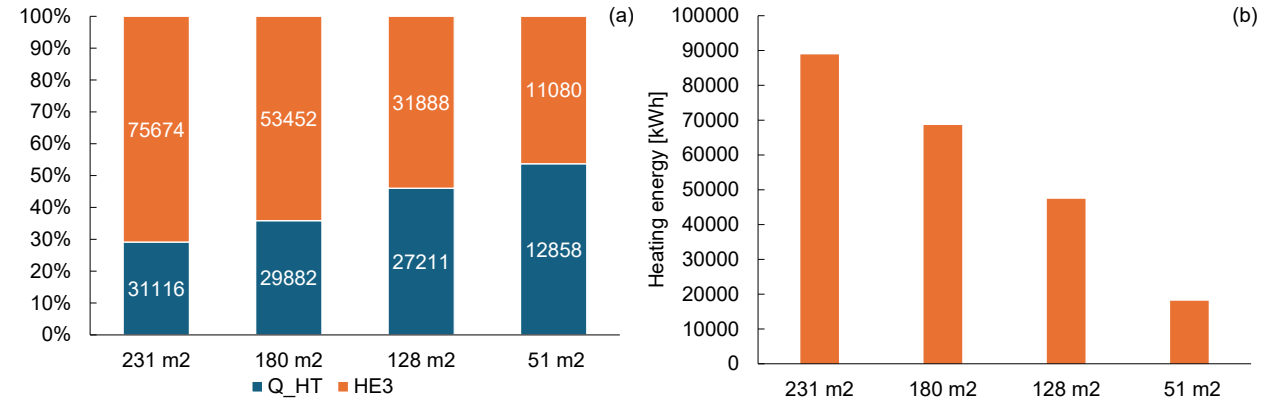

Figure 55: Energy balance (kWh) of the substation and solar system during summer (a) and average season (b) in Palermo

The KPIs reported in Table 29 describe the overall performances of the analyzed system by considering the most relevant components and their relationship with dynamic user load.

The solar covering of the thermal load during the winter period has a linear decreasing trend when passing from 231 m^2 to 128 m^2 cases, the last case shows a higher decreasing ratio since the solar system cannot provide the required thermal level to supply the user load. The fraction covered by the DHN is complementary to the previous one and ranges between 26.2% to 72.6%, showing that also in the best solar covering and warm climate, a relevant amount of heating energy is supplied by the DHN.

The fraction of cooling load covered by the absorption chiller shows a slight decrease in the first three cases and a drastic decrease in the last one, due to missed requirements in terms of the thermal level of the absorber generator, the complementary part is covered by the compression chiller.

The solar efficiency shows a quite constant trend with a slight increase in the case of the minor solar surface, due to higher temperature lift between inlet and outlet of the collectors. The absorber COP maintains the same values for the first three cases and shows a relevant derating in the last one, due to the lack of energy to the absorber and a fixed energy requirement and thermal level at the evaporator. Finally, the EER of the compression chiller maintains a stable level despite the increase in cooling demand when passing from the first to the last case.

Table 29: KPI for the Palermo case

KPI	231 m^2	180 m^2	128 m^2	51 m^2
$f_{sol,w}$	73.8%	65.5%	54.5%	27.4%
$f_{DHN,w}$	26.2%	34.5%	45.5%	72.6%
$f_{abs,s}$	33.6%	32.1%	28.7%	12.3%
ε_{solar}	52.8%	53.2%	53.2%	54.5%
COP_{abs}	0.79	0.79	0.77	0.70
EER	4.6	4.6	4.6	4.6

The analysis of the winter operation mode for the Verona case shows relevant differences from the previous case. Figure 56 shows the energy balance of the substation for the Verona case during winter operation mode. In this case, the contribution of HE1 is dominant over the other heat exchangers (Figure 56a), thus revealing that the role of DHN in supplying heat to the user is basilar for almost all winter operation periods in all cases. Unlike the Palermo case, the increasing trend of the HE1 contribution is here evident, the energy share of HE2 and HE3 is consequently linearly reduced. The prosumer operation, performed by HE3 is marginal in all cases, this result is clearly visible in Figure 56b: its share of energy produced by the solar system ranges from 28.6% (27419 kWh) for the nominal size to 14.9% (3835 kWh) for the minimum size.

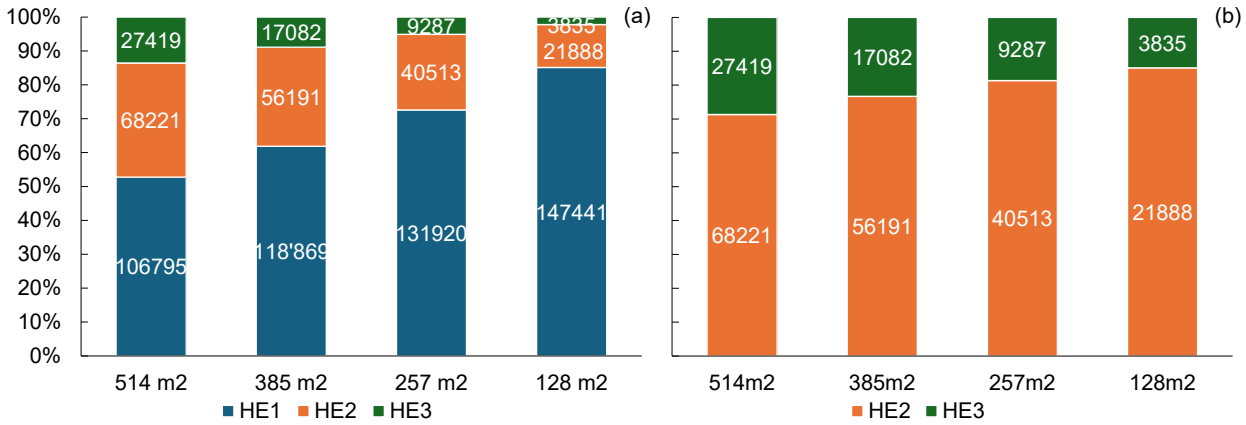

Figure 56: Energy balance (kWh) of the substation during winter in Verona. Energy distribution among the three heat exchangers (a) and energy sharing of the amount of energy produced by the solar system (b)

The simulation results for the summer operation mode (Figure 57a) show that the prosumer mode is dominant in the amount delivered to the absorption generator. This dominance is evident for all the sizing scenarios but is worthy of notice that the absolute values of Q_HT decrease, underlining that, although the relevant excess of energy is produced, the solar system is not oversized. The average operation season (Figure 57b) shows a trend that is similar to the Palermo case, also in terms of absolute values of energy supplied to the thermal grid, although the solar collector surface is relevantly different, this is due to the different solar irradiation and different operating periods.

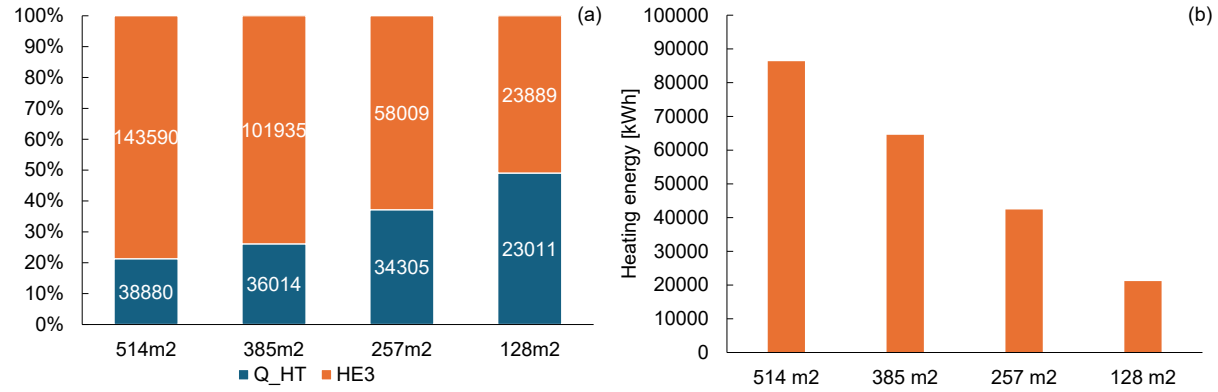

Figure 57: Energy balance (kWh) of the substation and the solar system during summer in Verona (a) and average season (b)

In all cases, the bidirectional access to the thermal grids allows meeting the demand when the solar energy is not enough and avoids dissipating the excess heat produced when there is no request from the loads (user or absorption chiller).

The KPIs for Verona case (Table 30) reveal that, despite the solar sizing adapted to the peak load, the solar load covering fraction during the winter period is about 50% lower in all sizing cases if compared to the Palermo climate. In this context, the presence of DHN for load supply is necessary since its load-covering fraction ranges from 61% to 87.1% when passing from the maximum to the minimum solar collector size. Conversely, the fraction of load covered by the absorption chiller during summer shows better performances than in the Palermo case, revealing that such a system can offer valid support even in the cooling period; the $f_{abs,s}$ slightly decrease when passing from 514 m^2 to 257 m^2 case, then it undergoes to a drastic derating.

The solar efficiency maintains a quite constant behavior for all size scenarios, the COP of the absorption chiller shows its maximum values that tend to decrease more evidently only in the last case. Finally, the EER is constant for all the considered solar sizing, although the amount of cooling load covered by the absorption chiller increases complementary to $f_{abs,s}$.

Table 30: KPI for the Verona case

KPI	514 m^2	385 m^2	257 m^2	128 m^2
$f_{sol,w}$	39.0%	32.1%	23.5%	12.9%
$f_{DHN,w}$	61.0%	67.9%	76.5%	87.1%
$f_{abs,s}$	43.0%	39.3%	37.1%	23.6%
ε_{solar}	49.3%	49.7%	49.9%	50.7%
COP_{abs}	0.80	0.78	0.78	0.74
EER	4.3	4.3	4.3	4.3

6.3. Economic Analysis

One of the most relevant barriers that hinder the penetration of renewable energy, especially in retrofit operations, is the investment cost. In the last decades, several countries adopted state incentivization provisions to foster new sustainable technologies.

The economic analysis was carried out considering that the described system was introduced within an existing baseline system as a retrofit operation. The baseline system comprises the same user that DHN entirely supplies for the heating demand and the vapor compression chiller for the cooling one.

The estimation of the capital expenditure (CAPEX) regards the installation of the solar collector system (including pipelines and auxiliaries), absorption chiller, thermal storage, and the expansion of the substation to change from simple thermal consumer to prosumer.

The solar collector CAPEX estimation is affected by the size of the proposed system which is considerably higher than the small system for single house application for DHW (<10 m^2) and, conversely, lower than the solar district heating application (>1000 m^2). The market references are given for the two aforementioned applications, an average estimation was performed due to the size range of the current analysis. The Danish Energy Agency releases yearly the market trend for a wide set of technologies, for the solar collector technology the costs range between 320 €/m^2 and 470 €/m^2 [156]. The International Renewable Energy Agency (IRENA) reports a range variable from 409 USD/kW to 1000 USD/kW for some European Countries [157]. Considering the nominal efficiency of the selected solar collector technology (η=0.68), the technology of the collector (high vacuum), and the high performance declared by manufacturers, the estimated CAPEX for the present analysis was 500 €/m^2. The Operational Cost (OPEX) is composed of two main components: maintenance costs and operating costs. For the solar system, the yearly maintenance costs are estimated on a fixed tariff of 250€ plus a variable cost proportional to the collector's surface: 1 €/m^2. The operating costs of the solar system are related to the electricity consumption to supply the circulating pump and the dry cooler operated to dissipate the excess heat during the eventual moments of thermal grid curtailment, i.e., situations during which the grid dealer can't receive the excess heat by the prosumer. In these cases, to avoid the overheating of the collectors, a safety dry cooler is operated.

The absorption chiller CAPEX was estimated by considering several sources. In [158] a solar-coupled absorption system was presented; the CAPEX of the absorption chiller was 472 €/kW (referred to as the cooling nominal capacity). In [159] an absorption chiller was coupled with a Fresnel solar plant with a specific cost of 288 €/kW, in [160] a CAPEX ranging between 314 and 571 €/kW is reported with an Operation and Maintenance cost of 0.17 €/kWh (cooling), comprehensive of electricity needed to activate the circulating pumps. Considering the range explored and the maturity of the absorption technology, the CAPEX selected for the present study is 411.6 €/kW, with a maintenance cost of 0.05 €/kWh, the first referred to the nominal cooling capacity, the second to the cooling energy produced for one year.

For the assessment of the thermal storage CAPEX, the large volume should be considered. Analogously to the solar system, the selected sizes are among the most usual sizes

recognized by the market: the domestic tanks with a volume that usually doesn't exceed 0.5 m^3 and large storage tanks used for district heating systems whose volume typically is higher than 1000 m^3. The European Association for Storage of Energy, for the selected size range, suggests 1200 €/m^3 [161]. An installation of a high-stratification storage tank performed within SunHorizon project [162] showed a CAPEX of approximately 1500 €/m^3. Also in this case an average value of 1350 €/m^3 was assessed.

Finally, the installation cost for expanding the substation should be considered. A substation equipped with a single heat exchanger (simple consumer) is installed in the reference case. The simulation takes into account a substation equipped for the prosumer operation with three heat exchangers and the relative auxiliaries (piping, valves, circulator, sensors, etc.). The Danish Energy Agency [163] presents a range varying between 30 and 70 €/kW. The first value refers to the substation whose nominal capacity is analog to those implemented in the present study, so that value was adopted as reference CAPEX.

A summary of Investment Costs is indicated in Table 31. The impact of the solar system on the overall CAPEX is the most relevant in almost all cases. When the solar collector surface is lower, the relevance decreases and the absorption chiller has a higher weight (45% and 63% for Palermo – 128 m^2 and 51 m^2 for absorption chiller versus 43%, 25% for solar system). The storage and substation have a lower weight on the total investments, equal to 12 % for Palermo and ranging between 15 and 18 % for Verona.

Table 31: Investment Costs for the Simulated Scenarios

	Palermo case				**Verona case**			
	231 m^2	180 m^2	128 m^2	51 m^2	514 m^2	385 m^2	257 m^2	128 m^2
Solar collectors	115500€	90000€	64000€	25500€	257000€	192500€	128500€	64000€
Thermal Storage	15525€	12150€	8640€	3510€	34695€	26055€	17415€	8640€
Absorption chiller	65854€	65854€	65854€	65854€	65854€	65854€	65854€	65854€
Substation	8918€	8918€	8918€	8918€	21350€	21350€	21350€	21350€
TOT CAPEX	**205797€**	**176922€**	**147412€**	**103782€**	**378899€**	**305759€**	**233119€**	**159844€**

The Operation Expenditure costs (OPEX) consider both the operation cost due to the purchase of electricity and heat and the maintenance costs.

The price of electricity was estimated by considering both Italian electricity prices for 2023 presented by Eurostat (non-domestic users, yearly consumption ranging between 20 and 500 MWh) [164], the same data are confirmed by the Italian Regulatory Authority for Energy, Networks and Environment (ARERA) [165]. The price of heat was assessed by considering the price list for 2023 released by the company that manages the district heating system for the municipality of Verona [166]. A yearly average price was calculated by considering the

monthly variation presented by the company for the user that requests less than 25000 Mcal per month. The price of both energy vectors is indicated in Table 32.

Table 32: price of energy vectors

	Price
Electricity	0.2044 €/kWh
Heat (from DHN)	0.1786 €/kWh

Finally, the yearly OPEX costs are indicated in Table 33. Electricity is the most relevant contribution among the expenditures for the Palermo case, the expenditure for purchasing heat from DHN increases when the solar collector surface decreases, in the last scenario (51 m^2) electricity and heat have the same weight in the overall balance. In the Verona case, the heat purchase always shows the most relevant contribution and, in terms of absolute values of OPEX, Verona shows expenditures three times higher than Palermo, due to the higher heat demand.

Table 33: Operation Expenditure costs, comprehensive maintenance and operating costs

	Palermo case				**Verona case**			
	231 m^2	180 m^2	128 m^2	51 m^2	514 m^2	385 m^2	257 m^2	128 m^2
Maintenance	1741 €	1635 €	1456 €	764 €	2347 €	2081 €	1872 €	1248 €
Electricity	3634 €	3328 €	3399 €	3400 €	3683 €	3507 €	3485 €	3624 €
Heat (DHN)	1382 €	1802 €	2331 €	3604 €	19073 €	21230 €	23561 €	26333 €
TOT OPEX	**6757 €**	**6765 €**	**7186 €**	**7768 €**	**25103 €**	**26818 €**	**28917 €**	**31204 €**

The OPEX of the baseline scenario was calculated by considering that the entire heat demand is supplied by the DHN and the cooling demand by the existing chiller (Table 34).

Table 34: Operation Expenditure Costs of the Baseline Scenario

	Palermo Baseline	Verona Baseline
Electricity	3225 €	3411 €
Heat (from DHN)	4943 €	30155 €
TOT OPEX	8168 €	33566 €

The economic evaluations will be based on two yearly components: the Cash Flow (CF) and the Incomes obtained by the heat sold to the grid (I_{th}).

The cash flow (CF) resulting from the difference between the yearly OPEX of the baseline system compared to the simulated scenarios was calculated as indicated in Eq. (44).

$$CF_i = OPEX_{baseline} - OPEX_{scen,i} \quad (44)$$

To define the maximum amount of income that yearly can be achieved through savings (determined by the Cash Flow) and by selling heat to the grid, I_{th} was defined as indicated in Eq (45).

$$I_{th} = Q_{HE3} \times p_{sell\_DHN} \quad (45)$$

Q_{HE3} is the total amount of heat exchanged by the HE3 and p_{sell_DHN} is the selling price of heat to the DHN. In the theoretical case, the maximum income considers selling all the excess heat produced by the solar system at the same price as heat purchase. Table 35 shows the maximum theoretical income yearly achievable for each simulated scenario, I_{th} contribution is predominant on the yearly balance. While the cost to purchase electricity is higher in the simulated scenarios if compared with the simulated ones, the CF is higher than zero because of the heat savings achieved by the solar collectors.

Table 35: Maximum incomes yearly achievable for each scenario

	Palermo case				**Verona case**			
	231 m²	180 m²	128 m²	51 m²	514 m²	385 m²	257 m²	128 m²
CF	1412 €	1404 €	983€	400€	8463 €	6748 €	4649 €	2361 €
I_{th}	33767 €	24821 €	15964 €	5812 €	45959 €	32786 €	19595 €	8732 €
TOT INCOMES	**35178 €**	**26224 €**	**16946 €**	**6212 €**	**54422 €**	**39534 €**	**24243 €**	**11093 €**

The selected comparison parameter was the Net Present Value (NPV) which offers a direct method to evaluate and compare the feasibility of investments proposed for each scenario. The NPV was calculated according to Eq. (46).

$$NPV = \sum_{t=0}^{N} \frac{FC_t}{(1 + WACC)^t} \quad (46)$$

Where WACC is the Weighted Average Cost of Capital and N is the foreseen lifetime of the components. The WACC estimation is mainly related to the technology proposed for the investment. In this case, the selected WACC considers the calculations performed in 2022 for Heating Companies and Heat Exchangers in the Netherlands, actively operating in the field of District Heating [167]. WACC is fixed at 4.23% and N=20 years.

Starting from the maximum theoretical income reported in Table 35 a sensitivity analysis was carried out to analyze the effects of introducing the prosumer role within the system. I_{th} component was varied by considering variables both Q_{HE3} and p_{DHN} (Eq.(45). In a real system it could happen that the thermal grid manager can't accept the thermal energy that a prosumer is available to inject into the grid, due to several factors (low demand, unavailability to partialize the centralized heat generators, hydraulic interferences, etc.).

During these moments a thermal curtailment occurs (analogously to the electrical grid with renewable energy powerplants) and the prosumer must reject to the environment the excess heat produced by the solar collectors since the storage is at full capacity. In these circumstances an additive cost is considered in the energetic and economic calculations: the activation of a safety dry-cooler, installed to avoid the super-heating and stagnation of collectors. In the economic analysis a curtailment ratio ranging from 0 to 100% was considered (it means that the DHN manager accepts all the heat released by the HE3 for 0% curtailment and cuts off all the heat available in the case of 100% curtailment). The p_{sell_DHN} (price of heat sold to the DHN) was varied between 0% and 100% p_{DHN} (price of heat purchased to the DHN), to explore the whole range of p_{sell_DHN} that can be negotiated between the prosumer and the DHN manager and its effects on the economic profitability in a long-term perspective.

For each scenario, an NPV matrix was produced by using a tailored script created in Matlab R2023b environment, it shows the trend of NPV achieved by variating the curtailment ratio (%cur) and the price of heat sold to the DHN (p_{sell_DHN}).

A map of the NPV trend for the scenario of Palermo – 231 m^2 is shown in Figure 58. The line expressing the value NPV=0 represents the front between the conditions that make the investment profitable or vice versa. The intercept between the zero-NPV line and x-axes, p_{sell_DHN} (NPV=0), (that represents the price of heat sold to the grid expressed as a ratio of the purchase price of heat) represents the minimum selling price of heat to the DHN which makes profitable the investment. The intercept with y-axes, $\%_{cur}$ (NPV=0), (that represents the curtailment ratio) represents the maximum allowable curtailment ratio which makes the investment profitable.

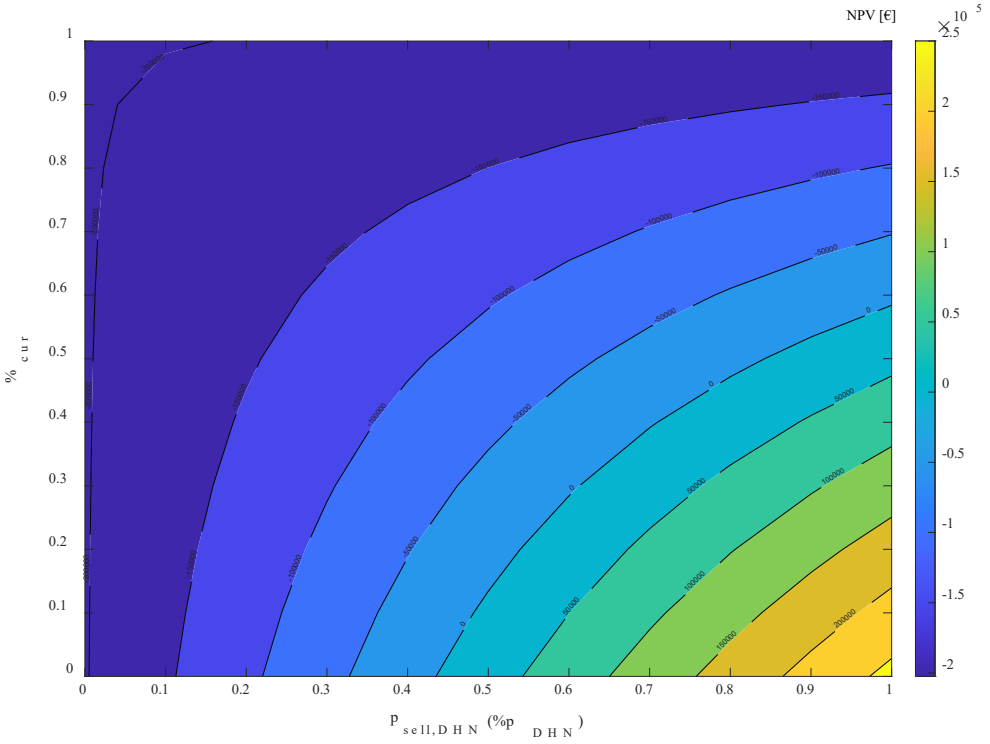

Figure 58: NPV behavior map for Palermo - 231 m^2 scenario

Table 36 reports the couples of intercepts of the zero-NPV front for all the simulated scenarios. The main result arising from the observation of this data is that the profitability decreases when the collector's surface decreases. This is due to the decrease of incomes arising from selling heat to the grid, even though in the best-case scenarios (Palermo – 231 m2 and Verona 514 m^2) the minimum allowable selling price ratio is high (respectively 43.5% and 45.4% of the purchasing price) since it is referred to a limit condition that marks the passage between profitability and vice versa. It means that, for a fixed NPV aim, the minimum selling price could be unacceptable from the DHN manager; as an example, concerning Figure 58, if the investment aims to obtain an NPV of 100 k€ after 20 years, the heat must be sold at a price higher than the 66% of the purchasing price. Consequently, the DHN manager should buy from the prosumer at that price and sell at p_{DHN} with a very low profit margin, which could be higher than its generation costs.

An analog consideration could be done with the maximum curtailment limit allowable for the profitability condition. Since curtailment can occur both for technical needs and economic reasons, the increase in the selling price of heat can determine a higher curtailment ratio.

The two scenarios with the smallest solar collector's surface present negative values of NPV in all the conditions.

Table 36: values of intercept between the zero - NPV front and axes

	Palermo case				**Verona case**			
	231 m^2	180 m^2	128 m^2	51 m^2	514 m^2	385 m^2	257 m^2	128 m^2
p_{sell_DHN} (NPV=0)	0.435	0.496	0.644	/	0.454	0.511	0.668	/
$\%_{cur}$ (NPV=0)	0.584	0.521	0.368	/	0.565	0.506	0.344	/

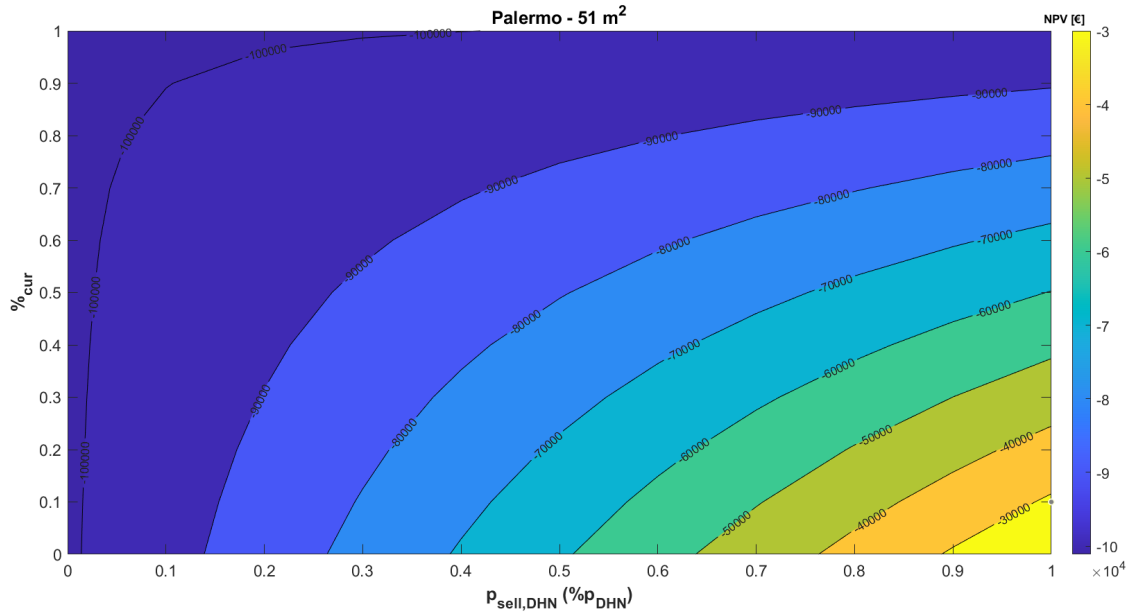

Figure 59: NPV behavior map for Palermo - 51 m² scenario

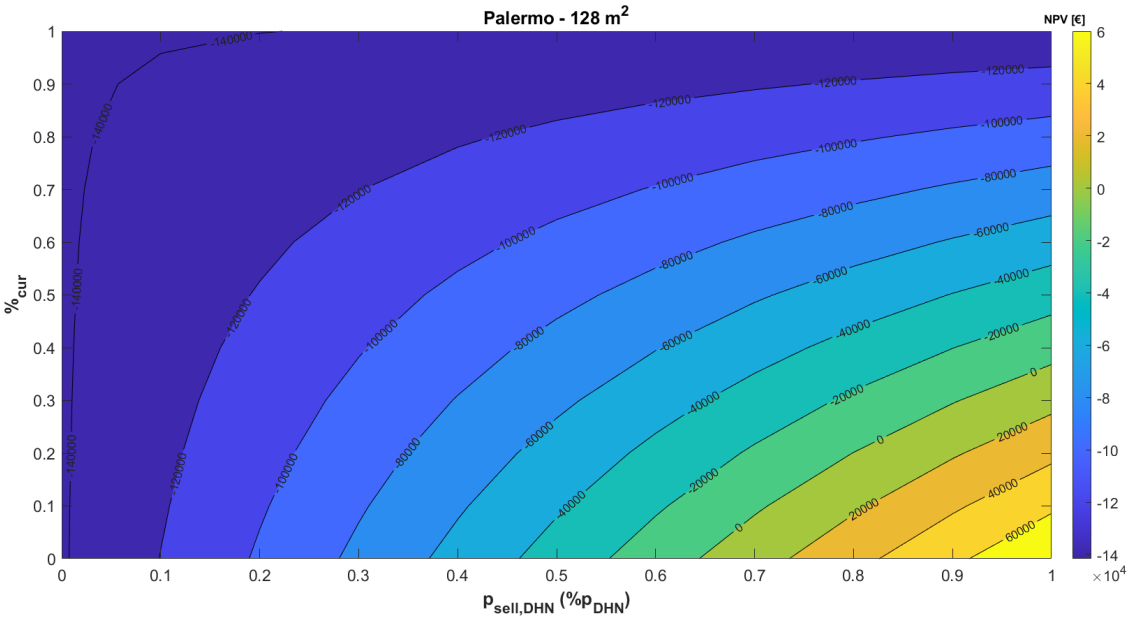

Figure 60: NPV behavior map for Palermo - 128 m² scenario

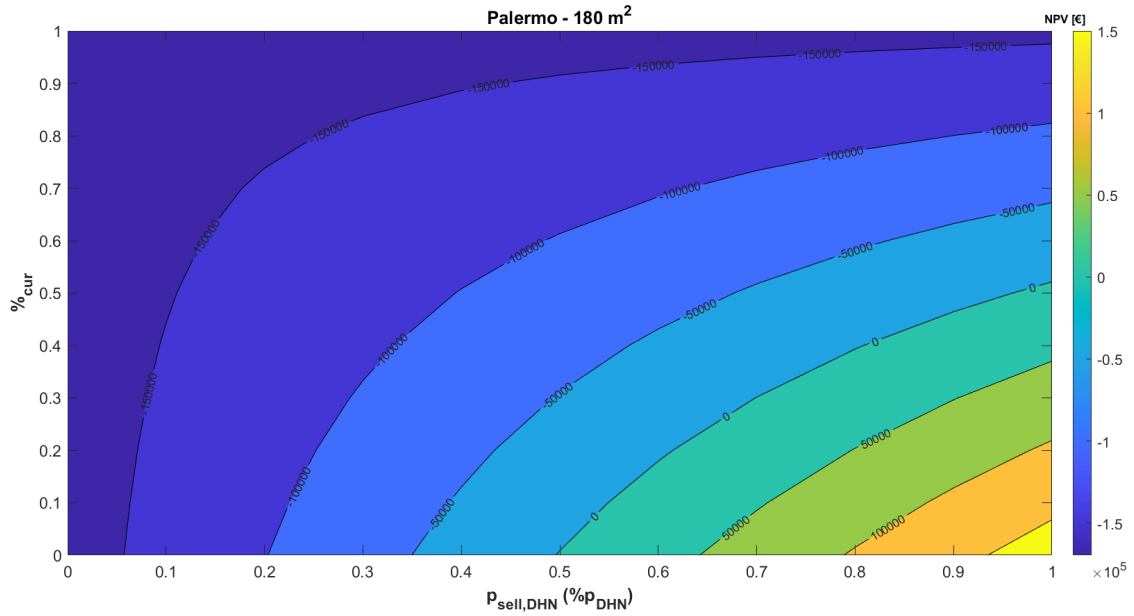

Figure 61: NPV behavior map for Palermo - 180 m² scenario

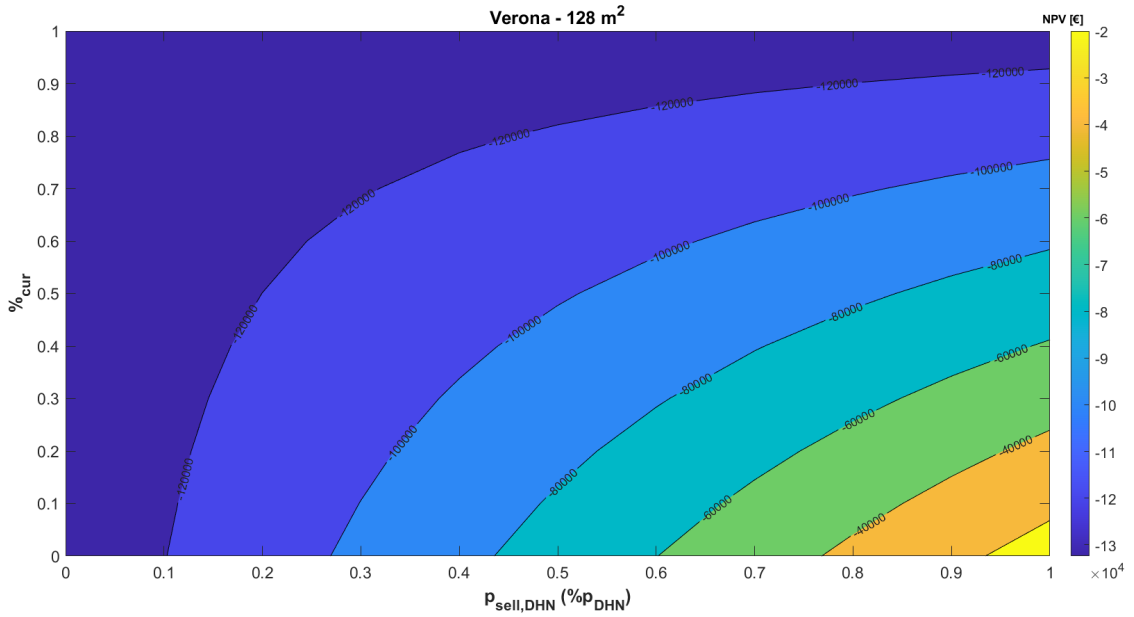

Figure 62: NPV behavior map for Verona - 128 m² scenario

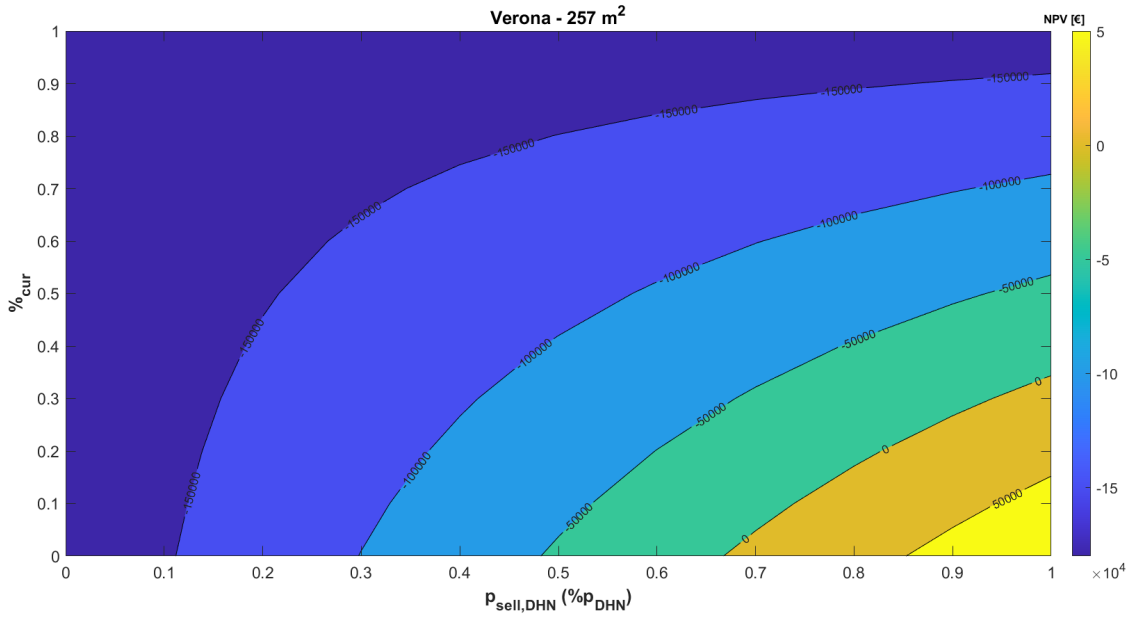

Figure 63: NPV behavior map for Verona - 257 m² scenario

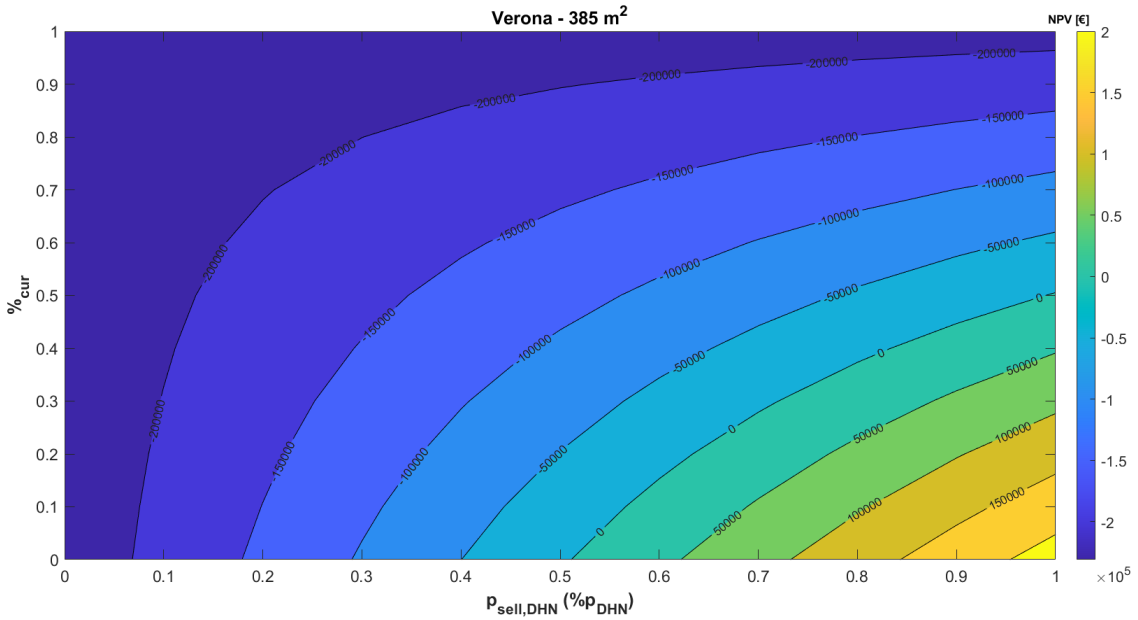

Figure 64: NPV behavior map for Verona - 385 m² scenario

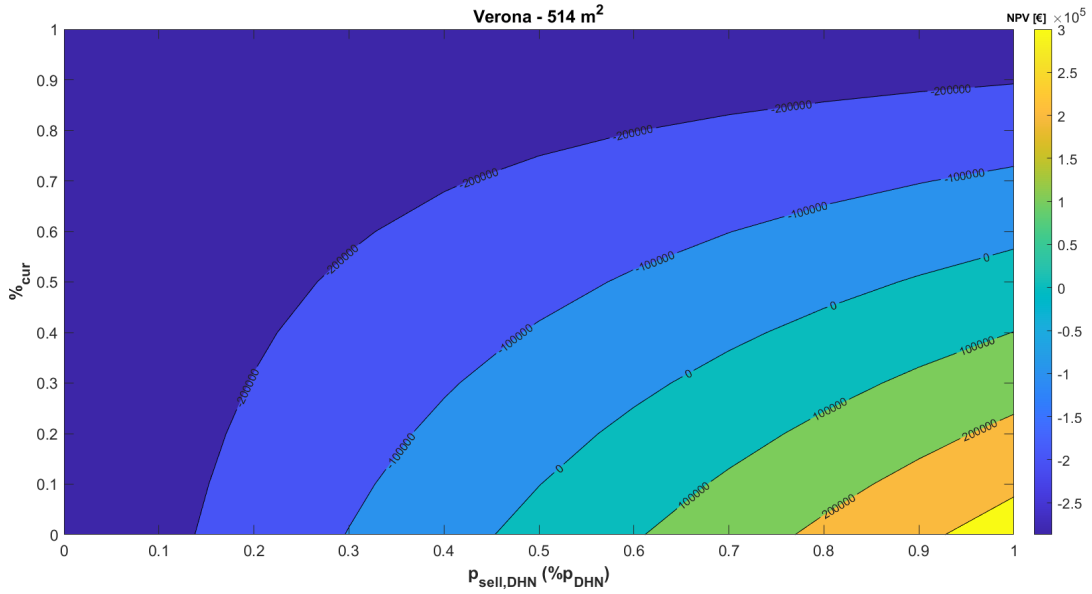

Figure 65: NPV behavior map for Verona - 514 m² scenario

As arising from comparing the difference in electricity costs between baseline (Table 34) and simulated scenarios (Table 33), it's evident that the proposed technologies don't introduce an improvement but, conversely, a slight worsening. The KPIs for the absorption chiller show the low covering of cooling demand by its application in the simulated case (Table 29 and Table 30), this suggests that the investment cost for this technology doesn't produce a relevant benefit in terms of money savings, while the cost for heat supply from the grid is reduced in all scenarios.

Another scenario for each location was considered: the absence of the absorption chiller in the retrofit operation. This evaluation was performed only for the maximum solar collector's surface. The investment costs are reduced, and the expenditures for electricity supply are slightly higher than the baseline (due to the auxiliaries of the substation and solar system), but the overall OPEX is lower since the maintenance costs of absorption chiller are avoided, and the expenditure to purchase heat from the DHN, analogously to the aforementioned scenarios. Finally, a higher amount of heat is potentially available to be injected into the grid (all the heating energy produced during the summer period is not supplied to the user and can be theoretically injected into the grid). A summary of the main indicators is reported in Table 37, the Cash Flow is higher than in the previous cases, but the theoretical income I_{th} is lower.

Table 37: main economic indicators for the scenarios without absorption chiller

	Palermo 231 m² no-sorption	Verona 514 m² no-sorption
CAPEX	139943 €	313045 €
OPEX	5908 €	24068 €
CF	2260 €	9468 €
I_{th}	39369 €	53155 €

The NPV indicator (Figure 66) shows relevant improvements if compared to the previous 8 scenarios, because of lower investment costs and higher cash flows. Avoiding the installation of the absorption chiller lets to achieve better economic performances, the zero–NPV front moves to lower values of psell,DHN and higher values of %cur (Table 38), this means that profitability is ensured even when the market conditions are critical and the selling price should be lowered and a high curtailment ratio is imposed.

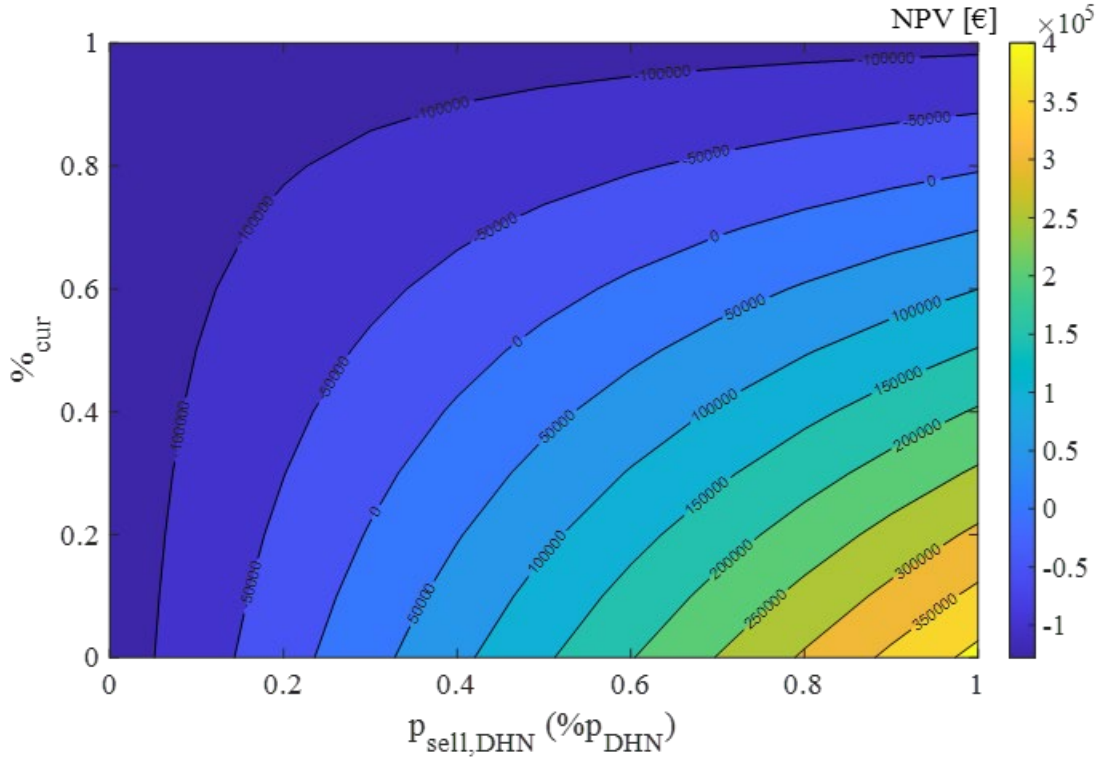

Figure 66: NPV behavior map for Palermo - 231 m² - no absorption scenario

Table 38: values of intercept between the zero - NPV front and axes. No sorption scenarios

	Palermo 231 m² no-sorption	Verona 514 m² no-sorption
psell_DHN (NPV=0)	0.2357	0.2880
%cur (NPV=0)	0.7905	0.7365

6.4. Optimization analysis

The substation and local heat and cold generation equipment were designed considering the user's energy requirements. One of the aims of the PhD project was the research of a flexible tool for studying the DHN systems, its capacity expansion analysis, and the capability to study the prosumer's introduction. The same system was reproduced in nPro tool [168], a virtual simulation tool designed to assist in the planning of district energy systems, particularly focusing on heating and cooling networks. It addresses the critical need for effective software solutions in the early conceptual design phase, enabling users to create customized demand profiles and simulate various energy scenarios. The tool offers several functionalities such as demand profile generation, thermal network simulation, energy hub design optimization, and economic analysis.

The nPro tool implements a calculation methodology that consists of two main modules: demand profile generation and thermal network calculation, followed by design optimization and operation simulation. In the first step, the tool generates energy demand profiles for various applications, including space heating, domestic hot water, space cooling, process cooling, and electricity demands (plug loads and e-mobility). Profiles are created with an hourly resolution, which is generally sufficient for subsequent energy hub optimization. The generation process uses a degree-day approach, which calculates heating and cooling demands based on the temperature difference between outdoor and indoor settings. The profiles can also be imported by the user from an external source.

The Thermal Network simulation aggregates the loads of all buildings and determines the load at the energy hub, structuring the energy model for the simulation of the thermal network. Then, the optimization model uses a mixed-integer linear programming approach, which is common in techno-economic models for energy systems (as described in Chapter 2). This allows for the consideration of various energy conversion and storage technologies, enabling the design of cross-sectoral energy hubs. The optimization calculation includes peak load constraints to ensure that the annual energy demand profiles can be met for every hour of the year. The design optimization results provide optimal generation and storage capacities for each technology, along with key performance indicators. Finally, once the system is optimized, its operation is simulated using a linear programming model to optimize the dispatch of all technologies over a full year, again using an hourly resolution with 8760 time steps.

The tool also lets to carry on a sensitivity analysis that functions similarly to multi-objective optimization, generating Pareto-efficient solutions to help users find optimal energy systems with varying degrees of sustainability.

The building loads (described in Paragraph 6.1) were imported, together with weather data through the import tool (Figure 67).

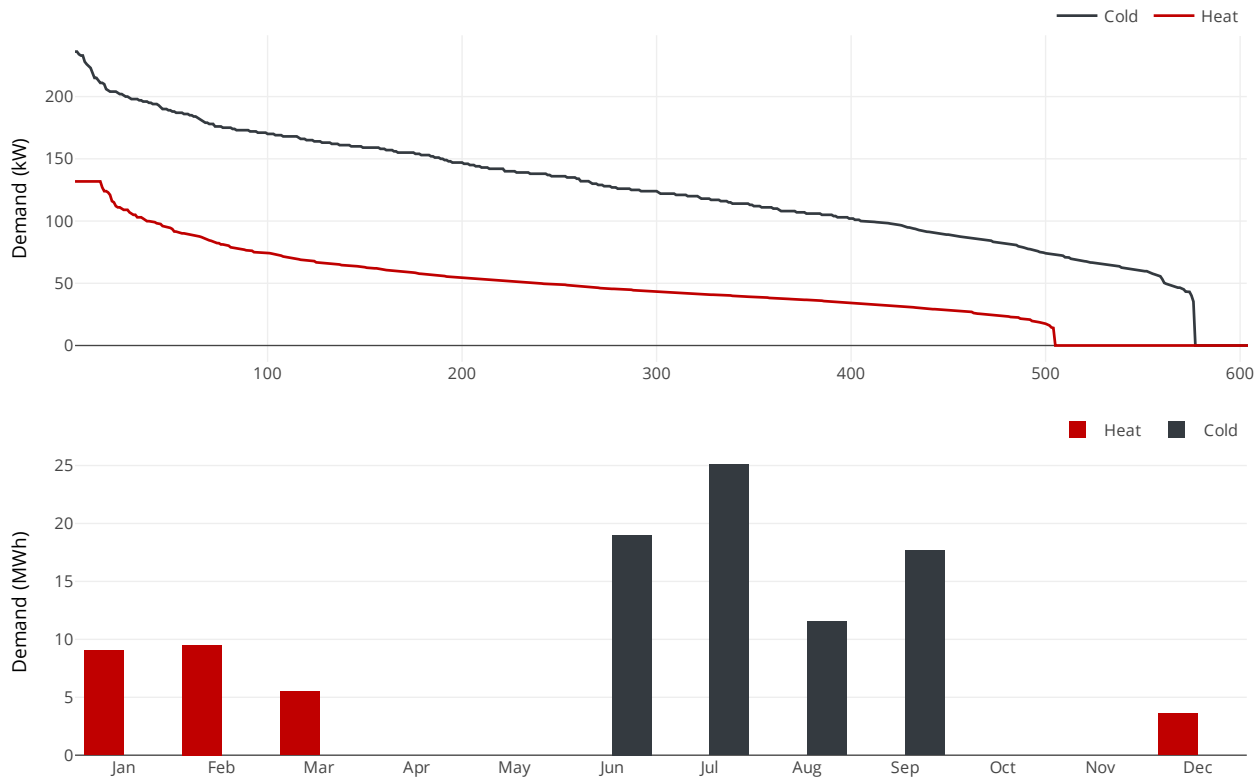

Figure 67: Heating and cooling demands for the case of Palermo. Duration curve (up) and Monthly values (down)

Then, the energy hub was defined by selecting the technologies modeled in TRNSYS (Figure 68). In this case, the detailed thermal model of the prosumer substation is out of the scope of simulation, since the aim is the overall analysis of the depicted system.

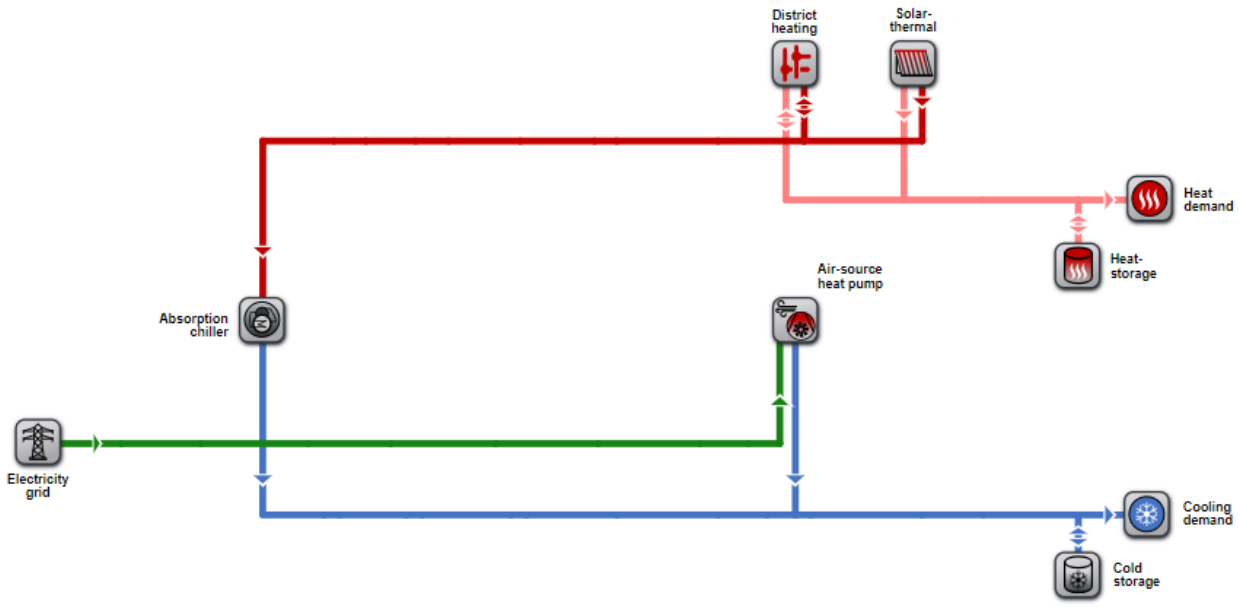

Figure 68: Energy hub modeling in nPro Tool, reproducing the system described in Figure 51

In the first phase, the technology set implemented in the energy hub was sized by adopting the Palermo 231 m^2 case, assuming that no thermal curtailment is imposed, and all the solar energy production is delivered to the user and DHN. The energy prices reported in Table 32

were set, furthermore, three fixed heat feed-in prices were set: 4.47 c€/kWh (25% heat purchase price), 8.93 c€/kWh (50% heat purchase price), and 13.4 c€/kWh (75% heat purchase price). nPro tool lets to consider a limit of heat feed-in into the grid, then, considering 242 MWh/year the maximum energy produced by solar collector field, as retrieved by TRNSYS simulation, three levels of curtailment were introduced in nPro: unlimited (0% curtailment), limit at 169.7 MWh (30% curtailment), limit at 96.8 MWh (60% curtailment).

Finally, 9 simulations were performed by considering fixed technology size, the three feed-in prices, and the three curtailment conditions, one scenario that foresees the total curtailment of feed-in energy (in this case the heat selling price does not affect the energy and economic simulation) and a scenario that simulates a null heat feed-in price and no curtailment. 11 Scenarios were considered (Table 39).

Table 39: acronyms of simulations performed in nPro tool for fixed technology sizes

	0% heat purchase price	*25% heat purchase price*	*50% heat purchase price*	*75% heat purchase price*
0 % curtailment	0C0P	0C25P	0C50P	0C75P
30 % curtailment		30C25P	30C50P	30C75P
60% curtailment		60C25P	60C50P	60C75P
100% curtailment	100C0P			

The following emission and primary energy factors were set, according to [169], [170]:

Table 40: emission factors and primary energy factors for electricity and district heating imports

	CO_2 emission factor [g/kWh]	*Primary Energy Factor*
Electricity import	256	2.1
District heating import	210	0.6

The optimization calculations include both technology sizing and operation. In the examined case the technology sizing is fixed, so the optimization is concentrated only on the optimal energy allocation to minimize the costs. In general, in nPro, the optimization mathematical model attempts to minimize the Total Annualized Costs (TAC) with the following equation:

$$\min TAC = C_{inv} + C_{o\&m} + (C_{el} - R_{el}) + C_{ngas} + C_{biogas} + C_{biom} + (C_{dh} - R_{dh}) + (C_{dc} - R_{dc}) + (C_{H2} - R_{H2}) + C_{CO2}$$

with

- C_{inv}: Annualized investment costs of all technologies
- $C_{o\&m}$: Annual maintenance and repair costs
- C_{el}: Cost of electricity purchased from the power grid
- R_{el}: Feed-in revenues for electricity fed into the power grid
- C_{ngas}: Cost of gas purchased from the gas grid
- C_{biogas}: Costs for biogas purchase

- C_{biom}: Costs for biomass purchase
- C_{dh}: Costs for heat procurement from an (external) heat network
- R_{dh}: Feed-in revenue for heat fed into an (external) heat network
- C_{dc}: Costs for cold procurement from an (external) cooling network
- R_{dc}: Feed-in revenue for cold fed into an (external) cooling network
- C_{H2}: Costs for hydrogen purchase
- R_{H2}: Feed-in revenues for hydrogen
- C_{CO2}: Costs for direct or indirect CO2 emissions

Figure 69 shows the heat balance on the energy hub for each simulated scenario. The first three scenarios, in which no curtailment is imposed, present an identical behavior, invariant with heat selling price. The solar collector field operates at its maximum producibility (242 MWh), and the excess heat is entirely delivered to the thermal grid. A small amount of heat imported to the grid is always present to balance the lack of solar production due to adverse weather conditions (7 MWh). The absorber heat demand is null in these three scenarios that foresee no thermal curtailment, the deduction is that from an economic point of view, it is always more convenient to sell energy to the DHN rather than operate the absorption chiller and save electrical energy, since the entire cooling demand (73 MWh) is covered by the vapor compression chiller (Figure 70). The three simulations in which a 30% thermal curtailment is implemented show relevant differences if compared to the previous ones. Although solar energy production is unvaried, the thermal feed-in is lower and the absorption chiller operation is enhanced, by maintaining identical values for each of the three scenarios (51 MWh for Absorption heat demand). The amount of energy stored is higher in the 30C25P case, this is due to the lower selling price that lets the optimization model deliver more heat to the heating and cooling system rather than to the thermal grid. Even in this case, the energy import from DHN shows invariant values. The cooling supply is mostly covered by the vapor compression chiller (43MWh), and the absorption chiller supplies the remaining 42.5% (31 MWh). The simulation results of the three scenarios where 60% of curtailment is imposed show that solar collector production is lowered. On 242 MWh produced, 72 MWh were curtailed, and the remaining part was delivered both to the user and DHN. The heat import has the same value as the previous cases (7 MWh). The absorption operation presents the same behavior as the 30% curtailment scenarios, due to the curtailment, the available excess heat generation is delivered to maximize the thermally driven cooling energy conversion. The last two scenarios adopt the most extreme conditions and are useful to trace a theoretical border of the depicted system's behavior. In the 100% curtailment case, all the excess heat is curtailed, and the solar generation is optimized to supply the user and absorption chiller. In the other case, even though there are no curtailment limits, the heat selling price is null and the optimization model maximizes the absorption operation to minimize the electricity import.

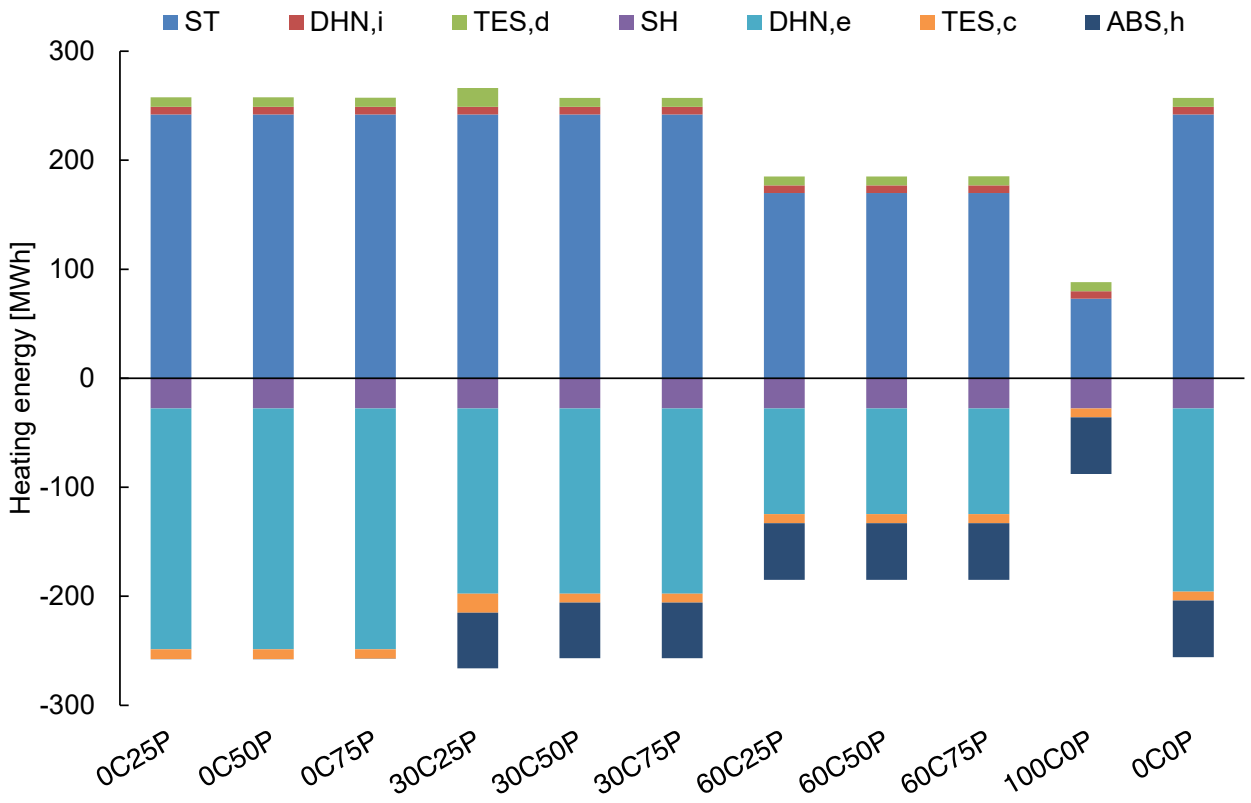

Figure 69: Heat balance on the energy hub. ST-Solar Thermal heat production, DHN,i-District Heating Import, TES,d-Thermal Energy Storage discharge, SH-Space Heating demand, DHN,e-District Heating export (feed-in), TES,c-Thermal Energy Storage charging, ABS,h-Absorption Chiller heat demand

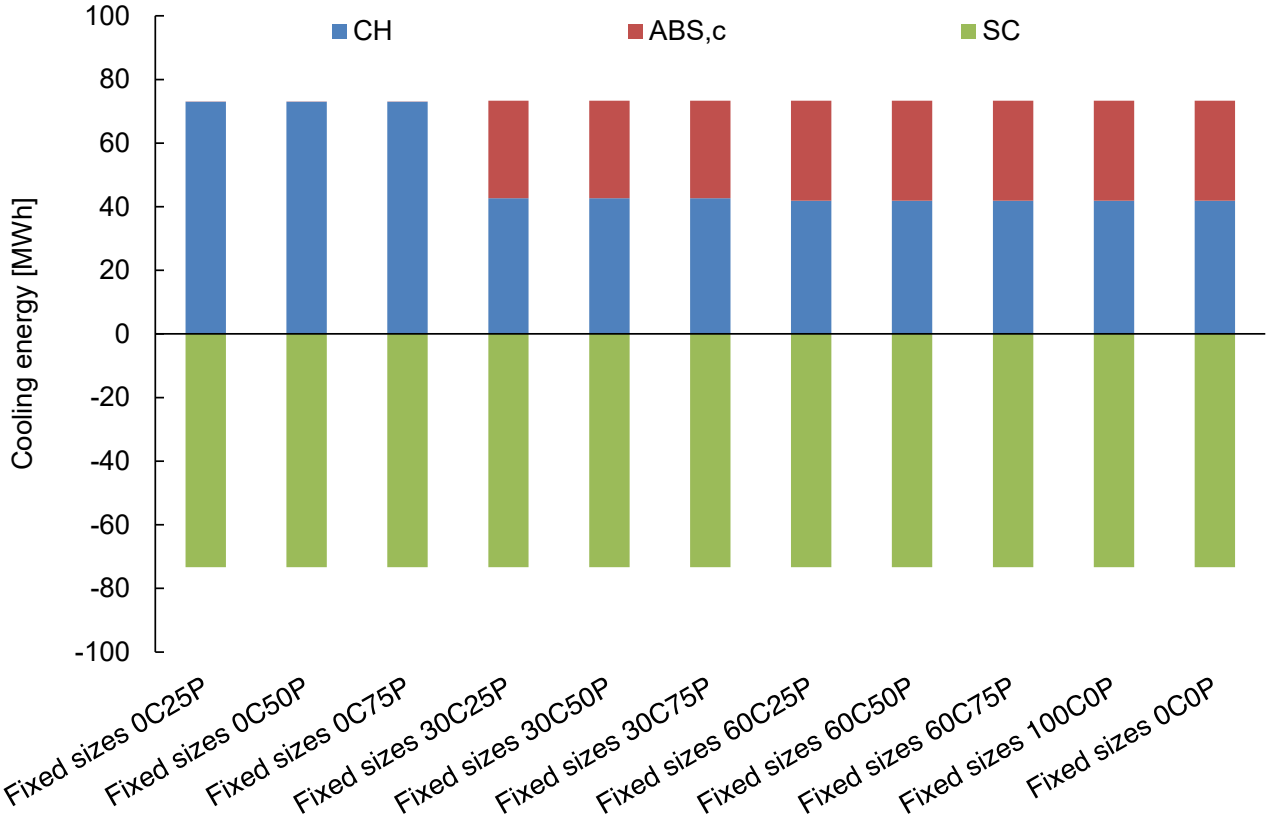

Figure 70: Cooling balance on the energy hub. CH - Vapor compression chiller, ABS,c - Absorption Chiller Cooling supply, SC - Space Cooling demand

The economic analysis in nPro follows the German VDI Guideline 2067 (Economic Efficiency of Building Technology Systems - Fundamentals and Cost Calculation). It evaluates the financial viability by considering all investments related to the building energy systems, the heating network, and central components in the energy center (energy hub). The net present value method is applied to calculate the annuities of investments, using the specified interest rate and the technical lifespan of the technology. These annuities are combined with all annual costs to determine the total annual costs or revenues. If the resulting annual costs are positive, the project will have a positive net present value at the end of its duration, indicating economic viability. Conversely, if the annual costs are negative, the project is deemed economically unfeasible. Revenues also include those earned by the energy system operator from the building owners to meet heating, cooling, and electricity demands. These revenues can be represented in nPro as volumetric prices (€/kWh), capacity prices (€/kW), and base prices (€/year). As per VDI 2067, residual values at the end of the technology lifespan are also accounted for. For instance, if a component like the heating network has a longer technical lifespan than the project duration, its residual value will generate revenue in the final year. Depreciation of value occurs linearly over lifespan. If the technology's lifespan is shorter than the project's duration, a replacement investment must be made during the project.

The one-time costs include:

- Investments in technologies (building energy system, heating network, and energy center),
- Subsidies on investments (listed separately, not part of the investments),
- Lump sum costs (listed separately, not part of the investments).

In addition, annual costs are incorporated into the economic feasibility analysis. These costs remain nominally constant throughout the observation period but are discounted using the net present value method:

- Energy costs (e.g., for electricity import),
- Maintenance costs (calculated as a percentage of the investment),
- Revenues (e.g., from electricity feed-in or heat demand coverage),
- CO2 costs, and
- Other operating costs (e.g., insurance and administrative expenses).

The economic feasibility calculation generates several financial indicators, such as net present value, internal rate of return, and amortization period, which are used to evaluate the project's profitability from an economic standpoint.

Furthermore, the Levelized Cost of Heat (LCoH) is calculated as annual costs divided by the heat demand covered by the system. If the system covers additional demands, such as plug loads, e-mobility, or hydrogen, the levelized costs of heat are usually of little relevance. Then, Levelized Costs of Energy (LCoE) are calculated as annual costs divided by all energy demands covered by the system (heat, cold, electricity, etc.).

In the present study, the economic data presented in section 6.3 were adopted for the simulations.

In Figure 71 the LCoH vs the Specific CO_2 emissions per heat demand is presented. The general trend for LCoH is decreasing when the selling price of heat increases since revenues counterbalance the costs (or overcome them), the curtailment ratio has a secondary effect, even if the lower LCoH are related to the lower curtailment ratios. The two border scenarios (0C0P and 100C0P) collapsed at the same point because in both cases the economic relationship with the thermal grid is null, furthermore, they have the same electrical energy consumption (for the chiller) and the same DHN import, thus achieving the same environmental indicator. The three scenarios adopting 0% curtailment show higher specific emission values since the absorption chiller isn't activated and higher electricity consumption is achieved. Since optimization relies only on the economic criterion (it's also possible to set a multi-objective optimization), the model attempts to maximize the revenues achieved by the thermal feed-in, neglecting the environmental aspects related to higher electricity consumption for the vapor compression chiller activation. This behavior is not present in the other simulations due to the introduction of curtailment. In those cases, the model attempts to minimize the curtailment by delivering the amount of energy that the thermal grid is not available to accept to the absorption chiller. Finally, the two negative values are obtained by the high revenues.

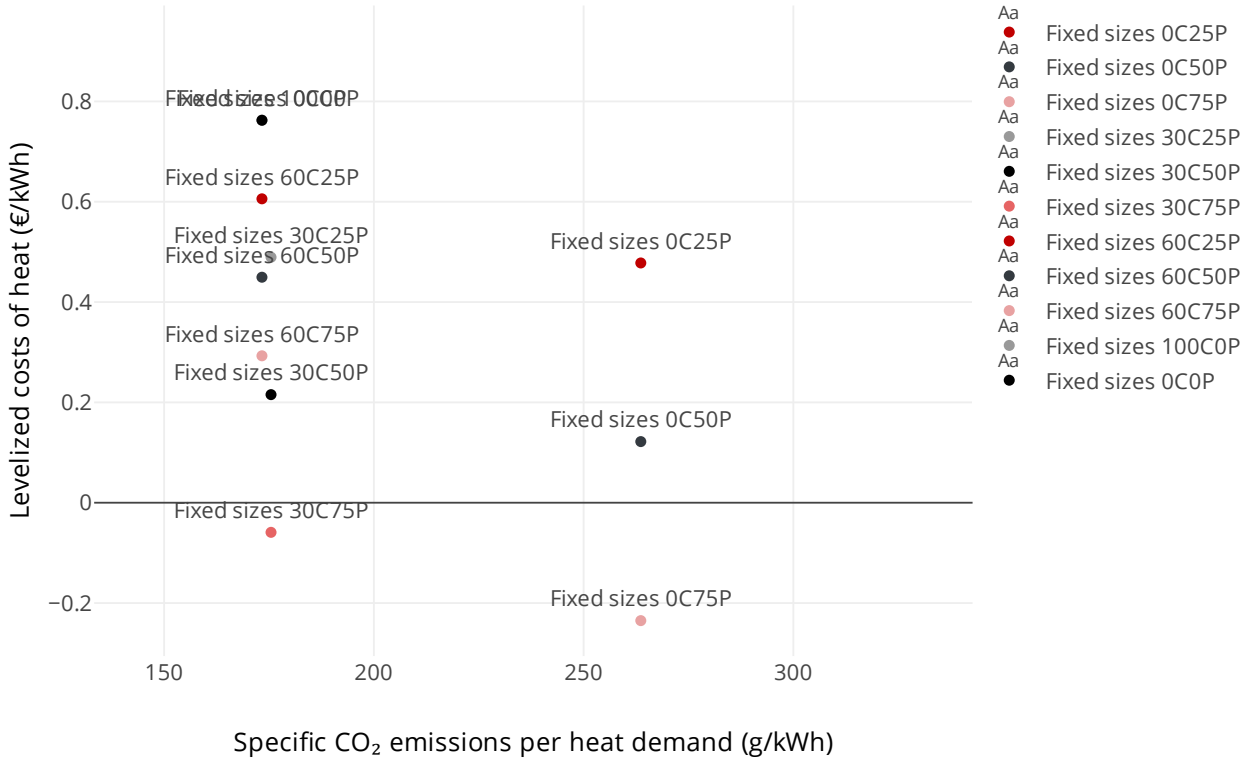

Figure 71: Levelized cost of heat vs Specific CO_2 emission - comparison of the 11 simulated scenarios

Table 41, Table 42, and Table 43 report the comparison of the 11 simulated scenarios from the energetic and economic points of view.

The economic KPIs reveal that only curtailment ratios lower or equal to 30% and heat feed-in prices higher than 50% buying price show positive indexes, although with scarce relevance for 20 years. The LCoH presents lower values than the DHN import price only in three cases (0C50P, 0C75P, 30C75P).

The environmental indicators reveal that the three scenarios with null curtailment have the higher impacts in terms of emissions and primary energy consumption, due to the higher electricity import for cooling purposes.

Table 41: Heat demand and Generation - Comparison of the 11 simulated scenarios with fixed technology sizing

Heat demand and generation		0C25P	0C50P	0C75P	30C25P	30C50P	30C75P	60C25P	60C50P	60C75P	100C0P	0C0P
Space heating	MWh	27.7	27.7	27.7	27.7	27.7	27.7	27.7	27.7	27.7	27.7	27.7
District heating import	MWh	6.9	6.9	6.9	6.9	6.9	6.9	6.9	6.9	6.9	6.9	6.9
Heat from solar thermal	MWh	242.0	242.0	242.0	242.0	242.0	242.0	170.0	170.0	170.0	73.0	242.0
District heating feed-in	MWh	221.0	221.0	221.0	170.0	170.0	170.0	97.0	97.0	97.0	0.0	168.0
Solar Collector area	m²	231	231	231	231	231	231	231	231	231	231	231
Curtailed generation potential	MWh	0.0	0.0	0.0	0.0	0.0	0.0	72.0	72.0	72.0	168.0	0.0
Yield per collector area	kWh/m²	1'046	1'046	1'046	1'046	1'046	1'046	736	736	736	316	1'046
Heat storage												
Storage capacity	kWh	268.0	268.0	268.0	268.0	268.0	268.0	268.0	268.0	268.0	268.0	268.0
Charging energy	MWh	8.8	8.8	8.5	17.4	8.2	8.2	8.2	8.2	8.3	8.2	8.2
Discharging energy	MWh	8.8	8.8	8.5	17.4	8.2	8.2	8.2	8.2	8.3	8.2	8.2
Full charging cycles		33	33	32	65	30	31	30	30	31	30	30

Table 42: Economic KPIs - Comparison of the 11 simulated scenarios with fixed technology sizing

Economic KPIs		0C25P	0C50P	0C75P	30C25P	30C50P	30C75P	60C25P	60C50P	60C75P	100C0P	0C0P
Net present value	€	-110'339	20'932	152'493	-88'202	12'771	113'968	-131'118	-73'503	-15'760	-188'864	-188'864
Amortization period	years	0	18	10	0	19	11	0	0	0	0	0
Internal rate of return	%	0.0%	1.1%	7.1%	0.0%	0.7%	5.4%	0.0%	0.0%	0.0%	0.0%	0.0%
Levelized costs of heat	€/kWh	0.478	0.122	-0.235	0.489	0.215	-0.059	0.606	0.45	0.293	0.762	0.762
Levelized costs of energy	€/kWh	0.131	0.033	-0.064	0.134	0.059	-0.016	0.166	0.123	0.08	0.209	0.209
Energy costs per floor area	€/m²	2.66	0.68	-1.31	2.72	1.20	-0.33	3.37	2.50	1.63	4.24	4.24
Mon. energy costs per area	€/m²	0.22	0.06	-0.11	0.23	0.10	-0.03	0.28	0.21	0.14	0.35	0.35

Table 43: Emissions and primary energy estimation - Comparison of the 11 simulated scenarios with fixed technology sizing

Emissions and primary energy		0C25P	0C50P	0C75P	30C25P	30C50P	30C75P	60C25P	60C50P	60C75P	100C0P	0C0P
CO_2 emissions	t	7.3	7.3	7.3	4.9	4.9	4.9	4.8	4.8	4.8	4.8	4.8
CO_2 emissions per floor area	kg/m²	1.465	1.465	1.465	0.975	0.975	0.975	0.963	0.963	0.963	0.963	0.963
Primary energy	MWh	52	52	52	32	32	32	32	32	32	32	32
Primary energy per floor area	kWh/m²	10	10	10	6	6	6	6	6	6	6	6

After having adopted the fixed technology sizing resulting from TRNSYS modeling, a new simulation was run on nPro, without fixing the size of the substation's equipment, but launching the optimization calculation that includes also the nominal size. The two intermediate curtailment and heat feed-in price scenarios were considered since they reproduce conditions closer to a real thermal market. Four simulations were run for the following scenarios: 30C25P, 30C50P, 60C25P, and 60C50P.

The heat balance and solar collector sizing shown in Table 44 reveal that the MILP optimization model decreased the nominal size of solar thermal plant, in order to decrease the total annual costs. Furthermore, when the curtailment increases, the solar collector surface is decreased to achieve at least the heat generation that can be delivered to the user or to the grid, without any curtailment. The TES capacity is lower than the previous cases, there is a small capacity increase when passing from 30% curtailment to 60%, attempting to store a balanced amount of energy that from one side lets to avoid the curtailment and, on the other side, doesn't increase the CAPEX more than the necessary level.

Table 44: Heat demand and Generation - Comparison of the 4 simulated scenarios with optimized technology sizing

Heat demand and generation		30C25P	30C50P	60C25P	60C50P
Space heating	MWh	27.7	27.7	27.7	27.7
District heating import	MWh	10.0	10.0	13.8	13.8
Heat from solar thermal	MWh	182.0	182.0	108.0	108.0
District heating feed-in	MWh	164.0	164.0	94.0	94.0
Solar Collector area	m²	174	174	103	103
Curtailed generation potential	MWh	0	0	0	0
Yield per collector area	kWh/m²	1'046	1'046	1'046	1'046
Heat storage					
Storage capacity	kWh	160.0	160.0	167.0	167.0
Charging energy	MWh	6.7	6.7	6.0	6.0
Discharging energy	MWh	6.7	6.7	6.0	6.0
Storage volume	m³	6.89	6.89	7.191	7.191
Full charging cycles		42	42	36	36

Table 45 shows the cooling demand and generation arising from the simulations. The optimization model, in the absence of any constraints, didn't choose to introduce the absorption chiller, although it lets save energy in the operational phase. All the cooling demand is supplied by the vapor compression chiller that is present in the energy hub and doesn't represent an additional cost.

Table 45: Cooling demand and generation -Comparison of the 4 simulated scenarios with optimized technology sizing

Cooling demand and generation		30C25P	30C50P	60C25P	60C50P
Space cooling	MWh	73	73	73	73
Air-source chiller					
Generated cold	MWh	73	73	73	73
Electricity demand	MWh	23	23	23	23
Full load hours	h/year	310	310	310	310

The Economic KPIs show negative indexes regarding the NPV, except for the 30C50 case, due to the revenues arising from higher feed-in than the 60C50P case (Table 46). The LCoH and LCoE show lower values than the analog scenario simulation carried out with fixed equipment size. Conversely, the environmental and primary energy indicators show an increase in CO_2 emissions and primary energy consumption in comparison with the previous simulations, due to the absence of the absorption chiller (Table 47).

Table 46: Economic KPIs -Comparison of the 4 simulated scenarios with optimized technology sizing

Economic KPIs		30C25P	30C50P	60C25P	60C50P
Net present value	€	-54'490	42'920	-69'851	-14'018
Amortization period	years	0	13	0	0
Internal rate of return	%	0.0%	4.0%	0.0%	0.0%
Levelized costs of heat	€/kWh	0.326	0.062	0.368	0.217
Levelized costs of energy	€/kWh	0.089	0.017	0.101	0.059
Energy costs per floor area	€/m²	1.81	0.35	2.05	1.20
Mon. energy costs per area	€/m²	0.15	0.03	0.17	0.10

Table 47: Emissions and primary energy estimation -Comparison of the 4 simulated scenarios with optimized technology sizing

Emissions and primary energy		30C25P	30C50P	60C25P	60C50P
CO_2 emissions	t	8.0	8.0	8.8	8.8
CO_2 emissions per floor area	kg/m²	1.597	1.597	1.76	1.76
Primary energy	MWh	54.1	54.1	56.4	56.4
Primary energy per floor area	kWh/m²	10.9	10.9	11.3	11.3

Finally, Figure 72 shows the same previous trend in which the LCoH decreases when curtailment decreases and feed-in price increases. The specific emissions of 60% curtailment scenarios are higher than the 30% ones because of higher energy imports from DHN.

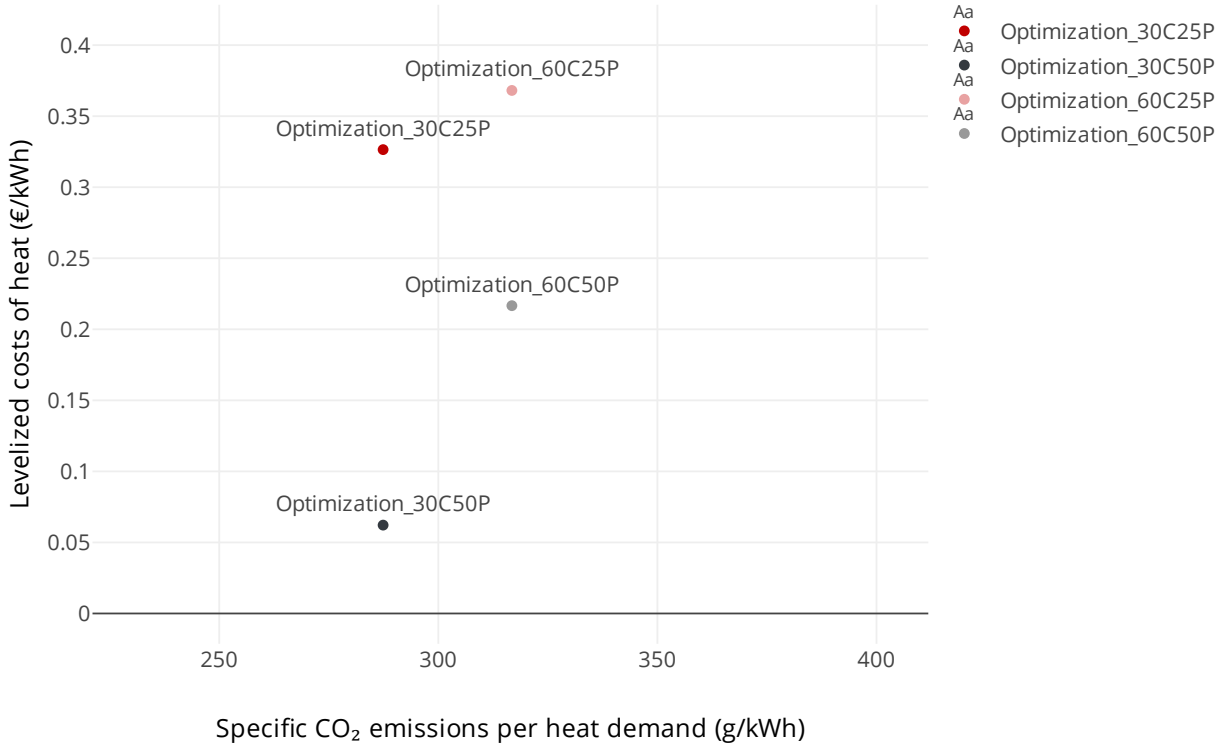

Figure 72: Levelized cost of heat vs Specific CO_2 emission - Comparison of the 4 simulated scenarios with optimized technology sizing

7. Conclusions

The presented research tries to offer a wide exploration of the integration of thermal energy systems, particularly focusing on the role of thermal prosumers within district heating and cooling networks. This research is focused on a timely and relevant issue, given the increasing emphasis on sustainable energy solutions and the urgent need to transition towards low-carbon energy systems. The findings of this thesis are particularly significant in the European context, where the integration of renewable energy sources into existing energy infrastructures is critical for achieving decarbonization targets.

The first part of the thesis traces the foundational framework for understanding the complexities and opportunities associated with the integration of renewable energy sources and the role of thermal prosumers in enhancing the sustainability and efficiency of these systems.

Section 1 introduces the fundamental concepts of district heating and cooling systems, outlining their importance in the context of energy efficiency and sustainability. After a brief description of historical development and current research on DHC systems, the role of providing centralized heating and cooling solutions to urban areas is highlighted. The advantages of DHC systems in improving energy efficiency, lowering greenhouse gas emissions, and improving energy security are stressed. A significant focus of this chapter is the current state of DHC systems in Italy, where the integration of renewable energy sources is becoming increasingly critical. The chapter discusses the challenges faced by existing DHC networks, including infrastructural limitations, economic viability, and the need for modernization to accommodate renewable energy inputs. The introduction of thermal prosumers is a potential and feasible solution to these challenges, as they can contribute to the decentralization of energy production and enhance the overall resilience of the energy system.

A wide focus on district heating capacity expansion models is depicted in Section 2, underlining the role of these instruments in future strategic energy planning and the importance of capacity expansion in meeting future energy demands and integrating renewable energy sources. The technical and economic barriers that influence capacity expansion are identified. The need for innovative configurations and upgrading measures to enhance the efficiency of existing DHC systems is clearly emphasized by the literature research. The findings suggest that a proactive approach to capacity expansion, supported by robust policy frameworks and financial incentives, is crucial for achieving the integration of renewable energy sources and enhancing the sustainability of district heating networks. Starting from a free simulation tool, a capacity expansion analysis for district heating in Italy was carried out. It considers factors such as population growth, urbanization, and the increasing demand for sustainable energy solutions and the potential for integrating diverse renewable energy sources, including biomass, solar thermal, and waste heat, into existing DHC networks. The analysis showed the importance of developing a comprehensive heat atlas, which serves as a geospatial representation of heating and cooling demands alongside potential supply sources. This tool is deemed essential for effective planning and decision-making in the expansion of DHC systems. The outcomes presented a different mix of energy sources employed for the future DHC system, according to the energy policy

adopted by the Governments. Natural gas will play a relevant role in the short-term transition towards the zero emissions targets.

Besides the technical barriers, the legislative and economic frameworks are crucial for the development of novel thermal grids, especially for the introduction of new actors, such as the prosumers. In section 3 the critical issue of heat pricing and third-party access within district heating systems are discussed to explore the existing models and their implications for thermal prosumers and consumers. The pricing mechanisms should balance economic viability with the need to incentivize renewable energy integration, parallelly, they should promote competition and ensure fair access to energy markets. The analysis revealed that starting from the actual model, several innovative improvements can be adduced since they rely on traditional district heating systems. The introduction of prosumers promotes both competition with centralized producers and novel cooperativity models to access the energy services. Innovative business models can accommodate the different interests of the involved stakeholders while promoting the overall sustainability of the energy system. The findings suggest that a collaborative approach, supported by clear regulatory guidelines, is essential for fostering a competitive and inclusive energy market. The insights gained from these chapters are crucial for informing policymakers, energy planners, and industry stakeholders as they navigate the complexities of energy transition.

Section 4 goes inside the technical heart of prosumer's systems. The thermal modeling of a prosumer's substation in DHNs was there presented. It was implemented in TRNSYS 18 environment and validated against experimental results available in the literature for a similar setup. Results showed a good agreement between experimental and simulated results for both the energy and thermal response of the system, with relative errors lower than 5% or 10%, respectively. Assuming a solar thermal field composed of high vacuum solar thermal panels as a district generation plant, simulations were performed for two different geographical locations, i.e. Palermo (Csa-Köppen classification) and Berlin (Cfb-Köppen classification). Results showed that the prosumer substation allowed for a total exploitation of the heat produced by the solar distributed generation system, thus avoiding any waste of excess heat production from the solar source into the environment; also, the embedded controls could provenly meet the desired water temperature setpoints. In the presence of an unstable energy source, such as the solar one, the examined substation with bi-directional heat exchange allows for full energy exploitation to supply the final user, through the heat purchase from the DHN in case of a lack, or sale to the network in the case of an excess of local production by the solar DG. In the examined configuration, the surplus heat supplied to the grid ranged between 29% and 66% of the total amount of energy exchanged by the substation, while the self-consumption accounted for up to 21.2% and 30.6%, respectively for Palermo and Berlin. Being the solar source not sufficient to supply the heat demand, the need for a relevant heat supply from the DHN was assessed, accounting for 16.3% and 56.9% of the total exchanged heat for Palermo and Berlin, respectively. These results highlight the crucial role that a substation with bi-directional heat exchange can play to promote distributed heat generation by intermittent renewables such as solar energy. In DHNs comprising large users with continuous or asynchronous heat demands (large tertiary, sports centers, hospitals, etc.), the surplus heat produced by solar plants and supplied to the network could be effectively exploited by these remote users,

lowering the share of heat produced by fossil fuels or electricity in conventional boilers or heat pumps. The proposed model represents a viable tool to perform analyses aimed at identifying the optimal capacity and spatial distribution of such distributed renewable systems, for a given set of prosumers connected to the network, and to investigate rational pricing mechanisms to promote effective coordinated management of equipment. In the future, further research will be aimed at refining the model with additional hydraulic analysis and evaluating the influence of the dynamic behavior of energy users within the integrated energy communities.

After analyzing the “heart” of prosumer systems, the research tried to open an overview of their “brain” in Section 5. The reported study investigated the behavior of a thermal prosumer equipped with HPs when variation in the electricity prices is adopted to increase flexibility. More specifically, the effects of market constraints on HP operation and cost saving (primarily the energy price) were analyzed. A TRNSYS model of a thermal prosumer substation equipped with an HTHP and serving an office building was implemented and validated by using experimental data available from past works. A heuristic profit-oriented management strategy of HP was developed and implemented in the dynamic simulations. The proposed strategy aimed at minimizing the costs sustained to meet the thermal demand and maximizing the profits when selling thermal energy to the DHN. Six different scenarios were investigated, each one related to different economic conditions imposed by the TSO to promote flexibility. The analysis pointed out the key role of electricity prices in the operation of HP. Indeed, for given selling and purchasing prices of heat, the results showed an increase in the operating time of HTHP when decreasing the electricity price, as expected. Moreover, results from economic analysis highlighted that in the “Neutral” scenario, which was characterized by the absence of incentives or governmental actions that promoted flexibility, profits could be also achieved. The introduction of tax cuts and incentives for flexibility led to a relevant increase in profits in the case of a surplus in electricity production (almost +67%). In case of a deficit in electricity generation, an increase in the price component related to network cost will reduce the profits achievable by producing heat onsite through HPs. Finally, the presented study showed that in the context of smart electrical and thermal grids, HPs achieve flexibility for both of them and attempt to simultaneously optimize efficiency and economic profitability. The effect of incentives on the profit increase was investigated through the introduction of two simulation scenarios that include the random variation of prices in the presence or absence of incentives. The outcomes lead to reflecting on a methodology that proposes economic incentives for grid flexibility to balance the eventual inequalities, rather than to increase the profits. The study opens the discussion on future studies that should focus on thermal grids composed of substation clusters that include different typologies of DG, with a special focus on renewable technologies. The analysis of the substation’s performances should be characterized while considering constraints related to DHN architecture, the capability of the network to consume the heat provided by prosumers, and the coordination of DR programs for heat and electricity. Heat pricing methods and third-party access conditions should be approached through a systematical method to support the decision of policymakers in the process of renewable energy community creation.

Some of the open issues of Section 5 were addressed in the Section 6. The novel system reported presents a perspective for future district heating system frameworks. The bi-directional operation will give a chance for the integration of renewable energy sources within the district heating network components, thus introducing the concept of “renewable energy community” applied to thermal energy. The simulation model shows the operation flexibility of a prosumer substation and offers a reliable tool to optimize a thermal prosumer substation equipped with a renewable energy source generation plant. The economic analysis further underscores the viability of these systems and considers the interface with the grid. The study aimed to present an economic framework that depends on grid operating conditions (curtailment) and market (price of heat purchased and sold), the economic performances are obtained for a wide spectrum of cases. While the initial investment in solar thermal technology and absorption chillers may not yield immediate financial benefits, the long-term savings from reduced energy costs and the ability to sell excess heat back to the grid present a compelling case for their adoption. The cash flow analysis indicates that, despite higher electricity costs in some scenarios, the overall financial performance remains positive due to the significant heat savings achieved by utilizing solar energy. This highlights the importance of considering both operational expenditures and potential income from heat sales when evaluating the economic feasibility of thermal prosumer systems. For this reason, the higher the solar plant, the higher the potential income and the profitability results. The dynamic simulation proved that the introduction of a thermally driven chiller doesn’t enhance economic performance by exploiting a “free” energy source. This deduction cannot be applied to all heating and cooling systems since it is strictly related to the single study case but opens the discussion about the effective feasibility of trigenerative systems. They need an in-depth analysis of each investigated system. The future perspectives for thermal prosumer systems are promising. As the demand for sustainable energy solutions continues to grow, the development of advanced simulation tools and methodologies will be crucial in optimizing the design and operation of these systems. Future research should focus on addressing the existing infrastructural, technological, and legislative barriers that currently impede the widespread adoption of prosumer models. This includes exploring innovative control strategies, enhancing seasonal thermal storage solutions, and refining market mechanisms to better accommodate the unique characteristics of prosumer-based energy systems. Moreover, the integration of smart grid technologies and digital platforms can facilitate real-time monitoring and management of energy flows, further enhancing the efficiency and reliability of district heating networks. Collaborative efforts among stakeholders, including policymakers, energy providers, and consumers, will be essential in creating a supportive regulatory framework that encourages investment in renewable energy technologies and promotes the establishment of thermal energy communities. In future works, the introduction of energy market constraints will open a perspective on the application of bi-directional thermal substations within DHNs. An analysis of the limitations imposed by energy market rules will enable a new methodology to assess the optimal size of thermal plants and new logic to be set on the substation controls. The optimized exploitation of renewable energy sources integrated into the prosumer systems and the implementation of power-to-heat technologies will foster effective decarbonization of the district heating and cooling sectors. Furthermore, an optimization analysis of a high vacuum solar system integrated into a district heating network was carried out. Key findings indicate

that integrating a high vacuum solar system can significantly enhance the thermal energy supply, particularly during peak demand periods. The analysis reveals that optimal configurations can lead to substantial reductions in operational costs and greenhouse gas emissions, thereby contributing to the sustainability goals of the DHC system. Additionally, the study highlights the importance of adaptive control strategies that can respond to fluctuating energy demands and solar availability, ensuring that the system operates at peak efficiency. The concept of a trigenerative system undergoes a significant revision since the absorption chiller isn't valued positively by the MILP optimization model that, in this case, relies only on economic parameters. Integrating solar thermal technologies into DHC systems not only supports the transition towards renewable energy sources but also aligns with broader sustainability objectives. The ability to adaptively manage energy supply in response to varying demand and resource availability is crucial for maximizing the benefits of such integrations. Overall, the analysis reinforces the importance of innovative approaches in optimizing the performance of thermal energy systems. It highlights the need for ongoing research and development to refine these optimization methodologies, ensuring that district heating networks can effectively leverage renewable energy sources to meet future energy demands sustainably. This work contributes valuable insights for policymakers and energy planners aiming to enhance the resilience and efficiency of urban energy systems in the face of evolving energy challenges.

Finally, the thesis systematically addresses the integration of renewable energy sources, waste heat recovery, and the development of theoretical frameworks for DHC systems. A notable aspect of the research is its emphasis on the potential of district heating systems to enhance energy efficiency and sustainability. The analysis demonstrates that district heating can effectively balance supply and demand, particularly when combined with fluctuating renewable energy sources. The novelty of this research lies in its comprehensive approach to integrating various elements of thermal energy systems.

In 2011 Jeremy Rifkin gave the definition of "Third Industrial Revolution" [171], a visionary framework for reshaping global economies by integrating new technologies, renewable energy systems, and collaborative social models. This research work wants to contribute actively, giving a contribution to realize that futuristic program by opening the way to a multi-sectorial analysis, necessary to face the challenges that energy transition will present.

References

[1] "Data - Eurostat." Accessed: Oct. 01, 2024. [Online]. Available: https://ec.europa.eu/eurostat/web/main/data

[2] "Energy consumption in households - Statistics Explained." Accessed: Oct. 01, 2024. [Online]. Available: https://ec.europa.eu/eurostat/statistics-explained/index.php?title=Energy_consumption_in_households

[3] H. Lund *et al.*, "4th Generation District Heating (4GDH): Integrating smart thermal grids into future sustainable energy systems," *Energy*, vol. 68, pp. 1–11, Apr. 2014, doi: 10.1016/J.ENERGY.2014.02.089.

[4] C. Stănişteanu, "Smart Thermal Grids – A Review," *The Scientific Bulletin of Electrical Engineering Faculty*, vol. 0, no. 0, Apr. 2017, doi: 10.1515/sbeef-2016-0030.

[5] S. Buffa, M. Cozzini, M. D'Antoni, M. Baratieri, and R. Fedrizzi, "5th generation district heating and cooling systems: A review of existing cases in Europe," *Renewable and Sustainable Energy Reviews*, vol. 104, pp. 504–522, Apr. 2019, doi: 10.1016/J.RSER.2018.12.059.

[6] S. Boesten, W. Ivens, S. C. Dekker, and H. Eijdems, "5th generation district heating and cooling systems as a solution for renewable urban thermal energy supply," *Advances in Geosciences*, vol. 49, pp. 129–136, Sep. 2019, doi: 10.5194/ADGEO-49-129-2019.

[7] R. Zeh *et al.*, "Large-Scale Geothermal Collector Systems for 5th Generation District Heating and Cooling Networks," *Sustainability 2021, Vol. 13, Page 6035*, vol. 13, no. 11, p. 6035, May 2021, doi: 10.3390/SU13116035.

[8] "AIRU - Annuario 2023," 2024. doi: https://www.airu.it/#ANNUARIO.

[9] "Gazzetta Ufficiale." Accessed: Oct. 09, 2024. [Online]. Available: https://www.gazzettaufficiale.it/atto/serie_generale/caricaDettaglioAtto/originario?atto.dataPubblicazioneGazzetta=2011-11-03&atto.codiceRedazionale=11A14397&elenco30giorni=false

[10] G. Mendes, C. Ioakimidis, and P. Ferrão, "On the planning and analysis of Integrated Community Energy Systems: A review and survey of available tools," Dec. 01, 2011, *Pergamon*. doi: 10.1016/j.rser.2011.07.067.

[11] A. Revesz *et al.*, "Developing novel 5th generation district energy networks," *Energy*, vol. 201, p. 117389, Jun. 2020, doi: 10.1016/J.ENERGY.2020.117389.

[12] L. Horstink *et al.*, "Collective Renewable Energy Prosumers and the Promises of the Energy Union: Taking Stock," *Energies 2020, Vol. 13, Page 421*, vol. 13, no. 2, p. 421, Jan. 2020, doi: 10.3390/EN13020421.

[13] A. M. Jodeiri, M. J. Goldsworthy, S. Buffa, and M. Cozzini, "Role of sustainable heat sources in transition towards fourth generation district heating – A review," *Renewable and Sustainable Energy Reviews*, vol. 158, p. 112156, Apr. 2022, doi: 10.1016/J.RSER.2022.112156.

[14] J. Vivian, X. Jobard, I. Ben Hassine, and J. Hurink, "Smart Control of a District Heating Network with High Share of Low Temperature Waste Heat," in *Conference: 12th Conference on Sustainable Development of Energy, Water and Environmental Systems - SDEWES 2017*, 2017. Accessed: Oct. 02, 2024. [Online]. Available: https://www.researchgate.net/publication/320281076

[15] R. Candela, M. L. Di Silvestre, P. Gallo, E. R. Sanseverino, G. Sciume, and G. Zizzo, "A Remuneration Model of Energy Community Members in Italy," *2022 Workshop on Blockchain for Renewables Integration, BLORIN 2022*, pp. 206–211, 2022, doi: 10.1109/BLORIN54731.2022.10028072.

[16] D. Wang, J. Carmeliet, and K. Orehounig, "Design and Assessment of District Heating Systems with Solar Thermal Prosumers and Thermal Storage," *Energies 2021, Vol. 14, Page 1184*, vol. 14, no. 4, p. 1184, Feb. 2021, doi: 10.3390/EN14041184.

[17] I. Elizarov and T. Lickleder, "ProsNet - A Modelica library for prosumer-based heat networks: Description and validation," in *Journal of Physics: Conference Series*, L. D. Scartezzini J.-L. Smith B., Ed., IOP Publishing Ltd, 2021. doi: 10.1088/1742-6596/2042/1/012031.

[18] D. Zinsmeister, T. Lickleder, F. Christange, P. Tzscheutschler, and V. S. Perić, "A comparison of prosumer system configurations in district heating networks," *Energy Reports*, vol. 7, pp. 430–439, Oct. 2021, doi: 10.1016/J.EGYR.2021.08.085.

[19] M. Gross, B. Karbasi, T. Reiners, L. Altieri, H.-J. Wagner, and V. Bertsch, "Implementing prosumers into heating networks," *Energy*, vol. 230, 2021, doi: 10.1016/j.energy.2021.120844.

[20] M. Pipiciello *et al.*, "The bidirectional substation for district heating users: experimental performance assessment with operational profiles of prosumer loads and distributed generation," *Energy Build*, vol. 305, p. 113872, Feb. 2024, doi: 10.1016/J.ENBUILD.2023.113872.

[21] M. H. Kim, D. W. Kim, D. W. Lee, and J. Heo, "Experimental Analysis of Bi-Directional Heat Trading Operation Integrated with Heat Prosumers in Thermal Networks," *Energies 2021, Vol. 14, Page 5881*, vol. 14, no. 18, p. 5881, Sep. 2021, doi: 10.3390/EN14185881.

[22] M.-H. Kim, D.-W. Lee, D.-W. Kim, and J. Heo, "Experimental analysis of heat prosumers under low temperature thermal network," in *Journal of Physics: Conference Series*, L. D. Scartezzini J.-L. Smith B., Ed., IOP Publishing Ltd, 2021. doi: 10.1088/1742-6596/2042/1/012102.

[23] T. Lickleder, D. Zinsmeister, I. Elizarov, V. Perić, and P. Tzscheutschler, "Characteristics and Challenges in Prosumer-Dominated Thermal Networks," *J Phys Conf Ser*, vol. 2042, no. 1, p. 012039, Nov. 2021, doi: 10.1088/1742-6596/2042/1/012039.

[24] D. Zinsmeister *et al.*, "A prosumer-based sector-coupled district heating and cooling laboratory architecture," 2023, doi: 10.1016/j.segy.2023.100095.

[25] T. Testasecca, P. Catrini, M. Beccali, and A. Piacentino, "Dynamic simulation of a 4th generation district heating network with the presence of prosumers," *Energy Conversion and Management: X*, vol. 20, p. 100480, Oct. 2023, doi: 10.1016/J.ECMX.2023.100480.

[26] H. Kauko, K. H. Kvalsvik, D. Rohde, N. Nord, and Å. Utne, "Dynamic modeling of local district heating grids with prosumers: A case study for Norway," *Energy*, vol. 151, pp. 261–271, 2018, doi: 10.1016/j.energy.2018.03.033.

[27] T. Lickleder, T. Hamacher, M. Kramer, and V. S. Perić, "Thermohydraulic model of Smart Thermal Grids with bidirectional power flow between prosumers," *Energy*, vol. 230, p. 120825, Sep. 2021, doi: 10.1016/J.ENERGY.2021.120825.

[28] H. Li, J. Hou, T. Hong, and N. Nord, "Distinguish between the economic optimal and lowest distribution temperatures for heat-prosumer-based district heating systems with short-term thermal energy storage," *Energy*, vol. 248, Jun. 2022, doi: 10.1016/j.energy.2022.123601.

[29] H. Li, J. Hou, Z. Tian, T. Hong, N. Nord, and D. Rohde, "Optimize heat prosumers' economic performance under current heating price models by using water tank thermal energy storage," *Energy*, vol. 239, p. 122103, Jan. 2022, doi: 10.1016/j.energy.2021.122103.

[30] A. Penkovskii, V. Stennikov, and A. Kravets, "Bi-level modeling of district heating systems with prosumers," *Energy Reports*, vol. 6, pp. 89–95, 2020, doi: 10.1016/j.egyr.2019.11.046.

[31] M. Bilardo, F. Sandrone, G. Zanzottera, and E. Fabrizio, "Modelling a fifth-generation bidirectional low temperature district heating and cooling (5GDHC) network for nearly Zero Energy District (nZED)," *Energy Reports*, vol. 7, pp. 8390–8405, Nov. 2021, doi: 10.1016/J.EGYR.2021.04.054.

[32] Y. J. Youn and Y. H. Im, "Analysis of operating characteristics of interconnected operation of thermal grids with bidirectional heat trade," *Appl Therm Eng*, vol. 229, p. 120608, Jul. 2023, doi: 10.1016/J.APPLTHERMALENG.2023.120608.

[33] P. Huang *et al.*, "A review of data centers as prosumers in district energy systems: Renewable energy integration and waste heat reuse for district heating," *Appl Energy*, vol. 258, 2020, doi: 10.1016/j.apenergy.2019.114109.

[34] J. Stock, F. Arjuna, A. Xhonneux, and D. Müller, "Modelling of waste heat integration into an existing district heating network operating at different supply temperatures," *Smart Energy*, vol. 10, p. 100104, May 2023, doi: 10.1016/J.SEGY.2023.100104.

[35] A. Kang, I. Korolija, and D. Rovas, "Photovoltaic Thermal District Heating: A review of the current status, opportunities and prospects," *Appl Therm Eng*, vol. 217, p. 119051, Nov. 2022, doi: 10.1016/J.APPLTHERMALENG.2022.119051.

[36] R. Alisic, P. E. Paré, and H. Sandberg, "Modeling and Stability of Prosumer Heat Networks," in *IFAC-PapersOnLine*, G. D.F., Ed., Elsevier B.V., 2019, pp. 235–240. doi: 10.1016/j.ifacol.2019.12.164.

[37] I. Postnikov, "Methods for optimization of time redundancy of prosumer in district heating systems," *Energy Reports*, vol. 6, pp. 214–220, 2020, doi: 10.1016/j.egyr.2019.11.065.

[38] V. Stennikov and I. Postnikov, "Search the optimal ratio of system's component reliability parameters and the heat capacity of prosumers in the district heating system," in *E3S Web of Conferences*, C. V. R. K. E. T. V. V. K. L. B. M. S. A. N. M. S. C. S. C. S. M. G. T. E. Novitsky N.N. Serttter B., Ed., EDP Sciences, 2020. doi: 10.1051/e3sconf/202021902004.

[39] I. Postnikov, "Providing the Reliability of Heating of Prosumers taking into account the Functioning of Their Own Heat Sources in District Heating Systems," in *2019 International Multi-Conference on Industrial Engineering and Modern Technologies, FarEastCon 2019*, Institute of Electrical and Electronics Engineers Inc., 2019. doi: 10.1109/FarEastCon.2019.8934913.

[40] M. Jiang, C. Rindt, and D. M. J. Smeulders, "Optimal Planning of Future District Heating Systems—A Review," *Energies 2022, Vol. 15, Page 7160*, vol. 15, no. 19, p. 7160, Sep. 2022, doi: 10.3390/EN15197160.

[41] H. Dorotić, T. Pukšec, D. R. Schneider, and N. Duić, "Evaluation of district heating with regard to individual systems – Importance of carbon and cost allocation in cogeneration units," *Energy*, vol. 221, p. 119905, Apr. 2021, doi: 10.1016/J.ENERGY.2021.119905.

[42] S. Calixto, M. Cozzini, R. Fedrizzi, and G. Manzolini, "A New Method for the Techno-Economic Analysis and the Identification of Expansion Strategies of Neutral-Temperature District Heating

and Cooling Systems," *Energies 2024, Vol. 17, Page 2159*, vol. 17, no. 9, p. 2159, Apr. 2024, doi: 10.3390/EN17092159.

[43] A. Delangle, R. S. C. Lambert, N. Shah, S. Acha, and C. N. Markides, "Modelling and optimising the marginal expansion of an existing district heating network," *Energy*, vol. 140, pp. 209–223, Dec. 2017, doi: 10.1016/j.energy.2017.08.066.

[44] A. Lerbinger, I. Petkov, G. Mavromatidis, and C. Knoeri, "Optimal decarbonization strategies for existing districts considering energy systems and retrofits," *Appl Energy*, vol. 352, p. 121863, Dec. 2023, doi: 10.1016/J.APENERGY.2023.121863.

[45] D. F. Dominković, G. Stunjek, I. Blanco, H. Madsen, and G. Krajačić, "Technical, economic and environmental optimization of district heating expansion in an urban agglomeration," *Energy*, vol. 197, p. 117243, Apr. 2020, doi: 10.1016/j.energy.2020.117243.

[46] F. Wendel, M. Blesl, L. Brodecki, and K. Hufendiek, "Expansion or decommission? – Transformation of existing district heating networks by reducing temperature levels in a cost-optimum network design," *Appl Energy*, vol. 310, p. 118494, Mar. 2022, doi: 10.1016/j.apenergy.2021.118494.

[47] C. Shao, M. Shahidehpour, and Y. Ding, "Market-Based Integrated Generation Expansion Planning of Electric Power System and District Heating Systems," *IEEE Trans Sustain Energy*, vol. 11, no. 4, pp. 2483–2493, Oct. 2020, doi: 10.1109/TSTE.2019.2962756.

[48] L. Grundahl, S. Nielsen, H. Lund, and B. Möller, "Comparison of district heating expansion potential based on consumer-economy or socio-economy," *Energy*, vol. 115, pp. 1771–1778, Nov. 2016, doi: 10.1016/j.energy.2016.05.094.

[49] E. Guelpa, G. Mutani, V. Todeschi, and V. Verda, "A feasibility study on the potential expansion of the district heating network of Turin," *Energy Procedia*, vol. 122, pp. 847–852, Sep. 2017, doi: 10.1016/j.egypro.2017.07.446.

[50] S. Nielsen and L. Grundahl, "District Heating Expansion Potential with Low-Temperature and End-Use Heat Savings," *Energies 2018, Vol. 11, Page 277*, vol. 11, no. 2, p. 277, Jan. 2018, doi: 10.3390/EN11020277.

[51] E. Guelpa, G. Mutani, V. Todeschi, and V. Verda, "Reduction of CO2 emissions in urban areas through optimal expansion of existing district heating networks," *J Clean Prod*, vol. 204, pp. 117–129, Dec. 2018, doi: 10.1016/j.jclepro.2018.08.272.

[52] G. Spirito, A. Dénarié, F. Fattori, G. Muliere, M. Motta, and U. Persson, "Assessing district heating potential at large scale: Presentation and application of a spatially-detailed model to optimally match heat sources and demands.," *Appl Energy*, vol. 372, p. 123844, Oct. 2024, doi: 10.1016/J.APENERGY.2024.123844.

[53] C. Delmastro, G. Mutani, and L. Schranz, "The evaluation of buildings energy consumption and the optimization of district heating networks: a GIS-based model," *International Journal of Energy and Environmental Engineering*, vol. 7, no. 3, pp. 343–351, Sep. 2016, doi: 10.1007/S40095-015-0161-5/FIGURES/5.

[54] J. Lambert and H. Spliethoff, "A Nonlinear Optimization Method for Expansion Planning of District Heating Systems with Graph Preprocessing," 2023, doi: 10.52202/069564-0238.

[55] G. Mutani, V. Todeschi, E. Guelpa, and V. Verda, “Building Efficiency Models and the Optimization of the District Heating Network for Low-Carbon Transition Cities,” pp. 217–241, 2020, doi: 10.1007/978-3-030-31459-0_14.

[56] D. Connolly *et al.*, “The role of district heating in decarbonising the EU energy system and a comparison with existing strategies,” 2013. doi: https://api.semanticscholar.org/CorpusID:6681829.

[57] P. A. Østergaard, H. Lund, J. Z. Thellufsen, P. Sorknæs, and B. V. Mathiesen, “Review and validation of EnergyPLAN,” *Renewable and Sustainable Energy Reviews*, vol. 168, p. 112724, Oct. 2022, doi: 10.1016/J.RSER.2022.112724.

[58] M. Jaskólski and P. Bućko, “Modelling Long-Term Transition from Coal-Reliant to Low-Emission Power Grid and District Heating Systems in Poland,” *Energies 2021, Vol. 14, Page 8389*, vol. 14, no. 24, p. 8389, Dec. 2021, doi: 10.3390/EN14248389.

[59] A. Sandvall, M. Hagberg, and K. Lygnerud, “Modelling of urban excess heat use in district heating systems,” *Energy Strategy Reviews*, vol. 33, p. 100594, Jan. 2021, doi: 10.1016/J.ESR.2020.100594.

[60] A. Sandvall and K. B. Karlsson, “Energy system and cost impacts of heat supply to low-energy buildings in Sweden,” *Energy*, vol. 268, p. 126743, Apr. 2023, doi: 10.1016/J.ENERGY.2023.126743.

[61] S. Robu, M. Lupu, and V. Daud, “The Impact of Distributed Heat Pumps on the District Heating System,” in *2021 9th International Conference on Modern Power Systems (MPS)*, IEEE, Jun. 2021, pp. 1–6. doi: 10.1109/MPS52805.2021.9492548.

[62] J. Z. Thellufsen, S. Nielsen, and H. Lund, “Implementing cleaner heating solutions towards a future low-carbon scenario in Ireland,” *J Clean Prod*, vol. 214, pp. 377–388, Mar. 2019, doi: 10.1016/j.jclepro.2018.12.303.

[63] “Renewable and Waste Heat Recovery for Competitive District Heating and Cooling Networks REWARDHeat”, doi: https://rewardheat.tokni.com/.

[64] “Hotmaps Project - The open source mapping and planning tool for heating and cooling.” Accessed: Aug. 09, 2024. [Online]. Available: https://www.hotmaps-project.eu/

[65] U. Persson and S. Werner, “Effective Width: The Relative Demand for District Heating Pipe Lengths in City Areas”, Accessed: Aug. 09, 2024. [Online]. Available: http://www.diva-portal.orghttp://urn.kb.se/resolve?urn=urn:nbn:se:hh:diva-6014

[66] H. Lund, “Theory: Choice awareness theses,” *Renewable Energy Systems: A Smart Energy Systems Approach to the Choice and Modeling of 100% Renewable Solutions: Second Edition*, pp. 15–34, Jan. 2014, doi: 10.1016/B978-0-12-410423-5.00002-X.

[67] R. Loulou, E. Wright, G. Giannakidis, and K. Noble, “Energy Technology Systems Analysis Programme,” 2016, Accessed: Mar. 14, 2024. [Online]. Available: http://www.iea-etsap.org/web/Documentation.asp

[68] “Joint Research Centre Data Catalogue - The JRC European TIMES Energy System Model - European Commission.” Accessed: Aug. 22, 2024. [Online]. Available: https://data.jrc.ec.europa.eu/collection/id-00287

[69] “GAINS Model.” Accessed: Aug. 24, 2024. [Online]. Available: https://gains.iiasa.ac.at/models/

[70] H. Li, Q. Sun, Q. Zhang, and F. Wallin, "A review of the pricing mechanisms for district heating systems," *Renewable and Sustainable Energy Reviews*, vol. 42, pp. 56–65, Feb. 2015, doi: 10.1016/J.RSER.2014.10.003.

[71] D. F. Dominković, M. Wahlroos, S. Syri, and A. S. Pedersen, "Influence of different technologies on dynamic pricing in district heating systems: Comparative case studies," *Energy*, vol. 153, pp. 136–148, Jun. 2018, doi: 10.1016/J.ENERGY.2018.04.028.

[72] S. Syri, H. Mäkelä, S. Rinne, and N. Wirgentius, "Open district heating for Espoo city with marginal cost based pricing," in *International Conference on the European Energy Market, EEM*, IEEE Computer Society, Aug. 2015. doi: 10.1109/EEM.2015.7216654.

[73] V. Stennikov and A. Penkovskii, "The pricing methods on the monopoly district heating market," in *Energy Reports*, Elsevier Ltd, Feb. 2020, pp. 187–193. doi: 10.1016/j.egyr.2019.11.061.

[74] S. Oh and S. K. Kim, "Impact of heat price regulation on the optimal district heating production mix and its policy implications," *Energy*, vol. 239, Jan. 2022, doi: 10.1016/j.energy.2021.122305.

[75] L. Bai, P. Pinson, and J. Wang, "Variable heat pricing to steer the flexibility of heat demand response in district heating systems," *Electric Power Systems Research*, vol. 212, Nov. 2022, doi: 10.1016/j.epsr.2022.108383.

[76] W. Liu, D. Klip, W. Zappa, S. Jelles, G. J. Kramer, and M. van den Broek, "The marginal-cost pricing for a competitive wholesale district heating market: A case study in the Netherlands," *Energy*, vol. 189, Dec. 2019, doi: 10.1016/j.energy.2019.116367.

[77] S. Selvakkumaran, L. Eriksson, and I.-L. Svensson, "How do business models for prosumers in the district energy sector capture flexibility?," *Energy Reports*, vol. 7, pp. 203–212, 2021, doi: 10.1016/j.egyr.2021.08.154.

[78] "THIRD-PARTY ACCESS TO DISTRICT HEATING NETWORKS A report to Finnish Energy," 2018. doi: https://energia.fi/wp-content/uploads/2018/05/Third-Party_Access_to_District_Heating_Networks_FINAL_REPORT_20180509-1.pdf.

[79] V. Bürger, J. Steinbach, L. Kranzl, and A. Müller, "Third party access to district heating systems - Challenges for the practical implementation," *Energy Policy*, vol. 132, pp. 881–892, Sep. 2019, doi: 10.1016/j.enpol.2019.06.050.

[80] M. Pipiciello, M. Caldera, M. Cozzini, M. A. Ancona, F. Melino, and B. Di Pietra, "Experimental characterization of a prototype of bidirectional substation for district heating with thermal prosumers," *Energy*, vol. 223, 2021, doi: 10.1016/j.energy.2021.120036.

[81] M. A. Ancona, L. Branchini, B. Di Pietra, F. Melino, G. Puglisi, and F. Zanghirella, "Utilities Substations in Smart District Heating Networks," *Energy Procedia*, vol. 81, pp. 597–605, Dec. 2015, doi: 10.1016/J.EGYPRO.2015.12.044.

[82] M. A. Ancona, L. Branchini, A. De Pascale, and F. Melino, "Smart District Heating: Distributed Generation Systems' Effects on the Network," *Energy Procedia*, vol. 75, pp. 1208–1213, Aug. 2015, doi: 10.1016/J.EGYPRO.2015.07.157.

[83] J. Eric and B. Vad, "'Progression of District Heating-1st to 4th generation'", Accessed: Mar. 07, 2024. [Online]. Available: www.4dh.dk

[84] R. H. S. Winterton, "Where did the Dittus and Boelter equation come from?," *Int J Heat Mass Transf*, vol. 41, no. 4–5, pp. 809–810, Feb. 1998, doi: 10.1016/S0017-9310(97)00177-4.

[85] D. Schmidt and K. Lygnerud, “Low Temperature District Heating as a Key Technology for a Successful Integration of Renewable Heat Sources in our Energy Systems”, doi: 10.18086/eurosun.2022.04.12.

[86] M. Norişor, D. Ban, R. Pătraşcu, and E. Minciuc, “COMPLEX, ENERGY, ECONOMIC AND ENVIRONMENTAL ANALYSIS OF DIFFERENT SOLUTIONS FOR INTEGRATING SOLAR THERMAL PANELS (PT) IN TO DISTRICT HEATING SUBSTATION (DHS),” *U.P.B. Sci. Bull., Series C*, vol. 84, no. 3, p. 2022.

[87] “SDH project”, doi: https://www.solar-district-heating.eu/.

[88] “SDHp2m project”, [Online]. Available: https://wayback.archive-it.org/12090/20190928022107/https://ec.europa.eu/inea/en/horizon-2020/projects/h2020-energy/heating-cooling/sdhp2m

[89] “RES DHC project”, doi: https://www.res-dhc.com/it/informazioni/h2020-res-dhc/.

[90] S. Brand, “TVP Solar - Solar Keymark Certificate,” Jun. 2017. doi: https://www.dincertco.de/logos/011-7S1890%20F.pdf.

[91] M. Database, “Meteonorm Version 8 - Meteonorm (en).” Accessed: Mar. 04, 2021. [Online]. Available: https://meteonorm.com/en/meteonorm-version-8

[92] “EN 14825:2018 - Air conditioners, liquid chilling packages and heat pumps, with electrically driven.” Accessed: Jan. 09, 2023. [Online]. Available: https://standards.iteh.ai/catalog/standards/cen/304fe3bd-b611-4f34-8ca2-8ace2d476d89/en-14825-2018

[93] “UNI/TS 11300-4:2016 - UNI Ente Italiano di Normazione.” Accessed: Jan. 09, 2023. [Online]. Available: https://store.uni.com/en/uni-ts-11300-4-2016

[94] “EN 12831:2003 - Heating systems in buildings - Method for calculation of the design heat load.” Accessed: Jan. 09, 2023. [Online]. Available: https://standards.iteh.ai/catalog/standards/cen/5a4acdae-ff13-4411-8b0b-b54c65c4f91c/en-12831-2003

[95] “CEN/TR 15615:2008 - Explanation of the general relationship between various European standards and.” Accessed: Jan. 09, 2023. [Online]. Available: https://standards.iteh.ai/catalog/standards/cen/d7208116-9623-4117-8d99-4c81230c6f5e/cen-tr-15615-2008

[96] M. Dongellini, C. Naldi, and G. L. Morini, “Seasonal performance evaluation of electric air-to-water heat pump systems,” *Appl Therm Eng*, vol. 90, pp. 1072–1081, 2015, doi: https://doi.org/10.1016/j.applthermaleng.2015.03.026.

[97] I. Grossi, M. Dongellini, A. Piazzi, and G. L. Morini, “Dynamic modelling and energy performance analysis of an innovative dual-source heat pump system,” *Appl Therm Eng*, vol. 142, pp. 745–759, 2018, doi: https://doi.org/10.1016/j.applthermaleng.2018.07.022.

[98] Szulgowska-Zgrzywa, Malgorzata and Piechurski, Krzysztof, “The influence of thermal load profile of building on the air/water heat pump efficiency simulation,” *E3S Web Conf.*, vol. 116, p. 89, 2019, doi: 10.1051/e3sconf/201911600089.

[99] M. Cannistraro, E. Mainardi, and M. Bottarelli, "Mathematical Modelling of Engineering Problems Testing a dual-source heat pump," vol. 5, no. 3, pp. 205–210, 2018, doi: 10.18280/mmep.050311.

[100] T. Lickleder, T. Hamacher, M. Kramer, and V. S. Perić, "Thermohydraulic model of Smart Thermal Grids with bidirectional power flow between prosumers," *Energy*, vol. 230, 2021, doi: 10.1016/j.energy.2021.120825.

[101] "REPowerEU." Accessed: Nov. 19, 2024. [Online]. Available: https://commission.europa.eu/strategy-and-policy/priorities-2019-2024/european-green-deal/repowereu-affordable-secure-and-sustainable-energy-europe_en

[102] F. Ceglia, E. Marrasso, G. Pallotta, C. Roselli, and M. Sasso, "The State of the Art of Smart Energy Communities: A Systematic Review of Strengths and Limits," *Energies 2022, Vol. 15, Page 3462*, vol. 15, no. 9, p. 3462, May 2022, doi: 10.3390/EN15093462.

[103] G. E. Dino, C. Raimondi, F. Gracceva, E. R. Sanseverino, and A. Piacentino, "The Renewable Energy Communities: An Innovative Application to a Small Mountain Italian Municipality," *2024 International Conference on Renewable Energies and Smart Technologies, REST 2024*, 2024, doi: 10.1109/REST59987.2024.10645387.

[104] M. Krug, M. R. Di Nucci, M. Caldera, and E. De Luca, "Mainstreaming Community Energy: Is the Renewable Energy Directive a Driver for Renewable Energy Communities in Germany and Italy?," *Sustainability 2022, Vol. 14, Page 7181*, vol. 14, no. 12, p. 7181, Jun. 2022, doi: 10.3390/SU14127181.

[105] A. A. Kebede, T. Kalogiannis, J. Van Mierlo, and M. Berecibar, "A comprehensive review of stationary energy storage devices for large scale renewable energy sources grid integration," *Renewable and Sustainable Energy Reviews*, vol. 159, p. 112213, May 2022, doi: 10.1016/J.RSER.2022.112213.

[106] A. Bartolini, F. Carducci, C. B. Muñoz, and G. Comodi, "Energy storage and multi energy systems in local energy communities with high renewable energy penetration," *Renew Energy*, vol. 159, pp. 595–609, Oct. 2020, doi: 10.1016/J.RENENE.2020.05.131.

[107] F. Alsokhiry, P. Siano, A. Annuk, and M. A. Mohamed, "A Novel Time-of-Use Pricing Based Energy Management System for Smart Home Appliances: Cost-Effective Method," *Sustainability 2022, Vol. 14, Page 14556*, vol. 14, no. 21, p. 14556, Nov. 2022, doi: 10.3390/SU142114556.

[108] C. Wulf, P. Zapp, and A. Schreiber, "Review of Power-to-X Demonstration Projects in Europe," *Front Energy Res*, vol. 8, p. 547456, Sep. 2020, doi: 10.3389/FENRG.2020.00191/BIBTEX.

[109] J. Z. Thellufsen *et al.*, "Smart energy cities in a 100% renewable energy context," *Renewable and Sustainable Energy Reviews*, vol. 129, p. 109922, Sep. 2020, doi: 10.1016/J.RSER.2020.109922.

[110] H. Lund, "Renewable heating strategies and their consequences for storage and grid infrastructures comparing a smart grid to a smart energy systems approach," *Energy*, vol. 151, pp. 94–102, May 2018, doi: 10.1016/J.ENERGY.2018.03.010.

[111] E. Guelpa, A. Bischi, V. Verda, M. Chertkov, and H. Lund, "Towards future infrastructures for sustainable multi-energy systems: A review," *Energy*, vol. 184, pp. 2–21, Oct. 2019, doi: 10.1016/J.ENERGY.2019.05.057.

[112] A. Bloess, W. P. Schill, and A. Zerrahn, "Power-to-heat for renewable energy integration: A review of technologies, modeling approaches, and flexibility potentials," *Appl Energy*, vol. 212, pp. 1611–1626, Feb. 2018, doi: 10.1016/J.APENERGY.2017.12.073.

[113] D. Fischer and H. Madani, "On heat pumps in smart grids: A review," *Renewable and Sustainable Energy Reviews*, vol. 70, pp. 342–357, Apr. 2017, doi: 10.1016/J.RSER.2016.11.182.

[114] J. Le Dréau and P. Heiselberg, "Energy flexibility of residential buildings using short term heat storage in the thermal mass," *Energy*, vol. 111, pp. 991–1002, Sep. 2016, doi: 10.1016/J.ENERGY.2016.05.076.

[115] L. Zhang, N. Good, and P. Mancarella, "Building-to-grid flexibility: Modelling and assessment metrics for residential demand response from heat pump aggregations," *Appl Energy*, vol. 233–234, pp. 709–723, 2019, doi: https://doi.org/10.1016/j.apenergy.2018.10.058.

[116] W. Meesenburg, T. Ommen, and B. Elmegaard, "Dynamic exergoeconomic analysis of a heat pump system used for ancillary services in an integrated energy system," *Energy*, vol. 152, pp. 154–165, Jun. 2018, doi: 10.1016/J.ENERGY.2018.03.093.

[117] Z. E. Lee, Q. Sun, Z. Ma, J. Wang, J. S. MacDonald, and K. Max Zhang, "Providing Grid Services With Heat Pumps: A Review," *ASME Journal of Engineering for Sustainable Buildings and Cities*, vol. 1, no. 1, Feb. 2020, doi: 10.1115/1.4045819.

[118] P. Manner, I. Alapera, and S. Honkapuro, "Domestic heat pumps as a source of primary frequency control reserve," *International Conference on the European Energy Market, EEM*, vol. 2020-September, Sep. 2020, doi: 10.1109/EEM49802.2020.9221902.

[119] L. Bartolucci, S. Cordiner, V. Mulone, and M. Santarelli, "Ancillary Services Provided by Hybrid Residential Renewable Energy Systems through Thermal and Electrochemical Storage Systems," *Energies 2019, Vol. 12, Page 2429*, vol. 12, no. 12, p. 2429, Jun. 2019, doi: 10.3390/EN12122429.

[120] G. M. Tina, S. Aneli, and A. Gagliano, "Technical and economic analysis of the provision of ancillary services through the flexibility of HVAC system in shopping centers," *Energy*, vol. 258, p. 124860, Nov. 2022, doi: 10.1016/J.ENERGY.2022.124860.

[121] W. Meesenburg, W. B. Markussen, T. Ommen, and B. Elmegaard, "Optimizing control of two-stage ammonia heat pump for fast regulation of power uptake," *Appl Energy*, vol. 271, p. 115126, Aug. 2020, doi: 10.1016/J.APENERGY.2020.115126.

[122] A. Arteconi and F. Polonara, "Assessing the Demand Side Management Potential and the Energy Flexibility of Heat Pumps in Buildings," *Energies 2018, Vol. 11, Page 1846*, vol. 11, no. 7, p. 1846, Jul. 2018, doi: 10.3390/EN11071846.

[123] J. Vivian, E. Prataviera, F. Cunsolo, and M. Pau, "Demand Side Management of a pool of air source heat pumps for space heating and domestic hot water production in a residential district," *Energy Convers Manag*, vol. 225, p. 113457, Dec. 2020, doi: 10.1016/J.ENCONMAN.2020.113457.

[124] I. Ibrahim, C. O'Loughlin, and T. O'Donnell, "Virtual Inertia Control of Variable Speed Heat Pumps for the Provision of Frequency Support," *Energies 2020, Vol. 13, Page 1863*, vol. 13, no. 8, p. 1863, Apr. 2020, doi: 10.3390/EN13081863.

[125] T. B. Harild Rasmussen, Q. Wu, and M. Zhang, "Primary frequency support from local control of large-scale heat pumps," *International Journal of Electrical Power & Energy Systems*, vol. 133, p. 107270, Dec. 2021, doi: 10.1016/J.IJEPES.2021.107270.

[126] L. Romero Rodríguez, J. Sánchez Ramos, S. Álvarez Domínguez, and U. Eicker, "Contributions of heat pumps to demand response: A case study of a plus-energy dwelling," *Appl Energy*, vol. 214, pp. 191–204, Mar. 2018, doi: 10.1016/J.APENERGY.2018.01.086.

[127] V. Z. Gjorgievski, N. Markovska, A. Abazi, and N. Duić, "The potential of power-to-heat demand response to improve the flexibility of the energy system: An empirical review," *Renewable and Sustainable Energy Reviews*, vol. 138, p. 110489, Mar. 2021, doi: 10.1016/J.RSER.2020.110489.

[128] S. Bechtel, S. Rafii-Tabrizi, F. Scholzen, J. R. Hadji-Minaglou, and S. Maas, "Influence of thermal energy storage and heat pump parametrization for demand-side-management in a nearly-zero-energy-building using model predictive control," *Energy Build*, vol. 226, p. 110364, Nov. 2020, doi: 10.1016/J.ENBUILD.2020.110364.

[129] T. Q. Péan, J. Salom, and R. Costa-Castelló, "Review of control strategies for improving the energy flexibility provided by heat pump systems in buildings," *J Process Control*, vol. 74, pp. 35–49, Feb. 2019, doi: 10.1016/J.JPROCONT.2018.03.006.

[130] Z. You, M. Zade, B. Kumaran Nalini, and P. Tzscheutschler, "Flexibility Estimation of Residential Heat Pumps under Heat Demand Uncertainty," *Energies 2021, Vol. 14, Page 5709*, vol. 14, no. 18, p. 5709, Sep. 2021, doi: 10.3390/EN14185709.

[131] L. Schibuola, M. Scarpa, and C. Tambani, "Demand response management by means of heat pumps controlled via real time pricing," *Energy Build*, vol. 90, pp. 15–28, Mar. 2015, doi: 10.1016/J.ENBUILD.2014.12.047.

[132] S. Buffa, A. Soppelsa, M. Pipiciello, G. Henze, and R. Fedrizzi, "Fifth-Generation District Heating and Cooling Substations: Demand Response with Artificial Neural Network-Based Model Predictive Control," *Energies 2020, Vol. 13, Page 4339*, vol. 13, no. 17, p. 4339, Aug. 2020, doi: 10.3390/EN13174339.

[133] J. Barco-Burgos, J. C. Bruno, U. Eicker, A. L. Saldaña-Robles, and V. Alcántar-Camarena, "Review on the integration of high-temperature heat pumps in district heating and cooling networks," *Energy*, vol. 239, p. 122378, Jan. 2022, doi: 10.1016/J.ENERGY.2021.122378.

[134] N. Nord, M. Shakerin, T. Tereshchenko, V. Verda, and R. Borchiellini, "Data informed physical models for district heating grids with distributed heat sources to understand thermal and hydraulic aspects," *Energy*, vol. 222, p. 119965, May 2021, doi: 10.1016/J.ENERGY.2021.119965.

[135] L. Frölke, T. Sousa, and P. Pinson, "A network-aware market mechanism for decentralized district heating systems," *Appl Energy*, vol. 306, 2022, doi: 10.1016/j.apenergy.2021.117956.

[136] M. Loesch, D. Hufnagel, S. Steuer, T. Fabßnacht, and H. Schmeck, "Demand side management in smart buildings by intelligent scheduling of heat pumps," *2014 IEEE International Conference on Intelligent Energy and Power Systems, IEPS 2014 - Conference Proceedings*, pp. 209–214, 2014, doi: 10.1109/IEPS.2014.6874181.

[137] X. Yan, Y. Ozturk, Z. Hu, and Y. Song, "A review on price-driven residential demand response," *Renewable and Sustainable Energy Reviews*, vol. 96, pp. 411–419, Nov. 2018, doi: 10.1016/J.RSER.2018.08.003.

[138] A. Coelho, J. Iria, F. Soares, and J. P. Lopes, "Real-time management of distributed multi-energy resources in multi-energy networks," *Sustainable Energy, Grids and Networks*, vol. 34, p. 101022, Jun. 2023, doi: 10.1016/J.SEGAN.2023.101022.

[139] T. Dengiz, P. Jochem, and W. Fichtner, "Demand response with heuristic control strategies for modulating heat pumps," *Appl Energy*, vol. 238, pp. 1346–1360, Mar. 2019, doi: 10.1016/J.APENERGY.2018.12.008.

[140] "EN ISO 52000-1:2017." Accessed: May 06, 2021. [Online]. Available: http://store.uni.com/catalogo/en-iso-52000-1-2017?josso_back_to=http://store.uni.com/josso-security-check.php&josso_cmd=login_optional&josso_partnerapp_host=store.uni.com

[141] "High temperature heat pump KWP | Kroll Energy GmbH." Accessed: Feb. 24, 2023. [Online]. Available: http://www.kroll.de/en/high-temperature-heat-pump-kwp/

[142] S. Kuboth, F. Heberle, T. Weith, M. Welzl, A. König-Haagen, and D. Brüggemann, "Experimental short-term investigation of model predictive heat pump control in residential buildings," *Energy Build*, vol. 204, p. 109444, Dec. 2019, doi: 10.1016/J.ENBUILD.2019.109444.

[143] F. D'Ettorre, P. Conti, E. Schito, and D. Testi, "Model predictive control of a hybrid heat pump system and impact of the prediction horizon on cost-saving potential and optimal storage capacity," *Appl Therm Eng*, vol. 148, pp. 524–535, Feb. 2019, doi: 10.1016/J.APPLTHERMALENG.2018.11.063.

[144] Z. Lee, K. Gupta, K. J. Kircher, and K. M. Zhang, "Mixed-integer model predictive control of variable-speed heat pumps," *Energy Build*, vol. 198, pp. 75–83, Sep. 2019, doi: 10.1016/J.ENBUILD.2019.05.060.

[145] G. E. Dino, V. Palomba, E. Nowak, and A. Frazzica, "Experimental characterization of an innovative hybrid thermal-electric chiller for industrial cooling and refrigeration application," *Appl Energy*, vol. 281, p. 116098, 2021, doi: 10.1016/j.apenergy.2020.116098.

[146] "Teleriscaldamento tariffe e costi in Veneto." Accessed: Feb. 02, 2023. [Online]. Available: https://www.ilteleriscaldamento.eu/teleriscaldamento_veneto.htm

[147] F. Giunta and S. Sawalha, "Techno-economic analysis of heat recovery from supermarket's CO2 refrigeration systems to district heating networks," *Appl Therm Eng*, vol. 193, 2021, doi: 10.1016/j.applthermaleng.2021.117000.

[148] "Arera: Dati e statistiche." Accessed: Apr. 10, 2024. [Online]. Available: https://www.arera.it/dati-e-statistiche

[149] Ashrae, "ANSI/ASHRAE/IES Addenda be, bm, bn, bo, bp, br, bs, bu, bv, cf, cl, cm, cq, ct, cu, cv, cw, cy," 2021, Accessed: Mar. 12, 2024. [Online]. Available: www.ashrae.org

[150] "Commercial Reference Buildings | Department of Energy." Accessed: Mar. 12, 2024. [Online]. Available: https://www.energy.gov/eere/buildings/commercial-reference-buildings

[151] "UNI/TR 11552:2014 - UNI Ente Italiano di Normazione." Accessed: Mar. 12, 2024. [Online]. Available: https://store.uni.com/en/uni-tr-11552-2014

[152] D. P. Hiris, O. G. Pop, and M. C. Balan, "Preliminary sizing of solar district heating systems with seasonal water thermal storage," *Heliyon*, vol. 8, no. 2, p. e08932, Feb. 2022, doi: 10.1016/j.heliyon.2022.e08932.

[153] “Kältemaschinen.” Accessed: Mar. 14, 2024. [Online]. Available: https://www.baelz.de/systeme/absorptionskaelte

[154] J. Cervera-Vázquez, C. Montagud-Montalvá, and J. M. Corberán, “Science and Technology for the Built Environment Sizing of the buffer tank in chilled water distribution A/C systems,” 2016, doi: 10.1080/23744731.2016.1131569.

[155] “Home - Aermec.” Accessed: Mar. 14, 2024. [Online]. Available: https://global.aermec.com/it/

[156] “Technology Data for Individual Heating Plants | The Danish Energy Agency.” Accessed: May 23, 2024. [Online]. Available: https://ens.dk/en/our-services/technology-catalogues/technology-data-individual-heating-plants

[157] E. Press *et al.*, “Renewable Power Generation Costs in 2020,” 2021, Accessed: May 23, 2024. [Online]. Available: www.irena.org

[158] A. G. Papatsounis *et al.*, “Operation assessment of a hybrid solar-biomass energy system with absorption refrigeration scenarios,” *Energy Sources, Part A: Recovery, Utilization, and Environmental Effects*, vol. 44, no. 1, pp. 700–717, Mar. 2022, doi: 10.1080/15567036.2022.2049929.

[159] J. J. Roncal-Casano, P. Taddeo, J. Rodriguez-Martín, J. Muñoz-Antón, and A. A. Velasco, “Techno-economic comparison of a solar absorption chiller and photovoltaic compression chiller,” *36th International Conference on Efficiency, Cost, Optimization, Simulation and Environmental Impact of Energy Systems, ECOS 2023*, pp. 2661–2672, 2023, doi: 10.52202/069564-0239.

[160] U. States Department of Energy, “Combined Heat and Power Technology Fact Sheet Series ADVANCED MANUFACTURING OFFICE,” 2017, doi: https://www.energy.gov/sites/prod/files/2017/06/f35/CHP-Absorption%20Chiller-compliant.pdf.

[161] “Energy Storage Technology Descriptions-EASE-European Associaton for Storage of Energy Thermal hoT WaTer STorage Thermal energy STorage 1. Technical description”, Accessed: May 30, 2024. [Online]. Available: www.ease-storage.eu

[162] “SunHorizon.” Accessed: Jun. 05, 2024. [Online]. Available: https://sunhorizon-project.eu/

[163] “Technology Data for Generation of Electricity and District Heating | The Danish Energy Agency.” Accessed: May 30, 2024. [Online]. Available: https://ens.dk/en/our-services/technology-catalogues/technology-data-generation-electricity-and-district-heating

[164] “Electricity price statistics - Statistics Explained.” Accessed: Jun. 05, 2024. [Online]. Available: https://ec.europa.eu/eurostat/statistics-explained/index.php?title=Electricity_price_statistics#Electricity_prices_for_non-household_consumers

[165] “Prezzi finali dell’energia elettrica per i consumatori industriali - Ue a Area euro - Arera.” Accessed: Jun. 05, 2024. [Online]. Available: https://www.arera.it/dati-e-statistiche/dettaglio/prezzi-finali-dellenergia-elettrica-per-i-consumatori-industriali-ue-a-area-euro

[166] “La tariffa base del teleriscaldamento e acqua calda sanitaria-Comune di Verona”, doi: https://www.ilteleriscaldamento.eu/teleriscaldamento_veneto.htm.

[167] D. Harris and A. L. Figurelli, “The WACC for Heating Companies and Heat Exchangers in the Netherlands The WACC for Heating Companies and Heat Exchangers in the Netherlands PREPARED BY PREPARED FOR NOTICE The WACC for Heating Companies and Heat Exchangers in the Netherlands,” 2022.

[168] M. Wirtz, “nPro: A web-based planning tool for designing district energy systems and thermal networks,” *Energy*, vol. 268, p. 126575, Apr. 2023, doi: 10.1016/J.ENERGY.2022.126575.

[169] “Serie-storiche-emissioni-di-gas-serra-sintesi – EMISSIONI.” Accessed: Dec. 01, 2024. [Online]. Available: https://emissioni.sina.isprambiente.it/serie-storiche-emissioni-di-gas-serra-sintesi/

[170] “Pubblicato in Gazzetta Ufficiale il DECRETO LEGISLATIVO 14 luglio 2020, n. 73 (Attuazione della direttiva (UE) 2018/2002 che modifica la direttiva 2012/27/UE sull’efficienza energetica) - ENEA - Dipartimento Unità per l’efficienza energetica.” Accessed: Dec. 01, 2024. [Online]. Available: https://www.efficienzaenergetica.enea.it/vi-segnaliamo/pubblicato-in-gazzetta-ufficiale-il-decreto-legislativo-14-luglio-2020-n-73-attuazione-della-direttiva-ue-2018-2002-che-modifica-la-direttiva-2012-27-ue-sull-efficienza-energetica.html

[171] J. Rifkin and J. Linton, “THE READING ROOM The Third Industrial Revolution,” no. 416, pp. 37–39, 2011, doi: 10.1049/et:20080718.